Identification of MLL-AF9 related target genes and microRNAs involved in leukemogenesis

Dissertation zur Erlangung des Doktorgrades der Naturwissenschaften (Dr. rer. nat.)

an der Fakultät für Biologie der

Ludwig-Maximilians-Universität München

Durchgeführt am Forschungszentrum des Dr. von Haunerschen Kinderspitals der Ludwig-Maximilians-Universität München

vorgelegt von

Katrin Kristina Fleischmann

München, 3. Mai 2012

Erstgutachterin: Frau Prof. Dr. Elisabeth Weiss

Zweitgutachter: Herr Prof. Dr. Michael Schleicher

Sondergutachter: Herr Prof. Dr. Adelbert Roscher

Tag der Abgabe: **03.05.2012**

Tag der mündlichen Prüfung: **17.09.2012**

What is a scientist after all?

It is a curious man looking through a keyhole,

the keyhole of nature, trying to know what's going on.

Jacques Yves Cousteau

Preamble and Acknowledgments

How to explain the change from evolutionary ecology to tumor biology?

After my diploma thesis in evolutionary ecology and a major in ecology, I was facing some skepticism while being interviewed for PhD positions in the biomedical field.

What was my motivation to study biology? Why do I continue to feel this strong enthusiasm for this field? For me, it was always the grand question **"How does life work?"** that drove me and which may interconnect almost every aspect within natural sciences. Only when we strive to get answers to this grand question we may reach an understanding as to what happens in disease.

I am profoundly grateful to my dear colleagues Dr. Julia von Frowein, Dr. Thomas Magg and Dr. Uta Fuchs who supported me to become one of their colleagues at the research center of the Dr. von Haunerschen Kinderspital. Since then, innumerable great and inspiring discussions allied us. With them and many other splendid colleagues at our research center (among them Kristin Hähnel, Carola Laudano, Rita Meilbeck and many others who may forgive that I can not name all), I shared a vivid exchange of information and cordial coffee breaks. They all made every-day-life at our research center always joyful and worthwhile.

I profoundly thank Prof. Dr. Adelbert Roscher for his experimental advice and supervision, many stimulating discussions, for directing my thesis over these years and for his help when it was most crucial.

Further great thanks go to: Prof. Dr. Elisabeth Weiss for her friendly support and for representing this thesis at the Faculty of Biology of the Ludwig-Maximilians Universität München. PD Dr. Irene Schmid whose friendly support has always been of great value for my research at the Dr. von Haunerschen Kinderspital and for providing insights into the clinical oncology. PD Dr. Philipp Pagel for bioinformatical collaboration, stimulating discussions and open ears in a truly remarkable cooperation. Prof. Dr. Arndt Borkhardt for the initiation of this work and for supporting me while he was still at our institute.

And last but not least to: My dearest Markus, with whom I could share endless happy moments in nature and every-day-life while traveling, climbing and going on ski-randonnée, for taking care of a healthy work-life-balance. My loving parents Sigrid and Prof. Dr. Rudolf Schröck for supporting me in my interests and in every way anyone could wish. My brother and fellow scientist Dr. Florian Schröck for his friendship and interest in my work and for seeing it from a different angle. My family and friends for their friendship and support.

This work has been supported by the Graduiertenkolleg 1202 „Oligonucleotides in Cell Biology and Therapy" from the Deutsche Forschungsgemeinschaft.

1 Index

2 List of figures

3 List of tables

4 Summary

The translocation t(9;11)(p22;q23), leading to the leukemogenic hybrid gene and fusion protein MLL-AF9, is one of the most frequent translocations in infant acute myeloid leukemia (AML) and particularly associated with monoblastic AML (FAB classification M5). MLL and AF9 wildtype proteins play essential roles in embryogenesis and hematopoiesis and lead to transcriptional initiation (MLL) and elongation (AF9) of their target gene transcripts. The fusion protein MLL-AF9 is believed to combine these properties, leading to increased activation of target genes.

AML in childhood is a malignant type of leukemia with currently insufficient therapeutic options, as survival rates are still low with a 5-year overall survival of 57%. Therefore, this study set out to identify genes and miRNAs downstream of MLL-AF9 which could serve as potential targets in new therapeutic strategies.

The function of MLL-AF9 was investigated by efficient and specific knockdown via siRNAs in the AML M5 cell line THP1 which harbors this t(9;11) translocation. MLL-AF9 is known to change the expression of target genes via epigenetic mechanisms. To ensure that a reversal of these effects can be detected, the experimental setting included a prolonged knockdown over eight days. Besides biological assays, comprehensive gene and miRNA expression profiles following *MLL-AF9* knockdown were generated.

Endogenous MLL-AF9 protein showed low solubility and appeared to be prone to aggregate making its quantitation by Western blot difficult. *HOXA9* expression, however, could be utilized as a surrogate marker for MLL-AF9 protein reduction since its levels are increased via direct interaction between MLL-AF9 and the *HOXA9* promoter.

A highly significant reduction of 0.3 µm in cell diameter was detected after *MLL-AF9* knockdown which we hypothesize to be due to AF9 protein co-aggregation with MLL-AF9 because deletion of the AF9 homolog leads to an abnormally large phenotype in yeast. Additionally, our gene expression data suggested that the observed cell size reduction could be due to changes in intracellular ion concentrations and / or reduced ribosomal biogenesis.

Gene expression profiling revealed transcripts of 1269 genes to be differentially expressed. Together with functional gene ontology analyses, these results argued for a more differentiated state of MLL-AF9 depleted THP1 cells. Our data suggest effects of MLL-AF9 on differentiation and apoptosis as well as on calcium signaling, estrogen signaling, immunosurveillance and the heat-shock / unfolded protein response. Among the deregulated transcripts, a set of 40 likely candidates for mediation of the leukemogenic effects of MLL-AF9 was prioritized via a rating

strategy. Of these, 8 appear to be prone to therapeutic exploitation as they fall into protein classes well known as „druggable“.

MicroRNA expression screening yielded 23 differentially expressed miRNAs after *MLL-AF9* knockdown. A subset of these was selected for further validation via single-assay qRT-PCR and confirmed differential expression for 7 out of 11 tested microRNAs. Among these, miR-511, as the strongest differentially expressed miRNA, was additionally shown to be significantly upregulated in phorbol 12-myristate 13-acetate (PMA) differentiated THP1 cells. This observation is consistent with the hypothesis that miR-511 plays a role in the differentiation process of monoblasts. Expression strength was inversely correlated between miR-511 and 445 *in silico* predicted miR-511 targets within *MLL-AF9* knockdown samples. A subset of these was selected for experimental validation. Here, a trend towards reduced expression of eight predicted targets was detected after miR-511 mimic treatments in THP1 cells.

Our study revealed processes as well as novel candidate genes and miRNAs for mediation of MLL-AF9 leukemogenic effects, thus expanding previous knowledge of *MLL*-aberrant leukemia. Subsequent investigations of these candidates may aim to further evaluate their potential for new therapeutic strategies.

5 Zusammenfassung

Die Translokation t(9;11)(p22;q23), die zu dem leukämogenen Hybridgen und Fusionsprotein MLL-AF9 führt, ist eine der häufigsten Translokationen der frühkindlichen akuten myeloischen Leukämie (AML) und ist besonders mit dem monoblastischen Subtyp (FAB Klassifikation M5) assoziiert. Die MLL und AF9 Wildtyp-Proteine üben essentielle Funktionen in der Embryogenese und Hämatopoese aus und führen zur Initiation (MLL) und Elongation (AF9) der Transkription ihrer Zielgene. Das Fusionsprotein MLL-AF9 soll diese Eigenschaften kombinieren und so zu einer erhöhten Aktivität von Zielgenen führen.

AML im Kindesalter ist ein maligner Leukämietyp mit bislang unzureichenden Therapieoptionen, da die 5 Jahres Überlebensraten bei 57% liegen. Somit war das übergeordnete Ziel dieser Studie Gene und miRNAs zu identifizieren, die MLL-AF9 nachgeschaltet sind und die potentiell mit neuen therapeutischen Strategien beeinflusst werden können.

Die Wirkung von MLL-AF9 wurde mittels einer effizienten und spezifischen Stilllegung durch siRNAs in der Zellline THP1, die diese t(9;11) Translokation trägt, untersucht. Es ist bekannt, dass MLL-AF9 über epigenetische Mechanismen zu Veränderungen in der Expression seiner Zielgene führt. Um sicherzustellen, dass die Umkehr dieser Auswirkungen nachgewiesen werden kann, wurde ein experimentelles Protokoll gewählt, das eine über acht Tage anhaltende Supprimierung von MLL-AF9 einschloss. Neben Untersuchungen der biologischen Auswirkungen wurden umfassende Gen- und miRNA-Expressionsprofile nach Stilllegung von *MLL-AF9* generiert.

Endogenes MLL-AF9 Protein war schwer löslich und schien zur Aggregatbildung zu neigen, was die verlässliche Quantifizierungen mittels Western Blot verhinderte. Jedoch konnte die Expressionsstärke von *HOXA9* als Ersatz-Marker für die Reduktion des MLL-AF9 Proteins verwendet werden, da die Transkription von *HOXA9* über eine direkte Interaktion zwischen MLL-AF9 Protein und dem *HOXA9* Promotor erhöht wird.

Eine hochsignifikante Reduktion des Zelldurchmessers um 0,3 µm wurde nach Stilllegung von MLL-AF9 beobachtet. Wir haben die Hypothese, dass dies durch eine Co-Aggregation des AF9 Proteins mit MLL-AF9 bedingt sein könnte, da die Deletion des AF9 homologs in Hefe zu einer abnorm erhöhten Zellgröße führt. Des Weiteren legten unsere Genexpressionsdaten nahe, dass die reduzierte Zellgröße durch Veränderungen der intrazellulären Ionenkonzentrationen und / oder durch reduzierte Ribosomen-Biogenese bedingt sein könnte.

Genexpressionsanalysen zeigten die differentielle Expression von 1269 Genen. Zusammen mit funktionellen Gen-Ontologieanalysen sprachen die Ergebnisse für einen differenzierteren

Zustand der Zellen nach Verminderung von MLL-AF9. Unsere Daten weisen auf Effekte von MLL-AF9 auf die Differenzierung, die Apoptose und die Immunüberwachung hin, sowie auf die Beteiligung von Kalzium- und Östrogen-Signalwegen sowie der Hitzeschock- und Protein-Missfaltungs-Antwort (heat-shock / unfolded protein response) bei der MLL-AF9 vermittelten Leukämogenese. Unter den differentiell regulierten Transkripten konnten mittels einer Bewertungs-Strategie 40 vielversprechende Kandidaten für die Vermittlung des leukämogenen Effekts von MLL-AF9 priorisiert werden. Darunter wurden acht identifiziert, die für die therapeutische Nutzung prädestiniert erscheinen, da die kodierten Proteine in Proteinklassen fallen welche häufige Angriffspunkte für Medikamente darstellen.

Das erstellte miRNA Expressionsprofil zeigte 23 differenziell exprimierte miRNAs nach *MLL-AF9* Stilllegung. Eine Untergruppe dieser miRNAs wurde für die Validierung mittels qRT-PCR ausgewählt. Dabei bestätigte sich die differenzielle Expression bei sieben der elf getesteten miRNAs. Unter diesen zeigte sich miR-511, die am stärksten differentiell exprimierte miRNA, als zusätzlich signifikant hochreguliert nach der Differenzierung von THP1 Zellen mittels phorbol 12-myristate 13-acetate (PMA). Diese Beobachtung ist stimmig mit der Hypothese, dass miR-511 eine Rolle innerhalb des Differenzierungsprozesses von Monoblasten spielen könnte. Nach *MLL-AF9* Stilllegung wurde eine inverse Korrelation der Expression zwischen miR-511 und 445 seiner *in silico* vorhergesagten Zieltranskripte beobachtet. Ein Teil davon wurde zur experimentellen Validierung ausgewählt. Nach einer Erhöhung der zellulären miR-511 Konzentration mittels sogenannter „mimics“ in THP1 Zellen zeigte sich bei acht vorhergesagten Zielgenen ein Trend zu reduzierter Expression.

Unsere Studie identifizierte Prozesse sowie neue Kandidaten-Gene und -miRNAs für die Vermittlung der leukämogenen Effekte von MLL-AF9 und erweitert damit das bisherige Wissen um *MLL*-aberrante Leukämien. Zukünftige Forschung an diesen Kandidaten sollte zur weiteren Evaluierung ihres Potentials hinsichtlich neuer therapeutischer Strategien führen.

6 Introduction

6.1 Genetic aberrations in leukemia

Acute leukemias are malignancies of the hematopoietic system. They are caused by the accumulation of genetic aberrations in progenitor cells which lead to a block in cell differentiation and to an increase in cell proliferation (Stavropoulou, et al. 2010). In childhood, acute leukemias are the most prevalent forms of cancer, with acute lymphoblastic leukemia (ALL) being the most common form, followed by the more aggressive acute myeloid leukemia (AML), while chronic myeloid leukemia (CML) and chronic lymphoblastic leukemias (CLL) are rare (Kufe, et al. 2003; Bender-Götze, et al. 2003; Deschler, et al. 2006).

For AML, accounting for 15-20% of leukemias in childhood (Deschler, et al. 2006), new targeted therapies are urgently needed due to the aggressiveness of the disease and relative low survival rates (5-year overall survival of 57%, (Creutzig, et al. 2005)).

The majority of children with AML, i.e. 50-80%, harbor leukemic cells with clonal chromosomal aberrations (Raimondi, et al. 1999; Deschler, et al. 2006). Among these are numerous translocations resulting in hybrid genes and fusion proteins (Deschler, et al. 2006). Chromosomal aberrations involving the *mixed-lineage leukemia* gene (*MLL*) at 11q23 are the most common form, being present in 20% of childhood AML cases (Hollink, et al. 2009) and in 51% of very young AML patients (below 2 years of age) (Balgobind, et al. 2011).

Originally, these *MLL* aberrations were detected in a subset of acute leukemias with especially dismal prognosis and in leukemic blasts expressing surface markers of both the myeloid and lymphoid lineage. Thus the associated gene was named *mixed-lineage leukemia* (*MLL*) (Mirro, et al. 1986). *MLL* has been found to be translocated to over 50 different partner genes, whose associated leukemias nevertheless represent an entity (Meyer, et al. 2006; Slany 2009). The most common form of *MLL* gene rearrangement in AML is the translocation t(9;11)(p22;q23), resulting in the fusion protein MLL-AF9 (Jansen, et al. 2005).

6.2 The genes *MLL*, *AF9*, *MLL-AF9* and their functions

Unraveling the molecular mechanism by which MLL fusion proteins lead to deregulated gene expression might assist the development of new, targeted therapies for this type of leukemia. The following short overview on the two participating genes and functions of their proteins shall summarize the pre-existing knowledge and illustrate the potential molecular function of the fusion protein.

Gene deletion and disruption experiments yielded information on the biological role of the corresponding proteins, e.g. in the mouse model.

Mll gene disruption experiments in the mouse are embryonically lethal for homozygous *Mll* -/- animals. *Mll* is widely and dynamically expressed in the mouse embryo, indicating its importance in embryogenesis. (Yu, et al. 1995) Its expression is required to maintain the expression of *Hox* genes in early embryogenesis (Gan, et al. 2010; Yu, et al. 1998). Here, *Hox* genes are essential for correct positioning of segmented structures (vertebrae, limbs, digestive and reproductive tracts), while they also play a definitive role in normal proliferation and differentiation of hematopoietic stem and progenitor cells (He, et al. 2011a). Heterozygous *Mll* +/- mice show retarded growth, hematopoietic abnormalities, and bidirectional homeotic transformation of the axial skeleton, as well as sternal malformations (Yu, et al. 1995). Conditional knock-out alleles leading to a *Mll* loss in the hematopoietic lineage revealed phenotypically normal fetal hematopoiesis but massive mortality at 3 weeks of age with surviving animals being anemic, thrombocytopenic, and showing a significant reduction of bone marrow hematopoietic stem / progenitor cells (Gan, et al. 2010). Consequently, *Mll* must be considered as an essential gene in embryogenesis and hematopoiesis.

Homozygous deletion of *Af9* leads to homeotic skeletal anomalies and perinatal death in mice but has no effect on hematopoiesis (Collins, et al. 2002). Nevertheless, *AF9* is highly expressed in human hematopoietic stem cells and appears to be important for erythro- and megakaryopoiesis (Pina, et al. 2008). The effects of *Af9* deletion on the axial skeleton, suggested an involvement of *Hox* gene expression. Af9 was later confirmed as a regulator of *Hox* genes, which points to an analogous role to Mll in embryogenesis (Collins, et al. 2002).

Specific features of *MLL* and *AF9* genes, transcripts and proteins are summarized in table 1 and compared to the average of human genes and transcripts. This comparison stresses the large size of the two genes and their transcripts as well as their unusual large number of encompassed exons and transcription variants.

Table 1: **Comparison of *MLL* and *AF9* genes and transcripts to the average of human genes and transcripts.**

	MLL	AF9	human transcripts (mean)
location	11q23	9p22	n.a.
strand	forward	reverse	n.a.
gene size [nts]	90 334	280 879	36 974
transcript size [nts]	11 910	6 772	1 371
number of exons	36	11	7.7
cleavage site position [amino acid]	2 666 and 2 718	none known	n.a.
polypeptide size [amino acids]	3 969	568	n.a.
protein size [kDa]	320 (MLL-N) and 180 (MLL-C)	63	n.a.
number of transcript variants	18	11	8
number of protein coding transcript variants	13	6	n.a.

Given gene information on *MLL* and *AF9* refers to the consensus coding sequences from Ensemble data base. Features are compared to the mean of human genes as described by Chacko et al. (2009). nt = nucleotides, n.a. = not analyzed

MLL, a histone 3 lysine 4 (H3K4) methylase and member of the trithorax / MLL gene family, is a large protein which is rapidly cleaved by taspase 1 (TASP1) into the subunits MLL-N (320 kDa) and MLL-C (180 kDa). These MLL subunits interact via the FY-rich domain N-terminal region (FYRN) of MLL-N and the FY-rich domain C-terminal region (FYRC) and Su(var)3-9, Enhancer-of-zeste, Trithorax (SET) domain of MLL-C. This interaction has been shown to be necessary for the stability of MLL-N and the correct nuclear sublocalization of MLL-C subunits (Hsieh, et al. 2003; Yokoyama, et al. 2002). As depicted in figure 1, the MLL-N / MLL-C dimer is the core of a large protein complex, in which MLL-N together with Menin and LEDGF confers nuclear localization pattern and target gene selection, while the MLL-C and associated proteins are responsible for activating changes in the chromatin (Slany 2009). Additionally, the CxxC zinc finger domain of MLL-N maintains the expression of specific genes (Erfurth, et al. 2008; Cierpicki, et al. 2010). The MLL complex is believed to be recruited by transcription factors to initiate RNA synthesis. H3K4 methylation is universally introduced around transcription start sites of all transcribed genes, and it has been estimated that each H3K4 methyltransferase is responsible for methylation of more than 1000 gene loci. (Slany 2009) In leukemogenic fusions, breakpoints of MLL cluster in a 8.3 kb region of chromosome 11

containing *MLL* exons 8 to 14. They result in MLL fusion proteins which retain about 1300 N-terminal amino acids of MLL and include the DNA binding AT-hooks and the CxxC domain which protects target gene CpG dinucleotides from methylation (Langer, et al. 2003; Hsieh, et al. 2003).

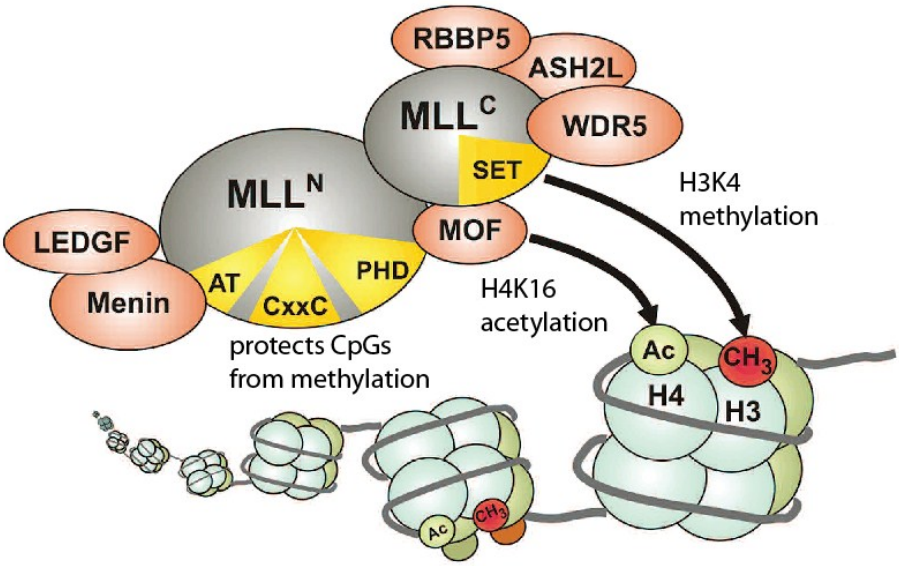

Figure 1: **The MLL complex and its molecular functions.** MLL-N together with Menin and lens epithelium-derived growth factor (LEDGF) confers subnuclear localization and target gene selection, while the MLL-C and associated proteins (histone acetyltransferase MYST1 (MOF), retinoblastoma-binding protein 5 (RBBP5), ASH2-like (ASH2L) and WD-repeat containing protein 5 (WDR5)) are responsible for activating changes in the chromatin (histone 4 lysine 16 (H4K16) acetylation and H3K4 trimethylation). CxxC zinc finger domain (CxxC) of MLL-N has been shown to bind unmethylated CpG dinucleotides and to protect them from methylation. The plant (PHD) homeodomain is involved in protein-protein interactions, thus regulating the recruitment of repressive factors.(Slany 2009) AT, AT-hook (binding to the minor groove of DNA); H4K16, lysine 16 of histone 4; H3K4, lysine 4 of histone 3; Ac, acetyl group; CH3, methyl group. Figure modified from Slany, 2009.

About 200 C-terminal amino acids of AF9 are retained in fusions to MLL and harbor a protein interaction domain. In contrast, the chromatin-targeting N-terminal YEATS domain (named after `YNK7', `ENL', `AF-9', and `TFIIF small subunit') is lost in MLL fusions. (He, et al. 2011b) Like other frequent fusion partners of MLL, AF9 is a component of the super elongation complex (SEC) and the Dot1 complex (DotCom) and interacts with the protein complex components via its C-terminal protein interaction domain which is retained in MLL fusions. SEC clears paused RNA polymerase II (Pol II) for elongation, while DotCom leads to raised histone 3 lysine 79 (H3K79) methylation and thus both complexes lead to transcriptional activation. These findings led to a model, where MLL fusion proteins activate gene expression by binding to (MLL) target genes and – unlike MLL – automatically recruiting SEC or DotCom, leading to

transcriptional activation and elongation independent of other, otherwise necessary, additional factors (figure 2). (Slany 2009; Mohan, et al. 2010; Margaritis, et al. 2008) Because many MLL fusion partners are proteins of the SEC or DotCom complexes (besides AF9, i.e. AF4, AFF4, ENL, ELL, AF10 and AF17), this model offers an explanation, why different MLL fusion proteins may lead to similar changes in gene expression and to leukemogenesis.

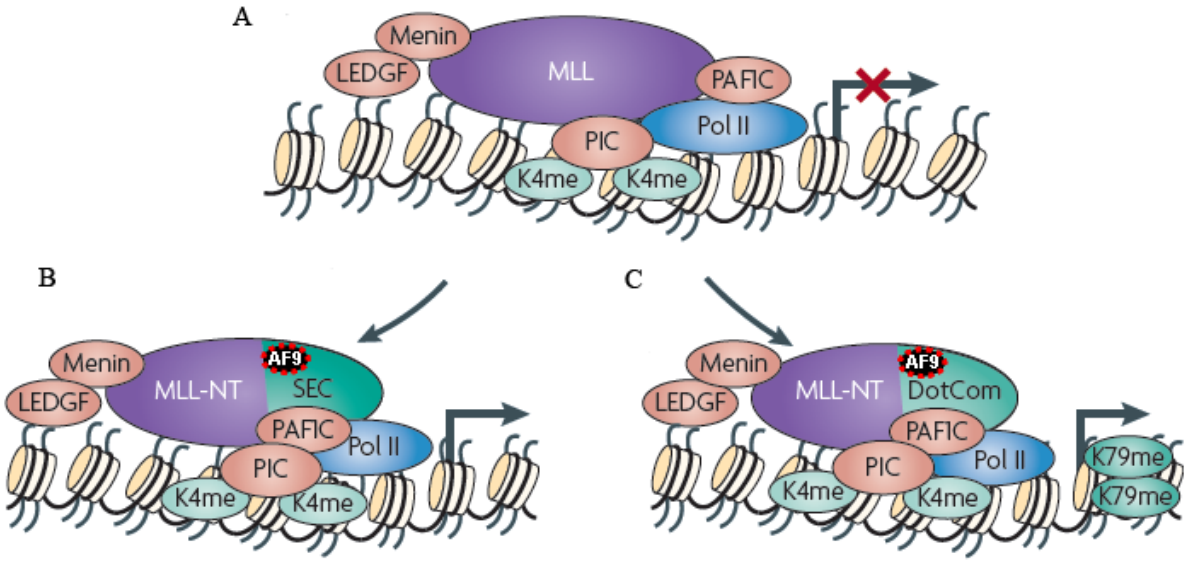

Figure 2: **Model of MLL complexes and their functions (A)** MLL complex needs additional factors for transcriptional activation. **(B)** Complex generated by fusions of MLL with proteins of the super elongation complex (SEC) (e.g. AF9), is believed to automatically recruit SEC complex, leading to transcriptional activation. **(C)** Complex generated by fusions of MLL with proteins of DotCom (e.g. AF9), is believed to directly activate transcription via histone 3 lysine 79 methylation. MLL-NT, N-terminal part of MLL; LEDGF, lens epithelium-derived growth factor; SEC, super elongation complex; DotCom, Dot1 complex; Pol II, polymerase II; K4me, methylated lysine 4 of histone 3; K79me, methylated lysine 79 of histone 3. RNA polymerase-associated factor 1 complex (PAF1C) is a transcriptional elongation factor, the preinitiation complex (PIC) is necessary for transcription. Figure modified from Mohan et al., 2010.

MLL fusions have been assigned to two functional categories dependent on the subcellular localization of their native fusion partner proteins. Fusions with partner proteins with nuclear localization (e.g. AF4, AF9, ENL, AF10 and ELL) by far represent the larger group of leukemic MLL-fusions, while the only common cytoplasmic fusion partner is ALL1-fused gene from chromosome 6 (AF6). It has been noticed that the less frequent MLL translocations to cytoplasmic partners occur mainly in adult patients, indicating weaker transforming activities. (Ayton, et al. 2001; Slany 2009)

Altogether, MLL and AF9 proteins play essential roles in embryogenesis and hematopoiesis and lead to transcriptional initiation (MLL) and elongation (AF9) of their target gene transcripts. The fusion protein MLL-AF9 is believed to combine these properties, leading to increased activation

via transcriptional initiation and elongation of target gene transcripts. Resulting from this knowledge, new therapeutic strategies are under investigation which aim to intervene with DNA binding of MLLs CxxC domain or with the assembly of MLL fusion proteins with elongation complexes. However, a main concern with these approaches is that the physiological functions of the involved proteins will also be abrogated, thereby leading to toxicity. (Slany 2009) Other potential therapeutic targets lie downstream of MLL fusion proteins. In this context, detailed information on gene expression influenced by specific MLL-fusion proteins, as aimed in this study, is still lacking.

6.3 The role of *MLL-AF9* fusion gene in leukemia

MLL-AF9 is either by itself sufficient to initiate acute leukemia or essential secondary mutations are rapidly acquired: *Mll-AF9* chimeric mice (generated by knock-in of partial human *AF9* sequence into the *Mll* genomic region of the mouse) showed non-malignant expansion of myeloid precursor cells and subsequently developed acute myeloid leukemia (Corral, et al. 1996; Dobson, et al. 1999). Mice transplanted with bone marrow stem / progenitor cells which were retrovirally transduced to carry a *MLL-AF9* cDNA sequence, develop AML and harbor leukemia stem cells (LSC). These LSC confer leukemia - even when only very few are transplanted into mice (Krivtsov, et al. 2006; Somervaille, et al. 2006). Krivtsov et al. (2006) additionally showed that the self-renewal associated mRNA expression signature of leukemic stem cells resembles the profile of *MLL*-rearranged AML patients.

A important source of information to understand the transforming effects of a fusion gene are expression studies. Classic gene expression studies do not include small RNA species, so that in we employ the term “gene expression” for analyses of coding and non-coding transcripts exclusive of small RNA species. Transcript levels of miRNAs are denoted as miRNA expression.

There is some prior knowledge on gene expression correlated to MLL-fusion proteins. However, these data are derived either from patient studies or from introduction of the cDNA sequence in cell lines or primary cells. Retroviral transductions of cDNA sequences may lead to supraphysiologic expression of the fusion protein with absence of natural occurring isoforms. Patient studies have to struggle with diverse genetic backgrounds and cell types of samples. Such problems can mask many downstream effects. Therefore, knockdown of endogenous *MLL*-fusion proteins in leukemia cell lines may present an alternative tool. According to genomic DNA gains and losses as well as gene expression patterns, the monoblastic AML cell line THP1 has been described to be a faithful model system for leukemia with genomic aberrations (Rucker, et al. 2006). The most common *MLL* translocation in AML (*MLL-AF9*) is strongly associated

infant AML and with the AML subclass M5 of the French-American-British (FAB) classification systems that describes monoblastic and monocytic phenotypes (Chowdhury, et al. 2003; Jansen, et al. 2005). Among seven described cell lines carrying the *MLL-AF9* translocation, THP1 is the only one established from an infant AML M5 leukemia patient (Drexler, et al. 2004; Tsuchiya, et al. 1980) and thus may be regarded as a representative model. In previous studies employing RNAi, the effect of *MLL-AF9* knockdown on the expression of a few selected genes was investigated in this cell line (Kawagoe, et al. 2001; Pession, et al. 2003). So far, however, no comprehensive data is available on differential transcription after specific knockdown of endogenous *MLL*-fusion genes.

6.4 MicroRNAs and their role in hematologic malignancies

MicroRNAs are small (~ 22 nt long), abundant and highly conserved endogenous RNAs which regulate gene expression by translational inhibition and mRNA destabilization (Bartel 2004). MicroRNAs (miRNAs) are either transcribed from independent miRNA genes encompassing a single or a cluster of miRNAs or are located in introns or even exons of (protein coding) genes. Their biogenesis and mode of action is depicted in figure 3. At present, 1424 miRNAs are known in humans and their number is still rising.

Evidence from transcription and protein studies has led to the notion that mRNA targets of miRNAs are plentiful in number, ranging between dozens and hundreds of mRNAs per miRNA (Lim, et al. 2005; Hammond 2006; Baek, et al. 2008). Embryonic lethality has been observed in mammals for the knock-out of miRNA pathway components (*Dicer*, *DGCR8* and *Ago2*), highlighting the significance of this gene regulatory mechanism (Babiarz, et al. 2009).

After two decades of research since their discovery, the regulatory role and importance of miRNAs in normal development and cellular homeostasis, as well as in human pathogenesis and basic cellular functions including proliferation, differentiation and apoptosis, is widely accepted (Hwang, et al. 2006; Hammond 2006).

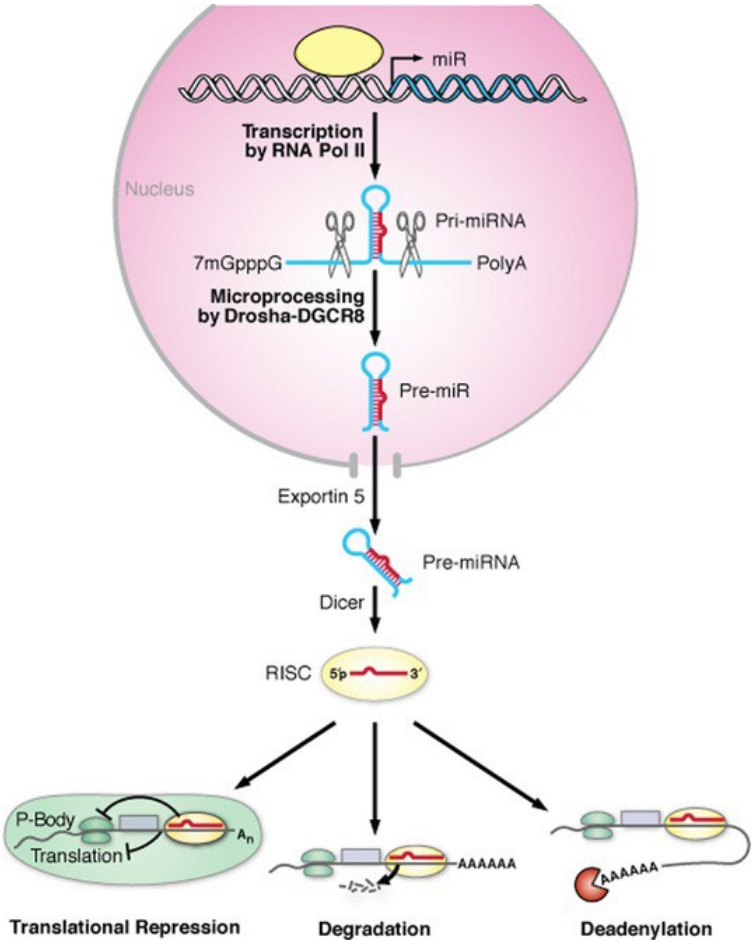

Figure 3: **MicroRNA biogenesis and mode of action**. A primary transcript, the pri-miRNA, is transcribed by polymerase II and processed into the precursor miRNA (pre-miRNA, a 60 to 70 nt long stem loop intermediate) by drosha (a RNase III endonuclease) and the cofactor DiGeorge syndrome critical region gene 8 (DGCR8). The pre-miRNA is actively transported from the nucleus to the cytoplasm by exportin-5 and further processed by dicer (also a RNase III endonuclease) into the mature, about 22 nt long, miRNA double strands bearing two-nucleotide 3'-overhangs. It is presumed that drosha, not dicer, imparts the specificity of the whole cleavage process. One strand of the mature miRNAs gets preferentially incorporated into the RNA induced silencing complex (RISC), a process which is regulated depending on the miRNA double strand sequence and is guided by other proteins (Hutvagner 2005). The incorporated, active miRNA strand identifies target molecules via sequence complementarity, allowing mismatches and loops and thus leading to the regulation of numerous different targets. The binding of RISC to a target leads to mRNA cleavage, translational inhibition and mRNA deadenylation and might even lead to transcriptional inhibition on DNA level. (Bartel 2004; Landthaler, et al. 2004; Standart, et al. 2007) Figure from Cordes et al., 2010.

An important role for miRNAs in tumorigenesis has been shown (Calin, et al. 2002; Calin, et al. 2004; Cimmino, et al. 2005) and abnormal miRNA expression is a common feature of human malignancies. MicroRNAs are extensively involved in cancer pathogenesis of solid tumors by controlling the expression of protein-coding tumor suppressors and oncogenes. (Hwang, et al. 2006; Kasinski, et al. 2011) Lu et al. (2005) showed that miRNA profiles classify tissue origin, differentiation state, cancer versus non-cancer state and even leukemia subtypes. In this context,

a profile of 217 miRNAs proofed more informative than a profile of 16000 mRNAs, highlighting the highly valuable information content of miRNA profiles (Lu, et al. 2005).

Recently, in a number of patient studies, miRNAs have been found to be differentially expressed among distinct cytogenetic groups of AML. However, the specific signatures differ among studies, a phenomenon which has been ascribed to the lack of standardization of the analytic methods used by different groups. Concerning *MLL*-aberrant AML patient samples, the fact that different subtypes, e.g. *MLL* translocations with a cytoplasmic and a nuclear translocation partner, are grouped together may cause additional problems in obtaining specific information on the miRNAs involved. (Marcucci, et al. 2011)

Guenther et al. (2005) could show that the SET domain of wild-type MLL binds to a vast number of miRNA loci. This was the first published direct link between MLL and miRNAs. Recently, miRNAs were shown to be downregulated in *MLL-AF4* infant ALL as a consequence of CpG hypermethylation (Stumpel, et al. 2011).

Nakamura et al. (2007) found miRNAs differentially expressed in cell lines harboring *MLL* translocations compared to pro-B cell lines without these aberrations. Popovic et al. (2009) reported that miR-196b is upregulated by MLL as well as MLL fusion proteins in mouse bone marrow progenitors and appeared to contribute to immortalization and block of differentiation. Mi et al. (2010) showed that the miR-17-92 cluster, which has been previously associated with solid tumors, is highly expressed in *MLL*-aberrant leukemia and enhances proliferation and colony-forming capacity of mouse bone marrow progenitor cells.

Taken together, these reports suggest that miRNAs play an important role in *MLL*-aberrant leukemogenesis. However - as argued for gene expression analyses (4.3) - studies with patient samples and techniques leading to overexpression of *MLL* fusions have limitations.

The necessity for further studies on the effects of specific *MLL*-rearrangements on miRNA expression – as aimed in our study - has already been acknowledged (Marcucci, et al. 2011). This is especially important, as miRNAs are anticipated to proof useful for targeted cancer therapies. *In vivo* proof-of-principle for application of miRNA-based cancer therapies has already been obtained in a number of animal studies. (Kasinski, et al. 2011)

6.5 Aim of this study

The general aim of our study was to identify new potential therapeutic targets for *MLL*-aberrant acute myeloid leukemia. Specifically, we decided to focus our work on the relatively common *MLL-AF9* translocation in view of the still poor prognosis of the associated AML.

In our experimental approach we aimed to define the downstream effects of MLL-AF9 both on the cellular phenotype and on functional endpoints as well as on gene and miRNA expression.

As a prerequisite the technical goals to be achieved were:

- » selecting an appropriate cell line as model
- » designing and evaluating specific and efficient siRNAs that target the breakpoint of *MLL-AF9* while not disturbing wildtype *MLL* or *AF9* expression
- » confirming efficient knockdown of *MLL-AF9*
- » setting up an experimental design that achieves a prolonged knockdown of *MLL-AF9*
- » constraining the masking of MLL-AF9 specific effects by the strong mitogenic influence of fetal bovine serum (FBS) within the culture

In the biological context we aimed at evaluating the differential expression data concerning the functional processes involved in *MLL-AF9* translocation and in respect to their potential relevance in the mediation of MLL-AF9 leukemogenic effects. Finally distinct candidate genes and miRNAs with potential as new therapeutic targets should be sorted out.

For this specific purpose we planned to devise a strategy for rating and prioritization of candidate targets that includes

- » gene ontology analyses to identify the functional processes involved
- » disease ontology analyses to identify genes linked to leukemic disease conditions
- » comparisons of our *in vitro* data to published *in vivo* expression data

7 Material and Methods

7.1 Cell and molecular biological methods

7.1.1 Cell culture

THP1 cells were purchased from DSMZ (Deutsche Sammlung von Mikroorganismen und Zellkulturen GmbH, Braunschweig, Germany) and aliquots were frozen in liquid nitrogen after 5 passages. Cells were maintained in RPMI 1640 with 10% heat inactivated fetal calf serum, 100 Units Penicillin per ml and 0.1 mg/ml Streptomycin (all PAA Laboratories, Pasching, Austria) at a density of 0.05-0.5×10^6 cells/ml in a humidified 37°C / 5% CO_2 incubator. Experiments were started one day after splitting cells, in the exponential growth phase. Every two to three months, fresh aliquots of the cells were thawed for experiments. MCF-7 and HELA cell lines were obtained from DSMZ and cultured in RPMI 1640 supplemented as for THP1.

For serum reduced conditions, cells were gently washed in Dulbecco's PBS and resuspended in DMEM / Ham's F12 medium containing 1 g/L BSA (all PAA Laboratories, Pasching, Austria) and 0.5 % Fetal Bovine Serum (#10270, Lot 41G3681K, Gibco, Life Technologies, Carlsbad, CA, USA). These culture conditions result in THP1 cells proliferating over at least 6 days, while showing a clearly reduced proliferation level (doubling time was reduced from 1.08 days to 1.34 days over four days in 0.5% FBS).

For induction of monocyte-macrophage differentiation of THP1 cells, 20 nM phorbol 12-myristate 13-acetate (Sigma-Aldrich, St. Louis, MO, USA) was added to the culture for 48 hours and effect on morphology was confirmed via microscopy.

7.1.2 SiRNAs and miRNA mimics

For establishing *MLL-AF9* specific knockdown, six siRNAs were designed according to scores from *sfold Sirna* (Ding, et al. 2001), *DISR* (Vert, et al. 2006) and *siDESIGN Center* (Thermo Scientific, Waltham, MA, USA) against *MLL-AF9* breakpoint in THP1 cell line. Table 2 gives sense and antisense sequences of *MLL-AF9* specific siRNAs. SiRNAs were dissolved in 1 x siRNA buffer (Dharmacon, Lafayette, CO, USA). SiR_1 and siR_2 were unmodified (MWG Biotech, Ebersberg, Germany), while siR_5 was ON-TARGET*plus*™ modified (Dharmacon, Lafayette, CO, USA) and siR_3, siR_4 and siR_6 were Silencer Select® modified (Ambion, Life Technologies, Carlsbad, CA, USA). Silencer Select® and ON-TARGET*plus*™ are proprietary chemical modifications of the companies and not precisely specified.

Table 2: **THP1-breakpoint specific siRNA sequences against *MLL-AF9*.**

siRNA name	sense strand (5'-3')	antisense strand (5'-3')
siR_1	AAG**UCUGAACAACCCAGUC**-dTdT	**GACUGGGUUGUUCAGA**CUU-dTdT
siR_2	AAAGAAAAG**UCUGAACAACCC**-dTdT	**GGGUUGUUCAGA**CUUUUCUUUU-dTdT
siR_3	AAGAAAAG**UCUGAACAACC**-dTdT	**GGUUGUUCAGA**CUUUUCUU-dTdT
siR_4	CAAAAGAAAAG**UCUGAACA**-dTdT	**UGUUCAGA**CUUUUCUUUUG-dTdT
siR_5	ACCAAAAGAAAAG**UCUGAA**-dTdT	**UUCAGA**CUUUUCUUUUGGU-dTdT
siR_6	GAAAAG**UCUGAACAACCCA**-dTdT	**UGGGUUGUUCAGA**CUUUUC-dTdT

Sequences of siRNAs that were designed and tested in this study are given. Sequences in bold correspond to *AF9* part of *MLL-AF9*. dT = deoxythymidine

For analysis of transfection efficiency, AF488 labeled AllStars Negative siRNA (Qiagen, Hilden, Germany) was employed. As negative controls, Silencer Select negative control #1 and #2 siRNAs (Ambion, Life Technologies, Carlsbad, CA, USA) were used (proprietary sequences of Ambion).

MiR-511 and negative control #1 mimics (Pre-miR™ miRNA Precursor Molecules, Ambion, Life Technologies, Carlsbad, CA, USA) were employed for miRNA upregulation studies in THP1 cells. These small, chemically modified double-stranded RNA molecules are designed to mimic endogenous mature miRNAs and do not need to be further processed by the cell.

7.1.3 Transfections of siRNAs, miRNA-mimics and shRNA plasmids

Six chemical transfection methods (Dreamfect (OZ Biosciences, Marseille cedex, France), Dmrie-C (Invitrogen, Carlsbad, CA, USA), HiPerFect (Qiagen, Hilden, Germany), FuGene HD (Roche, Basel, Switzerland), Lipofectamine LTX and Lipofectamine 2000 (both Invitrogen, Carlsbad, CA, USA)) were tested in THP1 cells. Transfections were performed according to suppliers' protocols. Electroporation was carried out using an EPI 2500 device (Laborgeräte Fischer, Heidelberg, Germany) with 200 V for 10 msec. Finally, transfections of siRNAs in THP1 cell line were performed with 8.9 µl Dreamfect™ (OZ Biosciences, Marseille cedex, France) and a final concentration of 50 nM siRNA added to 1 ml cell culture medium containing 5×10^4 cells in a 12-well format (Greiner, Kremsmuenster, Germany) according to supplier's protocol. To ensure a *MLL-AF9* knockdown which efficiently reaches the protein level and leads to changes in the expression of MLL-AF9 target genes, experiments were performed over eight (or, as indicated, over twelve) days with repeated siRNA transfections on day 0, 3, 6 (and 10). Before each transfection event, cell densities were determined by Cellscreen microscopy and cells were reseeded at 5×10^4 cells per ml in 12- well formats.

Transfections for miRNA upregulation studies were performed with 8.9 µl Dreamfect™ (OZ Biosciences, Marseille cedex, France) and a final concentration of 30 nM miRNA mimics added to 1 ml cell culture medium containing 5×10^4 cells in a 12-well format (Greiner, Kremsmuenster,

Germany) according to supplier's protocol. Serum reduced conditions (see section 7.1.1) were employed to maintain similar conditions as in which *MLL-AF9* knockdown specific miR-511 overexpression was observed. The resulting upregulation of miR-511 resembled approximately the expression strength of the strongest expressed endogenous miRNA in this cell line.

For stable transfection of THP1, two shRNA plasmids against *MLL-AF9* and one containing a control shRNA were constructed (table 3) by utilizing pSIF1-H1-Puro shRNA vector (System Biosciences, Mountain View, CA, USA). ShRNAs were under the polymerase III RNA promoter H1 as described in the supplier's protocol. Puromycin resistant marker was replaced by a cassette of cGFP under CMV promoter, and a truncated version of the surface marker LNGFR under EF1 promoter (Magg, et al. 2009). THP1 cells were transfected with a Nucleofector® II Device and Human Monocyte Nucleofector® Kit (both Lonza, Basel, Switzerland) and nucleofector program Y-001. LNGFR served for positive selection of transfected THP1 cells with immunomagnetic CD271 (LNGFR) microbeads and MS columns (both Miltenyi Biotec, Bergisch Gladbach, Germany).

Table 3: **Overview of THP1-breakpoint specific shRNA sequences.**

shRNA name	strand	sequence (5'-3')
shRNA #4	sense	GATCC**CAAAAGAAAAGTCTGAACA**CTTCCTGTCAGATGTTCAGACTTTTCTTTTGTTTTTG
shRNA #4	antisense	AATTCAAAAA**CAAAAGAAAAGTCTGAACA**TCTGACAGGAAGTGTTCAGACTTTTCTTTTGG
shRNA #6	sense	GATCC**GAAAAGTCTGAACAACCCA**CTTCCTGTCAGATGGGTTGTTCAGACTTTTCTTTTTG
shRNA #6	antisense	AATTCAAAAA**GAAAAGTCTGAACAACCCA**TCTGACAGGAAGTGGGTTGTTCAGACTTTTCG
non-targeting shRNA	sense	GATCC**TGGTTTACATGTCGACTAA**CTTCCTGTCAGATTAGTCGACATGTAAACCATTTTTG
non-targeting shRNA	antisense	AATTCAAAAA**TGGTTTACATGTCGACTAA**TCTGACAGGAAGTTAGTCGACATGTAAACCAG

ShRNA sequences as employed for generation of shRNA plasmids for stable transfection of THP1 cells. Sequences designed for being processed into siRNAs are depicted in bold.

7.1.4 Confocal fluorescence microscopy

For detecting the localization of siRNA within the cells, confocal fluorescence microscopy was employed. Here, 1×10^5 AF488 siRNA transfected THP1 cells were stained with 4,6-diamidino-2-phenylindole (DAPI, Sigma-Aldrich, St. Louis, MO, USA). Cells were centrifuged onto object slides at 200×g for 3 minutes, mounted in Aqua-Poly/Mount (Polysciences, Eppelheim, Germany) and analyzed via an Olympus IX81 confocal microscope using the UPLanSApo 60x/1.35 oil objective (Olympus, Hamburg, Germany).

7.1.5 Cell diameter and proliferation

Proliferation and cell diameter were measured via Cellscreen System (Innovatis, Bielefeld, Germany) on an Olympus IX 50 microscope. This system is a non-invasive, automated analysis system that captures and evaluates microscopic images of cell cultures. It allows to repeatedly measure a multi-well plate by taking images of pre-adjusted regions of interest (ROIs) and analyzes cell number and cell diameter through digital image recognition (examples of images are shown in figure 4).

Cellscreen Microscopy was performed in 12 well formats (Greiner, Kremsmuenster, Germany) with 62 ROIs equivalent to 8% of the surface area of each well. Cells were allowed to settle to the bottom of the well on the Cellscreen microscope for 20 minutes prior to measurement to ensure that all cells were within the focus of the microscope. Measurement times were kept below 45 minutes to reduce room temperature (RT) and CO_2 concentration effects. To test if cell size was significantly altered between *MLL-AF9* knockdown and control treatments, a Welch's *t* test was performed over five replicate experiments after confirmation of normal distribution via Shapiro-Wilk normality test. For analyses, all knockdown treatments (siR_3 and siR_4) were compared to all non-targeting control treatments (n-tg_1 and n-tg_2).

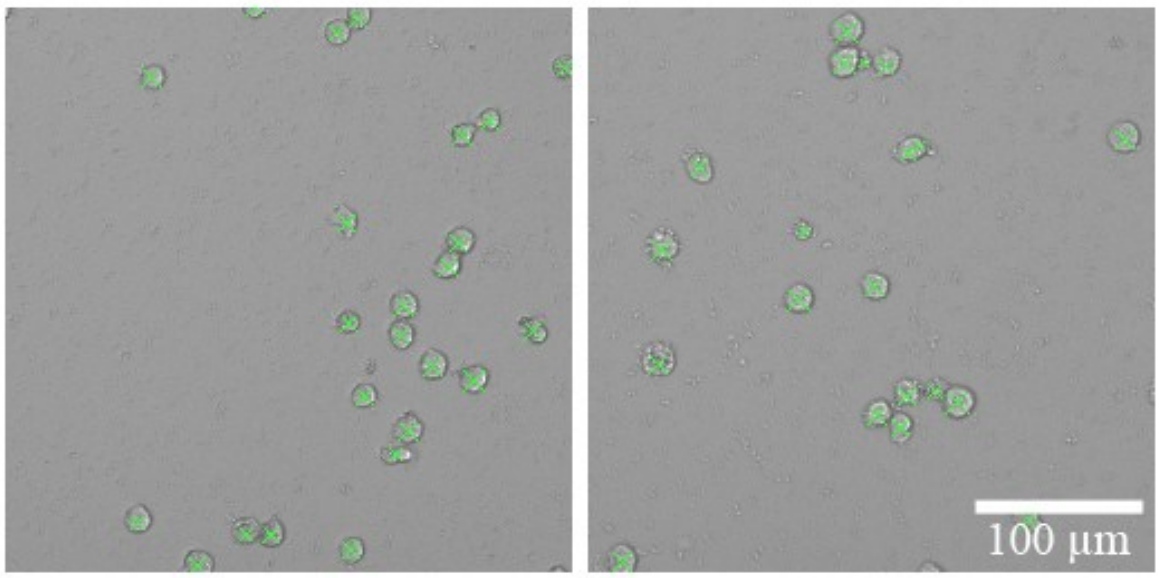

Figure 4: **Example of Cellscreen image evaluation.** Depicted are enlarged sections (each corresponding to ¼) of two regions of interest (ROIs) from *MLL-AF9* knockdown (left) and control treatments (right). Cell number and size is evaluated via an automated analysis system, which generates green marks (crosses) on the cells within the images.

Cell Proliferation Kit I (MTT) (Roche, Basel, Switzerland) was employed according to supplier's protocol to measure metabolic activity of viable cells from which proliferation may be deduced. Briefly, after gentle mixing, 100 µl of transfected cell suspension was taken from 6

transfection replicate wells per treatment, incubated with 10 µl MTT reagent for 4.5 hours and solved over night with 100 µl solubilization solution. Spectrophotometric read out was performed on a GENios (TECAN, Maennedorf, Switzerland) microplate reader.

7.1.6 Flow cytometric measurements

Flow cytometric measurements were performed on a BD FACSCanto™ (BD Biosciences, Franklin Lakes, NJ, USA) with FACS Diva Software v 5.0.3.
Flow cytometric analyses and figures were created with Cyflogic v.1.2.1 (CyFlo Ltd., Turku, Finland).

7.1.6.1 Transfection efficiency

Transfection efficiency was measured by flow cytometry (FCM) after transfection with AF488-labeled AllStars Negative siRNA (Qiagen, Hilden, Germany). Washing with 1 mg/ml dextran sulphate in PBS ensured that no siRNA was attached to the surface of the cells (Zelphati, et al. 1996). Cell viability was measured by 7-AAD exclusion staining via FCM and by trypan blue exclusion staining in hemocytometer counts.

7.1.6.2 Monitoring of stable transfected cells

Surface LNGFR was stained with phycoerythrin (PE)–anti-LNGFR antibody (Miltenyi Biotec, Bergisch Gladbach, Germany) and together with GFP served to monitor percentage of stable transfected cells within the culture by flow cytometry.

7.1.6.3 Cell cycle analysis

Cells were fixed in 70% ethanol at -20°C for a minimum of 2 hours and washed in PBS prior to staining for 30 minutes in PI/Triton X-100 buffer (0.1% Triton X-100 (Sigma-Aldrich, St. Louis, MO, USA), 0.2 mg/ml RNase A (Qiagen, Hilden, Germany), 20 µg/ml propidium iodide (Sigma-Aldrich, St. Louis, MO, USA) in Dulbecco's PBS (PAA Laboratories, Pasching, Austria)). For analysis of flow cytometry data, cell doublets and aggregates were removed and gates were set to quantify the amount of cells within the three cell cycle phases G0/G1, S and G2; apoptotic cells lie within the sub-G0 area (figure 5).

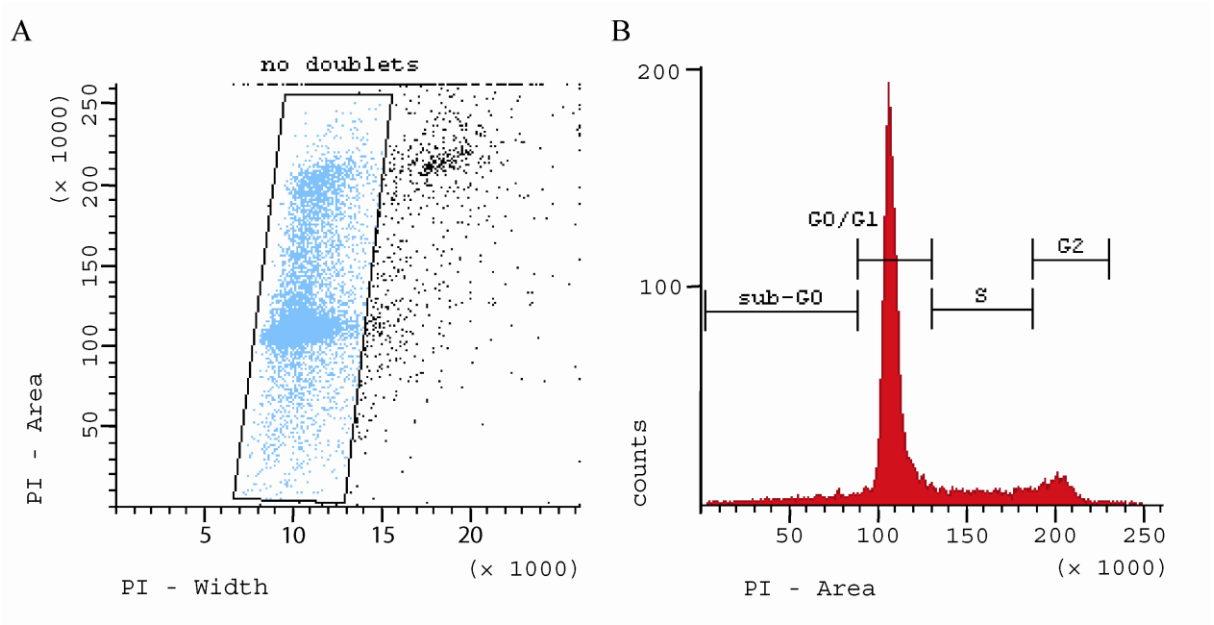

Figure 5: **Cell cycle Analysis of THP1 cells by flow cytometry. (A)** Cell doublets and aggregates were removed from analysis by "no doublets" gate within dot blots of propidium iodide (PI) width to area. **(B)** Area of propidium iodid signal was displayed and gates were set to quantify the amount of cells within the three cell cycle phases G0/G1, S and G2. Apoptotic cells lie within the sub-G0 area.

7.1.6.4 Apoptosis detection

For analysis of apoptosis, an intracellular staining of cleaved PARP1 was performed (Kaufmann, et al. 1993). Cells were fixed with 70% ethanol at -20°C for a minimum of 2 hours. Cells were washed in PBS (PAA Laboratories, Pasching, Austria) prior to permeabilization and staining with Foxp3 Staining Buffer Set (eBioScience, San Diego, CA, USA) and FITC conjugated rabbit polyclonal anti-PARP cleavage site (214/215) specific antibody (Invitrogen, Carlsbad, CA, USA) according to supplier's protocol. Briefly, cells were incubated for 30 minutes in fixation/permeabilization buffer, washed once and further incubated for 30 minutes in permeabilization buffer and stained in 100 µl permeabilization buffer with 5 µl of fluorescently labeled antibody.

We used a second technique for analysis of apoptosis: staining of cells with Annexin V-PE Apoptosis Detection Kit I (BD Biosciences, Franklin Lakes, NJ, USA) with 7-AAD and Annexin V-PE according to supplier's protocol.

7.1.7 RNA extraction and determination of RNA concentration, purity and integrity

Total RNA was extracted with miRNeasy Mini Kit (Qiagen, Hilden, Germany) according to supplier's protocol. Samples were lysed in Qiazol and stored at -80°C until extraction. Extracted RNA samples were stored at -80°C.

RNA concentration and purity (absorption 260 nm / 280 nm) was analyzed using a Nanodrop ND-1000 Spectrophotometer (Nanodrop Technologies, Wilmington, DE, USA). RNA integrity was determined by capillary electrophoresis with RNA 6000 Nano LabChip Kit on a 2100 Bioanalyzer (both Agilent Technologies, Santa Clara, CA, USA). Here, a RNA integrity number (RIN) is determined from characteristics of the electropherogram, where a high RIN (maximum is 10) stands for intact, non-degraded RNA (Schroeder, et al. 2006). RNA samples with a RIN above 7.0 or 8.0 have been described to yield reliable miRNA and gene transcript qRT-PCR results (Mishra, et al. 2009; Fleige, et al. 2006). For all profiling samples A260/A280 was above 2.0 and RIN was above 9.3.

7.1.8 Reverse transcriptase quantitative real-time PCR

Genomic DNA elimination reaction and reverse transcription was carried out with 300 – 600 ng total RNA and QuantiTect Reverse Transcription Kit (Qiagen, Hilden, Germany) according to supplier's protocol.

Quantitative real-time PCR was performed in triplicates with iQ^{TM}-SYBR® Green Supermix (Biorad, Hercules, CA, USA) with 0.6 µl template cDNA, 0.3 µM forward and reverse primer (MWG Biotech, Ebersberg, Germany) in a total volume of 15 µl on a StepOnePlus^{TM} instrument (Applied Biosystems, Life Technologies, Carlsbad, CA, USA). Run method was: 95°C for 3 min, 40 cycles of 95°C for 15 sec, 56°C for 15 sec and 72°C for 1 min, followed by 72°C for 2 min. A subsequent melt curve was performed: 95°C for 1 min and 0.5°C steps from 55 to 95.5°C for 30 sec each.

Real time primer pairs were designed with Clone Manager Suite (version 7.11) software. Primer sites were separated by at least one intron if possible (except for transcripts with only one exon and the primer MDM2-001, designed to quantify only transcript variant 1). Primer sequences are given in supplementary table 1 on page 137. To ensure that no DNA contamination was present, melting curves were analyzed on all runs and primer pairs with small separating introns were employed. After testing for stable intra- and interexperimental expression, *UBC* and *RPL13A* were used as reference transcripts for normalization. Among ten tested transcripts, these control genes have previously been described as most stable expressed in bone marrow (Vandesompele,

et al. 2002). An approximately 100 % efficiency of qRT-PCR was confirmed via cDNA dilution series for *MLL-AF9*, *MLL*, *AF9*, *RPL13A* and *UBC*.

7.1.9 Gene expression profiling

Human Whole Genome Microarrays 4x44K v2 (arrayID 026652, Agilent Technologies, Santa Clara, CA, USA) were commissioned to and performed at IMGM Laboratories (Martinsried, Germany) with 100 ng total RNA input per sample.

Low Input Quick Amp Labeling Kit (Agilent Technologies, Santa Clara, CA, USA) was used to generate fluorescent complimentary RNA (cRNA) with a sample input of 100 ng total RNA. T7 RNA polymerase was used, which simultaneously amplifies target material and incorporates cyanine 3-labeled CTP. Nanodrop ND-1000 spectrophotometer (Nanodrop Technologies, Wilmington, DE, USA) was used to record cRNA concentration (ng/µl), RNA absorbance ratio (260nm/280nm) and Cyanine-3 dye concentration (pmol/µl) for all cRNA samples. cRNA yield and specific activity of dye incorporated in cRNA was calculated and fulfilled the requirements (yield of cRNA above 1.65 µg and specific activity above 9.0 pmol Cyanine-3 per µg cRNA). The RNA 6000 Nano LabChip Kit was used on the 2100 Bioanalyzer (both Agilent Technologies, Santa Clara, CA, USA) to analyze the quality of labeled non-fragmented cRNA. Following cRNA clean-up and quantitation (NanoDrop ND-1000, Nanodrop Technologies, Wilmington, DE, USA), 1.65 µg of each Cyanine-3-labeled cRNA sample was fragmented and prepared for One-Color based hybridization (Gene Expression Hybridization Kit, Agilent Technologies, Santa Clara, CA, USA). cRNA samples were hybridized at 65 °C for 17 hours on separate Whole Human Genome Microarrays (4x44K format). Afterwards microarrays were washed with increasing stringency using Gene Expression Wash Buffers (Agilent Technologies, Santa Clara, CA, USA) followed by drying with acetonitrile (Sigma-Aldrich, St. Louis, MO, USA). Fluorescent signal intensities (FI) were detected with Scan Control 8.4.1 Software on the Agilent DNA Microarray Scanner and extracted from the images using Feature Extraction 10.5.1.1 Software (both Agilent Technologies, Santa Clara, CA, USA). Analysis of the Agilent One-Color RNA Spike-In Plot was used to ensure equal and good performance of each single labeling and hybridization experiment.

7.1.10 MicroRNA profiling and confirmatory techniques

7.1.10.1 Quantitative microRNA detection via TaqMan miRNA Low Density Array and single assay qRT-PCR

Quantitative miRNA profiles were generated with TaqMan® Array Human MicroRNA Cards (Applied Biosystems, Life Technologies, Carlsbad, CA, USA), also known as TaqMan® Low Density Arrays (LDAs). These arrays cover 664 distinct miRNA assays which are spread over two low density array cards, the so-called plates A and B. MiRNA profiles were generated with preamplification according to supplier's protocol. An input of 350 ng total RNA per array card and sample pool was used. LDA runs were performed on an ABI PRISM® 7900HT machine and SDS 2.3 software (Applied Biosystems, Life Technologies, Carlsbad, CA, USA).

Quantitative real time PCR of single miRNAs was performed with TaqMan® miRNA assays (Applied Biosystems, Life Technologies, Carlsbad, CA, USA) according to the manufacturers' instructions. *RNU6B*, *RNU44* and *RNU48* assays were tested as internal references. *RNU48* showed the least intra- and interexperimental variance and thus was used as internal reference. Single assay miRNA measurements from experimental pools were performed after megaplex reverse transcription and preamplification according to supplier's protocol. Single assay miRNA measurements from individual experiments were performed with Taq Man® miRNA assays after 2-plex reverse transcription for the specific miRNA and the internal reference (RNU48) from 200 ng total RNA.

7.1.10.2 Semiquantitative microRNA detection via microarrays

Expression profiling via semiquantitative microarrays was commissioned to IMGM laboratories (Martinsried, Germany) and carried out with 100 ng total RNA input using Agilent Human miRNA Microarrays (8x15K) in combination with one-color based hybridization protocol. Prior to the labeling reaction, the total RNA samples were spiked with *in-vitro* synthesized oligonucleotides (MicroRNA Spike-In Kit, Agilent Technologies, Santa Clara, CA, USA) which served as an internal labeling control for linearity, sensitivity and accuracy. The spiked total RNA was treated with alkaline calf intestine phosphatase (CIP). Subsequently, the dephosphorylated RNA was labeled (miRNA Complete Labeling and Hyb Kit, Agilent Technologies, Santa Clara, CA, USA) using the T4 RNA ligase. All steps were carried out according to manufacturer's instructions.

After clean-up, Cyanine-3-labeled miRNA samples were prepared for one-color based hybridization (Complete miRNA Labeling and Hyb Kit, Agilent Technologies, Santa Clara, CA, USA). Each Cyanine-3-labeled miRNA sample was hybridized for 20 hours at 55°C on separate

Human miRNA Microarrays (Agilent Technologies, Santa Clara, CA, USA, AMADID 029297, 8x15K format). Afterwards, microarrays were washed with increasing stringency using Gene Expression Wash Buffers (Agilent Technologies, Santa Clara, CA, USA) followed by drying in acetonitril (Sigma-Aldrich, St. Louis, MO, USA).

Signals on the microarrays were detected with the Agilent Microarray scanner using Scan Control at IMGM.

7.2 Biochemical methods

7.2.1 Western blot

Protein samples were extracted from Qiazol organic phase. Phase separation was performed according to supplier's miRNeasy Mini Kit protocol (Qiagen, Hilden, Germany). To the organic phase of 700 µl Qiazol, 210 µl 100% ethanol was added and gently mixed. DNA was pelleted by centrifugation (7500×g, 5 min, 4°C). 1.05 ml isopropyl alcohol was added to the supernatant, mixed, incubated (10 min, RT) and centrifuged to pellet protein (12000×g, 10 min, 4°C). The protein pellet was washed three times with 1.4 ml guanidine-hydrochloride (0.3 M in 95% ethanol) and once with 1.4 ml 100% ethanol at RT for 20 min each, with subsequent centrifugation steps (7500×g, 5 min, 4°C). The protein pellet was dried at RT and resuspended in 2 % SDS and 1 volume Laemmli sample buffer and heated for 5 min to 95°C.

Alternatively, whole cell lysates were generated by either adding 2 × Laemmli sample buffer and incubating at 95°C for 5 min or by adding RIPA buffer (150 mM sodium chloride, 50 mM Tris, 1% Triton, 0.5% deoxycholate, 0.1% SDS, 1 × Complete Mini protease inhibitor cocktail) on ice, performing sonication on ice and subsequently adding one volume 2 × Laemmli sample buffer before loading on gels. Sonication was performed on a Sonifier S-250D digital ultrasonic (Branson Ultrasonics, Danbury, CT, USA) with cycles of 0.8 seconds pulse, 0.2 seconds pause for 4 seconds and an pulse amplitude of 10%.

Samples were loaded on self-casted 6% polyacrylamid gels with 4% stacking gel and run in 1 x Tris buffer (25 mM Tris, 0.2M glycine, 1%SDS) at 100 V and 50 mA for approximately one hour. PVDF membrane with 0.2 µm pore size was prewet in 100% methanol, and equilibrated for 15 min in transfer buffer (10 mM CAPS, pH 11, 0.05% SDS). Wet blotting was performed with transfer buffer in a Mini-Protean^{TM} 3 Cell (Biorad, Hercules, CA, USA) at 285 mA for one hour. Blots were blocked for 30 min in 1 × Rotiblock solution, rinsed in TBST (20 mM Tris-HCl, pH 7.6, 137 mM sodium chloride, 0.2% Tween20) and incubated over night at 4 °C with primary antibody. Primary antibodies were diluted in 1.5% milk powder in TBST containing 0.01% sodium azide. MLL1 antibody (A300-086A, Santa Cruz Biotechnology, Santa Cruz, CA,

USA), recognizes a N-terminal epitope and was diluted 1:2500. MLLT3 antibody (alias AF9, A300-597A, Santa Cruz Biotechnology, Santa Cruz, CA, USA) recognizes a C-terminal epitope and was diluted 1:2000. Blots were washed three times with TBST (10 min, RT) and incubated for 45 minutes with goat-anti-rabbit-HRP secondary antibody (sc-2004, Santa Cruz Biotechnology, Santa Cruz, CA, USA,) diluted 1:2500 in 1.5% milk powder / TBST. Blots were washed five times with TBST (10 min, RT) and bands were detected with Immun-Star HRP substrate on CL-XPosure™ Film.

Table 4: **Western blot reagents and supplier.**

Reagents	**Supplier**
CAPS	Roth, Karlsruhe, Germany
CL-XPosure™ Film	Thermo Scientific, Waltham, MA, USA
Complete Mini Protease Inhibitor Cocktail	Roche, Basel, Switzerland
Ethanol, absolute	Merck, Darmstadt, Germany
Glycine	Roth, Karlsruhe, Germany
Guanidine hydrochloride	Sigma-Aldrich, St. Louis, MO, USA
Immun-Star HRP substrate	Biorad, Hercules, CA, USA
Laemmli sample buffer	Sigma-Aldrich, St. Louis, MO, USA
Methanol, ≥99.9%	Roth, Karlsruhe, Germany
Milk powder	Roth, Karlsruhe, Germany
Polyacrylamid Rotiphorese Gel 30 (37.5:1)	Roth, Karlsruhe, Germany
PVDF membrane, 0.2 µm pore size	Biorad, Hercules, CA, USA
Rotiblock solution	Roth, Karlsruhe, Germany
SDS, ultra pure, 20% solution	National Diagnostics, Atlanta, GA, USA
Sodium azide	Merck, Darmstadt, Germany
Sodium chloride	Roth, Karlsruhe, Germany
Sodium deoxycholate	Sigma-Aldrich, St. Louis, MO, USA
Tris	Roth, Karlsruhe, Germany
Triton	Sigma-Aldrich, St. Louis, MO, USA
Tween20	Roth, Karlsruhe, Germany

7.2.2 TaqMan Protein Assay

TaqMan® Protein Assay (Applied Biosystems, Life Technologies, Carlsbad, CA, USA) is a new, alternative method to Western blotting and enables detection and relative quantitation of proteins in cultured mammalian cell and tissue lysates (figure 6).

To generate assay probes, antibodies against MLL and AF9 (see 7.2.1) were dialyzed (3 times for 2 h and once over night in 1 l PBS (PAA Laboratories, Pasching, Austria) at 4°C) to remove Tris via Slide-A-Lyzer® Mini Dialysis Unit (MWCO=7000, Thermo Scientific, Waltham, MA, USA). Subsequently, antibodies were biotinylated with Biotin-XX Microscale Protein Labeling Kit (Molecular Probes, Life Technologies, Carlsbad, CA, USA) according to supplier's protocol

and free biotin was removed by dialyzing as described before. To ensure efficient biotinylation of antibodies and removal of free biotin, a forced proximity test was performed according to supplier's protocol. This test was passed, indicating high quality biotinylation of antibodies.

To ensure equal number of cells lysed, cell suspensions were counted with one volume trypan blue in disposable C-chip hemocytometers (Peqlab, Erlangen, Germany). Samples were lysed in RIPA buffer on ice (see 7.2.1). For evaluation of TaqMan protein assay, cell lysates of THP1 and HELA (the latter expressing *MLL* wildtype but no *MLL-AF9*) were used and mixed in different proportions. HELA was used as background negative control for MLL-AF9 protein quantitation.

Antibody binding, ligation of oligonucleotide probes, protease digestion and quantitative real-timer PCR were performed according to supplier's protocol.

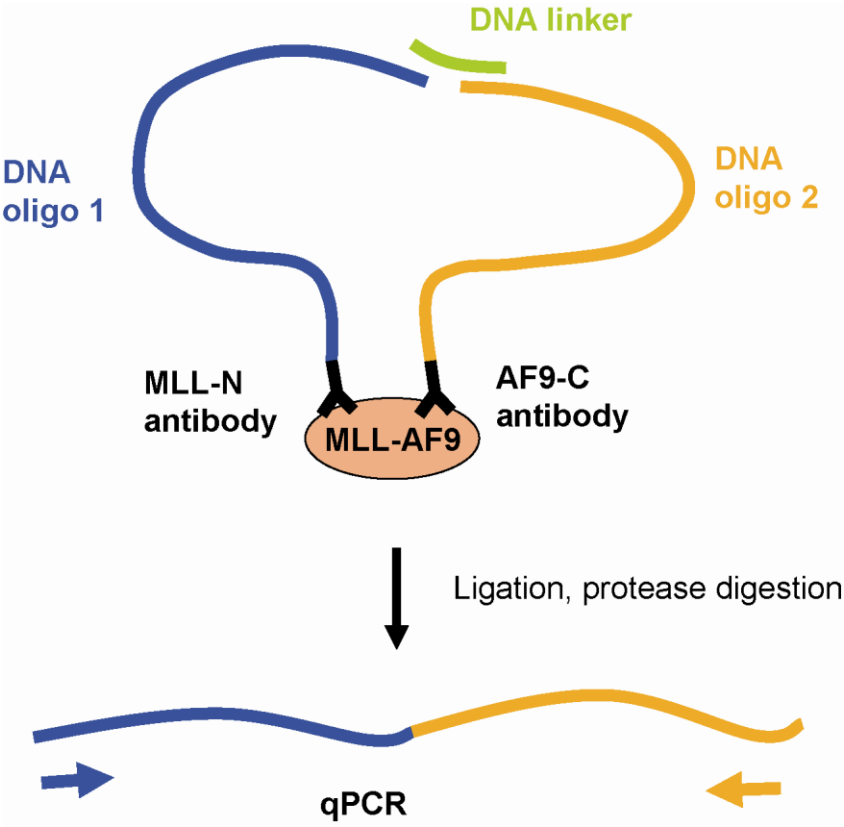

Figure 6: **TaqMan® Protein Assay generated to detect MLL-AF9 protein.** The TaqMan® Protein Assay is a new, alternative method to Western blotting and enables detection and relative quantitation of proteins in lysates. Antibodies (either two monoclonal or one polyclonal) are used to generate two assay probes, which consist of the antibodies linked to DNA oligonucleotides (shown in blue or yellow). After binding of the two antibodies in close proximity, i.e. on the same protein molecule, DNA oligonucleotides are ligated with the help of a DNA linker and are quantified by real-time PCR after protease digestion.

7.3 Biostatistical methods

7.3.1 Gene expression profiling data analysis

Green channel intensities from each data file were read for further analysis. Quality weights for each spot on every array were assigned based on several quality measures (e.g. saturation, uniformity, population outlier) as produced by Agilent Feature Extraction v10.5.1.1 (FE). Background correction was performed by FE and scaling was used for between array normalization.

Hierarchical clustering of arrays and principal component analyses were performed in collaboration with Dr. Philipp Pagel (Lehrstuhl für Genomorientierte Bioinformatik, Wissenschaftszentrum Weihenstephan, Technische Universität München) with the statistical language R (R Development Core Team 2008) using packages from the Bioconductor framework (Gentleman, et al. 2004). Analysis of differential expression between *MLL-AF9* knockdown and control treatments was carried out in R with the limma package (Smyth 2004) which fits a linear model for each gene and computes a moderated *t* statistic and its *p*-value (Smyth 2005). Limma is part of the Bioconductor project (Gentleman, et al. 2004). Adjustment for multiple testing was done using the method by Benjamini and Hochberg (Benjamini, et al. 1995). Thus, logarithmic fold-change ($\log_2$FC = $\log_2(Expression1 \div Expression2)$), *p*-value of the moderated *t* test and *p*-value after correcting for multiple testing were generated.

The unnormalized data showed an almost perfect logarithmic (log) intensity distribution which was more uniform than the background-corrected or the background-corrected and normalized data. In hierarchical clustering of arrays based on the Euclidean distance of log intensity profiles the treatments (*MLL-AF9* knockdown or control) clearly cluster together. In principal component (PC) analysis of arrays based on their expression profiles clearly the first PC is the knockdown, which is in good agreement with the hierarchical clustering results. No clear improvement is seen in PC analysis through background-correction and normalization. Additionally unnormalized data seem to be more consistent, e.g. more identical replicate probes are within the top regulated probes. Due to these findings unnormalized data were used for the differential expression analysis.

Agilent gene expression microarrays encompass a subset (999) of probes with 10 identical replicates and, depending on the transcript analyzed, between 1 and 13 non-identical probes. Nevertheless, because of regularly altered microarray layouts and different microarray designs (depending on the supplier), these replicates are all treated as independent data points in standard analyses, and a probe may show up as significantly regulated even though 9 other identical

replicates may not show differential expression. To evaluate the reliability of the results and to decide on a threshold *p*-value, a *t* test was performed over identical replicate probe sets for differentially expressed probes up to $p<0.05$. Here, probe sets showing a *p*-value below 0.05 were regarded as reliably differentially expressed. The percentage of significant replicates was plotted against the *p*-value threshold (figure 7). This showed a plateau of high percentage of significant identical replicates up to $p<0.03$, with an almost linear decline between $p<0.03$ and 0.06. Thus, to include the highest number of differentially expressed transcripts without raising the false positive rate, the cutoff *p*-value of the moderated *t* test was set below 0.03. Within the results, probes which did not show significant alteration over all identical replicates were removed.

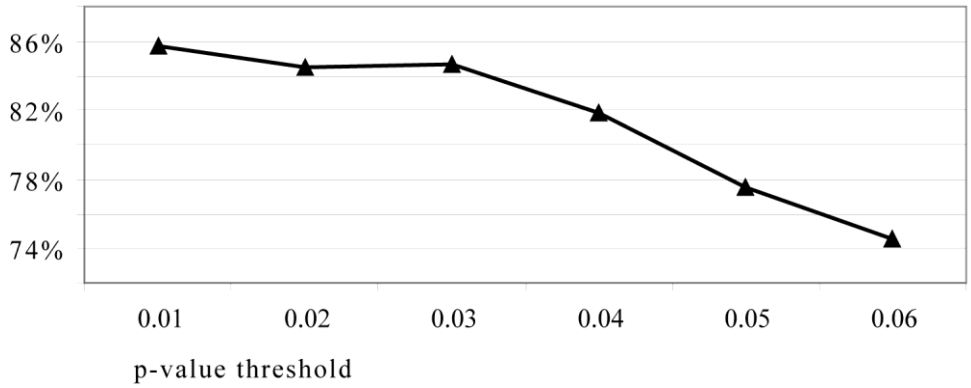

Figure 7: **Gene expression microarray analysis: Percentage of significant identical replicate probe sets as a function of *p*-value threshold.** Probe sets consist of ten identical replicate probes. Up to a *p*-value of 0.03 a plateau of high percentage of significant identical replicates is observed, with an almost linear decline following. Thus *p*-value cutoff was set to < 0.03.

According to experimental design strategies, probes which did not show a uniform regulation between *MLL-AF9* knockdown and non-targeting control treatments (i.e. both knockdown samples yielding either higher or lower FI values than the controls) were removed from the final results. This concerned five of 1350 deregulated probes.

Likewise, non-identical probes against gene transcripts were investigated with a *t* test if not all of these probes were significantly differentially expressed ($p<0.03$). In supplementary table 2 (on page 139), a sign (#) denotes that possibly only one splice variant of the gene transcripts is differentially expressed if probe signals were not overall significantly altered ($p<0.05$ in a paired *t* test).

Depending on the sequence of probes against *MLL* and *AF9* wildtype, these probes will also detect *MLL-AF9* transcript. This is the case for both *AF9* (alias *MLLT3*) probes which are complementary to exon 11 of *AF9* and for one out of four *MLL* probes which detects exon 6 of

MLL. As expected, these three probes showed significantly reduced signals (log_2FC -0.69 ±0.09 in *AF9* and -0.41 ±0.09 in *MLL*) in *MLL-AF9* knockdown samples. The other three probes detecting only *MLL* wildtype did not turn up as deregulated. *AF9* wildtype is only expressed at low level in THP1 whereas *MLL* wildtype is expressed in roughly similar amounts as *MLL-AF9* (according to qRT-PCR data). Thus it is consequential that the *AF9*-probes detecting both *AF9* wildtype and fusion mRNA show stronger downregulation compared to the *MLL*-probe detecting both *MLL* versions. These three probes influenced by the knockdown of *MLL-AF9* mRNA were excluded from the deregulated gene list.

Within the graphs displaying differentially expression of genes from microarray data, only the most significant probe per gene is shown in cases where multiple probes against one gene were differentially expressed. In these graphs, bars indicate standard error of the mean of 4 log_2FC ratios between *MLL-AF9* knockdown and control samples.

Gene expression strength was categorized in high, medium and low expression according to microarray average expression value, which is based on log geometric mean of fluorescent signal intensities (FIs): $\log_2 \sqrt{Expression1 \cdot Expression2}$. High expression was defined as ≥ 10.0, medium expression 7.0 – 9.99 and low expression < 7.0 average log_2 expression.

7.3.2 Quantitative LDA miRNA profiling data analysis

Data analysis of miRNA LDAs was performed in collaboration with Dr. Philipp Pagel (Lehrstuhl für Genomorientierte Bioinformatik, Wissenschaftszentrum Weihenstephan, Technische Universität München). All raw data tables from sds-files were imported into R programming language and software environment. A and B plates, on which the miRNA and control assays are spread, were merged into one table.

The canonical method in qPCR analysis is to use housekeeper genes as references before looking at treatment effects ($\Delta\Delta C_T$ method). As it is difficult to define reliable housekeeper in the case of miRNAs, it has been shown that normalizing to the overall mean instead outperforms the reference approach (Mestdagh, et al. 2009). Based on the observation of substantial distortion of log RQ values over the entire C_T range, we applied a LOESS normalization, similar to what is commonly used in the analysis of microarrays. This method works under the assumption that the majority of miRNAs is not differentially expressed and thus a LOESS curve fitted to the data can be used as reference. Cyclic LOESS normalization was applied to the data separately for the A and B plates. Cases of "undetermined" (no signal measured) cannot be handled in the statistical test. Analysis of differential expression between *MLL-AF9* knockdown and control treatments was carried out in the statistical language R with the limma package (Smyth 2004) (see section

7.3.1 for details). Adjustment for multiple testing was done using the method by Benjamini and Hochberg (Benjamini, et al. 1995). Log_2FC, *p*-value of the moderated *t* test and *p*-value after correcting for multiple testing were generated. MiRNAs which showed low expression, i.e. high threshold cycle (C_T values above 34.5) in both treatment groups were excluded form the analysis. MiRNAs with a *p*-value below 0.05 were regarded as differentially expressed. MiRNAs which were either turned "on" or "off" in both *MLL-AF9* knockdown versus both non-targeting control samples ("undetermined" versus C_Ts below 34.5) were added to the miRNA candidate list manually. For these, no ratio can be calculated but a lower limit of differential expression is reported as previously described (Dorsam, et al. 2004). Of the 664 distinct miRNAs detectable by this LDA, 73 are measured in duplicate. MiRNAs were removed from the candidate list if their replicate did not show concordant regulation.

7.3.3 Semiquantitative microarray miRNA profiling data analysis

Fluorescent signal intensities on Agilent Human miRNA Microarrays (8x15K) were detected with Scan Control 8.4.1 Software on the Agilent DNA Microarray Scanner and extracted from images using Feature Extraction 10.7.1.1 Software (all Agilent Technologies, Santa Clara, CA, USA) at IMGM laboratories (Martinsried, Germany). The software tool Feature Extraction 10.7.1.1 (FE) was used for quality control, visualization of the performance of microarray analysis and background correction. Data analysis was performed in collaboration with Dr. Philipp Pagel (Lehrstuhl für Genomorientierte Bioinformatik, Wissenschaftszentrum Weihenstephan, Technische Universität München). To avoid negative intensities which disrupt principal component analysis (PCA) and clustering after log transformation, a small constant (25) was added to all raw intensities before further analysis. This procedure usually helps to interpret data, especially of genes with low expression. Between-array normalization on the Cy3 intensity matrix was carried out with the quantile method. Hierarchical clustering of arrays based on the Euclidean distance of log intensity profiles after normalization was performed. Analysis of differential expression between *MLL-AF9* knockdown and control treatments was carried out in statistical language R with the limma package (see section 7.3.1 for details) (Smyth 2004). Adjustment for multiple testing was done using the method by Benjamini and Hochberg (Benjamini, et al. 1995). Log_2FC, *p*-value of the moderated *t* test and *p*-value after correcting for multiple testing were generated. In graphs, bars indicate standard error of the mean of 4 log_2FC ratios between *MLL-AF9* knockdown and control samples.

7.3.4 Correlation analysis of array and qRT-PCR data

To test reliability of array data (Human Whole Genome Microarray and miRNA LDAs) qRT-PCR was performed for selected transcripts / miRNAs. In each case, a linear regression model was fitted to the two data sets (log_2FC of array data versus log_2FC of qRT-PCR data) and Spearman's rank correlation was calculated as previously described (MAQC Consortium 2006). Linear regressions and Spearman's rank correlation coefficients were calculated with the statistical language R (R Development Core Team 2008). Spearman's rank correlation was employed because this limited data set could not be expected to show normal distribution. Regression analysis was based on the formula $y = mx + b$. The percent difference from the ideal slope was calculated as m-1. Differential expression was regarded as confirmed via qRT-PCR when log_2FC over both experimental pools was at least ±0.3 in the concordant direction.

7.3.5 Functional disease ontology analysis

Functional disease ontology analysis maps gene sets to diseases by highlighting statistically enriched (overrepresented) disease annotations of the encompassed genes. All differentially expressed (p<0.03) genes after *MLL-AF9* knockdown in THP1 were entered in functional disease ontology (FunDO) using the web version (Flatow, et al. 2009). Within FunDO, the disease association of each gene in the genome is annotated using the Disease Ontology and peer-reviewed evidence from GeneRIF (Osborne, et al. 2009). A condensed version of the Disease Ontology, Disease Ontology Lite, is used for the statistical analysis (Du, et al. 2009). Similar to functional gene ontology analysis, the significance of each disease association is evaluated by Fisher's exact test (Falcon, et al. 2007).

7.3.6 Functional gene ontology analysis

Functional gene ontology analysis maps gene sets to associated functional annotations by highlighting statistically enriched (overrepresented) annotations terms linked to the encompassed genes. Functional gene ontology analysis was performed with **D**atabase for **A**nnotation, **V**isualization and **I**ntegrated **D**iscovery v6.7 (DAVID) with an input of all deregulated genes (p<0.03) after *MLL-AF9* knockdown in THP1. Fold enrichment (FE) is calculated for each term by DAVID software. This calculation includes a biostatistical normalization procedure, so that ranking of terms slightly deviates as compared to the percent of differentially expressed genes contained in each functional term (% of total).

As recommended by DAVID (Huang, et al. 2009b), terms with equal or more than 1.5-fold enrichment and a p-value below 0.1 were manually screened for biological relevance. Annotation terms which contained the same subset of our differentially expressed genes were

seen as redundant and the more specific term was kept in the results. To further structure the results, the enriched ontology annotation terms were manually sorted into four functional higher-order terms within which they may play a role in this biological setting.

For all genes of the putative relevant functional terms, further information concerning important biological categories was collected: genes coding for kinases, for proteins with cell surface location, for receptors (via DAVID), for transcription factors (via DAVID and Pubmed gene data base) and for cytokines (via match to the genes with the annotation *cytokine* of Immunology Database and Analysis Portal (2011)).

7.3.7 MiRNA target prediction

MiRNA target prediction was performed for individual miRNAs with miRWalk software (Dweep, et al. 2011). MiRWalk employs 9 different prediction algorithms (DIANA-mT, miRanda, miRDB, miRWalk, PICTAR4 / PICTAR5, PITA, RNA22, RNAhybrid and TargetScan / TargetScanS) to scan 3'UTRs of genes for predicted miRNA binding sites. Results from these predictions were matched for differentially expressed transcripts in *MLL-AF9* knockdown, whose expression negatively correlated to that of the miRNA. For that purpose, the *p*-value threshold of differentially expressed genes was relaxed to $p<0.05$ (instead of the stringent $p<0.03$) in order to include the highest possible number of potentially relevant miRNA targets.

7.4 Prioritization of likely candidate genes

To prioritize likely candidate genes for mediation of MLL-AF9 leukemogenic effects within the genes which were differentially expressed after *MLL-AF9* knockdown, a step-wise approach was utilized.

By applying four criteria, a subset of differentially expressed genes was selected for literature research: (1) Genes with strong differential expression (more than ± 1.0 $\log_2$FC) (2) Genes which were linked to leukemia via functional disease ontology (FunDO) analysis (3) Top regulated genes ($\log_2$FC>± 1 and further top 5 genes) of different functional categories (higher-order terms) of functional gene ontology analysis (4) Genes which showed concordant regulation between our data set and published leukemia patient studies.

Information from literature research together with differential expression strength subsequently served to rate the potential importance of these genes in the context of the transforming activity of MLL-AF9 via a structured rating strategy (table 5).

Table 5: **Strategy to rate the potential role of selected, differentially expressed genes after *MLL-AF9* knockdown concerning mediation of MLL-AF9 leukemogenic effects.**

Rating category	Rating criteria
+++	Highly likely candidates for mediation of MLL-AF9 leukemogenic effects: Differentially expressed gene agrees with all of the following three terms: (1) Coherent regulation with described role in at least one of the following functions: differentiation of myeloid cells (mere association to differentiation is not sufficient), proliferation, growth, apoptosis, survival, senescence, self-renewal, immunosurveillance, energy-supply, regeneration. (2) Coherent regulation with linked association to leukemia via FunDO and / or comparison to published patient studies. (3) Differential expression of the gene $\geq \pm 0.5$ $\log_2$FC.
++	Likely candidates for mediation of MLL-AF9 leukemogenic effects: Differentially expressed gene agrees with two of the three above described criteria.
+	Genes whose regulation is coherent with its functional role in malignancies: Differential expressed gene agrees with either term (1) or term (2) of the three above described criteria.
○	Genes with a currently undefined role in malignancies due to a lack of relevant literature.
-	Genes whose regulation is incoherent with its functional role in malignancies or its association to leukemia.

8 Results

8.1 Experimental design and siRNA selection

Within AML, the *MLL-AF9* translocation is strongly associated with infant AML (Balgobind, et al. 2011) and with the AML subclass M5 of the French-American-British (FAB) classification systems (Chowdhury, et al. 2003) that describes monoblastic and monocytic phenotypes. Among seven cell lines carrying the *MLL-AF9* translocation, the cell line THP1 is the only one established from an infant AML M5 leukemia patient (Drexler, et al. 2004; Tsuchiya, et al. 1980) and thus this representative cell line was chosen for the study. According to genomic DNA gains and losses as well as gene expression, THP1 – like other leukemia cell lines – has been described to be a reliable model system for leukemia with genomic aberrations (Rucker, et al. 2006).

Due to the occurrence of off-target effects of siRNAs (Jackson, et al. 2010; Nature Publishing Group 2003), i.e. binding and downregulation of transcripts via imperfect complementarity, siRNA experiments should generally be designed with two different siRNA sequences against a single target. Only effects which can be seen in both siRNA treatments are considered to be true effects of the knockdown, whereas effects only seen in one are likely off-target effects. To control for off-target effects, two distinct siRNAs each (against *MLL-AF9* and non-targeting controls) were used. Both of these non-targeting control siRNAs have previously been described to have effects on mRNA expression (as all tested control siRNAs did), but the number of off-targets was relatively low in comparison to the total number of analyzed transcripts. Additionally, they affected distinct sets of mRNAs as seen by hierarchical cluster analysis. (Baum, et al. 2010) Thus, these two control siRNAs are unlikely to feign a *MLL-AF9* knockdown specific result by affecting a common transcript and thus can be efficiently used as control treatments.

8.1.1 Transfection method and efficiency

To establish an efficient and gentle siRNA transfection method for THP1 cells, electroporation and six different transfection reagents were tested. Fluorescently (AF488) labeled control siRNA and 7-AAD exclusion staining was used to determine transfection efficiency and percentage of viable cells by flow cytometry. Dreamfect, electroporation, Dmrie-C and HiPerFect were relatively efficient transfection methods, while FuGene HD, Lipofectamine LTX and Lipofectamine 2000 had transfection efficiencies below 25% (table 6). It seems that cationic lipids in combination with an additional component perform best for THP1 cells. Dreamfect was most efficient with 92.5 ±0.8% transfection rate (figure 8), while having the least effect on cell

viability (93.0 ±3.7% viable cells) and was selected for further studies. By fluorescence microscopy, we ensured that the siRNA did enter the cytoplasm (figure 9). A 50 nM final siRNA concentration resulted in maximum *MLL-AF9* knockdown.

Table 6: **Percentage of transfected and viable THP1 cells 24 h after transfection.**

technique	transfected [%]	viable [%]	components
Dreamfect	92.5	93.0	cationic lipids + cationic polymers
Electroporation	89.2	68.2	none
Dmrie-C	88.4	83.1	cationic lipids + cholesterol
HiPerFect	56.2	86.8	cationic lipids + neutral lipids
FuGene HD	23.6	90.4	lipids + other components
Lipofectamine LTX	22.5	92.8	cationic lipids
Lipofectamine 2000	13.3	92.7	cationic lipids

Transfection techniques were performed according to suppliers' protocols. Electroporation was performed as described in material and methods. Percentages were determined by flow cytometry of AF488-labeled siRNA and 7-AAD staining as described in material and methods.

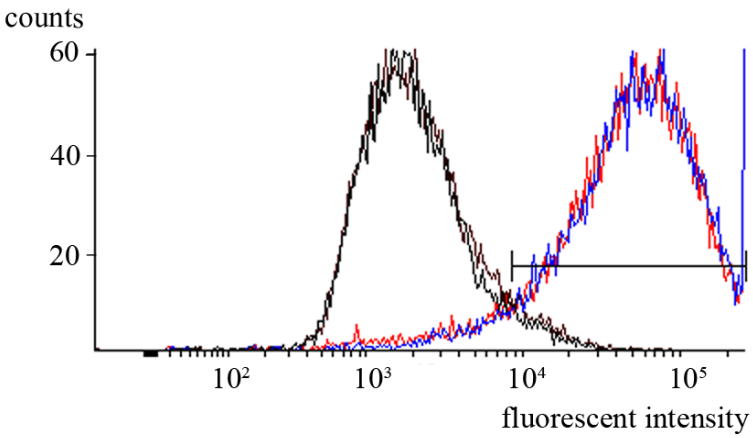

Figure 8: **Transfection efficiency of THP1 cells with Dreamfect**. Left (black) histograms are control siRNA treatments (non-fluorescent), while histograms on the right (red and blue) indicate transfections with AF488-labeled siRNA. Bar indicates gate set to analyze percentage of transfected cells. 1×10^4 cells were analyzed per sample. Measurements were performed by flow cytometry as indicated in material and methods.

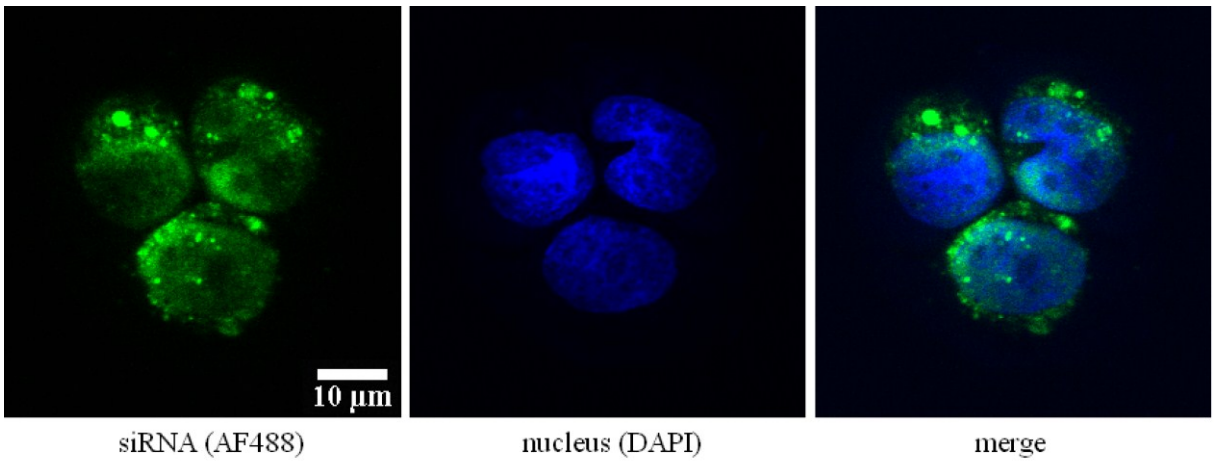

Figure 9: **Images of THP1 cells transfected with fluorescently labeled siRNA.** To evaluate, if siRNA efficiently enters the cytoplasm of THP1 cells, cells were transfected with Dreamfect and AF488-labeled siRNA, stained with DAPI and analyzed by confocal fluorescence microscopy 24 h after transfection.

8.1.2 Design and selection of efficient siRNAs against *MLL-AF9* in THP1 cells

To specifically target *MLL-AF9* without disturbing *MLL* and *AF9* wildtype expression levels, siRNAs were designed to target the THP1 specific fusion point of *MLL-AF9* transcript. Six siRNAs (siR_1 – siR_6) were designed (figure 10) according to scores from *sfold Sirna* (Ding, et al. 2001), *DISR* (Vert, et al. 2006) and *siDESIGN Center* (Thermo Scientific, Waltham, MA, USA) and tested in comparison to non-targeting control siRNA (table 7). While siR_5 resulted in a highly efficient knockdown of *MLL-AF9*, it was the only tested siRNA which also significantly reduced the mRNA level of one of the wildtype gene transcripts (in this case *MLL*). The other five siRNAs performed roughly equally well. For further studies, siR_3 and siR_4 were chosen due to their relatively central target position on the fusion breakpoint sequence while still having considerably distinct sequences (a shift of 3 nucleotides). The latter is important for minimizing off-target effects since for miRNA-like mRNA (off-) target recognition, the so-called seed-region of 6 – 7 nucleotides (nts) is most important. As the chemically modified siRNAs had a prolonged knockdown effect on the *MLL-AF9* transcript, these were used for this study.

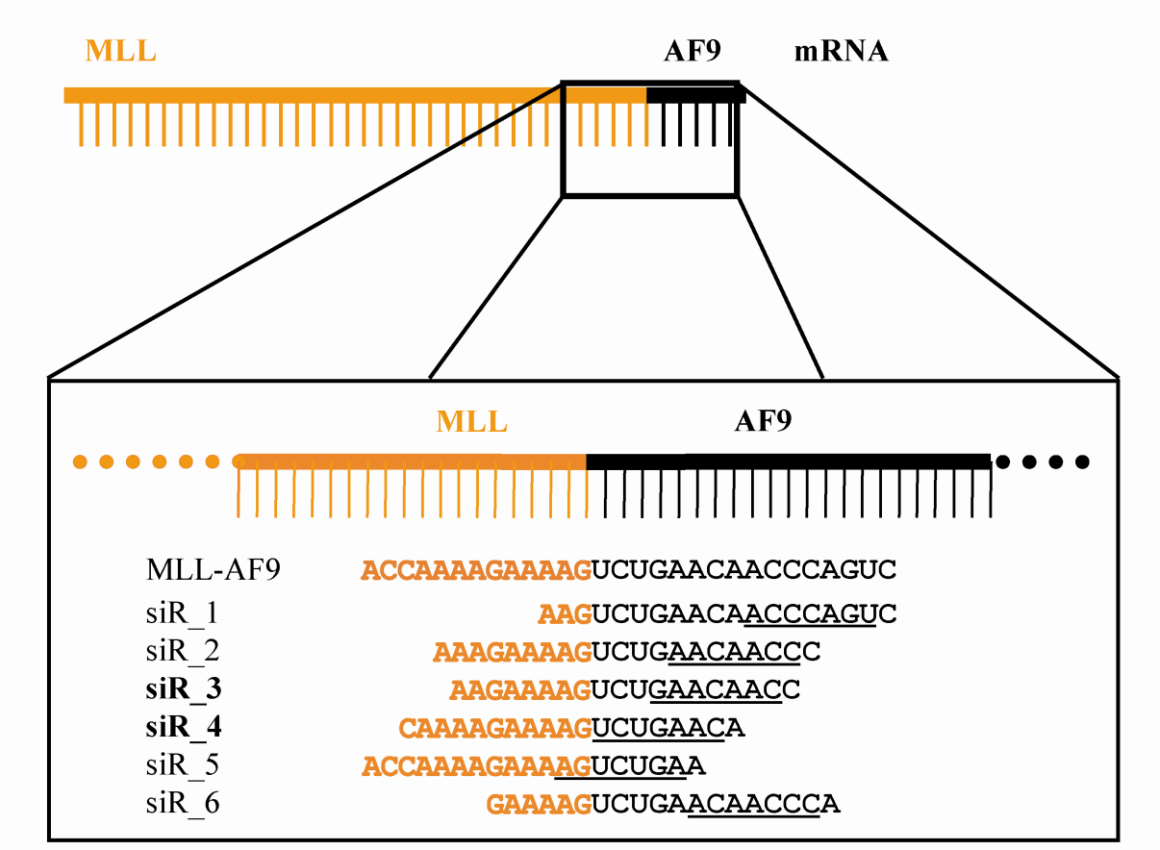

Figure 10: **Overview of the binding positions of all designed and tested siRNAs against *MLL-AF9*.** Alignments to *MLL-AF9* mRNA of THP1 cells are shown. Orange sequences represent the *MLL* and black sequences the *AF9* part of the fusion sequence. Underlined sequences correspond to seed regions for miRNA-like off-target effects. SiR_3 and siR_4 were selected for this study.

Table 7: **Results of tested siRNAs against *MLL-AF9* in THP1 cells.**

siRNA	MLL-AF9	MLL (wt)	AF9 (wt)	siRNA modification	duration
siR_1	0.54 ±0.05	1.17 ±0.13	1.52 ±0.33	no	< 48 h
siR_2	0.57 ±0.03	0.81 ±0.04	1.24 ±0.10	no	< 48 h
siR_3	0.45 ±0.02	0.71 ±0.04	1.09 ±0.09	yes	≥ 72 h
siR_4	0.58 ±0.06	1.63 ±0.12	2.42 ±0.33	yes	≥ 72 h
siR_5	0.18 ±0.01	0.39 ±0.03	1.66 ±0.08	yes	≥ 48 h
siR_6	0.56 ±0.05	1.34 ±0.05	1.38 ±0.18	yes	≥ 72 h

MLL-AF9, *MLL* and *AF9* transcript levels were analyzed by qRT-PCR 24 h after transfection. Expression levels relative to non-targeting control siRNA treatments ± standard error of the mean and duration of the *MLL-AF9* specific effect are given. SiRNAs that were selected for further experiments are shaded in grey. SiRNAs siR_3 - siR_6 were chemically modified as indicated in material and methods.

8.2 *MLL-AF9* knockdown

8.2.1 Experimental conditions

Two main aspects had to be considered for selecting an appropriate experimental setup: First, nothing is known about the half-life of MLL-AF9 protein, which might be significantly different to MLL protein. Second, MLL-AF9 leads to changes in the expression of target genes via epigenetic mechanisms (Mohan, et al. 2010; Slany 2009) whose reversal might take considerably more time than e.g. direct interaction by transcription factors (Ehrenhofer-Murray 2004; Cheng, et al. 2008). Thus a prolonged knockdown of *MLL-AF9* over several days was envisaged. To simplify the experimental procedure, we aimed at a stable transfection of THP1 cells with shRNA plasmids (two plasmids containing distinct shRNA sequences against MLL-AF9 and one with a control shRNA sequence). Surprisingly, though over 94% of cells remained positive for the surface selection marker LNGFR, only 1% of cells stayed positive for the GFP marker and no *MLL-AF9* knockdown could be observed via qRT-PCR. Three main reasons could account for this failure to downregulate *MLL-AF9*: (1) the H1 promoter of the shRNA could be inactivated like obviously the CMV promoter of GFP was, (2) shRNA levels could have been too low to efficiently affect *MLL-AF9* transcript levels or (3) the shRNA was not processed correctly. Because of the time-consuming generation of stable transfected THP1 cells, we decided to proceed with the study employing the tested, very efficient and gentle transient transfection of siRNAs into THP1 via Dreamfect. To nevertheless ensure a functionally efficient *MLL-AF9* knockdown, experiments were performed over eight days with repeated siRNA transfections on day 0, 3 and 6. Prior to each transfection event, cell densities were determined by Cellscreen microscopy and cells were reseeded at 0.05×10^6 cells per ml. Fetal bovine serum (FBS), containing growth factors, has previously been reported to affect miRNA expression, leading to a mitogenic miRNA profile (Paroo, et al. 2009). These effects might mask changes which result from the knockdown treatment. Thus fetal bovine serum levels were reduced to 0.5% from day 6 on. This concentration was determined to correspond to culture conditions in which THP1 cells remain proliferating over at least 6 days, while showing a clearly reduced proliferation level. Analyses were usually performed on day 8 of experiments which corresponds to 48 hours after serum reduction and last transfection.

8.2.2 Validation of *MLL-AF9* knockdown

Knockdown was efficient and reduced *MLL-AF9* transcript levels on day 8 of experiments to 22 ±6 % residual expression (figure 11 a), while *MLL* and *AF9* wildtype levels were not significantly altered at any time point (day 8 levels are shown in figure 12).

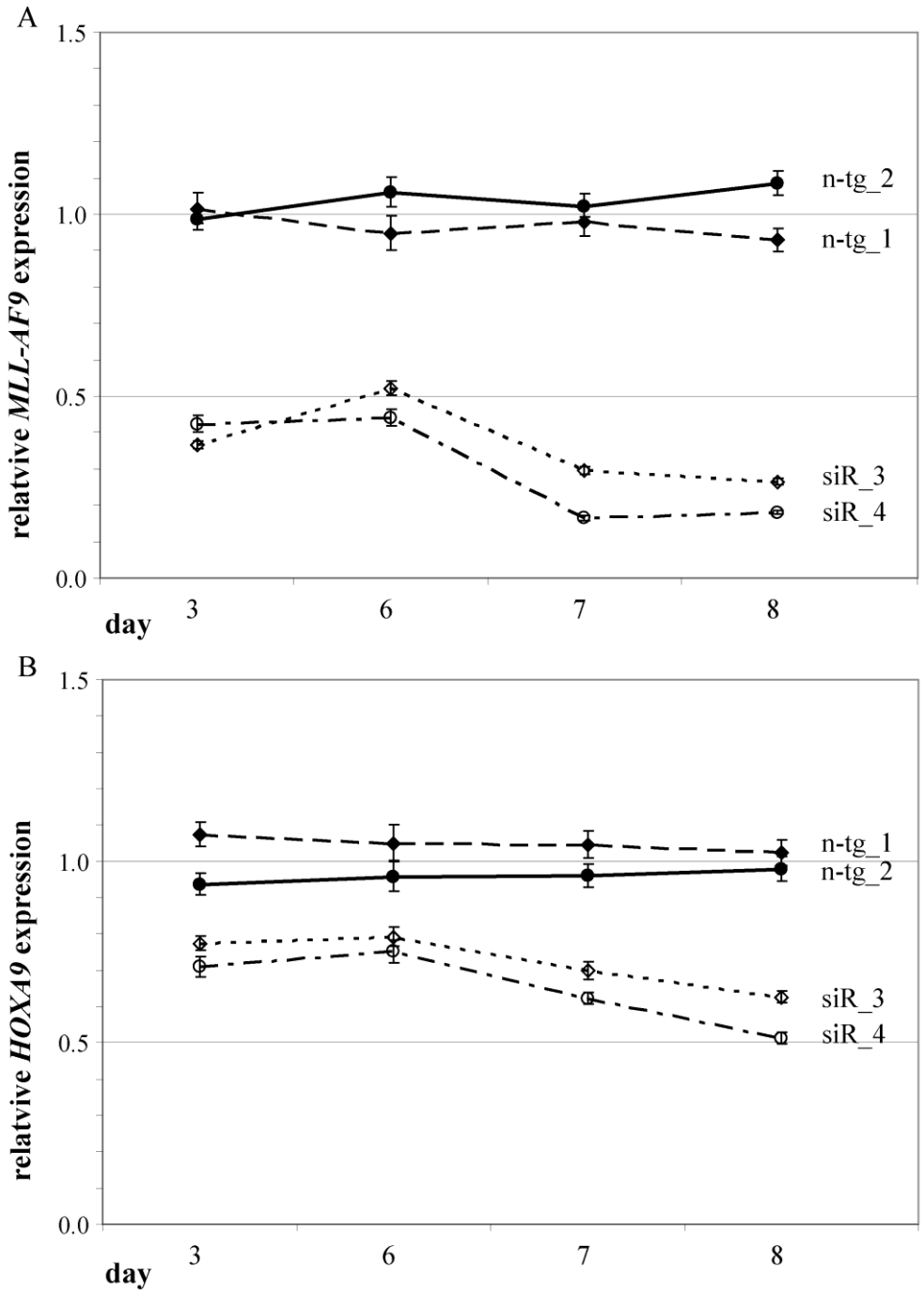

Figure 11: **Confirmation of *MLL-AF9* knockdown in THP1 cells over the experimental time course.** Employed were two siRNA against *MLL-AF9* (siR_3 and siR_4) and two non-targeting control siRNAs (n-tg_1 and n-tg_2). **(A)** Relative *MLL-AF9* transcript levels measured by qRT-PCR. **(B)** Relative *HOXA9* transcript levels which served as surrogate marker of MLL-AF9 protein reduction. MLL-AF9 has previously been shown to directly upregulate *HOXA9* transcription. Graphs represent data from five independent experiments. Bars indicate standard error of the mean.

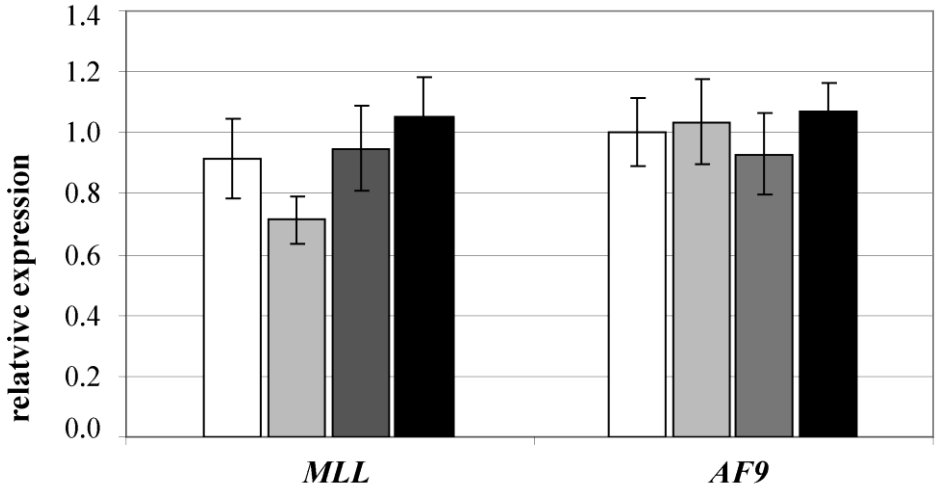

Figure 12: ***MLL* and *AF9* wildtype transcript levels in presence or absence of *MLL-AF9* knockdown in THP1 cells.** Relative transcript levels on day 8 of experiments are shown. Employed siRNA were: ☐ siR_3 and ▒ siR_4 against *MLL-AF9* and non-targeting control siRNAs ▒ n-tg_1 and ■ n-tg_2. Graph represents data from five independent experiments. Bars indicate standard error of the mean.

MLL-AF9 protein is hard to detect, which is already implied by the fact that other groups working with knockdown strategies to reduce endogenous *MLL-AF9* were not able to show reduction on protein level (Kawagoe, et al. 2001; Pession, et al. 2003). Here, MLL-AF9 from THP1 cells was detectable on Western blot by antibodies detecting MLL N-terminus or AF9 C-terminus in protein isolated from the organic phase of Qiazol (similar to Trizol) and redissolved in equal volumes of 2% SDS and 2 × Laemmli sample buffer (figure 13 a) or in equal volumes of 9.5M Urea / 2%CHAPS and 2 × Laemmli sample buffer. Several lines of evidence indicate that the observed band is specific for MLL-AF9: (1) it shows the predicted size (approximately 170 kDa), (2) it is detected by both, MLL (N-terminal) and AF9 (C-terminal) antibodies and (3) it is somewhat larger in MonoMac6 (MM6) cell line than in THP1 cells which is expected because MM6 cells harbor a further 3'-terminal breakpoint in *MLL*. However, due to the high amount of protein needed and because complete dissolution of intermediate protein precipitates can hardly be achieved following this isolation procedure, these samples were not employed for semiquantitative assessment of MLL-AF9 in knockdown experiments. Cell lysates prepared with standard lysis buffers (e.g. Laemmli sample buffer or RIPA buffer) were tested but did not lead to the MLL-AF9 specific band (figure 13 b). To overcome insufficient dissolution of MLL-AF9 protein or protein bound to DNA, sonication of cell lysates was tested. Surprisingly, MLL and AF9 wildtype could be readily detected in control lysates of MCF-7 or HELA cells, while no MLL or MLL-AF9 or AF9 specific band was detectable in THP1 lysates, even on the same Western blots (figure 13 c). This phenomenon may point to a higher tendency of MLL-AF9 to form protein aggregates as compared to wildtype MLL protein.

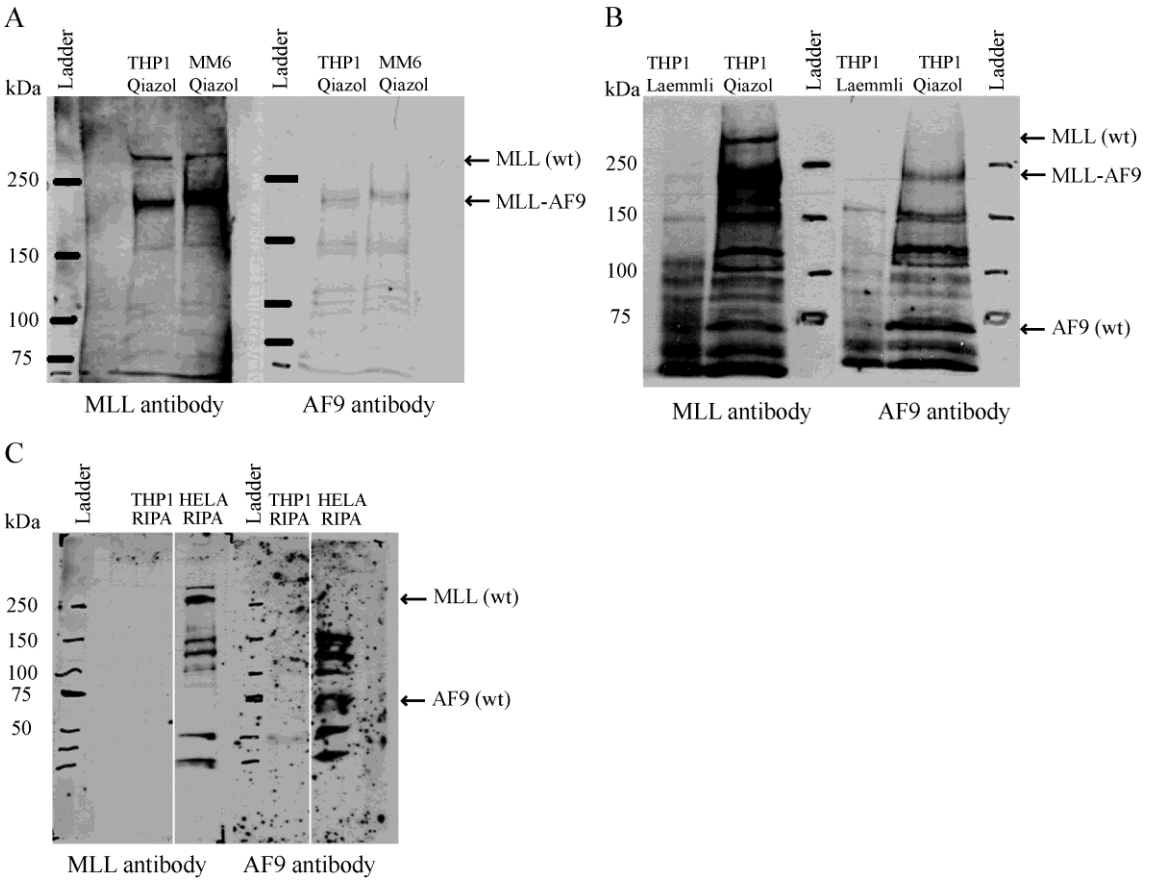

Figure 13: **Detection of MLL-AF9 by Western blot (A)** Identification of MLL-AF9 protein band in THP1 cells: As expected, MLL-AF9 band is larger (~11 kDa) in MonoMac6 (MM6) cell line as compared to THP1 cells, because of a further 3'-terminal breakpoint in *MLL*. MLL-AF9 band is stained by MLL (N-terminal) as well as by AF9 (C-terminal) antibody. Protein was extracted from Qiazol organic phase as described in material and methods. **(B)** MLL-AF9 band is not detectable by neither MLL nor AF9 antibody in THP1 cell lysates prepared with Laemmli sample buffer (or RIPA buffer) but is detectable in THP1 protein extracted from Qiazol organic phase. **(C)** In lysates prepared with RIPA buffer, neither MLL nor MLL-AF9 or AF9 bands are detectable in THP1 lysates, but wildtype MLL and AF9 bands are detectable in HELA control lysates (HELA cells express MLL and AF9 but do not carry *MLL-AF9* translocation). Shown is the image of a single blot from which two lanes were excised for clarity reasons. Similar results were obtained with MCF7 cell line lysates. Band above MLL wildtype band in HELA might be unprocessed MLL protein (430 kDa). MLL and AF9 wildtype bands were assigned due to the expected sizes of the proteins (320 kDa and 63 kDa respectively).

An alternative, new technique for relative quantitation of protein, TaqMan® Protein Assay (Applied Biosystems, Life Technologies, Carlsbad, CA, USA), was additionally tested for MLL-AF9 quantitation (figure 6 in material and methods, page 26). Unfortunately, despite promising quality control results for the assay probes, specific signal of MLL-AF9 was not high enough above background (ΔC_T>3) to yield reliable quantitative data. Disadvantageous binding sites for the antibodies (i.e. located far from each other on the large MLL-AF9 protein) or again, non-sufficient dissolution of MLL-AF9 protein, might explain this result.

To nevertheless ensure that *MLL-AF9* knockdown is effective on protein level, we analyzed *HOXA9* transcript level as a surrogate marker. *HOXA9* transcription is raised by MLL-AF9 through direct interaction between MLL-AF9 protein complex and *HOXA9* promoter (Erfurth, et al. 2008; Cierpicki, et al. 2010). A *MLL-AF9* knockdown specific reduction of *HOXA9* transcript to 57 ±8 % residual expression on day 8 was detected by qRT-PCR (figure 11 b). This finding clearly indicates a functionally sufficient reduction of MLL-AF9 protein.

8.3 Cellular phenotype and functional endpoints of *MLL-AF9* knockdown

To screen for cellular phenotype and functional consequences of our prolonged knockdown of *MLL-AF9* in THP1 cells, proliferation, apoptosis, cell cycle distribution and mean cell size was analyzed.

Proliferation: No significant differences in proliferation measured via Cellscreen microscopy on days 6, 7 and 8 and MTT-assay on day 8 were detected between MLL-AF9 depleted and control treatments. Likewise, no significant difference in proliferation was observed even in a prolonged experiment up to day 12 (figure 14).

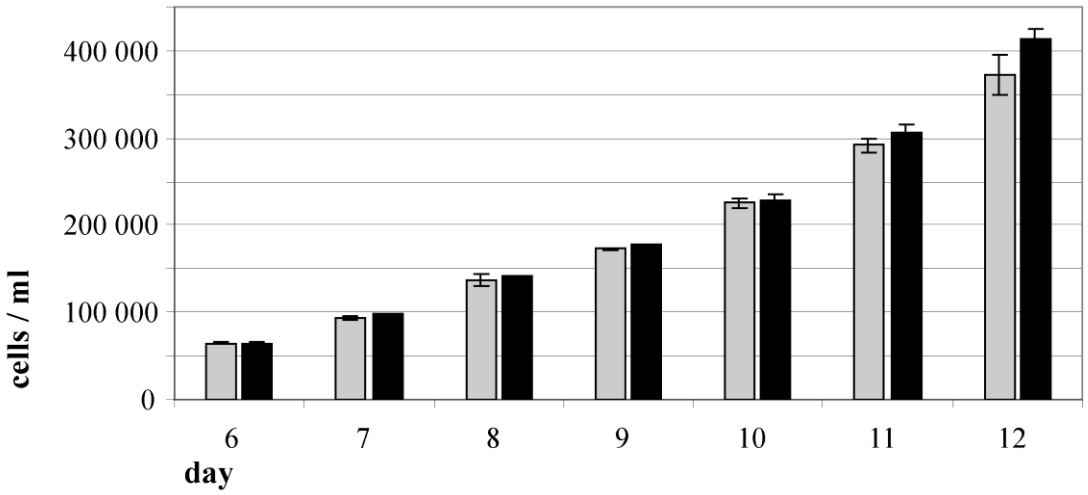

Figure 14: **Proliferation of THP1 cells in presence or absence of *MLL-AF9* knockdown.** □ *MLL-AF9* knockdown, ■ non-targeting control treatments. Cells were counted within culture wells by Cellscreen microscopy as described in material and methods. Three cell culture wells were analyzed per siRNA-treatment and day, each with 62 regions of interest (ROIs) equivalent to 8% of the surface or to ~ 5000 – 32000 cells. Graph represents one experiment with each siRNA-treatment performed in triplicate. Bars indicate standard error of the mean.

Apoptosis: Analysis of apoptotic cells via annexin V and 7AAD staining was difficult to interpret, due to raised autofluorescence of transfected THP1 cells. Thus detection of apoptotic cells was performed via anti-PARP1 cleavage site-specific antibody in flow cytometry on day 7, 8 and 9. No significant differences (figure 15) were detected. BAX is a proapoptotic gene

product and the *BCL-2* to *BAX* transcript ratio has been proposed to indicate survival or death following apoptotic stimuli (Oltval, et al. 1993). The mRNA expression of *BCL-2* and *BAX* on day 8 was analyzed via qRT-PCR, but did not reveal a significant alteration for *MLL-AF9* knockdown versus control samples.

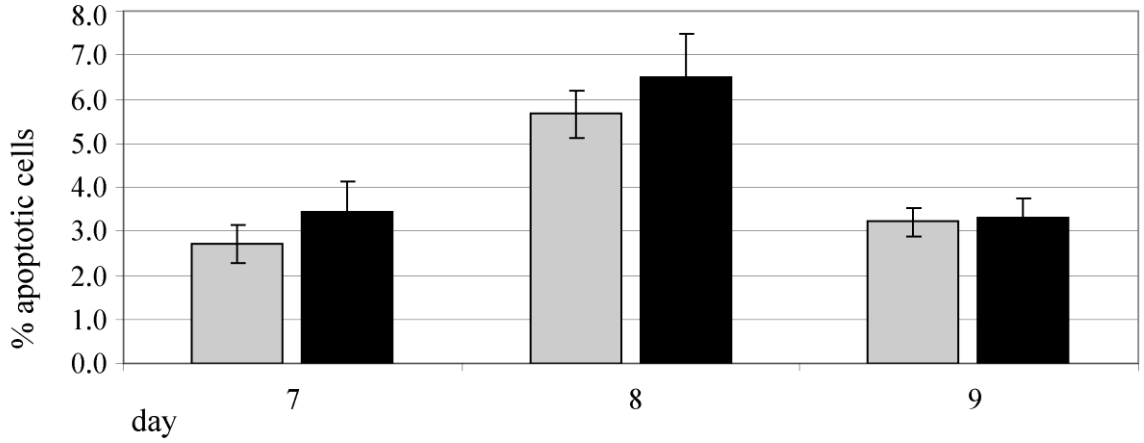

Figure 15: **Apoptosis of THP1 cells in presence or absence of *MLL-AF9* knockdown.** Percentage of apoptotic cells in □ *MLL-AF9* knockdown and ■ non-targeting control treatments were detected by flow cytometry after staining of cleaved PARP1 as described in material and methods. Graph represents one experiment with each treatment performed in triplicate. Bars indicate standard error of the mean.

Cell cycle distribution analysis was performed on day 7, 8 and 9 via flow cytometry. No significant differences in the fractions of cells within the cell cycle phases G0/G1, S and G2 were detected between *MLL-AF9* knockdown and control treatments (figure 16). Percentage of apoptotic cells within the sub-G0 area was also not significantly altered between these treatments.

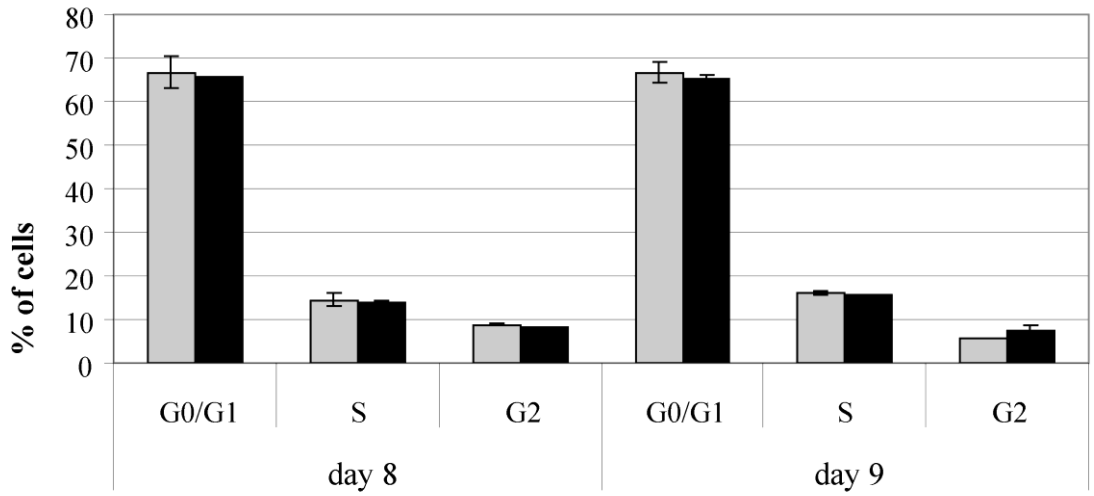

Figure 16: **Cell cycle distribution of THP1 cells in presence or absence of *MLL-AF9* knockdown.** Cell cycle analyses were performed by flow cytometry after staining with propidium iodide as described in material and methods. Percentage of cells within the three cell cycle phases are given for ▫ *MLL-AF9* knockdown (siR_3 and siR_4) and ■ non-targeting control (n-tg_1 and n-tg_2) treatments. Sub-G0 (apoptotic) cells are not displayed. Graph represents one experiment with treatments performed in duplicate. Bars indicate standard error of the mean.

Cell size: A highly significant and reproducible reduction of 0.3 µm in mean cell diameter was observed via Cellscreen microscopy on day 7 and 8 between *MLL-AF9* knockdown and control treatments (figure 17, *p*-value 0.0029 and 0.00088 respectively). In the material and methods section, two Cellscreen images are exemplarily shown (figure 4, page 18). Although the overall mean diameter of the cells varied over the experimental time course, the *MLL-AF9* knockdown specific reduction of cell size remained constant and highly significant.

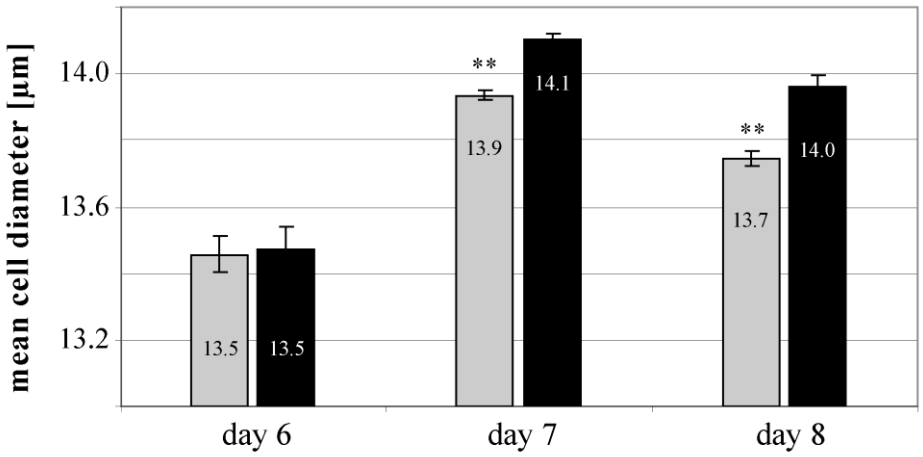

Figure 17: **Cell size of THP1 cells in presence or absence of *MLL-AF9* knockdown.** Cell diameter was significantly reduced in □ *MLL-AF9* knockdown as compared to ■ non-targeting control treatments from experimental day 7 onwards. Three cell culture wells were analyzed per siRNA-treatment and day, each with 62 regions of interest (ROIs) equivalent to 8% of the surface area and corresponding to ~ 5000 – 12000 cells. Graph represents data from five independent experiments, each performed in triplicates. Bars indicate standard error of the mean. Normal distribution was confirmed by Shapiro-Wilk normality test. ** Welch's *t* test $p<0.005$.

To test if the MLL-AF9 specific reduction in cell size is dependent on serum reduced conditions and prolonged *MLL-AF9* knockdown, additional experiments were performed without serum reduction (up to day 8) or with *MLL-AF9* knockdown already initiated in serum reduced conditions on day 0 (up to day 3). In neither experiment we could observe a MLL-AF9 specific reduction in mean cell diameter. These observations suggest that both, a prolonged knockdown as well as serum reduced conditions are necessary to reveal this *MLL-AF9* knockdown phenotypic effect.

We also tested if the MLL-AF9 specific reduction in cell size could be due to reduced proliferation rates. However, even in a prolonged experiment up to day 12 (6 days after serum reduction) no significant difference in cell densities between *MLL-AF9* knockdown and control treatments was observed (figure 14), while the MLL-AF9 specific reduction in cell size remained present up to day 11 (figure 18). Taken together, these pieces of evidence suggest that a reduced proliferation rate is not likely to be the cause of cell size reduction seen in *MLL-AF9* knockdown.

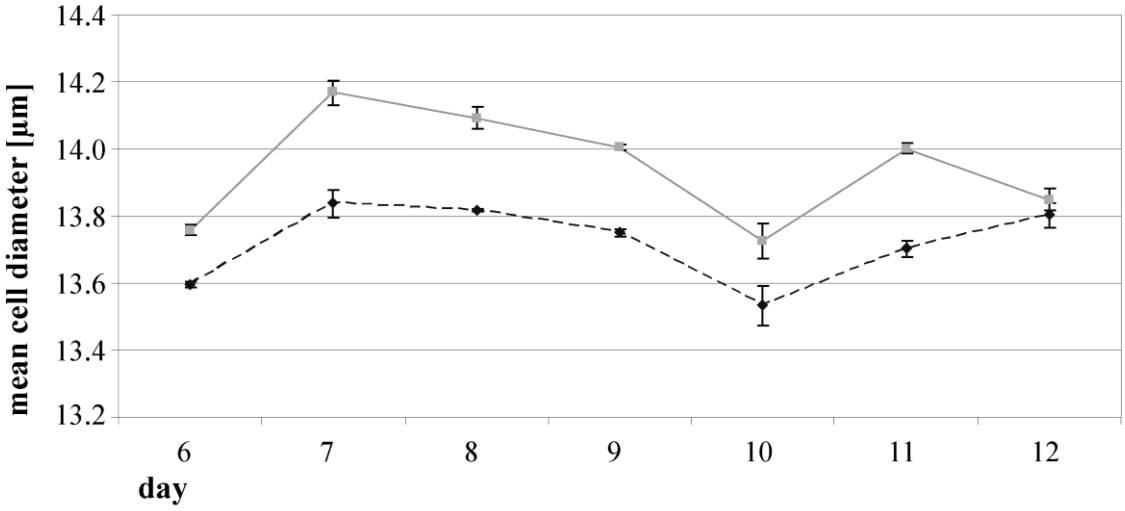

Figure 18: **Cell size of THP1 cells in presence or absence of *MLL-AF9* knockdown over the experimental time course.** Dotted line: *MLL-AF9* knockdown (siR_3 and siR_4), solid grey line: non-targeting control (n-tg_1 and n-tg_2). Three cell culture wells were analyzed per siRNA-treatment and day, each with 62 regions of interest (ROIs) equivalent to 8% of the surface area. Graph represents one experiment with each treatment performed in triplicate. Bars indicate standard error of the mean.

Cell shrinkage is a hallmark of apoptosis (Bortner, et al. 1998) and we considered the possibility that the observed difference in cell size is due to a raised basal levels of apoptosis. Camptothecin induced apoptosis (indicated by detection of cleaved PARP1) in otherwise untreated THP1 cells and led to a significant reduction in cell size. However, this treatment rapidly led to a much higher degree in cell size reduction and finally caused the cells to degrade.

This observation in conjunction with the fact that no raised apoptosis rate could be observed after *MLL-AF9* knockdown, suggests that apoptosis is not the cause of cell size reduction induced by *MLL-AF9* knockdown.

8.4 *MLL-AF9* knockdown dependent effects on gene expression

To understand the transforming activities of MLL-AF9 and to identify potential therapeutic targets downstream of MLL-AF9, more detailed knowledge about gene expression influenced by a common *MLL* fusion product, the MLL-AF9 protein, might be valuable. Thus, gene expression profiles were generated from *MLL-AF9* knockdown experiments. To this end, equal amounts of RNA from day 8 samples of five independent experiments were pooled for each of the four siRNA treatments.

To avoid initial loss of potentially relevant hits for screening purposes, probes with a *p*-value of the moderated *t* test below 0.03 were regarded as differentially expressed as relaxing the

threshold from 0.01 to 0.03 was shown to have little influence on the false positive rate (see 7.3.1 on page 27 for details).

8.4.1 Quality control of gene expression profiling results

Criteria of high quality gene lists from high-throughput biological studies have been described by Huang et al. (2009b) are complied by our *MLL-AF9* knockdown microarray data.

First, the gene list contained important marker genes as expected for the study, e.g. genes from the HOXA cluster (*HOXA7*, *HOXA9*, *HOXA11*) and the differentiation marker *CD14*.

Secondly, the gene list featured a reasonable number of genes, i.e. not extremely low or high (e.g., 100 – 2000). We detected 1269 differentially expressed genes, while 1000 targets have previously been postulated as targets of *MLL* and *MLL*-fusion proteins (Slany 2009).

Thirdly, most of the genes significantly pass the statistical threshold for selection. These 1269 genes match a *p*-value threshold of below 0.03.

Fourthly, a notable portion of up- or downregulated genes are involved in certain interesting biological processes, rather than being randomly spread throughout all possible biological processes. In our data set, genes were indeed found as highly enriched in biological processes (see section 8.4.3.3).

Fifthly, gene lists with different *p*-value thresholds consistently contained more enriched biology (concerning functional gene ontology results) than that of random lists.

Point six of Huang et al. (2009b), high reproducibility according to the generation of similar gene list under the same conditions, could not be evaluated due to high costs of gene profiling via microarray.

Seventhly, however, gene list data were partially confirmed by other independent wet lab tests, i.e. qRT-PCR. Quantitative real-time PCR was performed for 20 arbitrarily selected transcripts, which showed differential expression in microarray results ($p<0.01$). Among these, 19 were considered as confirmed ($\log_2$FC was $> \pm 0.3$ in concordant direction).

We calculated Spearman's correlations between microarray and qRT-PCR data and - though no data points lay around $\log_2 FC \pm 0$ because only differentially expressed genes were selected for qRT-PCR analyses - we added a linear regressions for comparison to the ideal correlation (perfect fit). Linear regressions between microarray and qRT-PCR data are close to the perfect fit: percent difference from the ideal slope was only -7.5% and 16.4% respectively for technical and biological validation (figure 19). Spearman's rank correlations were significant, both when identical RNA was sampled (Spearman's *Rho*=0.68, p=0.0009) and when RNA of independent biological experiments was sampled (Spearman's *Rho*=0.57, p=0.008).

Thus, these data support reliability of the generated microarray data as well as a high interexperimental reproducibility.

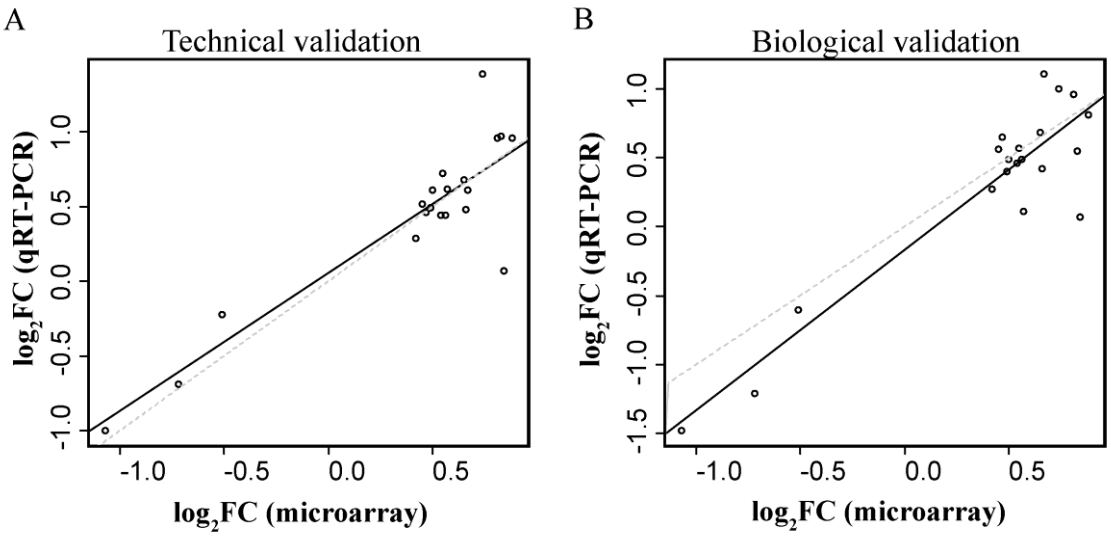

Figure 19: **Correlation between gene expression microarray and qRT-PCR results after *MLL-AF9* knockdown in THP1 cells.** To test reliability of microarray data, qRT-PCR was performed for 20 arbitrary chosen transcripts which showed differential expression (p<0.01) in microarray results. (These were: *ARHGAP26*, *CALR*, *CEBPB*, *CIITA*, *EGR2*, *EMP1*, *FOS*, *FUCA1*, *IL8*, *KCTD12*, *KIF26A*, *MAFB*, *NOTCH2*, *SOCS2*, *SULF2*, *TGFBR1*, *TSPAN14*, *VASH1*, *VDR* and *ZNF521*). Linear regression (black line) is shown in comparison to a perfect fit (= ideal slope, grey dotted line). **(A)** Technical validation: qRT-PCRs were performed in identical samples (RNA) which were measured on the microarrays (significant correlation, Spearman's *Rho*=0.68, p=0.0009). **(B)** Biological validation: qRT-PCRs were performed in additional sample pools of 2 independent experiments (significant correlation, Spearman's *Rho*=0.57, p=0.008). Linear regressions and Spearman's rank correlation coefficients including p-values were calculated with R. No data points are seen around $\log_2$FC ± 0 because only differentially expressed genes were selected for qRT-PCR.

8.4.2 Differentially expressed genes in *MLL-AF9* knockdown

Gene expression analysis was performed with whole human genome microarrays (Agilent), which detect 20194 unique genes with 31153 probes. Among these, 1345 probes representing transcripts of 1269 unique genes were found differentially expressed between *MLL-AF9* knockdown and control treatments on day 8 with a p-value of the moderated t test below 0.03. Of these, 814 gene transcripts were down- and 455 were upregulated in *MLL-AF9* knockdown samples.

Supplementary table 2 (page 139) shows all 1345 differentially expressed probes, including the information if all or only some of the probes against the transcripts of a gene were differentially expressed and if gene expression was validated by qRT-PCR.

Gene expression data were submitted to and accepted by Gene Expression Omnibus (GEO) database, the major public archive for high-throughput microarray- and sequence-based functional genomic data sets (Barrett, et al. 2011), under the accession number GSE36592.

8.4.3 Mediation MLL-AF9 leukemogenic effects: involved processes and subset selection of deregulated genes for prioritization of likely candidates

To identify biological processes potentially involved in mediation of MLL-AF9 leukemogenic effects, an enrichment analysis of functional gene ontology terms was performed with our data set of deregulated genes after *MLL-AF9* knockdown in THP1 cells (8.4.3.3, page 57).

To prioritize candidate genes for mediation of MLL-AF9 leukemogenic effects within the 1269 differentially expressed genes after *MLL-AF9* knockdown, four criteria were applied to select a subset of genes for further literature research:

(1) Genes with strong differential expression (more than ± 1.0 log_2FC).

(2) Genes which were linked to leukemia via functional disease ontology (FunDO) analysis.

(3) Top regulated genes (log_2FC>± 1 and further top 5 genes) of different functional categories (higher-order terms) based on functional gene ontology analysis.

(4) Genes which showed concordant regulation between our data set and published leukemia patient studies.

Altogether, these criteria yielded 92 genes that were then subjected to literature research. An overview of their known biological roles – where applicable in relation to leukemia or malignancies – was generated (supplementary table 3 on page 175).

This information, together with differential expression strength, was subsequently used to rate the potential importance of these genes concerning the transforming activity of MLL-AF9 via a structured rating strategy (table 5, page 33). Results are shown in table 8 on page 68.

In the following sections, results from each of the four selection criteria are presented.

8.4.3.1 Genes with strong differential expression

27 transcripts showed a more than ± 1.0 logarithmic fold-change (log_2FC). Among these, 13 were down- and 14 were upregulated (figure 20). 16 of these were not contained in any enriched gene ontology annotation of DAVID bioinformatical resource.

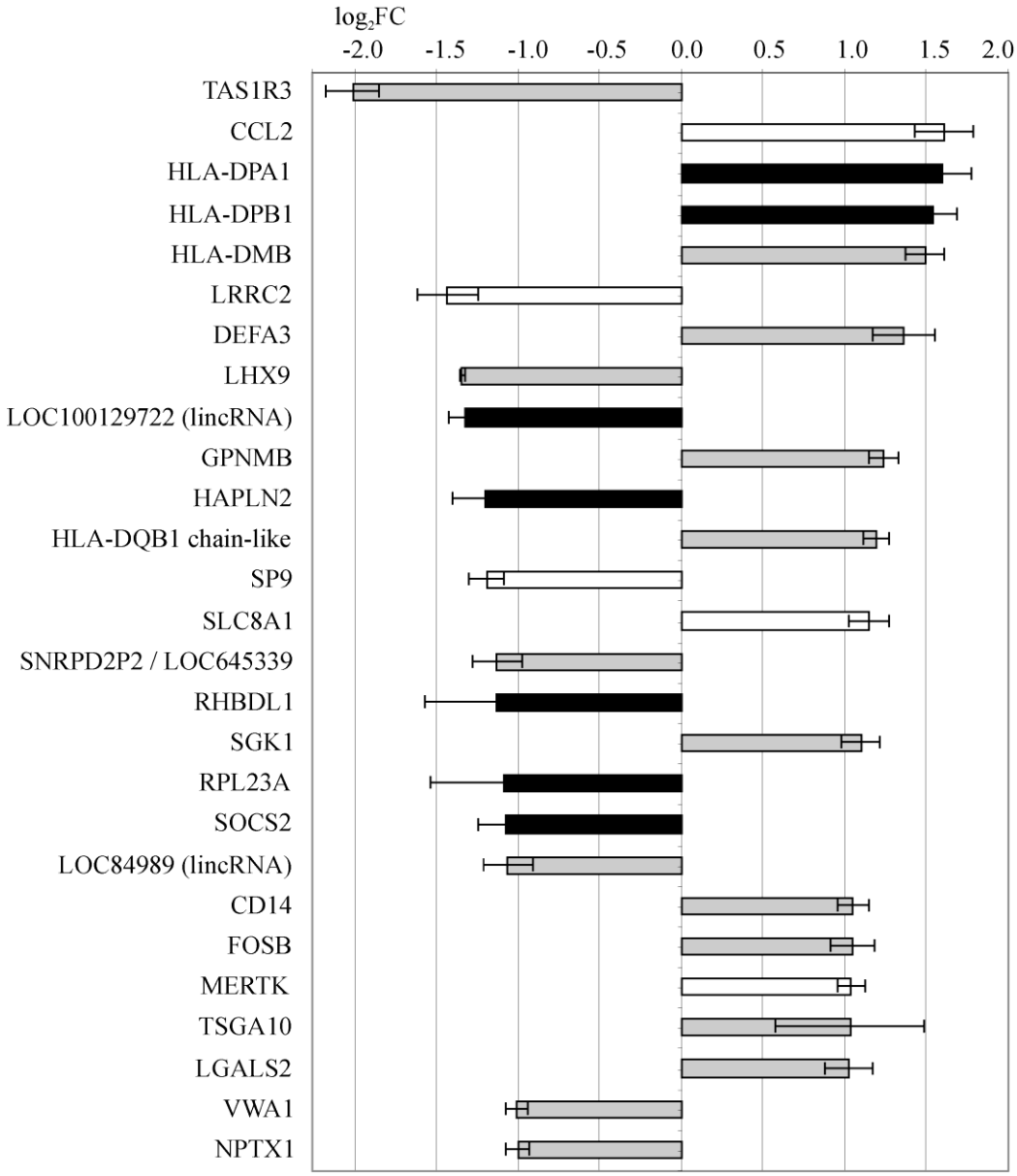

Figure 20: **Strongest differentially regulated transcripts from microarray data of *MLL-AF9* knockdown in THP1 cells.** All transcripts with > ±1.0 log_2FC and p<0.03 are displayed. Grayscale of columns indicates expression strength according to microarray fluorescent signal intensities: ■ high, ▣ medium and □ low expression (classified as described in material and methods, section 7.3.1). Bars indicate standard error of the mean as described in material and methods. Transcripts are sorted according to log fold change (strongest regulated on top). lincRNA = large intervening noncoding RNA.

TAS1R3: Taste receptor type 1 member 3, a glucose sensor which may be involved in energy supply (Mace, et al. 2009), was the most significant ($p=7.47\times10^{-8}$) and strongest regulated protein coding gene transcript (log_2FC -2.01) and showed medium expression strength according to the fluorescent signal intensity (FI). However, only one of three non-identical probes against *TAS1R3* showed this differential expression indicating the possibility that only a certain isoform is regulated dependent on MLL-AF9.

CCL2: The second strongest regulated gene transcript was the chemokine (C-C motif) ligand 2 (*CCL2*) with a $\log_2$FC of 1.61 and a *p*-value of 1.11×10^{-6}. CCL2 binds to chemokine (C-C motif) receptor 2 and 4 (CCR2 and CCR4). CCR2 is also found upregulated in a *MLL-AF9* knockdown specific manner. CCL2 displays chemotactic activity for monocytes and basophils.

HLA class II: The next three top differential expressed transcripts were two classical and one non-classical HLA class II gene: *HLA-DPA1*, *HLA-DPB1* and *HLA-DMB*. MHC class II proteins are selectively expressed in professional antigen presenting cells; besides monocytes these include macrophages, B-cells and dendritic cells (Ting, et al. 2002). Classical HLA class II proteins are expressed on the cell surface to present peptides to T-helper cells, while non-classical HLA class II proteins are involved in the process of peptide loading to classical HLA class II proteins (Shiina, et al. 2009). Further eleven HLA class II gene transcripts are upregulated in a *MLL-AF9* knockdown specific manner. These encompass genes of all types of classical HLA class II genes (*HLA-DP*, *-DQ* and *-DR*), as well as the two non-classical HLA class II genes *HLA-DMA* and *HLA-DMB*. These will be further described in the gene ontology annotation section (8.4.3.3).

Other noteworthy gene transcripts, downregulated with more than $\log_2$FC -1.0 were:

LHX9 of the LIM homeobox gene family, a developmentally expressed transcription factor with a suggested role in gonadal development;

LOC100129722 and *LOC84989*, encoding two large intervening noncoding RNAs (a group of RNAs which are usually associated with open chromatin signatures such as histone modification sites);

SP9: a transcription factor whose vertebrate homologs have a described role in embryo limb outgrowth (Kawakami, et al. 2004), are involved in the formation of regeneration epithelium (like Hoxa-9 and Hoxa-13) and were described as dedifferentiation marker of the mature skin epidermis in the axolotl (Satoh, et al. 2008);

RHBDL1: the rhomboid veinlet-like 1, whose Drosophila homolog has been implicated in the positive modulation of epidermal growth factor receptor signaling (Pascall, et al. 1998);

SOCS2: the suppressor of cytokine signaling 2, which is a negative regulator of cytokine receptor signaling via the Janus kinase pathway, suppresses the apoptotic effect of leukemia inhibitory factor (*LIF*) (Minamoto, et al. 1997), may play a regulatory role in insulin-like growth factor 1 (*IGF1*) receptor signaling (Dey, et al. 1998) and is induced by a wide number of cytokines and hormones (e.g. estrogen and GM-CSF) (Rico-Bautista, et al. 2006).

Other noteworthy gene transcripts upregulated with more than $\log_2$FC +1.0 were:

GPNMB: glycoprotein (transmembrane) nmb, a putative transmembrane glycoprotein which has been described to be involved in growth delay and reduction of metastatic potential in human melanoma (Weterman, et al. 1995);

CD14 molecule, a myelomonocytic differentiation antigen (Goyert, et al. 1988) and differentiation marker for maturating monocytes (Schwende, et al. 1996);

FOSB: the FBJ murine osteosarcoma viral oncogene homolog B, a component of the dimeric transcription factor AP-1, which displays subunit and context dependent effects on proliferation, differentiation and apoptosis (Hess, et al. 2004).

8.4.3.2 Functional disease ontology and gene association to leukemia

Gene Ontology (GO) is a collection of controlled vocabularies describing the biology of a gene product in an organism. Functional disease ontology (FunDO) analysis takes a list of genes and finds relevant diseases based on statistical analysis of the Disease Ontology annotation database and peer-reviewed evidence from GeneRIF (Osborne, et al. 2009). Within this process, an enrichment analysis is performed yielding fold enrichment and *p*-values for each term associated to the set of genes.

All 1269 differentially expressed genes ($p<0.03$) after *MLL-AF9* knockdown in THP1 were entered in FunDO (Flatow, et al. 2009), which recognized and analyzed 1034 genes. Of these, 122 of were found to be associated with diseases.

Figure 21 shows an overview of the top 5 diseases and the genes which map to them as well as a table listing the corresponding statistics. The disease term *leukemia* mapped on upmost position, with the 38 contained genes being 4.7-fold enriched with a highly significant *p*-value (3.4×10^{-15}). The terms *cancer* and *breast cancer* were also found to be associated with our differentially expressed gene list. The top-5 terms also included *Atherosclerosis* and *Diabetes mellitus*, two diseases in which immune cells play important roles. This fact might account for the association of these disease terms with our set of differentially expressed genes upon *MLL-AF9* knockdown.

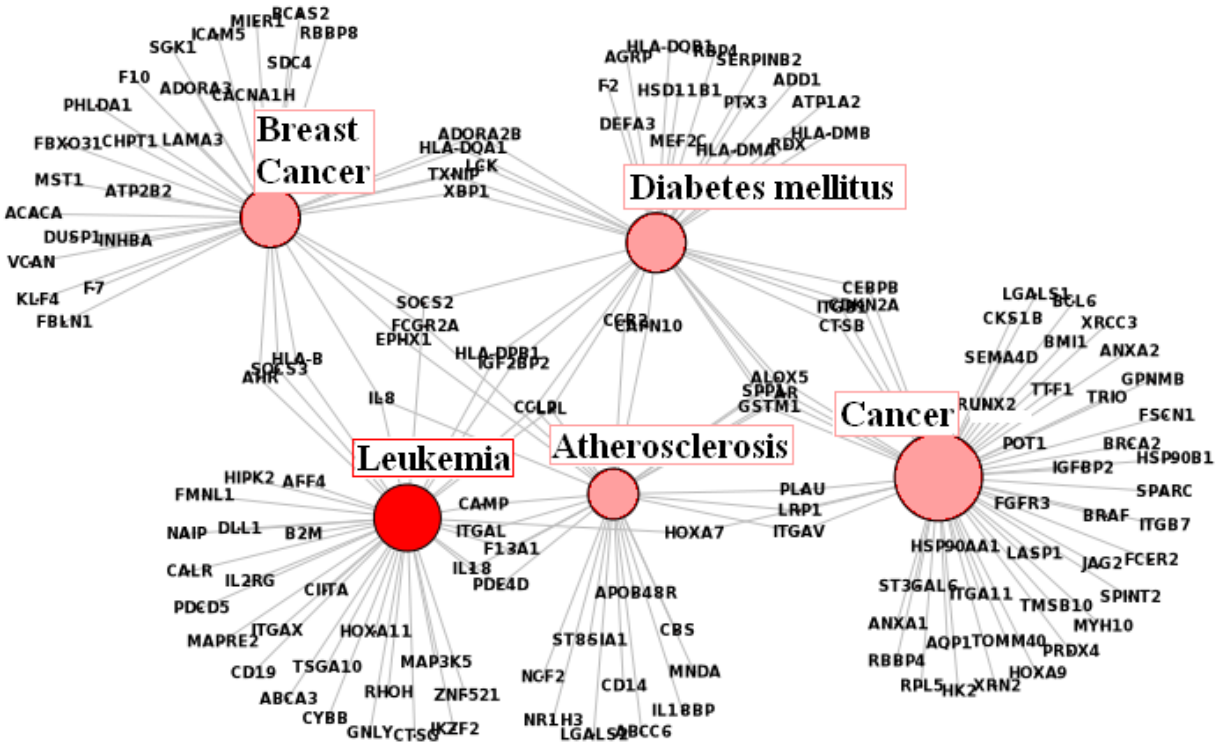

Top table position	FunDO Term	Number of Genes	% of List	Fold Enrichment	p-value	Bonferroni corrected p-value
1	Leukemia	38	12.1	4.7	3.4E-15	7.2E-13
2	Atherosclerosis	29	14.2	5.5	1.1E-13	2.2E-11
3	Diabetes mellitus	34	9.4	3.7	1.1E-10	2.3E-08
4	Cancer	50	6.8	2.6	6.7E-10	1.4E-07
5	Breast cancer	34	7.9	3.1	1.1E-08	2.2E-06

Figure 21: **Functional Disease Ontology (FunDO): The top 5 diseases associated with our set of differentially expressed genes after *MLL-AF9* knockdown in THP1 cells.** Shown are the top 5 associated diseases and the differentially expressed genes which map to them. For leukemia, the contained genes are additionally depicted in figure 22. The sizes of the disease nodes (red dots) are proportional to the number of associated genes. The *p*-value is calculated using Fisher's exact test.

Figure 22 shows the leukemia associated genes depicting their differential expression and expression strength. Supplementary table 3 (on page 175) includes an overview of the biological functions of these 38 genes according to literature research.

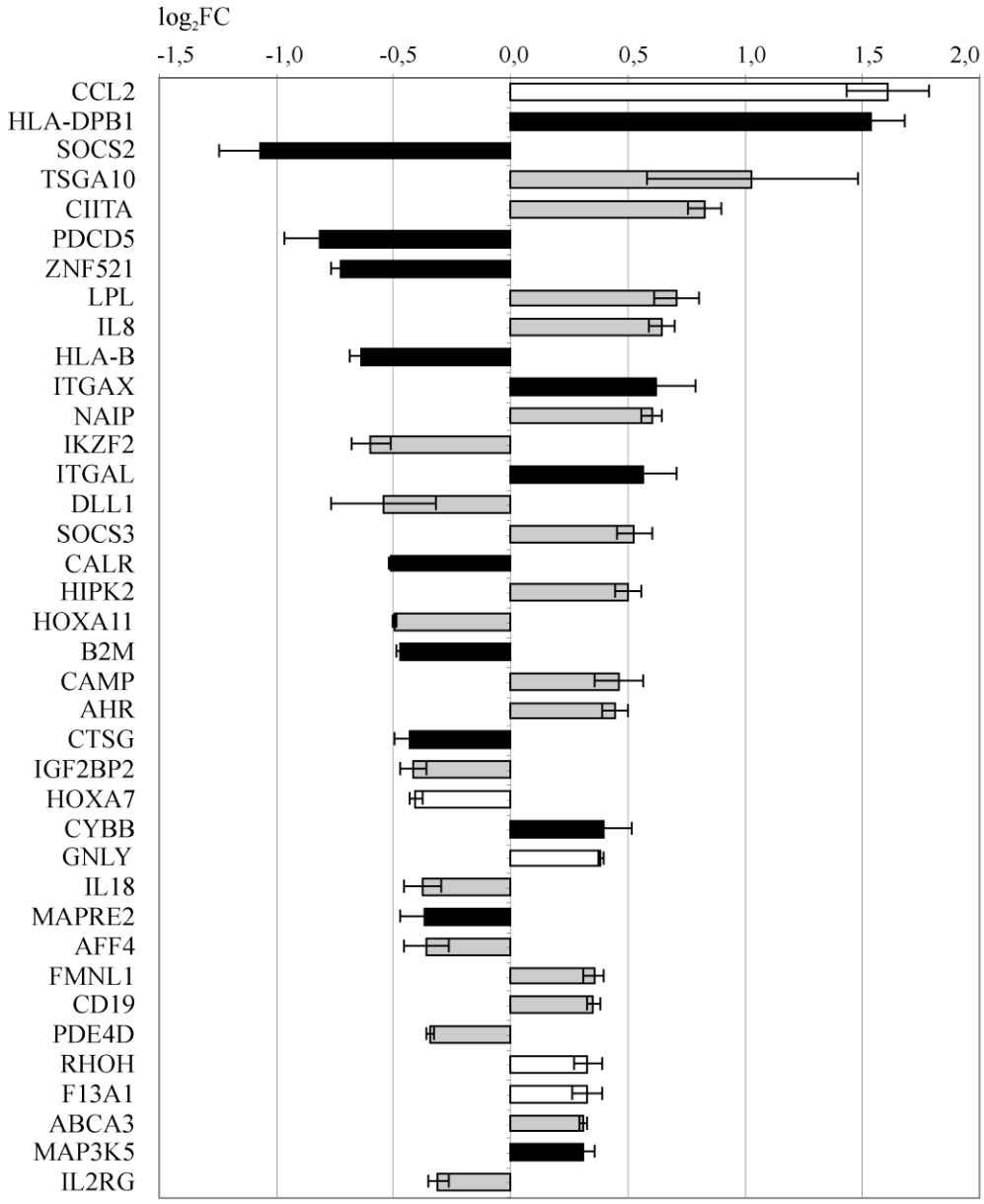

Figure 22: ***MLL-AF9* knockdown and "leukemia" associated genes**: Differentially expressed genes after *MLL-AF9* knockdown in THP1 cells (microarray results), which are associated with leukemia according to Functional Disease Ontology (FunDO) are shown. Grayscale of columns indicates expression strength according to microarray fluorescent signal intensities: ■ high, ▣ medium and □ low expression (classified as described in material and methods, section 7.3.1). Bars indicate standard error of the mean as described in material and methods. Transcripts are sorted according to $\log_2$FC.

Some of these transcripts do not reveal functional concordance with previously published roles in malignancies, while others do. For example, programmed cell death 5 (PDCD5) is a proapoptotic protein, and reduced levels of PDCD5 in AML and CML bone marrow cells compared to normal donor bone marrow cells were described (Ruan, et al. 2006; Ruan, et al. 2008). In contrast, a downregulation of PDCD5 transcript after reduction of leukemogenic MLL-AF9 protein was observed in our data set.

A transcript which regulation very well matches previous knowledge is zinc finger protein 521 (*ZNF521*), which we found as strongly downregulated in *MLL-AF9* knockdown cells. *ZNF521* is highly expressed in the most immature hematopoietic cells and declines with differentiation. Enforced expression leads to proliferation and decreases granulo-monocytic and erythroid differentiation. High expression has been associated with *MLL*-rearrangements and *ZNF521* silencing in THP1 cells led to impaired growth and clonogenicity. (Bond, et al. 2008)

The homeodomain interacting protein kinase 2 (*HIPK2*) is upregulated after MLL-AF9 depletion. HIPK2 is a described tumor suppressor, which - in response to DNA damage - phosphorylates the tumor suppressor PML, resulting in its stabilization. This phosphorylation is required for the ability of PML to cooperate with HIPK2 for the induction of cell death (Gresko, et al. 2009). Mutations of HIPK2 have been described in AML cases (Li, et al. 2007).

Insulin-like growth factor 2 mRNA binding protein 2 (*IGF2BP2* alias *IMP-2*) is downregulated in our *MLL-AF9* knockdown. It encodes a member of embryonically expressed IGF2 mRNA-binding proteins (IMPs: IMP1–3). IMP-1 has been shown to repress *IGF2* translation by binding to the 5' UTR of the *IGF2* mRNA (Nielsen, et al. 1999). *IGF2BP2* was previously found overexpressed in *MLL-AF4* positive acute B cell lymphoblastic leukemia (Stoskus, et al. 2011).

Calreticulin (*CALR*) is downregulated in a *MLL-AF9* knockdown-specific manner. CALR acts as a major Ca^{2+}-binding (storage) protein in the lumen of the endoplasmic reticulum and might be important for gene transcription (e.g. for glucocorticoid receptor regulated transcripts) (Burns, et al. 1994). It is also a chaperone and well-established effector of the unfolded protein response (Schardt, et al. 2011). The chaperone CALR inhibits the translation of *CEBPA*, which is a key myeloid transcription factor and a frequently disrupted in AML (Schardt, et al. 2011).

The aryl hydrocarbon receptor (*AHR*) was upregulated after our MLL-AF9 depletion. Upregulation of *AHR* has been shown to promote retinoic acid–induced differentiation of myeloblastic leukemia cells (Bunaciu, et al. 2011). The strongly differentially expressed transcripts *CCL2*, *HLA-DPB1* and *SOCS2* were already described in 8.4.3.1 of this chapter.

8.4.3.3 Functional gene ontology analysis

Functional gene ontology analysis systematically maps gene sets to associated functional annotations and statistically highlights the most overrepresented (enriched) biological annotations out of thousands of linked terms. This strategy increases the likelihood to identify the most relevant biological processes within the biological phenomena under study. (Huang, et al. 2009b)

Here, gene ontology analysis was performed with **D**atabase for **A**nnotation, **V**isualization and **I**ntegrated **D**iscovery v6.7 (DAVID) with an input of all deregulated genes (p<0.03) after *MLL-AF9* knockdown in THP1. This tool identifies enriched functional annotation terms associated with a gene list and clusters functionally similar terms into groups (cluster). Clustering annotation terms may help to identify related and redundant terms.

DAVID recognized 1159 of the 1270 distinct array probe IDs, which represented 1114 differentially expressed genes. From the resulting 289 functional annotation clusters encompassing 2191 functional annotation terms, 480 terms had at least a 1.5-fold enrichment and a p-value below 0.1 and were selected for further consideration (criteria suggested by Huang et al., 2009). As recommended by Huang et al., these 480 terms were then manually screened concerning biological relevance. Among these, 43 functional terms were considered as of potential biological relevance. These encompassed 331 differentially expressed genes (supplementary figure 1 a-i on pages 166 - 175). These 43 selected and enriched functional annotation terms were subsequently manually sorted into five functional higher-order terms (figure 23).

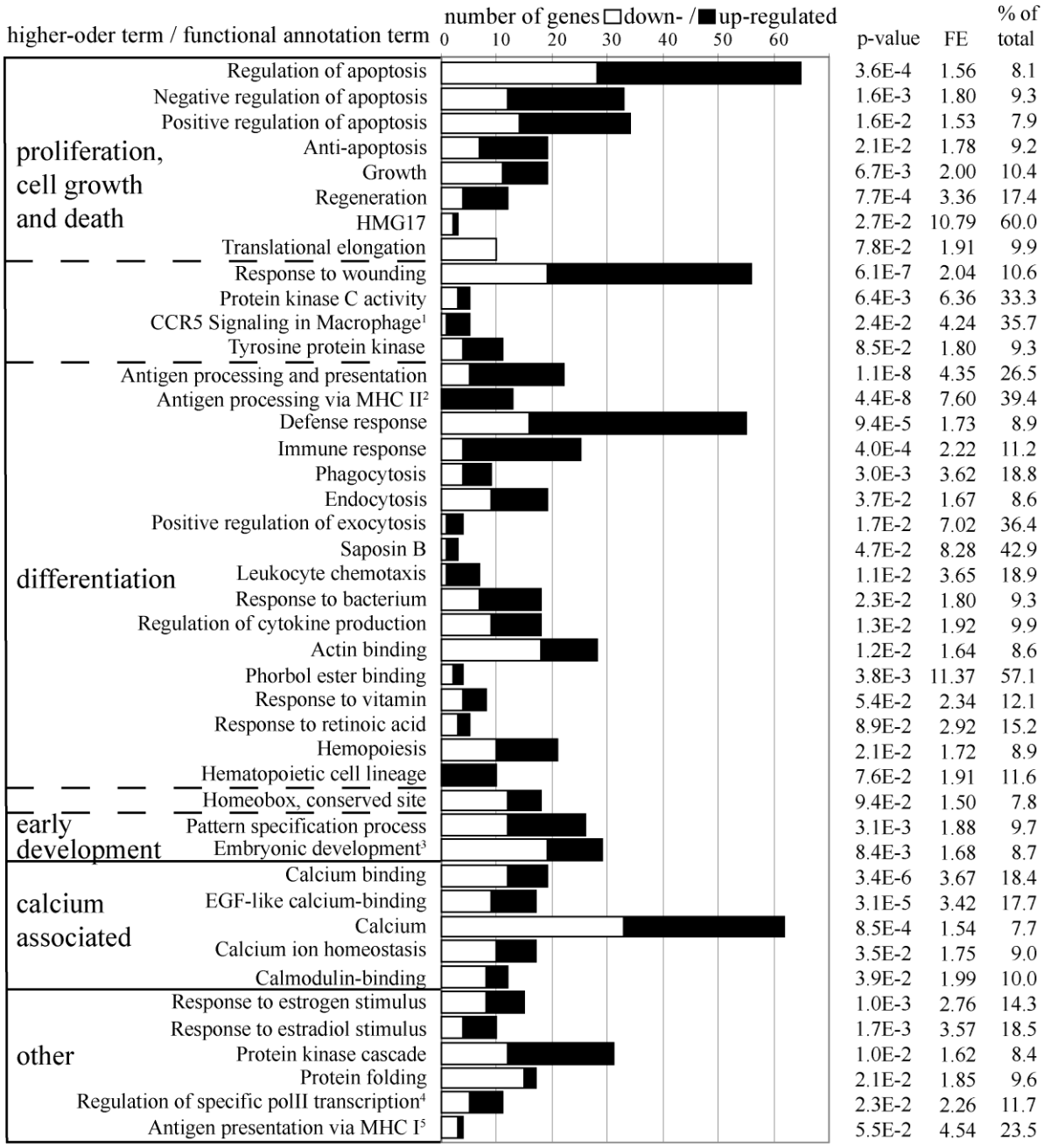

Figure 23: ***MLL-AF9*** **knockdown associated enriched functional gene annotations.** Functional annotation terms were manually assorted to 5 functional higher-order terms according to the major role of the biological process within this biological setting. Annotation terms which were assigned to two higher-order terms are depicted between these two, indicated by dotted division lines. Annotation terms which could not be assigned to one of the four specific higher-order terms are collected under the term "other". Some annotations were abbreviated as indicated by superscript numbers: [1]Pertussis toxin-insensitive CCR5 Signaling in Macrophage, [2]Antigen processing and presentation of peptide or polysaccharide antigen via MHC class II, [3]Embryonic development ending in birth or egg hatching, [4]Regulation of specific transcription from RNA polymerase II promoter and [5]Antigen processing and presentation of peptide antigen via MHC class I. Bars show proportion of □ down- and ■ upregulated genes after *MLL-AF9* knockdown in THP1 cells. Next to the bars, *p*-value, fold enrichment (FE) of annotation term and percent of differentially expressed genes within the term are given. All differentially expressed genes contained in each functional annotation term are shown in supplementary figure 1 a-i on pages 166 - 175.

The higher-order term "proliferation, cell growth and death" includes terms like *regulation of apoptosis*, *growth* and *translational elongation*, the higher-order term "differentiation" holds e.g. *antigen processing and presentation*, *phagocytosis*, *endocytosis*, *response to bacterium* and *hemopoiesis*, the higher-order term "early development" includes the two annotation terms *pattern specification process* and *embryonic development ending in birth or egg hatching* and the higher-order term "calcium associated" holds e.g. *calcium binding* and *calcium ion homeostasis*. The higher-order term "other" holds terms which could not be assorted to one of the other four higher-order terms, e.g. *response to estrogen stimulus* and *protein folding*. The strongest regulated genes of these higher-order terms (all genes with more than ±1.0 $\log_2$FC and further top 5 genes) were selected for further literature analysis. This approach provided 43 genes to be included in the assembly of genes for prioritization concerning mediation of MLL-AF9 leukemogenic effects.

The three most significantly enriched annotation terms were 1) *antigen processing and presentation*, 2) *antigen processing and presentation of peptide or polysaccharide antigen via MHC class II* and 3) *response to wounding* (*p*-values 1.1×10^{-8}, 4.4×10^{-8} and 6.1×10^{-7} respectively). The three most enriched ontology annotation terms according to fold enrichment were 1) *phorbol ester binding*, 2) *HMG17* (non-histone components of chromatin) and 3) *Saposin B* (describing lysosomal proteins containing a Saposin B domain), which were 11.4-, 10.8- and 8.3-fold enriched respectively. Except *HMG17,* all of these functional annotation terms were assigned to the higher-order term "differentiation".

In the following the functional annotation terms are presented in context with the higher-order terms to which they were assigned.

Twelve functional annotation terms were assigned to the higher-order term "proliferation, cell growth and death". Four of these were additionally assigned to "differentiation" (figure 23). The annotation term *regulation of apoptosis* included 65 genes, which can be further divided into *positive* or *negative regulation of apoptosis* and the term *anti-apoptotic*, describing direct effects on apoptosis. All terms encompassed up- and downregulated transcripts, and no preference in the direction of pro-apoptotic regulation can bee seen according to the number of associated transcripts. Positive regulators of apoptosis, which were upregulated in *MLL-AF9* knockdown were genes encoding e.g. *DUSP1*, the transcription factors *VDR*, *CEBPB*, *HIPK2*, *BCL6*, *INHBA*, *NOTCH1* and *SMAD3*, the kinases *PRKCE*, *LCK*, *TRIO*, *TGFBR1*, *CDKN2A*, *PRKCA*, *ERN1*, *MAP3K5* and the cell surface molecule *NOTCH2*. Vice versa, genes encoding negative

regulators of apoptosis, whose expression was reduced in *MLL-AF9* knockdown, were *SOCS2*, *SOX4*, *STAMBP*, *HSP90B1*, *ANXA4*, *CFL1*, *SMO*, *TMBIM6* and the transcription factors *MEF2C* and *GRIN1* as well as the kinase *BRAF* (supplementary figure 1 a, page 166).

Within the term *growth*, 58% of differential expressed transcripts were downregulated in *MLL-AF9* knockdown, among these the genes encoding *NINJ2*, *GSN*, *BRCA2*, *SMO*, the kinases *PRKCQ* and *FGFR3* and the transcription factors *AR* and *HOXA11*. The term *regeneration* is defined as the regrowth of a lost or destroyed body part, such as an organ or tissue. As such, it is related to growth and proliferation and holds some overlapping genes with the term *growth*.

The term *HMG17* describes a nucleosomal binding domain which facilitates binding of proteins to nucleosomes in chromatin. Accordingly, this term holds non-histone components of chromatin thought to be involved in unfolding higher-order chromatin structure, facilitating the transcriptional activation of genes (Porkka, et al. 2002) and affecting DNA replication, recombination and repair (Pogna, et al. 2010). Among the three genes within this term, *HMGN2* and *HMGN3* were downregulated and strongly expressed. *HMGN2* has been previously found overexpressed in CML and other cancer types, and an association to proliferation has been suggested (Kondos, et al. 1995). *HOXA9* overexpression has previously been found to upregulate *HMGN2* (Dorsam, et al. 2004), suggesting that the effect observed in our data set might be an indirect one via HOXA9 reduction.

A notable finding was that all of the of genes within the term *translational elongation* were downregulated. The ten encompassed genes mainly encode ribosomal proteins. Raised expression rates of ribosome components were previously associated with cell growth and proliferation and have been found in numerous cancer types (Andersen, et al. 2005; Ruggero, et al. 2003; Wang, et al. 2006).

The following four terms were assorted to both higher-order terms “proliferation, cell growth and death” and “differentiation”. Within the annotation *response to wounding*, 66% of the 56 genes were found upregulated. This functional process is associated with cell proliferation involved in wound healing, as well as with inflammatory responses. Monocytes are known to migrate into wound regions where they are involved in removing tissue debris and secreting factors that promote growth and biosynthetic activity of fibroblasts (Grinnell 1984). As such this functional annotation term might reflect a more differentiated status of the *MLL-AF9* knockdown monoblasts. It holds many immune response associated genes important for monocytic functions, among these the strongly upregulated *CCL2* and *CD14* as well as the genes encoding the transcription factor *CIITA*, the kinase *SGMS1* and the calcium binding protein *S100A12*.

The annotation *protein kinase C (PKC) activity* encompassed five kinases. Genes encoding the protein kinases C eta, theta and D3 (*PRKCH*, *PRKCQ*, *PRKD3*) were downregulated in *MLL-AF9* knockdown, while the genes for protein kinase C alpha (*PRKCA*) and epsilon (*PRKCE*) were upregulated. PRKCA is a so-called "conventional" protein C kinase, which requires diacylglycerol (DAG), Ca^{2+} and phospholipid hydrolysis for activation, while the other four PKCs are novel PKCs, which do not require Ca^{2+} for activation (Mellor, et al. 1998). PKC comprises a family of 12 related serine/threonine kinases connected with regulation of cell proliferation, differentiation, and other cellular functions (Schwende, et al. 1996). Increased PKC activity in monocytes enhances their initial adhesion and their differentiation into macrophages (Ceolotto, et al. 1999).

The functional annotation term *pertussis toxin-insensitive CCR5 signaling in macrophages* describes a pathway in which the dimeric transcription factor AP-1 is activated via calcium influx. AP-1 has subunit and context dependent effects on proliferation, differentiation and apoptosis (Hess, et al. 2004).

A growing body of evidence documents that myeloid malignancies are caused by genetic mutations that constitutively activate tyrosine kinases (Scott, et al. 2010). Nevertheless, only 4 (*NIN*, *FGFR3, TFG* and *ENST00000374440*) or 36% of transcripts within the annotation term *tyrosine protein kinase* were downregulated in *MLL-AF9* knockdown.

Under normal circumstances, the monoblast is the earliest precursor of the monocyte-macrophage maturation. Leukemic monoblasts, however, are halted in their differentiation at this stage. Monocytes and macrophages have important functions like the defense against certain microorganisms, the removal of damaged or dying cells and cell debris, antigen processing and presentation and the interaction with lymphoid cells in the cell-mediated immune reaction (Territo, et al. 1977). To perform these functions, certain characteristics are necessary that include a well-developed phagocytic activity, the ability to adhere to charged surfaces, motility, responsiveness to chemotactic stimuli, a rich content in lysosomal enzymes and the ability to kill certain microorganisms and to digest a wide variety of organic particles (Territo, et al. 1977). As these functions are increased during monocyte-macrophage maturation, the following 17 functional annotation terms were assorted to the higher-order term "differentiation".

The term *antigen processing and presentation* encompassed 22 genes, among these, 13 and 4 genes were also included in the more specific terms *antigen processing and presentation of peptide or polysaccharide antigen via MHC class II* (assigned to "differentiation"), and *antigen processing and presentation of peptide antigen via MHC class I* (assigned to "other"),

respectively. The remaining 5 genes (not contained in these more specific terms), included the strongly upregulated transcription factor and master controller of MHC class II, *CIITA* (Ting, et al. 2002), the downregulated *RFX5*, which activates transcription of MHC class II genes in cooperation with CIITA (Scholl, et al. 1997) and the upregulated cathepsin B (*CTSB*), encoding a lysosmal cysteine protease which plays an essential role in antigen processing for MHC class II presentation in macrophages (Katunuma, et al. 1994). In concordance with the strong activation of *CIITA*, all 13 differentially expressed transcripts of *antigen processing and presentation of peptide or polysaccharide antigen via MHC class II*, among these eleven HLA class II genes, were upregulated.

Other pieces of evidence from functional gene ontology analysis indicating a more differentiated status of the *MLL-AF9* knockdown cells were: the raised expression of 84% and 71% of genes within the annotations *immune response* and *defense response*, significant enrichment of differentially expressed genes within the terms *phagocytosis*, *endocytosis*, *positive regulation of exocytosis* and *Saposin B* domain proteins (lysosomal proteins), *leukocyte chemotaxis*, *response to bacterium*, *regulation of cytokine production* and *actin binding*. Actin binding proteins have been previously found to show altered expression and to be important in the differentiation of myeloid cells (Leung, et al. 1992).

The enrichment of genes within the annotations *phorbol ester binding*, *response to vitamin* and *response to retinoic acid* might be corresponding to differentiation, as PMA (a phorbol ester) as well as vitamin D (1,25-dihydroxyvitamin D3) and retinoic acid are well known differentiating agents for monoblasts (Matikainen, et al. 1994; Gemelli, et al. 2008; Schwende, et al. 1996).

The annotations *hemopoiesis* and *hematopoietic cell lineage* were also significantly enriched. The latter included solely upregulated transcripts like the differentiation marker for maturating monocytes, CD14 as well as several HLA class II genes, the cell adhesion molecule CD36, FCER2 (CD23) which mediates macrophage mediated lymphocyte tolerance (Swingler, et al. 2003), and colony stimulating factor 2 receptor, alpha (CSF2RA) which mediates control of the production, differentiation, and function of granulocytes and macrophages.

The term *homeobox, conserved site* was assorted to both higher-order terms “differentiation” and “early development”, while the two terms *pattern specification process*es and *embryonic development ending in birth or egg hatching* were only assorted to the higher-order term “early development”.

Homeobox transcription factors, in particular HOXA9, have previously been identified as deregulated by MLL fusion proteins (Kawagoe, et al. 2001; Cierpicki, et al. 2010). In our data,

the annotation *homeobox, conserved site* holds 18 genes. Among these, *EVX1*, *HMBOX1*, *HOXC4* and *LHX9* show an even more pronounced downregulation as the well known MLL-AF9 target *HOXA9*. Many homeobox genes play a role in *pattern specification process*es, which also showed up as an enriched ontology annotation and includes regulated genes such as *ROR2*, *EGR2*, *DLL1* and *MAFB*. *EGR2* encodes a transcription factor and tumor suppressor whose deletion leads to cancer cell proliferation. It inhibits neutrophil- and activates macrophage-specific genes and interacts with PU.1, a master transcription factor in macrophage differentiation (Gabet, et al. 2010).
Another functional annotation term assigned to the higher-order term "early development" is *embryonic development ending in birth or egg hatching*, where 66% of transcripts are found downregulated. These include a number of transcription factors, besides HOXA9 and HOXA7 for example the nuclear androgen receptor (*AR*), even-skipped homeobox 1 (*EVX1*) and retinoblastoma binding protein 8 (*RBBP8*).

Surprisingly, a high number of calcium associated genes were found to be differentially expressed, suggesting an important role of calcium signaling in this setting. Thus the higher-order term "calcium" was generated and included the functional annotations *calcium binding* ($p=3.4\times10^{-6}$, 3.67-fold enriched), where over 18% of all genes of this term were found differentially expressed, as well as the annotation *EGF-like calcium binding*, the terms *calcium* (meaning calcium dependent or calcium binding), *calcium ion homeostasis* and *calmodulin binding*. Among the included genes, *ATP2B2* encodes a plasma membrane pump whose rat homolog (97.9% identical to human) maintains a low free cytosolic Ca^{2+} concentration (Elwess, et al. 1997). Further deregulated transcripts are the bidirectional sodium/calcium exchanger *SLC8A1* (Mai, et al. 2010), *CCL2* (with a described role in calcium mobilization in primary cultured neurons (Banisadr, et al. 2005)), and *VDR*, encoding the receptor for 1,25-dihydroxyvitamin D3, which has been shown to cause a sustained increase of intracellular Ca^{2+} concentration (Sergeev 2005).

The higher-order term "other" contains functional annotations which could not be assorted to one of the other four higher-order terms.
These include the terms *response to estrogen / estradiol stimulus*. The latter of the two showed a stronger enrichment (3.57-fold) with 60% of its transcripts being upregulated. The strongest regulated of the 15 genes within these terms, however, was the strongly expressed and profoundly downregulated *SOCS2*.

Protein kinases play a role in a wide array of biological processes and are represented by over 500 genes. They are known to be involved in cell cycle control, embryonic development and cancer pathways, and thus constitute important drug targets (Manning, et al. 2002; Martin, et al. 2010). In our data, the enriched annotation *protein kinase cascade* contained 31 transcripts found to be differentially expressed in dependence of MLL-AF9. These include, e.g. ROR2, WNK1, MAP4K1, TGFBR1, MAP4K12, SYK and TYK2.

17 genes showed up within the enriched annotation term *protein folding*, and remarkably 15 (88%) of these were downregulated, including e.g. DNAJC, HSCB, HSP90AA1 and HSP90B1.

The significantly enriched term *regulation of specific transcription from RNA polymerase II promoter* included 6 up- and 5 downregulated transcripts, among them e.g. the transcription factors CIITA, VDR, IKZF2, DLX1 and MEF2C.

Within the functional annotation term *antigen processing and presentation of peptide antigen via MHC class I*, HLA-F transcript was upregulated, while HLA-B, B2M and CALR were downregulated. Two genes contained in the more general annotation term *antigen processing and presentation*, the downregulated heat shock proteins 70 (HSP90AA1) and 90 (HSPA2), are as well involved in peptide antigen presentation via MHC class I (Callahan, et al. 2008). MHC class I deficient tumor clones may escape T-cell immune responses, but might be more susceptible to natural killer (NK) cell-mediated lysis (Algarra, et al. 2004).

8.4.3.4 Comparison of *in vitro* gene expression data with published *in vivo* findings

Agreement of our *in vitro* data with previously published *in vivo* data might support biological relevance of these transcripts in *MLL*-aberrant leukemia.

Homeobox genes have been extensively associated with MLL and *MLL* aberrations in leukemia (Slany 2009; Ansari, et al. 2010; Afonja, et al. 2000; Kawagoe, et al. 2001; Pession, et al. 2003). Homeobox A9 (*HOXA9*), the best described and direct target of MLL and MLL-AF9 (Erfurth, et al. 2008; Cierpicki, et al. 2010), is downregulated in our data set as was expected. *HOXA7* and *HOXA11* were also significantly downregulated, while *HOXA10* was not differentially expressed after *MLL-AF9* knockdown (in microarray and qRT-PCR analyses). In contrast to expectations due to published findings (Afonja, et al. 2000), the Meis homeobox 1 gene (*MEIS1*) was not downregulated after *MLL-AF9* knockdown but slightly upregulated (log_2FC 0.32, p=0.03) although just above the employed microarray *p*-value cutoff of < 0.03.

Transcripts which have been shown to be class discriminating for *MLL* chimeric fusion gene associated AML patient samples (Ross, et al. 2004) were in part also deregulated in our *in vitro MLL-AF9* knockdown data set: expression of *HOXA9*, *SOCS2*, *PBX3* and *DACH1* was

concordantly altered, but expression of *HOXA5*, *PRG1*, *MICAL*, *CES1* and *AK2* was not affected.

Overlapping with the results of Ross et al.'s (2004) top-100 probe set selected by significance analysis of microarray (SAM) for *MLL* chimeric fusion gene AML were the six differentially expressed gene transcripts *DEXI*, *LGALS1*, *MBNL1*, *MEF2C*, *NKG7* and *RNPEP*.

Armstrong et al. (2002) compared gene expression profiles of patient samples with *MLL* translocated B-precursor ALL to other ALL and AML patient samples and described 13 upregulated transcripts. Although these *MLL*-rearranged cells were of a different cell type, *LGALS1* also turns up as deregulated in our data set. In a later study, *LGALS1* has been found to be a highly sensitive and specific biomarker of *MLL*-rearrangement in B-ALL and is likely induced by a MLL-dependent epigenetic modification (Juszczynski, et al. 2010). *LGALS1* has been described to promote escape from T cell dependent immunity and to confer immune privilege to tumor cells (Juszczynski, et al. 2010).

Kohlmann et al. (2005) identified transcripts which were commonly altered in their expression in *MLL*-rearranged samples, irrespective of their lineage (lymphoblastic or myeloid). Here, only *HOXA9* shows concordant regulation upon *MLL-AF9* knockdown in our *in vitro* study. They also describe the top-50 differentially expressed genes which classify AML with t(11q23) compared to other AML cases. Here, the genes *DACH1*, *HOXA7*, *HOXA9*, *PBX3*, *SOCS2* and *ZNF521* were concordantly regulated in our data set.

Further concordance compared to *in vivo* studies of *MLL*-aberrant AML as compared to other AML subtypes (Rozovskaia, et al. 2003; Bullinger, et al. 2004; Valk, et al. 2004) include *HLA-DRB4*, *HOXA9*, *PBX3*, *BMI1*, *MBNL1*, *MEF2C* and *SOCS2*.

Zheng et al. (2006) presented transcripts differentially expressed between CML chronic phase (CP) and blastic phase (BP), i.e. in the transition to an acute myeloid leukemia. Seven out of the 34 described BP versus CP distinguishing genes were also concordantly regulated in our data set: *SOCS2* (up in BP, down in *MLL-AF9* knockdown) and *FOS*, *FOSB*, *CEBPB*, *IL8*, *KLF4* and *S100A12* (down in BP and upregulated in *MLL-AF9* knockdown). This overlap might suggest importance of this gene set concerning aggressiveness of the leukemia.

Altogether, 20 genes showed concordant regulation to leukemia patient studies (figure 24) and thus were included in the gene list for further literature research.

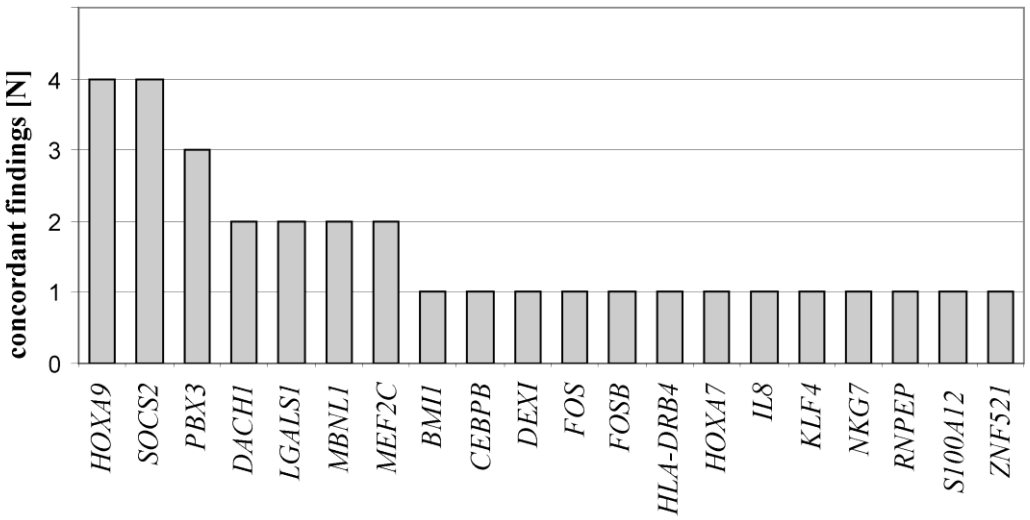

Figure 24: **Differentially expressed genes after *MLL-AF9* knockdown in THP1 cells with concordance to patient studies of acute leukemia.** The number of leukemia patient studies describing concordant differential expression are depicted on the y-axis. References to these studies for each gene are listed in supplementary table 3 on page 175.

8.4.4 Candidate genes with likely relevance in mediation of MLL-AF9 leukemogenic effects

The above described four criteria (see 8.4.3.1 - 8.4.3.4) yielded 92 genes that were subjected to literature research for potential biological function related to malignancies and leukemogenesis (figure 25).

Via a rating strategy, the 92 genes were assorted to five categories representing (1) highly likely candidates, (2) likely candidates for mediation of *MLL-AF9* leukemogenic effects, (3) genes whose regulation is coherent with its functional role in malignancies, (4) genes with a currently undefined role in malignancies due to a lack of relevant literature and (5) genes whose regulation is incoherent with its functional role in malignancies (material and methods section 7.4 on page 32).

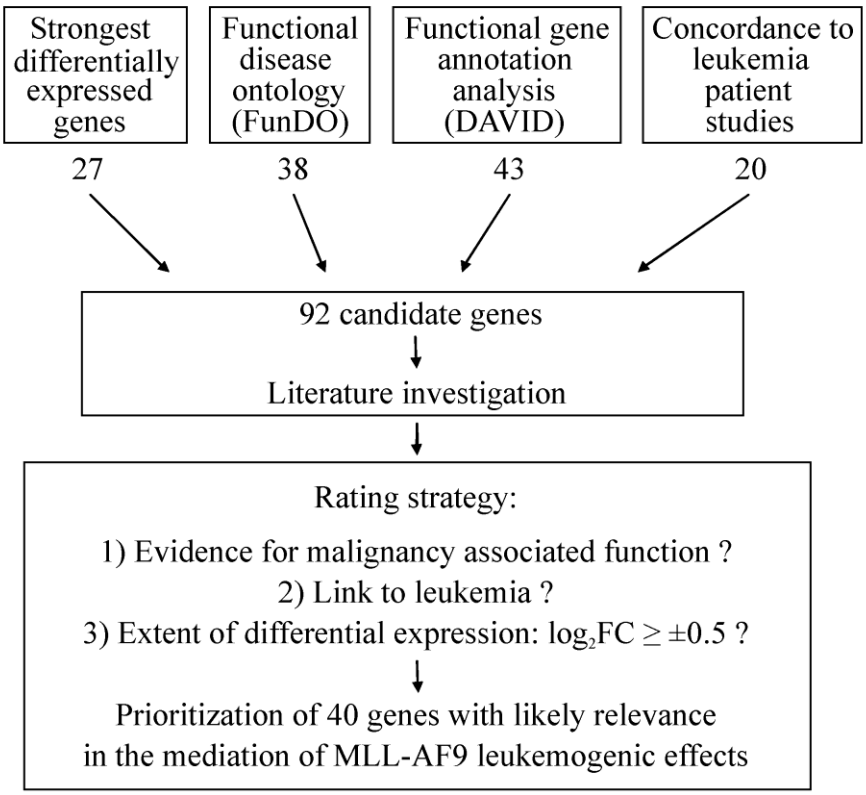

Figure 25: **Strategy to prioritize candidate genes for mediation of MLL-AF9 leukemogenic effects.** Four approaches (first line) were used to select 92 genes from the set of 1269 differentially expressed genes after *MLL-AF9* knockdown in THP1 cells. Subsequent to literature research, their likelihood to play a role in leukemogenesis was rated via a structured rating strategy (see material and methods section 7.4 on page 32 for details).

This strategy led to the prioritization of 40 genes as likely candidates for mediation of *MLL-AF9* leukemogenic effects (figure 27, page 71). An overview of all 92 genes with their assorted rating category is given in table 8 and the distribution of these genes over the rating categories is shown in figure 26. Additionally, supplementary table 3 (page 175) includes the information from literature research which was used to assort the genes to rating categories.

Within the candidate genes likely mediating MLL-AF9 leukemogenic effects, is e.g. the taste receptor and glucose sensor TAS1R3, the chemokine CCL2, the transcription factor SP9 which is involved in dedifferentiation, the suppressor of cytokine signaling SOCS2, the transcription factor and tumor suppressor EGR2, the transcription factor ZNF521, the tumor suppressor HIPK2 and the chaperon CALR which is involved in calcium signaling, in the unfolded protein response and in myeloid differentiation.

Table 8: **Rating of selected differentially expressed genes after *MLL-AF9* knockdown in THP1 cells concerning mediation of leukemogenic effects.**

Gene	Rating category	log_2FC	Official full name
ABCA3	-	0.31	ATP-binding cassette, subfamily A (ABC1), member 3
AFF4	+	-0.36	AF4/FMR2 family, member 4
AHR	++	0.44	aryl hydrocarbon receptor
ALOX5	-	0.76	arachidonate 5-lipoxygenase
ATP2B2	++	-0.69	ATPase, Ca++ transporting, plasma membrane 2
B2M	+	-0.47	beta-2-microglobulin
BMI1	++	-0.33	BMI1 polycomb ring finger oncogene
CALR	+++	-0.51	calreticulin
CAMP	+	0.46	cathelicidin antimicrobial peptide
CCL2	+++	1.61	chemokine (C-C motif) ligand 2
CD14	○	1.05	CD14 molecule
CD19	○	0.35	CD19 molecule
CD209	○	0.73	CD209 molecule
CD74	○	0.77	CD74 molecule, major histocompatibility complex, class II invariant chain
CEBPB	+++	0.53	CCAAT/enhancer binding protein (C/EBP), beta
CIITA	+++	0.83	class II, major histocompatibility complex, transactivator
CTSG	○	-0.43	cathepsin G
CYBB	+	0.4	cytochrome b-245, beta polypeptide
DACH1	++	-0.54	dachshund homolog 1 (Drosophila)
DEFA3	○	1.36	defensin, alpha 3, neutrophil-specific
DEXI	++	-0.56	Dexi homolog (mouse)
DLL1	+++	-0.54	delta-like 1 (Drosophila)
DRD5	○	-0.96	dopamine receptor D5
EGR2	++	0.81	early growth response 2
F13A1	○	0.33	coagulation factor XIII, A1 polypeptide
FMNL1	○	0.36	formin-like 1
FOS	+++	0.88	FBJ murine osteosarcoma viral oncogene homolog
FOSB	+++	1.05	FBJ murine osteosarcoma viral oncogene homolog B
GNLY	○	0.38	granulysin
GPNMB	++	1.24	glycoprotein (transmembrane) nmb
HAPLN2	○	-1.2	hyaluronan and proteoglycan link protein 2
HIPK2	+++	0.5	homeodomain interacting protein kinase 2
HLA-B	○	-0.64	major histocompatibility complex, class I, B
HLA-DMB	++	1.49	major histo-compatibility complex, class II, DM beta
HLA-DPA1	++	1.6	major histo-compatibility complex, class II, DP alpha1
HLA-DPB1	++	1.54	major histo-compatibility complex, class II, DP beta 1
HLA-DQA1	++	0.96	major histocompatibility complex, class II, DQ alpha 1

Gene	Rating category	log_2FC	Official full name
HLA-DQB1	++	1.19	Major histo-compatibility complex, class II, DQ beta 1
HLA-DRB4	++	0.45	major histocompatibility complex, class II, DR beta 4
HMBOX1	○	-0.95	homeobox containing 1
HOXA11	++	-0.5	homeobox A11
HOXA7	+	-0.41	homeobox A7
HOXA9	+++	-0.57	homeobox A9
HOXC4	++	-0.76	homeobox C4
HPX2	○	0.75	homeobox HPX-2
IFI30	○	0.91	interferon, gamma-inducible protein 30
IGF2BP2	+	-0.42	insulin-like growth factor 2 mRNA binding protein 2 (alias IMP-2)
IKZF2	++	-0.6	IKAROS family zinc finger 2 (Helios)
IL18	+	-0.38	interleukin 18
IL2RG	-	-0.31	interleukin 2 receptor, gamma
IL8	++	0.65	interleukin 8
ITGAL	○	0.57	integrin, alpha L / CD11A
ITGAX	○	0.62	integrin, alpha X / CD11C
KLF4	++	0.48	Kruppel-like factor 4
LGALS1	++	-0.41	lectin, galactoside-binding, soluble, 1
LGALS2	○	1.02	lectin, galactoside-binding, soluble, 2
LHX9	○	-1.34	LIM homeobox protein 9
LOC100129722	○	-1.32	hypothetical LOC100129722
LOC84989	○	-1.06	hypothetical LOC84989
LPL	○	0.71	lipoprotein lipase
LRRC2	○	-1.43	leucine rich repeat containing 2
MAP3K5	○	0.31	mitogen-activated protein kinase kinase kinase 5
MAPRE2	+	-0.37	microtubule-associated protein, RP/EB family, member 2
MBNL1	+	-0.34	muscleblind-like (Drosophila)
MEF2C	+++	-0.6	myocyte enhancer factor 2C
MERTK	○	1.04	c-mer proto-oncogene tyrosine kinase
NAIP	-	0.6	NLR family, apoptosis inhibitory protein
NKG7	+	-0.34	natural killer cell group 7 sequence
NPTX1	○	-1	neuronal pentraxin I
PBX3	+++	-0.51	pre-B-cell leukemia homeobox 3
PDCD5	-	-0.82	programmed cell death 5
PDE4D	++	-0.34	phosphodiesterase 4D, cAMP-specific
PRLR	-	0.64	prolactin receptor
RHBDL1	++	-1.13	rhomboid, veinlet-like 1
RHOH	+	0.33	ras homolog gene family, member H
RNPEP	+	-0.32	arginyl aminopeptidase (aminopeptidase B)
ROR2	++	0.81	receptor tyrosine kinase-like orphan receptor 2
RPL23A	○	-1.09	ribosomal protein L23a
RPS26	○	-0.85	ribosomal protein S26
S100A12	++	0.84	S100 calcium binding protein A12
SGK1	-	1.1	serum/glucocorticoid regulated kinase 1

Gene	Rating category	log_2FC	Official full name
SLC8A1	○	1.15	solute carrier family 8, member 1
SNRPD2P2	○	-1.13	small nuclear ribonucleoprotein D2 pseudogene 2 (LOC645339)
SOCS2	+++	-1.07	suppressor of cytokine signaling 2
SOCS3	-	0.53	suppressor of cytokine signaling 3
SOX4	++	-0.84	SRY (sex determining region Y)-box 4
SP9	++	-1.19	Sp9 transcription factor homolog (mouse)
TAS1R3	++	-2.01	Taste receptor, type 1, member 3
TSGA10	-	1.03	testis specific, 10
VDR	++	0.67	vitamin D (1,25- dihydroxyvitamin D3) receptor
VWA1	○	-1.01	von Willebrand factor A domain containing 1
ZNF521	+++	-0.73	zinc finger protein 521

Rating categories (based on biological role and differential expression): +++ highly likely candidates and ++ likely candidates for mediation of *MLL-AF9* leukemogenic effects, + genes whose regulation is coherent with its functional role in malignancies, ○ genes with a currently undefined role in malignancies due to a lack of relevant literature, - genes whose regulation is incoherent with its functional role in malignancies. Supplementary table 3 (on page 175) includes information from literature research which was used to assort the genes to the categories.

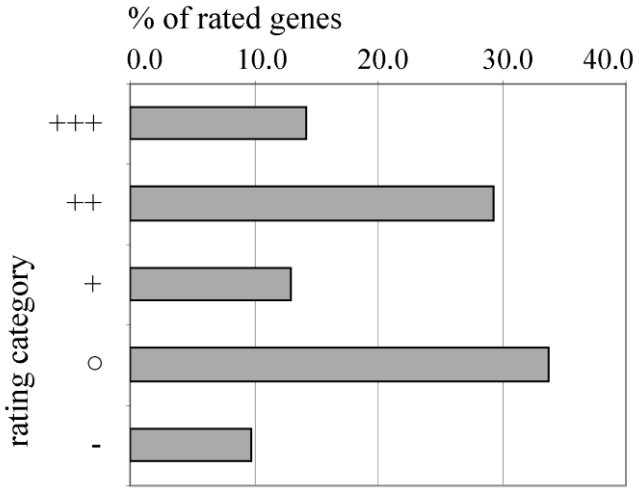

Figure 26: **Distribution of rating categories over the assessed 92 genes.** A rating strategy was employed to assort 92 selected, differentially expressed genes after *MLL-AF9* knockdown in THP1 cells concerning their potential as mediators of MLL-AF9 leukemogenesis. +++ highly likely candidates and ++ likely candidates for mediation of *MLL-AF9* leukemogenic effects, + genes whose regulation is coherent with its functional role in malignancies, ○ genes with a currently undefined role in malignancies due to a lack of relevant literature, - genes whose regulation is incoherent with its functional role in malignancies.

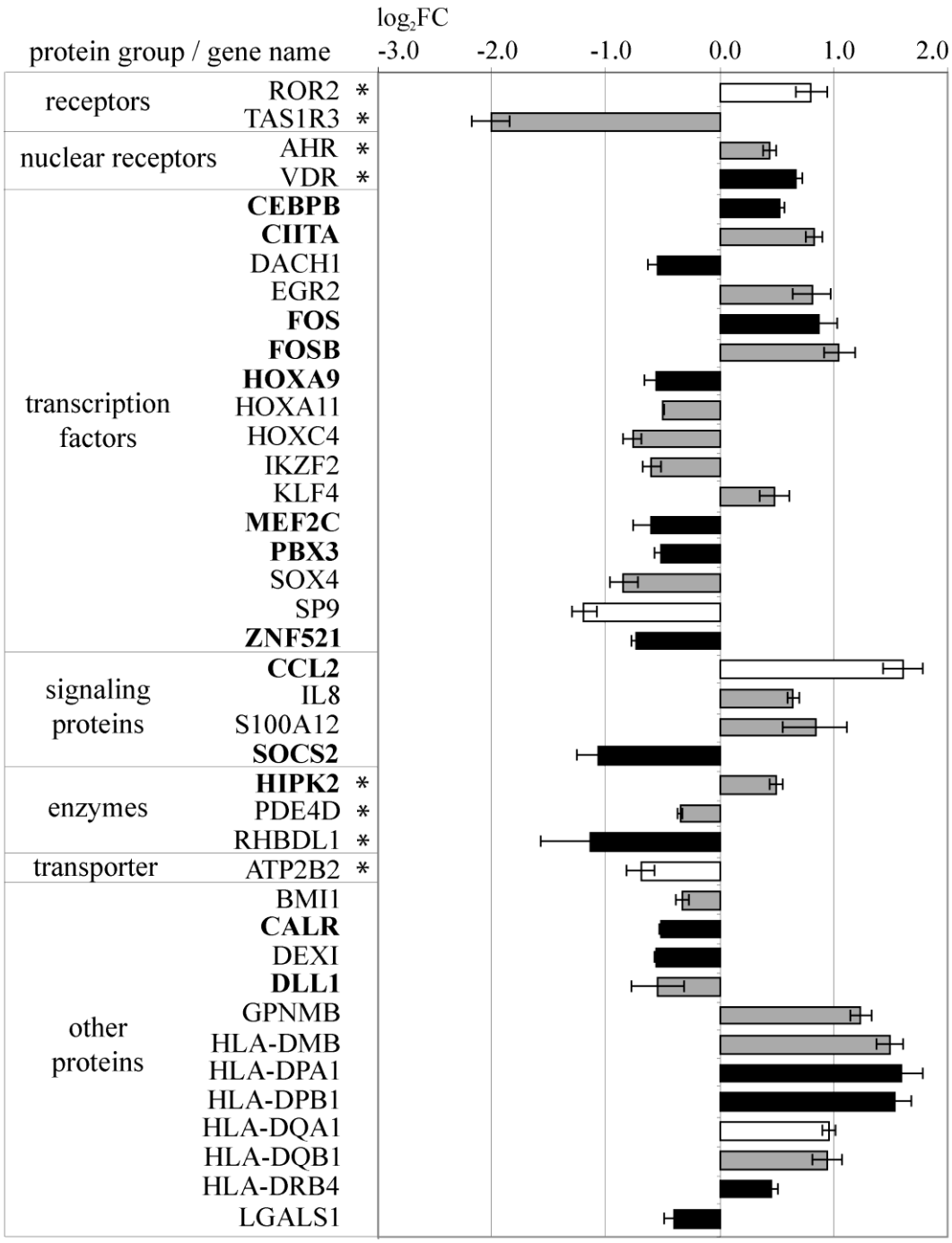

Figure 27: **Differentially expressed genes potentially involved in mediation of MLL-AF9 leukemogenic effects.** Differential expression after *MLL-AF9* knockdown in THP1 cells of 40 genes considered as likely candidates for mediation of leukemogenic effects of MLL-AF9. Gene names in bold indicate genes rated as highly likely candidates. Columns show log_2FC from microarray data of *MLL-AF9* knockdown versus control treatments on day 8. Bars indicate standard error of the mean as described in material and methods. Grayscale of columns indicates expression strength according to microarrays fluorescent signal intensities: ■ high, ▫ medium and □ low expression (classified as described in material and methods). Transcripts are sorted according to categories of encoded proteins and alphabetically. * Indicates genes coding for proteins which belong to conventionally druggable protein classes (see section 9.4.3, page 104 for details).

8.5 MicroRNAs in *MLL-AF9* knockdown

We hypothesized that the fusion protein MLL-AF9 is associated with differential expression of miRNAs. Such miRNAs might support the leukemogenic effect of MLL-AF9 and could yield a new category of potential therapeutic targets for the associated leukemia subtype. Therefore, a differential miRNA expression profile was generated after knockdown of endogenous *MLL-AF9* in THP1 cells.

8.5.1 *MLL-AF9* knockdown dependent effects on miRNA expression

Total RNA from day 8 samples of five independent experiments was pooled for each of the four treatments (two *MLL-AF9* knockdown and two controls). These samples were used for miRNA profiling via two different techniques. For quantitative TaqMan miRNA Low Density Arrays (LDAs), power calculations had revealed that at least eight replicates are needed to obtain over 90% power with a type I error rate below 0.0005 to detect a $\log_2$FC of ±1, given the observed standard deviations for most miRNAs (Chen, et al. 2009). To circumvent this high number of replicates, it was decided to additionally profile miRNAs from the same samples through a second independent technique. Semiquantitative Agilent Human miRNA Microarrays were chosen for this purpose. Supplementary table 4 (on page 185) shows differentially expressed miRNAs from both platforms.

Concerning data analysis of miRNA profiles, it is difficult to define reliable housekeeper. Normalizing the data to the overall mean instead, was shown to outperform the housekeeper reference approach (Mestdagh, et al. 2009). Thus, in collaboration with Dr. Philipp Pagel (Lehrstuhl für Genomorientierte Bioinformatik, Technische Universität München), we employed quantile normalization for semiquantitative microarrays (Agilent). For quantitative LDA profiles, we applied a novel strategy: LOESS normalization, which was based on the observation of substantial distortion of log RQ values over the C_T range. These methods work under the assumption that the majority of miRNAs are not differentially expressed.

Little is known, about how and to what extent the administration of an siRNA can disturb endogenous miRNA expression levels. In our study, we observed a strikingly high difference (Δ $\log_2$FC = 7.9) in the expression of miR-34c between the two non-targeting control siRNA treatments, which points to an off-target effect from one of these control siRNAs. Within the siRNAs designed to knockdown *MLL-AF9* a similar and reproducible (in LDA and Agilent microarray data) expression difference was seen in miR-100 (not detectable in one *MLL-AF9* knockdown treatment but strongly expressed (C_T 15.4) in the other). This finding underlines the

importance of using adequate controls for off-target effects in siRNA studies, like the study design employed here.

In semiquantitative microarray results, 37% of all covered (1048) miRNAs were detected above background and only two miRNAs (miR-328 and miR-744*) were differentially expressed with significance level of $p<0.05$. These miRNAs were not differentially expressed in the data set of quantitative LDAs.

Within the quantitative LDAs, 53% of all covered (664) miRNAs were detected above background. Among those, 15 reached significant ($p<0.05$) differential expression and additional 6 miRNAs were either turned "on" or "off" in both *MLL-AF9* knockdown versus both control samples ("undetermined" versus C_Ts below 34.5). For these, no exact ratio can be determined but - as previously described (Dorsam, et al. 2004) - a lower limit of differential expression was calculated. Among these 21 miRNAs considered as differentially expressed after *MLL-AF9* knockdown, 10 were down- and 11 upregulated (figure 28). The vast majority of differentially expressed miRNAs from quantitative LDA results, i.e. 20 miRNAs, was not detectable and the remaining one miRNA was not differentially expressed in the semiquantitative microarray measurements (supplementary table 4 on page 185).

Low correlation between LDAs and microarrays from the same samples has previously been described and the LDA was evaluated to display a higher sensitivity and specificity (Chen, et al. 2009). Because of this, the LDA was selected as the method of choice and its results applied to further validation.

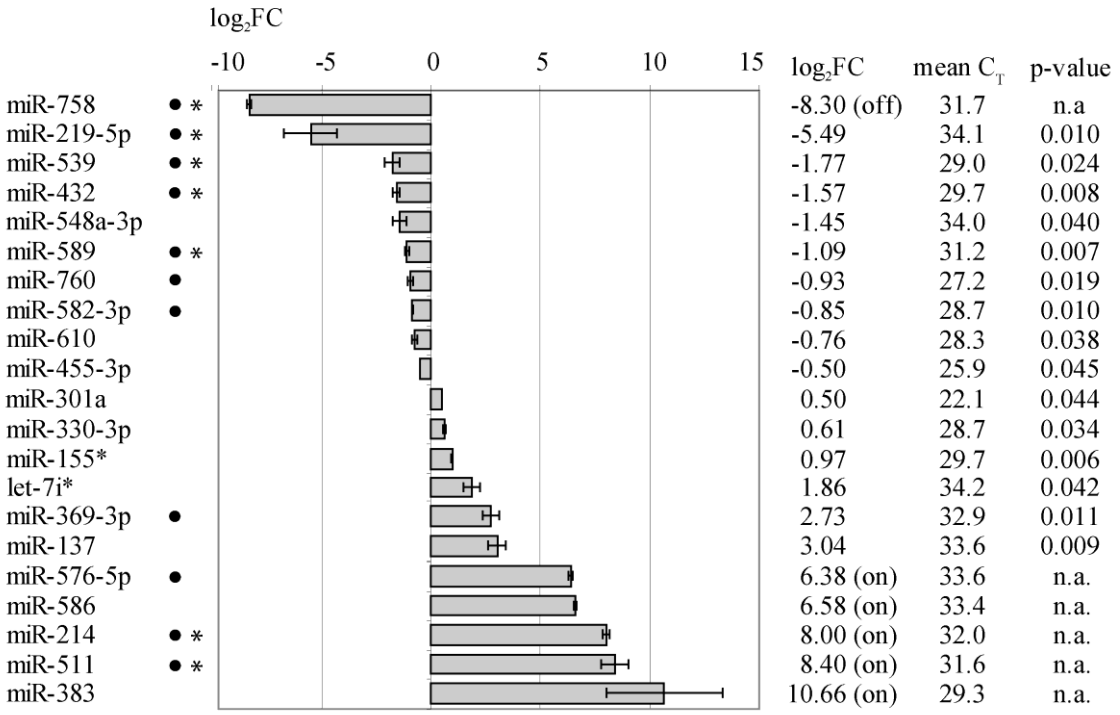

Figure 28: **Differentially expressed miRNAs after *MLL-AF9* knockdown in THP1 cells.** LDA analysis was utilized for quantitation of differential expression which is shown relative to non-targeting control siRNA treatments. Bars indicate standard error of the mean as described in material and methods. Transcripts are sorted from most down- to most upregulated. ● denotes miRNAs selected for single assay qRT-PCR confirmation, * indicates miRNAs which were confirmed via single assay qRT-PCR. Columns on the right show $\log_2$ fold change, mean threshold cycle (C_T) value (indicating expression strength) and *p*-value of the corresponding miRNA. For miRNAs which were turned „on“ or „off“, i.e. not detectable in either both control or both *MLL-AF9* knockdown samples, a lower limit of differential expression is reported as described in material and methods. Here no *p*-value can be calculated. n.a., not available.

Based on LDA results, 11 miRNAs were selected for single-assay qRT-PCR confirmation. Nine of these were selected according to strongest regulation and lowest variance of differential expression (miR-219-5p, miR-432, miR-539, miR-582-3p, miR-589, miR-758, miR-760, miR-511 and miR-214). Additional two miRNAs were selected due to predicted targets associated with leukemogenesis: miR-369-3p (potential targets e.g. ZNF521, SOCS2, B2M) and miR-576-5p (potential targets e.g. B2M, PSIP1, MAPRE2). Confirmatory qRT-PCR was performed in the pools of 5 experiments which had already been used for miRNA profiling (technical validation) and in replicate pools of additional two independent experiments (biological validation). Comparison of miRNA data generated by LDA and single-assay qRT-PCR showed a highly significant correlation between both quantitation methods (technical validation) and significant correlation when biological replicates were analyzed (figure 29). These findings support good technical and interexperimental reproducibility of our LDA miRNA profiling data. However, the linear regression between the two techniques showed a strong deviation from the perfect fit.

Percent difference from the ideal slope is -79.1% and -79.0% respectively for technical and biological validation. This suggests that in our data sets, the magnitude of differential expression of LDA profiling results emerge as more pronounced than data from single assay qRT-PCR.

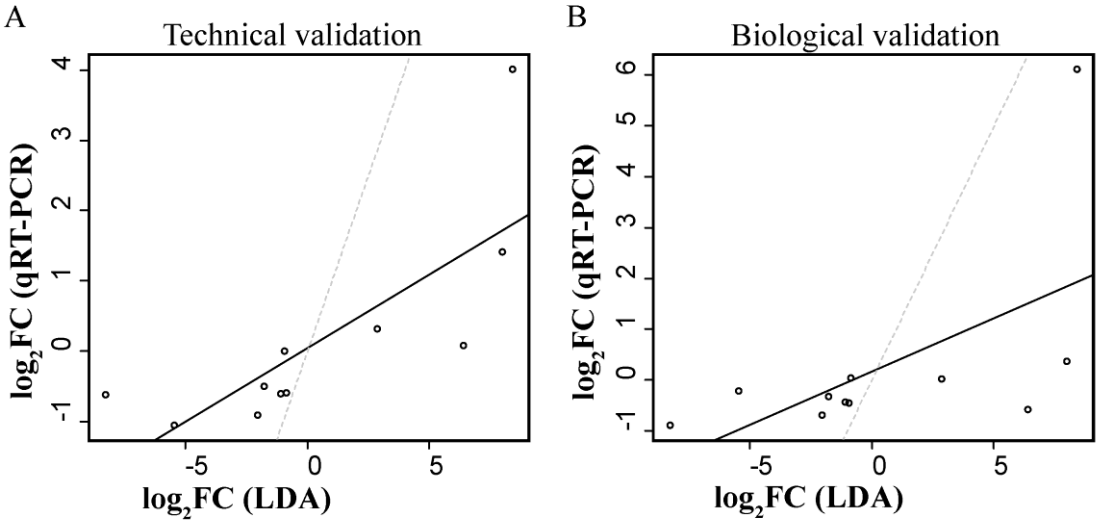

Figure 29: **Correlation between miRNA data from LDA and single assay qRT-PCR after *MLL-AF9* knockdown in THP1 cells.** MiRNA TaqMan low density array (LDA) data and single-assay qRT-PCR performed for 11 miRNAs which showed differential expression in LDA results (as described in the methods section) were compared. Linear regression (black line) is shown in comparison to a perfect fit (= ideal slope, gray dotted line). **(A)** Technical validation: single-assay qRT-PCRs were performed in identical samples ("pool 1", same reverse transcription and preamplification products) that were measured on the LDA (significant correlation, Spearman's *Rho*=0.92, p<2.2e-16). **(B)** Biological validation: single-assay qRT-PCRs were performed in additional sample pools of 2 independent experiments ("pool 2", significant correlation, Spearman's *Rho*=0.66, p=0.03). Linear regressions and Spearman's rank correlation coefficients including p-values were calculated with R.

As shown in table 9, among the 11 miRNAs selected for single assay qRT-PCR, 7 were confirmed to be differentially expressed (with a concordant regulation of at least ±0.3 $\log_2$FC). This suggests less reproducibility of miRNA profiling data as compared to gene expression data: 64% of miRNAs were confirmed via qRT-PCR as compared to 95% of genes.

Among the confirmed miRNAs, miR-511 showed the strongest differential expression and thus was chosen for further investigations. MiR-511 upregulation in a *MLL-AF9* knockdown-specific manner was additionally confirmed ($\log_2$FC 1.0, p=0.003) in three replicate experiments by qRT-PCR utilizing single-assay reverse transcription (instead of megaplex) without preamplification.

Table 9: **Confirmation of differential miRNA expression via single assay qRT-PCR.**

miRNA	log_2FC	SE
miR-511	5.07	± 1.05
miR-214	0.89	± 0.53
miR-432	-0.80	± 0.11
miR-758	-0.76	± 0.14
mir-219-5p	-0.64	± 0.42
miR-589	-0.52	± 0.08
miR-539	-0.41	± 0.09
miR-582-3p	-0.28	± 0.32
miR-576-5p	-0.25	± 0.33
miR-760	-0.22	± 0.23
miR-369-3p	0.17	± 0.15

Differential expression and standard error of the mean (SE) of miRNAs in *MLL-AF9* knockdown versus control in THP1 cells is given. MiRNAs concordantly regulated to LDA with > ± 0.3 log_2FC were regarded as confirmed (shaded in grey). Single assay qRT-PCRs were performed after megaplex reverse transcription and pre-amplification of experimental "pool 1" and "pool 2" samples.

All analyses were performed on day 8 samples which corresponds to a condition of 48 hours after serum reduction as described in 8.2.1. No differential expression of miR-511 on day 6 of experiments (i.e. before serum reduction) could be observed. To test if serum reduction was necessary to reveal this effect, miR-511 levels were also determined on day 8 samples of an experiment without serum reduction. Here, no differential expression of miR-511 was observed between *MLL-AF9* knockdown and controls. Thus, analogous to cell size reduction, serum reduced conditions are necessary to reveal the *MLL-AF9* knockdown specific effect on miR-511 expression.

8.5.2 Comparison of differential miRNA expression after *MLL-AF9* knockdown to data from patient studies

Recently, in a number of studies, miRNAs have been found to be differentially expressed among distinct cytogenetic groups of AML. However, the specific signatures differ among studies, a phenomenon which has been ascribed to the lack of standardization of the analytic methods used by different groups. (Marcucci, et al. 2011) An additional limitation for inter-study comparisons is the fact that novel human miRNAs are still being identified and thus studies performed just a few years ago may represent only a fraction of the presently known miRNAs. Nevertheless,

existing concordance of *in vivo* data to our *in vitro* data might point to potentially relevant miRNA candidates.

Class discriminating studies compare miRNA expression in certain types of leukemia to all other leukemia / cancer types. For these studies one should expect that miRNAs characterizing AML or *MLL*-aberrant leukemia should be inversely regulated after *MLL-AF9* knockdown. However, miRNAs more generally involved in the malignant state of the cells may not show up as differentially expressed in these patient data sets.

Lu et al. (2005) described a general downregulation of miRNAs in malignancies (including AML) and found clustering of samples according to miRNA expression with respect to tumor type and differentiation state. Three of the miRNAs we found upregulated in a MLL-AF9 dependent manner in our *in vitro* screen (miR-137, miR-214 and miR-301a) were shown by Lu et al. (2005) to have a reduced expression in AML versus all other samples.

Jongen-Lavrencic et al. (2008) profiled 260 miRNAs in 215 AML patient samples including 6 with *MLL* aberrations. They found 4 miRNAs being most discriminating for *MLL*-aberrant AML. However, none of these were differentially expressed in our *MLL-AF9* knockdown data set. We also searched Jongen-Lavrencics data set concerning the miRNAs we had validated to be significantly altered in a MLL-AF9 dependent manner. Here, miR-511 is reported as being downregulated in AML samples with *NPM1* and *CEBPA* abnormalities but upregulated in AML samples with inversion of chromosome 16 (Inv(16)) and *FLT3* internal tandem duplication (*Flt3*-ITD). In their study miR-214 was downregulated in AML samples with *CEBPA* abnormalities and *Flt3*-ITD. MiR-432 was found downregulated in AML samples with Inv(16) and *NPM1* aberrations but upregulated in AML with t(15;17).

Concordant to our *in vitro* study, Garzon et al. (2008) identified miR-219 to be upregulated in *MLL-AF6* and *MLL-AF9* positive AML versus all other AML cases.

An overview of concordant differential miRNA expression between our *in vitro* data and previous *in vivo* studies is given in table 10.

Table 10: **Overview of concordant differential miRNA expression between *in vitro MLL-AF9* knockdown and *in vivo* patient studies.**

miRNA	In class discriminating studies	Reference	In *MLL-AF9* knockdown
miR-137	↓ in AML	Lu et al. (2005)	↑ in LDA
miR-214	↓ in AML	Lu et al. (2005)	↑ in LDA and qRT-PCR
miR-214	↓ in AML with *CEBPA* abberations and *Flt3*-ITD	Jongen-Lavrencic et al. (2008)	↑ in LDA and qRT-PCR
miR-219	↑ in AML with *MLL-AF6* and *MLL-AF9*	Garzon et al. (2008)	↓ in LDA
miR-301a	↓ in AML	Lu et al. (2005)	↑ in LDA
miR-432	↑ in AML with t(15;17)	Jongen-Lavrencic et al. (2008)	↓ in LDA and qRT-PCR
miR-511	↓ in AML with *NPM1* and *CEBPA* abberations	Jongen-Lavrencic et al. (2008)	↑ in LDA and qRT-PCR

Comparison of our data to class discriminating (e.g. in AML versus all other leukemia samples) *in vivo* studies is shown.

8.5.3 Association of differentially expressed miRNAs to monocytic differentiation

Our differential gene expression profile (chapter 8.4) argued for a more differentiated state of *MLL-AF9* knockdown as compared to control cells. We aimed to explore if the *MLL-AF9* knockdown-specific differentially expressed miRNAs might also be related to differentiation. Publications concerning miRNAs in monocytic differentiation were thus examined, presuming that these miRNAs might be candidates for involvement in the differentiation block of leukemic monoblasts.

Lutherborrow et al. (2011) described 12 miRNAs differentially expressed between AML cases of FAB type M1 (immature myeloblasts) and FAB type M5 (more differentiated monoblasts / monocytes) and thus potentially involved in the differentiation block of M1 blasts and in differentiation along the monocytic lineage. Wang et al. (2011) studied miRNA expression in monocytic differentiation using PMA treated U937 cells and detected 32 upregulated and 12 downregulated miRNAs during differentiation. However, none of these miRNAs was found to be differentially expressed in our *MLL-AF9* knockdown study.

Tserel et al. (2011) detected miRNAs differentially expressed between monocytes and macrophages and thus potentially involved in macrophage differentiation. Among these were the upregulated miR-511 and miR-137, which we also detected as stronger expressed after *MLL-AF9* knockdown.

In our data, miR-511 was the strongest regulated of the confirmed differentially expressed miRNAs. To investigate if miR-511 is in deed associated to monocytic differentiation, THP1 cells were differentiated through the addition of phorbol 12-myristate 13-acetate (PMA) as previously described (Martino, et al. 2009). Monocyte / macrophage differentiation of THP1 cells was confirmed by Cellscreen microscopy: cells adhered tightly to the well surface and lost their round morphology (figure 30). Additionally, the transcript levels of *MLL-AF9* and *MLL*, and also of *AF9* and *HOXA9* were analyzed via qRT-PCR. As previously reported (Martino, et al. 2006), *MLL-AF9* and *MLL* mRNA levels were significantly reduced 48 hours after PMA addition (fold change 0.38 ±0.02 and 0.34 ±0.02), while additionally a significant reduction of *AF9* and *HOXA9* expression was detected, with fold change of 0.43 ±0.04 and 0.06 ±0.004 respectively.

MiR-511 expression was determined via single assay qRT-PCR in these samples. Indeed, miR-511 showed a significant twofold upregulation in PMA-differentiated compared to control treated THP1 cells (figure 31). This observation is consistent with the hypothesis that miR-511 plays a role in the differentiation process of monoblasts.

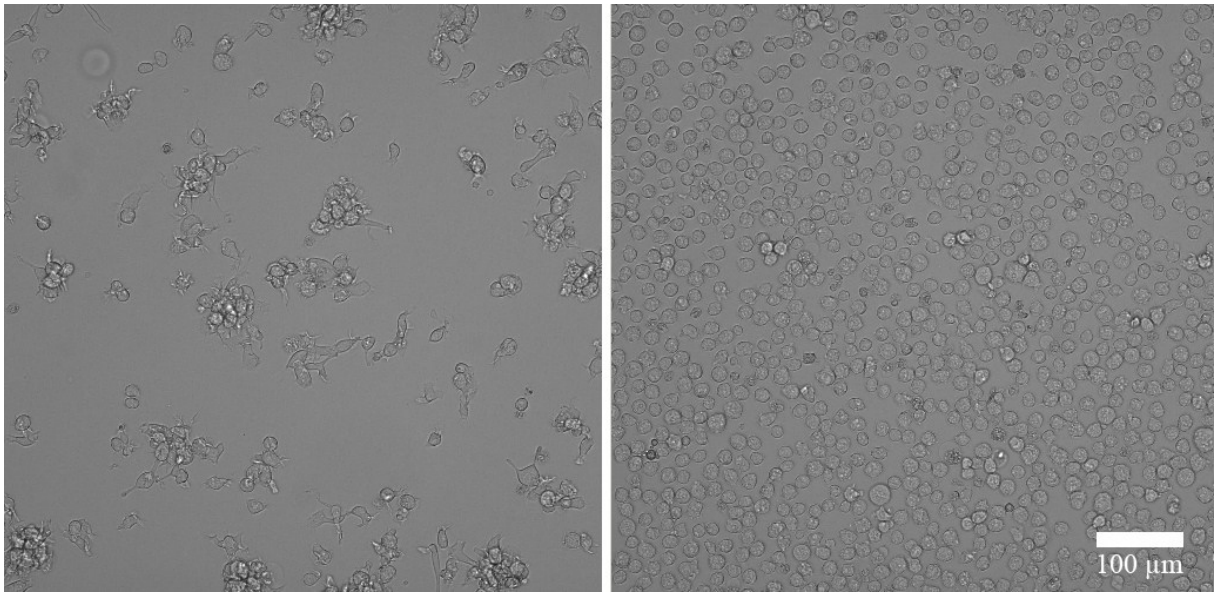

Figure 30: **Morphological changes of differentiated THP1 cells.** THP1 cells were treated for 48 h with phorbol 12-myristate 13-acetate (PMA, left image) and compared to control (right image). Cellscreen images of two regions of interest (ROIs) as described in material and methods are shown.

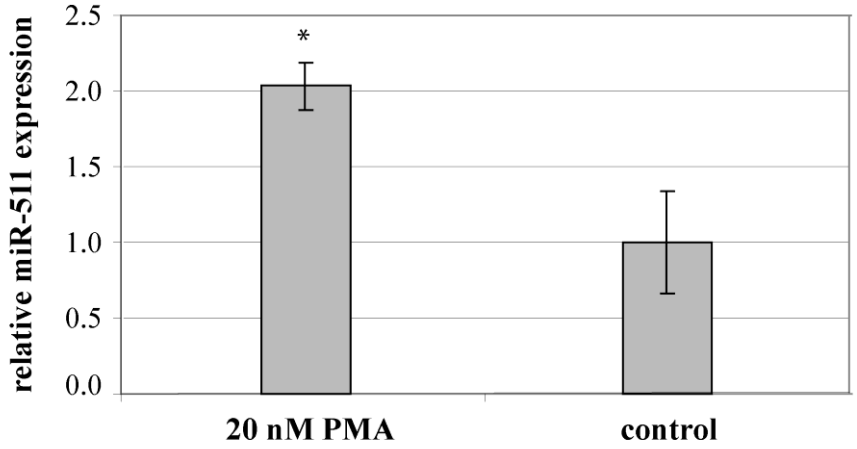

Figure 31: **Expression of miR-511 in differentiated THP1 cells**, 48 h after phorbol 12-myristate 13-acetate (PMA) addition. The experiment was performed in triplicate. Bars indicate standard error of the mean.* p=0.05

8.5.4 Potential direct targets of upregulated miR-511

Recently, the first two direct targets of miR-511, *TLR4* and *CD80*, have been experimentally validated (Tserel, et al. 2011). However, these two genes were not detected as differentially expressed in our data set. To further explore the functional role of miR-511, potential additional direct targets of this miRNA were searched via computational techniques.

Computational target prediction remains a complex task as evidenced by the existence of a large number of available algorithms which lead to notable different results. Employing more than one algorithm is thus recommended to improve the reliability of predictions. We performed an in-depth *in silico* target prediction for miR-511 using 9 different prediction algorithms via miRWalk (Dweep, et al. 2011). Among the predicted targets, potentially important ones within this biological setting were selected for further analysis. Figure 32 gives an overview of the selection process of predicted targets of miR-511 with potential 3'-UTR binding sites and includes information on their connection to leukemia. MiRWalk predicted a total of 8112 genes as potential targets for miR-511. Among these, according to our gene expression microarray results, 730 genes were differentially expressed upon *MLL-AF9* knockdown ($p<0.05$). Of those, 445 genes (61%) were downregulated and thus inversely correlated to miR-511 as expected for true miRNA-target gene pairs. These 445 potential target genes were then subjected to functional disease ontology (FunDO) analysis in order to identify leukemia and cancer associated genes. Five additional genes were added to the resulting list because of previously reported functional links to leukemia. As result, 19 leukemia and 22 cancer associated genes were recovered. These were rated by literature research to determine if the observed direction of regulation matched their described role in malignancy. Finally 9 genes (*AFF1 (alias AF4)*, *AFF4*, *FGFR1*, *FGFR3*,

IGF2BP2, *MAPRE2*, *DACH1*, *MDM2*, *MEF2C*) were selected as likely candidate targets of miR-511 within this biological setting.

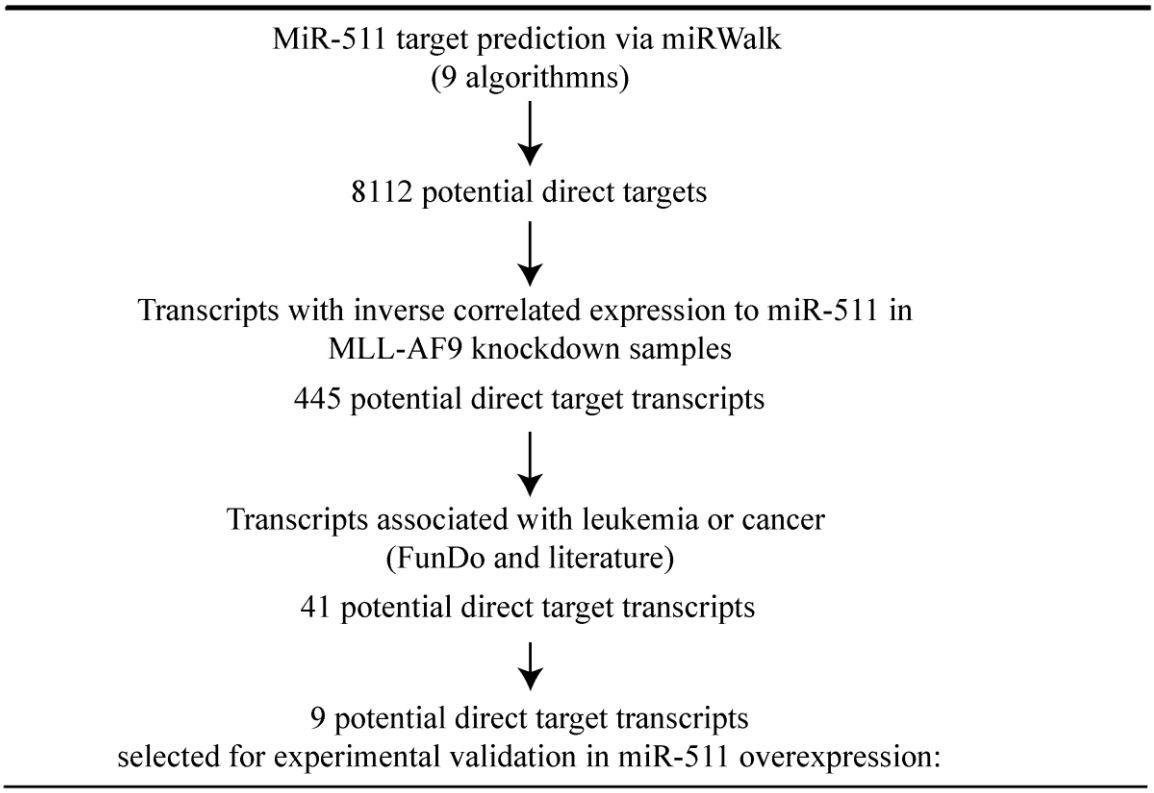

Gene	Disease association	Predicting algorithms	Function / link to malignancy
AFF1	FunDO: leukemia	3	Component of super elongation complex (SEC), which is recruited by many MLL-fusion proteins (Mohan et al., 2010)
AFF4	FunDO: leukemia	2	Component of super elongation complex (SEC), which is recruited by many MLL-fusion proteins (Mohan et al., 2010)
DACH1	Literature (see right)	2	Transcription factor, class discriminating gene for MLL chimeric fusion gene leukemia (Ross et al., 2004)
FGFR1	FunDO: cancer	4	Fibroblast growth factor receptor 1, translocations involved in myeloproliferative syndrome (EMS) including CML (Demiroglu et al., 2001; Sohal et al., 2001)
FGFR3	FunDO: cancer	4	Fibroblast growth factor receptor 3, translocation involved T-cell lymphoma, AML (Kang et al., 2009)
IGF2BP2	FunDO: leukemia	1	Insulin-like growth factor 2 mRNA binding, associated with MLL-AF4 leukemia (Stoskus et al., 2011)
MAPRE2	FunDO: leukemia	4	Tubulin binding protein, associated with Nup98-HOXA9 AML (Ghannam et al., 2004)
MDM2	Literature (see right)	2	Major regulator of tumor suppressor p53 (Okoshi et al., 2011), polymorphismn associated with AML (Phillips et al., 2010)
MEF2C	Literature (see right)	2	Transcription factor, class discriminating gene for MLL chimeric fusion gene (Ross et al., 2004)

Figure 32: **Overview of the selection process of predicted targets of miR-511 with potential 3'-UTR binding sites for experimental validation.** Included is information on their link to malignancy.

For confirmatory purposes, miR-511 upregulation experiments were performed in THP1 cell line via transfection of miR-511 or negative control mimics (Pre-miR™ miRNA Precursor Molecules). MiR-511 levels were determined via qRT-PCR and proofed to be strongly upregulated in miR-511 mimic treatments as compared to negative control mimic treated cells (log_2FC of 19.8 ±0.25). Levels of miR-511 after upregulation roughly resembled the expression strength of the strongest expressed endogenous miRNA in THP1. Expression of the selected 9 potential target genes was subsequently analyzed 48 and 72 h after treatment. Except for *DACH1*, an expected downregulation was observed, although these reductions in expression strengths did not reach significance (figure 33).

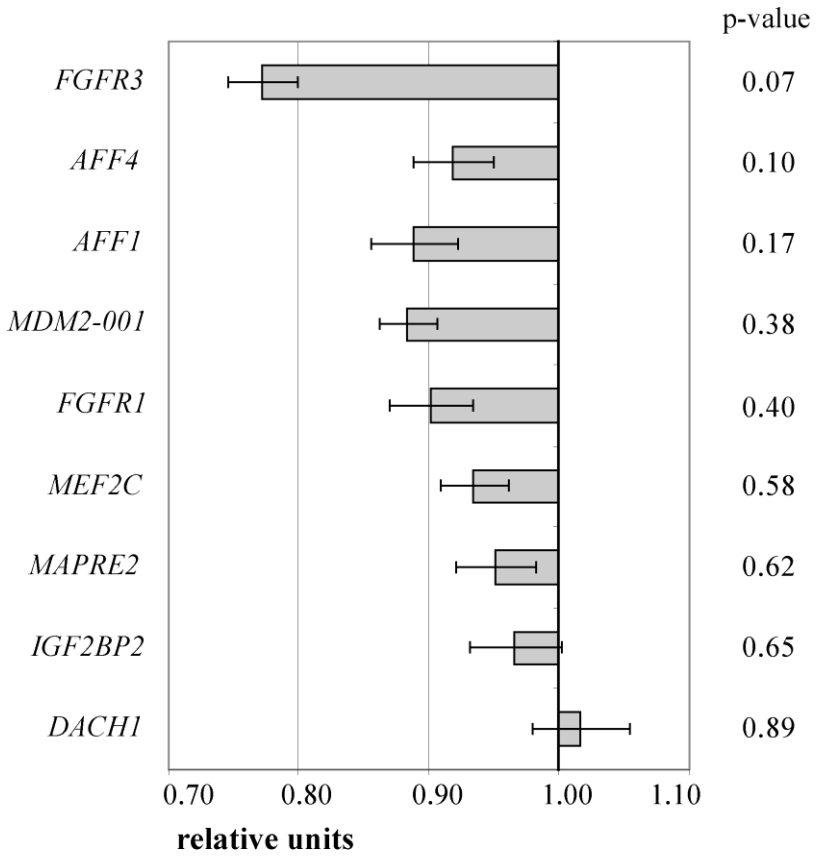

Figure 33: **Effect of transient upregulation of miR-511 in THP1 cells on potential direct target genes.** Expression levels were measured by qRT-PCR 48 and 72 h after transient transfection of miR-511 or control mimics under serum reduced conditions (0.5% FBS). Transcripts are sorted according to *p*-value. Graph represents four experimental data sets. Bars indicate standard error of the mean.

9 Discussion

In this study we employed RNAi to functionally interfere with endogenous *MLL-AF9* in the monoblastic cell line THP1. This technique served to deduce candidate genes and miRNAs for mediation of leukemogenic effects of MLL-AF9. Besides revealing downstream effects of MLL-AF9, our study aimed to identify new potential therapeutic targets of *MLL*-aberrant acute myeloid leukemia. This is relevant, as prognosis is still poor for this type of leukemia and because strategies aiming to interfere directly with MLL-AF9 function might be too toxic. We performed a specific and efficient knockdown of *MLL-AF9* in the cell line THP1 and for the first time describe, beside phenotypic changes, comprehensive gene and miRNA expression profiles in this setting. Both sources of information, gene expression and miRNA expression, may help with the identification of future therapeutic targets.

9.1 Experimental Design

We aimed to identify downstream effects of *MLL-AF9* via RNAi. The goal of our experimental design was to avoid conditions that lead to unspecific effects or to masking of MLL-AF9 specific effects. To this end a number of measures were taken: (1) To avoid the contamination of results by off-target effects, the experimental design included the utilization of two distinct, highly specific and effective siRNAs against *MLL-AF9* in THP1 cells as well as of two distinct control siRNAs. (2) The experimental design should allow sufficient time for reversal of potential epigenetic changes. This was accomplished by a prolonged duration of experiments over eight days. (3) We strived to constrain the masking of MLL-AF9 specific effects through the strong mitogenic influence of fetal bovine serum (FBS) by reduction of FBS to 0.5% from day 6 of experiments onwards. This FBS concentration was determined to lead to culture conditions in which THP1 cells remain proliferating over at least 6 days while showing a clearly reduced doubling rate. (4) To reduce the effects of interexperimental variation, samples were pooled from five independent experiments for the analysis of gene and miRNA profiles.

Altogether, these experimental steps resulted in a high reproducibility of the phenotypic as well as gene and miRNA expression data we generated. In functional disease ontology (FunDO) analysis, of all possibly associated disease terms, the term *leukemia* was significantly and on prime position associated with our differentially expressed gene data set, a fact which confirms the validity of our experimental approach in this biological context.

9.2 Confirmation of *MLL-AF9* knockdown

Efficiency of *MLL-AF9* knockdown was monitored on mRNA level over the time course of experiments and reached a residual expression of 22 ±6 % at the time point of gene and miRNA expression analyses (day 8).

MLL-AF9 protein is hard to detect by standard techniques, as suggested by previous studies not being able to show MLL-AF9 reduction on protein level after knockdown (Kawagoe, et al. 2001; Pession, et al. 2003). In our study, MLL-AF9 from THP1 cells could only be detected on Western blot performed with protein isolated from the organic phase of Qiazol (similar to Trizol) which is a strong denaturing agent. However, this kind of protein isolate was not suitable for quantitative procedures, because complete dissolution of intermediate protein pellets can hardly be achieved. Cell lysates generated with standard lysis buffers, e.g. Laemmli sample buffer or RIPA buffer, did not yield any MLL, AF9 or MLL-AF9 bands in THP1 samples. Surprisingly, however, MLL and AF9 wildtype was readily detected in MCF-7 and HELA control lysates with identical procedures.

A possible explanation is that MLL-AF9 binding to DNA is stronger as in MLL wildtype, leading to complexes which are not easily dissolved even after sonication. However, this would not explain the simultaneous non-detectability of MLL and AF9 wildtype protein in conventional THP1 protein lysates. Alternatively, a tendency of MLL-AF9 to form protein aggregates and co-aggregation of MLL and AF9 wildtype protein might explain this finding. This hypothesis is supported by the fact that *protein folding* was a significantly enriched functional gene ontology term associated with our differential gene expression set after *MLL-AF9* knockdown. Within this annotation term, the vast majority (88%) of transcripts was downregulated after *MLL-AF9* knockdown. Protein folding is a similar process in the test-tube and within cells and is dependent on certain positions in the amino acid sequence (Taubes 1996). Because MLL-AF9 is not a physiologically occurring protein, it might be more prone to form aggregates, a feature that – if confirmed – might play a role in MLL-AF9 related malignancy (chapter 9.4.1.4, page 92).

An alternative and innovative method we employed (TaqMan Protein Assay described on page 25) was also not sufficient to quantify MLL-AF9 protein. To overcome this problem, we utilized *HOXA9* transcript level as surrogate marker for MLL-AF9 protein level. This indirect method is able to indicate efficiency of *MLL-AF9* knockdown because *HOXA9* transcription is known to be raised through direct interaction between MLL-AF9 protein complex and the *HOXA9* promoter (Erfurth, et al. 2008; Cierpicki, et al. 2010). Thus we were able to indirectly confirm an efficient functional knockdown of MLL-AF9 in the cell line THP1 on protein level.

9.3 Cellular phenotype and functional endpoints of *MLL-AF9* knockdown

Various features such as cell cycle distribution, proliferation rate, apoptosis rate and mean cell size were assessed to screen for phenotypic and functional consequences of prolonged knockdown of *MLL-AF9* in THP1 cells.

In our study, we were not able to detect effects on proliferation, cell cycle or apoptosis with the techniques employed. Wiederschain et al. (2005) have previously demonstrated that MLL-AF9 and other MLL-fusion proteins can downregulate p53-mediated induction of p21, MDM2 and Bax and could thus act antiapoptotic. Kawagoe et al. (2001) and Pession et al. (2003) detected inhibition of cell growth and a moderate increase of apoptosis after 1 - 3 days after *MLL-AF9* knockdown in THP1 cells. However, experimental conditions between our and these studies are not directly comparable. While we performed a prolonged *MLL-AF9* knockdown via siRNAs over 8 days in the monoblastic leukemia cell line THP1, Kawagoe et al. (2001) and Pession et al. (2003) employed antisense oligodeoxyribonucleotides (ODNs) in THP1 and detected differences up to three days after *MLL-AF9* knockdown, while Wiederschain et al. (2005) expressed *MLL*-fusion constructs in epithelial and lymphoblastic leukemia cell lines. Alternatively, the lack of observable effects on proliferation and apoptosis in our study might be explained by the absence of sufficient apoptosis inducing stimuli, by residual MLL-AF9 protein level or by different secondary mutations within the cell line.

MLL-AF9 knockdown in THP1 led to a highly significant cell size reduction of about 0.3 µm. In order to retain cell size homeostasis, cells need to coordinate cell growth and division, while slowly growing cells tend to be smaller (Shin, et al. 2009). However, changes in proliferation, cell cycle distribution or apoptosis appear unlikely to be the underlying mechanisms of the cell size reduction we observed. Apoptosis is expected to lead to a high magnitude of cell size reduction and finally to cells dissolving into small vesicles. Thus we expected that these phenomena would all lead to a difference in cell number within our prolonged study design. However, we detected no effect on cell number even up to day 12 of *MLL-AF9* knockdown.

Genomic scale gene deletion analyses in the yeast *Saccharomyces cerevisiae* revealed 49 genes involved in cell size regulation without profoundly changing cell proliferation. Among these, the majority (71%) have putative human homologs (Zhang, et al. 2002). We searched our data set for differential expression of these human homologs. Indeed, two gene homologs whose deletion led to abnormally small yeast phenotypes were downregulated in our data set: the gene *RPL34* encoding a ribosomal protein involved in protein synthesis as well as the gene *RASGRF1* (ras protein-specific guanine nucleotide-releasing factor 1) encoding a signal transduction protein. Remarkably, repression of *RASGRF1* was recently linked to quiescence in very small

embryonic-like stem cells in adult murine tissues including bone marrow (Shin, et al. 2009) and thus repression of this gene might connect cell size with quiescence.

Deletion of the homolog of *AF9* (*ANC1*) led to an abnormal large phenotype in yeast (Zhang, et al. 2002). In our *MLL-AF9* knockdown within THP1 cells, *AF9* wildtype was not differentially expressed at transcript level. However, aggregation of MLL-AF9 protein – as suspected due to our biochemical findings (see 9.2 on page 84 and 9.4.1.4, page 92) – might account for this phenomenon. Partially folded proteins may form self-aggregates, e.g. due to mutations (Taubes 1996). If MLL-AF9 would co-aggregate AF9 due to a partial identical sequence, MLL-AF9 could render AF9 protein non-functional and – in analogy to deletion of yeast AF9 homolog – could lead to a cell size increase. Knockdown of *MLL-AF9* could alleviate AF9 co-aggregation thus returning its functional activity and reducing cell size. Supportive for this hypothesis is the fact that besides the MLL-AF9 band also the MLL and AF9 wildtype bands are non-detectable in conventional lysates of THP1 cells (8.2.2, page 42).

Cell size has been previously described to be largely determined by ribosome biogenesis, which is dependent on the activity of RNA polymerase I (Sun, et al. 2006a). Our expression data indeed point to reduced ribosome biogenesis after *MLL-AF9* knockdown as we observed reduced expression of *TTF1* (transcription termination factor, RNA polymerase I) as well as the upregulation of *CDKN2A* mRNA. TTF1 regulates RNA polymerase I, and thus rRNA transcription, while *CDKN2A* gene product p14/p19^{ARF} (ARF) is a tumor suppressor, which represses ribosome biogenesis by binding and inactivating the nucleolar localization motif of TTF1 (Lessard, et al. 2010). Additionally, all transcripts within the enriched gene annotation term *translational elongation* - among these seven encoding ribosomal proteins - were downregulated (see figure 23 on page 58 and supplementary figure 1 b on page 167).

Another contributing mechanism for the size reduction after MLL-AF9 depletion might be a raised intracellular (cytosolic) Ca^{2+} concentration, as previously described in many cell types (Tanaka, et al. 2004a; Koivusalo, et al. 2009). In this context, Ca^{2+} is believed to serve as a signal for activation of channels that mediate a net loss of ions, thus leading to a regulatory volume decrease (Koivusalo, et al. 2009). Our gene expression data support this possibility: the calcium transporter ATP2B2, which is responsible for maintaining low free cytosolic Ca^{2+} levels, as well as calreticulin (CALR), a major Ca^{2+} storage protein in the lumen of the endoplasmic reticulum, were found downregulated after *MLL-AF9* knockdown.

The aquaporines AQP1, AQP3 and AQP7P1 were downregulated in our data after *MLL-AF9* knockdown. Though this was not previously described to influence cell size, it seems

conceivable that reduced expression of aquaporines may inhibit water entry into the cells with the consequence of cell size reduction.

9.4 Differential gene expression profile after *MLL-AF9* knockdown

We analyzed differential gene expression profiles after *MLL-AF9* knockdown with the prospect to better understand the transforming activities of MLL-AF9 and to find downstream genes encoding proteins suitable as therapeutic targets.

We employed the term "gene expression" for analyses of coding and non-coding transcripts exclusive of small RNA species which are not typically included in these profiling techniques, while transcript levels of miRNAs are denoted as miRNA expression.

The goal of our data analysis of differential gene expression after *MLL-AF9* knockdown was to include the highest number of differentially expressed transcripts without rising the false positive rate. To this end, we rated the differential expression of identical replicate probe sets as a function of *p*-value cutoff. We detected a plateau of high percentage of significant identical replicate probes up to $p<0.03$ and a subsequent, almost linear decline with less stringent cutoffs. Thus, the cutoff *p*-value of the moderated *t* test was set to below 0.03.

This analysis resulted in 1269 unique genes being differentially expressed between *MLL-AF9* knockdown and control treatments. In line with our number of observed transcripts influenced by *MLL-AF9* knockdown, it has previously been estimated that *MLL* and *MLL*-fusion proteins target about 1000 genomic loci (Slany 2009).

Among the detected 1269 differentially expressed gene transcripts, the majority (64%) were found downregulated after *MLL-AF9* knockdown. Apparently, this data set contains both, direct targets of MLL-AF9 as well as an array of secondary changes in gene expression. Nevertheless, this regulatory imbalance confirms the hypothesis that MLL-AF9 mainly acts as a transcriptional activator as has been deduced from mechanistic studies of *MLL* aberrations (Slany 2009; Mohan, et al. 2010; Margaritis, et al. 2008).

To interpret this extensive gene expression data set, 1) functional gene ontology was employed to describe the biological processes behind the full data set (section 9.4.1), 2) a strategy to filter out and rate genes presumably important for mediation of leukemogenic effects of MLL-AF9 was created (section 9.4.2) and 3) an exploration of the latter gene set concerning their druggability was performed (section 9.4.3).

9.4.1 Biological processes potentially involved in mediation of MLL-AF9 leukemogenic effects

A standard procedure to track down biological meaning behind large lists of genes is enrichment analysis of functional gene ontology. This kind of analysis was performed for the set of differentially expressed genes after *MLL-AF9* knockdown in THP1 cells. The results should finally serve to identify processes which may be involved in MLL-AF9 mediated leukemogenesis. To structure the results consisting of 43 functional ontology annotation terms, these were grouped into 5 higher-order terms.

Based on the results (a simplified overview is given in table 11), we discuss in the following sections a number of biological processes and transcripts which we propose to be involved in mediation of MLL-AF9 leukemogenic effects.

Table 11: **Overview of *MLL-AF9* knockdown associated enriched functional gene annotations**

higher-oder term	/	functional annotation term
proliferation, cell growth and death		Regulation of apoptosis Negative regulation of apoptosis Positive regulation of apoptosis Anti-apoptosis Growth HMG17 Translational elongation
differentiation		Antigen processing and presentation Antigen processing via MHC II[1] Defense response Immune response Phagocytosis Endocytosis Positive regulation of exocytosis Saposin B Leukocyte chemotaxis Response to bacterium Regulation of cytokine production Actin binding Phorbol ester binding Response to vitamin Response to retinoic acid Hematopoietic cell lineage
early development		Homeobox, conserved site Pattern specification process Embryonic development[2]
calcium associated		Calcium binding Calcium ion homeostasis Calmodulin-binding
other		Response to estrogen stimulus Response to estradiol stimulus Protein folding Antigen presentation via MHC I[3]

This table depicts a simplified version of figure 23 on page 58. Functional annotation terms were manually assorted to 5 higher-order terms according to the major role of the biological process within this biological setting. Annotation terms which were assigned to two higher-order terms are depicted between these two, indicated by dotted division lines. Annotation terms which could not be assigned to one of the four specific higher-order terms are collected under the term "other". Some annotations were abbreviated as indicated by superscript numbers: [1]Antigen processing and presentation of peptide or polysaccharide antigen via MHC class II, [2]Embryonic development ending in birth or egg hatching, [3]Antigen processing and presentation of peptide antigen via MHC class I.

9.4.1.1 Proliferation, cell growth and cell death

We hypothesized that transcripts downstream of MLL-AF9 which are involved in proliferation, cell growth and cell death may contribute to the malignancy of MLL-AF9.

We found a high number of differentially expressed genes potentially playing a role in apoptosis. This suggests an effect on the apoptotic functions of the cells. However, the amount of apoptotic cells within *MLL-AF9* knockdown was not detectably altered. This might be due to the absence of a sufficient apoptotic stimulus in the culture or due to other conditions influencing the dynamic apoptosis network.

Some differentially expressed genes coding for anti-apoptotic regulator proteins showed reduced expression after *MLL-AF9* knockdown and thus might be involved in malignancy of *MLL-AF9* positive the cells. These were *SOCS2*, *MEF2C*, *STAMBP*, *HSP90B1*, *ANXA4*, *CFL1* and *BRAF* (see supplementary figure 1 b on page 167).

Two gene transcripts with HMG17-domains were strongly expressed and downregulated, while a third showed intermediate expression strength and was upregulated. This group of proteins contains non-histone components of chromatin thought to be involved in unfolding higher-order chromatin structure, facilitating the transcriptional activation of genes (Porkka, et al. 2002) and affecting DNA replication, recombination and repair (Pogna, et al. 2010). The included gene *HMGN2* has previously been found overexpressed in CML and other cancer types and association to proliferation has been suggested (Kondos, et al. 1995).

Expression rates of ribosomal proteins were previously associated with cell growth and proliferation and are altered in numerous cancer types (Andersen, et al. 2005; Ruggero, et al. 2003; Wang, et al. 2006). Thus, the finding that genes encoding ribosomal proteins (within the annotation term *translational elongation*) were downregulated as well as the occurrence of the annotation term *growth* in our MLL-AF9 depleted THP1 cells would point to an influence on proliferation or cell growth. However, this could not be observed on functional level implicating that potential effects may be either too weak to be detected by our tools or may be restricted to more unfavorable growth conditions.

9.4.1.2 Differentiation

We observed a raised expression of the monocytic maturation markers *CD14*, *BCL6*, *CEBPB*, *EGR2*, *FOS*, *KLF4*, *MAFB*, *MNDA* (Lutherborrow, et al. 2011; Klco, et al. 2011; Kelly, et al. 2000), *MHC class II* and *SERPINA1* (Abrink, et al. 1994) as well as a reduced expression of markers of immature cells of the monocytic lineage (*ELANE*, *CTSG* and *PRTN3*). This finding is strongly suggestive for maturation of THP1 monoblasts after *MLL-AF9* knockdown.

Gene ontology analysis of our data was also in line with a more differentiated state of the cells after MLL-AF9 reduction.

Monocytes are cells of the innate immune response responsible for phagocytotic uptake and digestion of microbes and particles (via lysosomes), antigen presentation as well as cytokine production and release (via exocytosis). Monocytes may adhere to vessel walls and migrate from the blood stream to tissues where they further differentiate into macrophages or dendritic cells. Within differentiation of monocytes, it has been suggested that phagocytosis is acquired prior to microbicidal activity, which again develops prior to locomotion (Glasser 1981).

The most significantly enriched functional annotations concerned antigen processing and presentation, especially via MHC class II. This is a major biological function of differentiated monocytes and macrophages. Upregulation of HLA class II gene transcripts has previously been associated with differentiation of monoblasts, while THP1 cells were observed to have reduced HLA class II expression levels compared to mature monocytes (Abrink, et al. 1994). We observed an upregulation of all differentially expressed genes within the category antigen processing and presentation via MHC class II. This finding might be explained by the transcriptional upregulation of the transcription factor and master controller of MHC class II, class II major histocompatibility complex transactivator *CIITA* (Ting, et al. 2002). Another transcriptional activator gene of MHC class II, regulatory factor X 5 (*RFX5*), was found downregulated, but can activate transcription only in cooperation with CIITA (Scholl, et al. 1997). *RFX5* was strongly expressed in our data set and its downregulation does not reduce MHC class II expression, suggesting that the residual level of RFX5 is sufficient for MHC class II expression.

Further genes indirectly indicating a more differentiated cellular status fell into the following monocyte / macrophage-related enriched annotation terms: *phagocytosis*, *regulation of cytokine production*, *endocytosis*, *defense response*, *response to bacterium*, *positive regulation of exocytosis*, *Saposin B* (lysosomal proteins), and *actin binding* (may indicating changes in cell shape and motility). Additionally, *phorbol ester binding*, *response to vitamin* and *response to retinoic acid* suggested links to the differentiating effects of PMA, 1,25- dihydroxyvitamin D3 and retinoic acid on monoblasts. All genes within the annotation *hematopoietic cell lineage* were upregulated, as was the majority of transcripts within the terms *immune response* and *defense response*.

Other genes (*EGR2*, *VDR*, *SP9* and *ZNF521*) of the differentiation associated annotations are discussed in section 9.4.2).

Taken together, these findings are consistent with the hypothesis that MLL-AF9 depletion leads to a partial release of the differentiation block in THP1 cells.

9.4.1.3 Early development

The three enriched ontology annotation terms *homeobox conserved site*, *pattern specification process* and *embryonic development ending in birth or egg hatching* were grouped to the higher-order term "early development". The wildtype genes involved in the *MLL-AF9* translocation, play essential roles in embryogenesis and their disruptions lead to homeotic transformations indicating a role in pattern specification (section 6.2, page 5). Thus deregulation within these terms might mainly be related to their wildtype functions. However, some of the genes encompassed in these annotations (e.g. *HOX* genes, *PBX3*, *HIPK2* and *BMI1*) have additionally been reported to play a role in leukemogenesis (Eklund 2007; Milech, et al. 2001; Li, et al. 2007; Yuan, et al. 2011a).

9.4.1.4 Calcium associated gene functions and protein folding

Our set of differentially expressed genes after *MLL-AF9* knockdown was significantly enriched in calcium associated annotation terms like *calcium-binding* and *calcium ion homeostasis*. This finding suggests that the cellular calcium homeostasis is influenced by MLL-AF9.

The charged calcium ion, together with the charged phosphate ion, is the primary signaling element of the cell. It is the most tightly regulated ion and influences every aspect of a cell's life and death, including differentiation, proliferation and apoptosis. Ca^{2+} binds to thousands of proteins and influences their localization, association and function. (Clapham 2007)

Decreased levels of intracellular Ca^{2+} may lead to endoplasmatic reticulum (ER) stress and thus activate the unfolded protein response (Schardt, et al. 2011).

Protein folding was an enriched annotation term with remarkable 88% of the transcripts being downregulated in *MLL-AF9* knockdown. In compartmentalized eukaryotic cells, integrity of the protein-folding environments has to be ensured in the cytosol, the endoplasmatic reticulum (ER) as well as in the mitochondria (Haynes, et al. 2010). To this end, cells contain compartment-specific chaperones as well as specific mechanisms protecting them from unfolded or misfolded protein: the heat-shock response in the cytoplasm, the unfolded protein response (UPR) in the ER and the mitochondrial UPR (Haynes, et al. 2010).

In our data set, genes encoding chaperones of all three compartments were downregulated: e.g. *HSP90AA1* and *PPIC* from the cytoplasm, *HSP90B1* and *CALR* from the ER and *HSCB* from

mitochondria (and the cytoplasm). This finding might be a consequence of the reduced expression of protein coding transcripts in general (64% of differentially expressed transcripts were downregulated) and ribosomal genes in particular. However, our biochemical findings on MLL-AF9 protein were suggestive of its disposition to aggregate (section 9.2, page 84). Thus reduced expression of protein folding genes may alternatively be caused by an attenuated heat-shock response within the cytoplasm due to less misfolded MLL-AF9 protein after MLL-AF9 depletion and / or an attenuated UPR, e.g. due to MLL-AF9 dependent effects on the cellular calcium ion homeostasis. Both mechanisms, the heat-shock response and the UPR, are interrelated as they share the proteasome and the eIF2alpa kinase regulatory pathway (Heldens, et al. 2011).

Heat shock proteins have previously been found to be overexpressed in a wide range of human cancers, including hematological malignancies (Yokoyama, et al. 2002) and evidence is accumulating for the involvement of the unfolded protein response in the pathogenesis of many tumor types as well as in AML linked to fusion genes (Schardt, et al. 2011). Thus, these interrelated mechanisms might also play a role within MLL-AF9 dependent leukemogenesis.

9.4.1.5 Estrogen signaling

Estrogen signaling was also a significantly enriched functional ontology term within our MLL-AF9 dependent gene expression data set and encompassed the terms *response to estrogen stimulus* and *response to estradiol stimulus*.

Promoter methylation of estrogen receptor has been previously associated with improved survival in adult AML patients and is reduced in AML of the subtypes M4 and M5 according to FAB classification (Li, et al. 1999). As *MLL-AF9* positive myeloid leukemias are mainly of the FAB type M5, this might point towards importance of estrogen regulated genes in MLL-AF9 leukemias.

A number of previous observations also point towards importance of estrogen signals in leukemogenesis and in particular in *MLL*-associated leukemogenesis: (1) high estrogen levels may lead to *MLL* gene aberrations, (2) *MLL*-rearrangements have a higher incidence in maternal ALL cases, (3) *MLL*-aberrant leukemia is associated with increased birth weight, which in turn is positively correlated with maternal estradiol levels (Aljurf, et al. 2011; Nagata, et al. 2006) and (4) proteins of the MLL family may bind to gene promoters in an estradiol-dependent manner (Ansari, et al. 2009; Ansari, et al. 2011).

MLL-fusion proteins might also indirectly influence the cellular protein level of estrogen receptor: The nuclear aryl hydrocarbon receptor AHR, which emerged as transcriptionally

suppressed by MLL-AF9 in our data set, is known to be important for estrogen receptor alpha ubiquitination and degradation (Bunaciu, et al. 2011).

A widespread crosstalk of retinoic acid and estrogen signaling to regulate gene expression in opposing directions was observed within a breast cancer cell line (Hua, et al. 2009). Retinoic acid is well known for promoting differentiation of monoblasts (Matikainen, et al. 1994). Also in line with these observations, stimulation of membrane-bound estrogen receptor inhibited retinoic acid-induced functional differentiation of HL-60 myeloblastic leukemia cells (Kauss, et al. 2008).

These findings support the hypothesis that hematopoietic progenitor cells, expressing high levels of estrogen receptor and / or being within an environment of strong estrogen signaling might be prone to transform into leukemic blasts. This transformation might arise via formation of *MLL*-aberrations which in turn support estrogen receptor expression and inhibit retinoic acid signaling pathways thus leading to a block in differentiation.

9.4.1.6 Evasion of immunosurveillance

We found a strong downregulation of *ZNF521* and reduced expression of most genes within functional terms related to MHC class I antigen presentation (the terms *antigen processing and presentation* as well as *antigen processing and presentation of peptide antigen via MHC class I*). This concerned downregulation of the genes *HLA-B*, *B2M*, *CALR*, *HSP90AA1* and *HSPA2* after *MLL-AF9* knockdown.

MHC class I deficient tumor clones have been found to be able to escape T cell immune responses, but might be more susceptible to NK cell-mediated lysis (Algarra, et al. 2004). The zinc finger transcription factor ZNF521 has previously been associated with enhanced MHC class I expression and reduced susceptibility to NK cell-mediated lysis (La Rocca, et al. 2009). Pig cells transgenic for human *HLA-E*/*B2M* are protected against human NK cell-mediated cytotoxicity (Weiss, et al. 2009). These facts support the importance of HLA class I and B2M proteins for avoiding NK cell-mediated lysis. In this context, MLL-AF9-associated, strong expression of *B2M* might suggest that MLL-AF9 positive cells are able to avoid NK cell-mediated cytotoxicity, a capability potentially being abrogated after knockdown.

We detected a strong transcriptional upregulation of all differentially expressed genes involved in antigen processing and presentation via MHC class II (see section 9.4.1.2 on page 91). Loss of MHC class II gene expression has previously been shown to be strikingly correlated with poor patient outcome and has been linked to decreased immunosurveillance via cytotoxic T cells in large B cell lymphoma patients (Rimsza, et al. 2004).

Additionally the enriched annotation term *leukocyte chemotaxis* might point towards changes related to immunosurveillance. This term included the strong transcriptional upregulated chemokine CCL2. AML blasts have been described to produce different amounts of CCL2 which influences the number of monocytes migrating towards AML blasts (Legdeur, et al. 2001). Plasma levels of CCL2 have been shown to be decreased in patients with AML of the FAB subtype M4 and M5 (Mazur, et al. 2007). Thus, upregulation of CCL2 might lead to improved immunosurveillance of M4 and M5 blasts. In this context, CCL2 has been proposed for adoptive immunotherapy (Legdeur, et al. 2001).

9.4.2 Candidate genes for mediation of MLL-AF9 leukemogenic effects

To prioritize likely candidates for mediation of MLL-AF9 leukemogenic effects within the 1269 differentially expressed genes after *MLL-AF9* knockdown, a subset of these genes had to be selected for further literature research concerning their potential as mediators of MLL-AF9 leukemogenic effects. To achieve this task, four criteria were applied as outlined in results section 8.4.3 (page 50).

Magnitude of differential expression is often taken as hint for biological importance or relevance. This approach, however, is not necessarily predictive and may depend on the specific functions of the encoded proteins (Huang, et al. 2009a). Therefore, besides the magnitude of differential expression, we aimed to cover a broader functional spectrum by additionally selecting genes according to functional gene ontology terms. Because we were especially interested in genes in context to leukemia, we added those genes that have already been linked to leukemia via functional disease ontology or leukemia patient studies.

Concerning the latter, one has to take into account that comparison of our *in vitro* data to *in vivo* data from patient samples remains difficult. Our data representing a homogenous cell population can only partly mirror events seen in heterogeneous cell populations from *in vivo* studies. Additionally, due to the quantity of resulting data from these array approaches, only selected differences in gene expression are be presented in most publications. These are e.g. the transcripts with best group-distinguishing properties or those with highest differential expression within these studies. These, however, do not necessarily give a comprehensive picture of the biological situation. For example, genes involved in the malignant state of leukemic cells in general are not necessarily expected to be discriminating for certain subsets of leukemias. Yet, a concordant regulation between our *in vitro* and previous *in vivo* data may support the hypothesis that these transcripts are relevant in leukemia.

The selecting approaches altogether yielded 92 genes that were subjected to literature research and a subsequent rating strategy with respect to potential relationship to leukemogenesis. Among these genes, a set of 40 candidates for mediation of leukemogenic effects of MLL-AF9 was prioritized. In the following these genes are discussed according to the protein classes they belong to (table 12).

Table 12: **Overview of differentially expressed genes potentially involved in mediation of MLL-AF9 leukemogenic effects**.

protein group	gene name	reg.	druggable
receptors	ROR2	up	*
	TAS1R3	down	*
nuclear receptors	AHR	up	*
	VDR	up	*
transcription factors	**CEBPB**	up	
	CIITA	up	
	DACH1	down	
	EGR2	up	
	FOS	up	
	FOSB	up	
	HOXA9	down	
	HOXA11	down	
	HOXC4	down	
	IKZF2	down	
	KLF4	up	
	MEF2C	down	
	PBX3	down	
	SOX4	down	
	SP9	down	
	ZNF521	down	
signaling proteins	**CCL2**	up	
	IL8	up	
	S100A12	up	
	SOCS2	down	
enzymes	**HIPK2**	up	*
	PDE4D	down	*
	RHBDL1	down	*
transporter	ATP2B2	down	*
other proteins	BMI1	down	
	CALR	down	
	DEXI	down	
	DLL1	down	
	GPNMB	up	
	HLA-DMB	up	
	HLA-DPA1	up	
	HLA-DPB1	up	
	HLA-DQA1	up	
	HLA-DQB1	up	
	HLA-DRB4	up	
	LGALS1	down	

Top-40 differentially expressed genes rated as likely candidates for mediation of leukemogenic effects of MLL-AF9. Gene names in bold indicate genes rated as highly likely candidates. Transcripts are sorted according to categories of encoded proteins and alphabetically. reg.: up- or downregulated after *MLL-AF9* knockdown in THP1; * Indicates genes coding for proteins which belong to conventionally druggable protein classes (see 9.4.3 on page 104 for details). This table depicts a simplified version of figure 27 which is displayed on page 71.

Receptors

One MLL-AF9 dependent transcript which was not encompassed in functional gene annotation results and has not been previously associated with leukemia or cancer, is the taste receptor type 1 member 3 (*TAS1R3*). It was strongly downregulated in MLL-AF9 depleted THP1 cells. As a heteromer with TAS1R2, this glucose sensor may contribute to the control of energy supply to the cell (Mace, et al. 2009) and(Nakajima, et al. 2006) thereby might facilitate a rapid reproduction of leukemic blasts. TAS1R3 could serve as a marker for leukemic MLL blasts and / or as a target or docking molecule for drugs. This target appears druggable as illustrated by a patent for the use and manufacturing of TAS1R3 receptor inhibitors to treat obesity and diabetes (PCT/EP2005/054760).

The upregulated gene *ROR2* encodes a receptor / coreceptor for Wnt5a and mediates noncanonical Wnt signaling (Minami, et al. 2010). It has been previously hypothesized that Wnt5a is a tumor suppressor in leukemogenesis acting through the Wnt5a/Ror2 noncanonical signaling pathway that inhibits Wnt canonical signaling (Yuan, et al. 2011b).

Nuclear receptors

The nuclear aryl hydrocarbon receptor (*AHR*) supports retinoic acid–induced differentiation of myeloblastic cells and might do so via downregulation of estrogen receptor signaling (see section 9.4.1.5 on page 93).

Transcription of vitamin D (1,25- dihydroxyvitamin D3) receptor (*VDR*), a ligand-inducible transcription factor, was upregulated in a *MLL-AF9* knockdown dependent manner. Its ligand, (1,25-dihydroxyvitamin D3) is capable of inducing *in vitro* monocyte / macrophage differentiation of both normal bone marrow progenitor cells and leukemic myeloid cell lines (Gocek, et al. 2010; McCarthy, et al. 1983).

Transcription factors

Sixteen transcription factors were within the top-40 gene set for mediation of leukemogenic effects of MLL-AF9. Among these, six, namely *CEBPB*, *CIITA*, *EGR2*, *FOS*, *FOSB*, and *KLF4* were upregulated and ten (*DACH1*, *HOXA9*, *HOXA11*, *HOXC4*, *IKZF2*, *MEF2C*, *PBX3*, *SOX4*, *SP9* and *ZNF521*) were downregulated after MLL-AF9 depletion.

The transcription factor CEBPB was previously shown to activate the promoter of PU.1, a tumor suppressor for AML (Mueller, et al. 2006). Additionally, activation of *CEBPB* expression was described to lead to differentiation and reduced proliferation of CML cells and is reactivated after imatinib treatment of *BCR/ABL* CML cells (Guerzoni, et al. 2006).

The class II major histocompatibility complex transactivator CIITA is the master controller of MHC class II expression. As described in section 9.4.1.2 (on page 91) upregulation of CIITA seems to be responsible for activation of all differentially expressed MHC class II encoding genes in our data set and is believed to be related to a more differentiated state of MLL-AF9 depleted monoblasts.

DACH1 gene, encoding dachshund homolog 1 (Drosophila), was shown to be overexpressed in *MLL*-aberrant leukemia (Ross, et al. 2004). DACH1 binds to the IL8 promoter and repressed it through AP1(JUN/FOS)- and NFKB-binding sites (Wu, et al. 2008). In concordance to this, IL8 is upregulated in a MLL-AF9 dependent manner in our study.

Early growth response 2 (*EGR2*) encodes a transcription factor and tumor suppressor involved in restriction of cancer cell proliferation. EGR2 interacts with PU.1, a master transcription factor in macrophage differentiation and upregulates macrophage-specific genes like colony stimulating factor 1 receptor (*CSF1R*). (Gabet, et al. 2010) Expression of ten identical probes detecting *CSF1R* was significantly higher after *MLL-AF9* knockdown in our data set although the individual probes were not within the employed microarray *p*-value cutoff of < 0.03.

Binding motifs of FBJ murine osteosarcoma viral oncogene homolog (*FOS*) and homolog B (*FOSB*) were found activated and being within the 30 'core' motifs explaining the expressional changes after PMA-differentiation in THP1 cells (Suzuki, et al. 2009). Both are components of the dimeric transcription factor AP-1, which can mediate gene regulation in response to cytokines, growth factors, stress signals, oncogenic stimuli, bacterial and viral infections. AP-1 has effects on proliferation, differentiation and apoptosis (Hess, et al. 2004).

HOX genes have been extensively linked to expression of *MLL*, *AF9* as well as to embryogenesis and hematopoiesis as described in introductory section 6.2 on page 6.

In the context of leukemia, homeobox A9 (*HOXA9*) is the best studied homeobox transcription factor and directly regulated by MLL-AF9 protein complex (Erfurth, et al. 2008; Cierpicki, et al. 2010). Its mouse homolog is overexpressed in hematopoietic stem and progenitor cells after *Mll-AF9* knock-in (Chen, et al. 2008). *HOXA9* knock-out in mice reduces the number of committed hematopoietic progenitor cells (Lawrence, et al. 1997). Overexpression of *Hoxa9* alone does not lead to leukemic transformation of primary bone marrow cells in mice but does in conjunction with *Meis1* overexpression (Kroon, et al. 1998). In our data set, however, *MEIS1* was not downregulated. In conjunction with BMI1, HOXA9 is essential for the self-renewal capacity of leukemic stem cells transformed by MLL-AF9 (Smith, et al. 2011).

Reduced *HOXA11* transcription was previously detected after PMA-induced differentiation of monocytic cell lines (Martino, et al. 2009; Wang, et al. 2011). In myeloid malignancies,

HOXA11 translocations were described (Mizoguchi, et al. 2009). Thus far, specific processes of HOXA11 influencing the development of leukemia could not be elucidated.

In our *MLL-AF9* knockdown, the transcription factor homeobox C4 (*HOXC4*) was even stronger downregulated as the well known MLL targets *HOXA9* and *HOXA11*. *HOXC4* has been previously detected to induce expansion of hematopoietic progenitor cells after *in vitro* overexpression (Daga, et al. 2000). The murine *HoxC4* was suggested to contribute to the stem cell character of mesenchymal stem cells (Phinney, et al. 2005).

IKZF2 (IKAROS family zinc finger 2 (Helios)) encodes a hematopoietic specific transcription factor involved in the regulation of lymphocyte development. A short isoform is overexpressed in patients with adult T-cell leukemia / lymphoma (Tabayashi, et al. 2007). Up to now, no link to myeloid leukemia or myeloid cell differentiation has been reported.

The transcription factor kruppel-like factor 4 (*KLF4*) is a marker for and inducer of monocytic and terminal macrophage differentiation (Klco, et al. 2011; Schuetz, et al. 2011). *KLF4* transcription was previously shown to be upregulated by CCL2 in induced-pluripotent mouse stem cells, along with the other key transcription factors of pluripotency, *Nanog*, *Sox2* and *Tbx3* (Hasegawa, et al. 2011). In concordance to that, CCL2 was upregulated in our MLL-AF9 depleted THP1 cells, so that the effect of MLL-AF9 on KLF4 might be indirect.

MEF2C is a member of the MADS box transcription enhancer factor 2 (MEF2) family. MEF2C was shown to promote myeloid progenitor proliferation (Johnnidis, et al. 2008) and is upregulated in leukemic stem cells of *MLL*-associated leukemia (Krivtsov, et al. 2006; Schuler, et al. 2008). Its mouse homolog was detected to be overexpressed in hematopoietic stem and progenitor cells after *Mll-AF9* knock-in (Chen, et al. 2008). *Mef2c* appears to act as a cooperating oncogene in leukaemogenesis that is unable to induce leukemia when expressed alone (Krivtsov, et al. 2006).

One isoform of the transcription factor pre-B-cell leukemia homeobox 3 (*PBX3*) was previously found to be preferentially expressed in leukemic cells (Milech, et al. 2001). PBX proteins function as part of large complexes with other homeodomain-containing proteins to regulate gene expression during developmental and / or differentiation processes. Together with *HOXA7*, *HOXA9* and *HOXA11* (all downregulated in our MLL-AF9 depleted THP1 cells), *PBX3* was previously negatively associated with the overall survival of cytogenetically abnormal AML patients (Li, et al. 2012).

SOX4 gene, encoding a leukemogenic transcription factor in mouse leukemias, has been described to be overexpressed in human AML samples (Sun, et al. 2006b).

Expression of the transcription factor *SP9* has not previously been linked to leukemia or cancer. It is involved in the formation of regeneration-epithelium and an early marker for dedifferentiation of keratinocytes in the axolotl (Satoh, et al. 2008). In this process, expression of *HoxA9* and *HoxA13* is also reduced – two transcripts, which are downregulated in our *MLL-AF9* knockdown, indicating similar regulation patterns between these two entirely different biological settings.

In healthy cells, *ZNF521* is highly expressed in the most immature hematopoietic cells and declines with differentiation. An enforced expression has been found to lead to proliferation and to a decrease in granulo-monocytic differentiation. Furthermore, high *ZNF521* expression levels have previously been associated with *MLL*-rearrangements in leukemia, while *ZNF521* silencing in THP1 cells was shown to lead to impaired growth and clonogenicity. (Bond, et al. 2008)

Signaling proteins

The chemokine (C-C motif) ligand 2 (CCL2) is produced by AML blasts and its levels influences the number of monocytes that migrate towards the blasts (Legdeur, et al. 2001). In this context, CCL2 seems to be involved in immunosurveillance (see section 9.4.1.6 on page 95).

Interleukin 8 (*IL8*) gene encodes a multifunctional CXC chemokine and chemoattractant for neutrophils in inflammation. It influences basophils and T cell function and may act as an angiogenic, proliferative, autocrine and metastatic factor. IL8 serum levels were raised in leukemia patients and IL8 was preferential released by myeloid blasts showing monocytic differentiation. (Vinante, et al. 1996) Thus, upregulation of this transcript might be associated with differentiation of monoblasts. Raised expression of IL8 may be mediated by downregulation of DACH1, a repressor of IL8 transcription (Wu, et al. 2008).

S100 calcium binding protein A12 (encoded by *S100A12*) has multiple proinflammatory activities including chemotaxis for monocytes and neutrophils (Kishimoto, et al. 2006) which implicates a potential role in immunosurveillance. S100A12 was described to be upregulated in PMA-differentiated U937 monocytes (Wang, et al. 2011).

SOCS2 encodes an anti-apoptotic regulatory protein and was previously reported as upregulated in a number of myeloid leukemias (Ross, et al. 2004; Valk, et al. 2004; Zheng, et al. 2006). Such agreement with *in vivo* studies may argue for a role of SOCS2 upregulation in AML, potentially being achieved via suppressing the apoptotic effect of leukemia inhibitory factor LIF (Minamoto, et al. 1997).

Enzymes

In response to DNA damage, the homeodomain interacting protein kinase 2 (encoded by *HIPK2*) phosphorylates and stabilizes the promyelocytic leukemia (*PML*) tumor suppressor protein. Phosphorylated PML cooperates with HIPK2 for the induction of cell death. (Gresko, et al. 2009) Loss of *Hipk2* increases susceptibility to radiation induced tumors in mice (Mao, et al. 2012) and mutations of *HIPK2* have been detected in AML cases (Li, et al. 2007).

Phosphodiesterase 4D, cAMP-specific (*PDE4D*) encodes a cAMP degrading enzyme. Stimulating the cAMP signaling pathway with a phosphodiesterase 4 (PDE4) inhibitor was previously shown to induce apoptosis in primary B cell chronic lymphocytic leukemic (B-CLL) (Dong, et al. 2010).

By gene annotation inferred from electronic annotation, rhomboid veinlet-like 1 drosophila homolog (encoded by *RHBDL1*) was suggested to posses serine-type endopeptidase activity and be involved in regulated intramembrane proteolysis and the subsequent release of functional polypeptides from their membrane anchors (UniProt Consortium 2012; National Center for Biotechnology Information 2012). RHBDL1 has been implicated in the positive modulation of epidermal growth factor receptor signaling (Pascall, et al. 1998) but so far has not been described as a component of leukemogenesis.

Transporter

The calcium ion transport ATPase ATP2B2 has previously been shown to be downregulated in PMA-differentiated U937 monocytes (Wang, et al. 2011). Raised expression of *ATP2B2* in our MLL-AF9 positive cells might be linked to estrogen signaling because estradiol and estrogen were previously described to decrease *ATP2B2* expression and activity (El Beialy, et al. 2010). Overexpression of *ATP2B2* was detected to lower intracellular Ca^{2+} and protect from apoptosis in breast cancer cells (VanHouten, et al. 2010). Endoplasmatic reticulum (ER) stress may be a consequence of decreased intracellular Ca^{2+} levels which in turn may activate the unfolded protein response (Schardt, et al. 2011).

Other proteins

BMI1 polycomb ring finger oncogene (*BMI1*) encodes a polycomb group protein described to be essential for reprogramming of myeloid progenitors into leukemia stem cells (Yuan, et al. 2011a) and, together with HOXA9, for the self-renewal capacity of leukemic stem cells transformed by *MLL-AF9* (Smith, et al. 2011). *BMI1* was previously described to be downregulated in PMA-differentiated U937 monocytes (Wang, et al. 2011).

Calreticulin (*CALR*) belongs to the group of calcium associated genes and is a multifunctional protein: 1) It can act as an important modulator of the regulation of gene transcription by nuclear hormone receptors. In this context, CALR was shown to inhibit retinoic acid-induced differentiation in neuronal cells (Dedhar, et al. 1994). 2) Calreticulin also acts as a major calcium-storage protein in the lumen of the endoplasmic reticulum (Burns, et al. 1994), with evidence for a role in reducing the cytotoxic effect of Ca^{2+} influx (Zhu, et al. 1999). 3) Calreticulin is a chaperone and well-established effector of the unfolded protein response (Schardt, et al. 2011) and inhibits the translation of *CEBPA*, which is a key myeloid transcription factor and a frequent target for disruption in AML (Schardt, et al. 2011; Foran 2010). Surprisingly, repression of *CEBPA* translation via CALR and the unfolded protein response has been recently linked to a number of other fusion proteins in AML (PML-RARA, BCR-ABL, AML1-MDS1-EVI1, CBFB-SMMHC) indicating the possibility of a common pathogenetic mechanisms in these cases (Schardt, et al. 2011). Inhibition of CALR via siRNA has been reported to restore the differentiation potential of leukemic cells (Schardt, et al. 2011).

Dexi mouse homolog (*DEXI*) is a dexamethasone-induced transcript which was within the top-100 probe set characterizing *MLL* chimeric fusion gene AML within the study of Ross et al. (2004). It is suspected to be a membrane protein that dimerizes either with itself or another protein. (Edgar, et al. 2001) Its function is so far unknown.

Delta-like 1 (Drosophila) (*DLL1*) is a NOTCH ligand. NOTCH activation has been causally linked to leukemia and cancer and NOTCH has been directly targeted by a peptide antagonist to inhibit proliferation in leukemia models (Moellering, et al. 2009). DLL1 also influences the differentiation of human hematopoietic progenitors into the B cells and NK cells (Jaleco, et al. 2001). DLL1 activated the NF-kappaB pathway via Notch in THP-1 cells (Itoh, et al. 2009), which in turn promotes cell survival (Breccia, et al. 2010). DLL1 also acts pro-proliferative via reduction of TNFalpha induced growth suppression and apoptosis in monoblastic leukemia U937 cells (Murata-Ohsawa, et al. 2004).

Glycoprotein (transmembrane) nmb (*GPNMB*) encodes a putative transmembrane (golgi) glycoprotein which has been described to be involved in growth delay and reduction of metastatic potential in human melanoma (Weterman, et al. 1995). *GPNMB* expression was upregulated during macrophage differentiation and acted as a negative regulator of macrophage inflammatory responses (Ripoll, et al. 2007). Thus upregulation of *GPNMB* might be associated with a more differentiated state of our MLL-AF9 depleted THP1 cells.

MHC class II genes (*HLA-DMB*, *HLA-DPA1*, *HLA-DPB1*, *HLA-DQA1*, *HLA-DQB1*, *HLA-DRB4*) were upregulated likely via raised expression of the transcription factor CIITA and are

regarded as a sign of differentiation of MLL-AF9 depleted THP1 monoblasts because antigen presentation via MHC class II is a key feature of monocytes (see 9.4.1.2 on page 91).

LGALS1 encodes lectin, galactoside-binding, soluble 1. This protein belongs to the galectines, a group of proteins which have been implicated in diverse biological processes including modulation of cell–cell and cell–matrix interactions (Wada, et al. 1997). LGALS1 promotes escape from T cell–dependent immunity and confers immune privilege to tumor cells. It is a highly sensitive and specific biomarker of *MLL*-rearrangement in B-ALL that is likely induced by a MLL-dependent epigenetic modification. (Juszczynski, et al. 2010)

In addition to these genes, two other strongly downregulated transcripts might be equally important although they escaped by the use of our prioritization strategy due to the absence of specific functional information: the large intervening noncoding RNAs (lincRNA) LOC100129722 and LOC84989. They belong to a group of RNAs which are usually associated with chromatin signatures such as histone modification sites. For example, HOTAIR is a lincRNA strongly overexpressed in breast cancer metastasis with prognostic value (Gupta, et al. 2010). HOTAIR was found to bind and redistributed genomic localization of a H3K27 methylase complex, leading to gene expression changes. (Gupta, et al. 2010) The lincRNAs found here might be the opening to a new field in respect to MLL-AF9 leukemogenesis, and might point to alternative opportunities for epigenetic-derived therapeutic strategies as compared to recent and challenging strategies to target methyltransferases via chemical inhibitors as described by Travers et al. (2011).

9.4.3 Genes considered as likely therapeutic targets

In the previous sections, we focused on genes and processes which are presumably important in mediating leukemogenic effects of MLL-AF9. However, some of these genes may not be suited well as therapeutic targets even though they may be involved in malignancy. Thus, we asked which genes of our top-40 set for mediation of leukemogenic effects of MLL-AF9 may be amenable for future therapies.

Three target classes, namely receptors (including nuclear receptors), enzymes and transporters encompass 88% of all currently known 435 therapeutic effect-mediating human protein targets of US Food and Drug Administration (FDA) approved and experimental drugs. This indicates that these classes encompass proteins especially amenable to drug development. However, “innovation peaks” may arise when new protein types emerge as novel drug targets. This was e.g. the case when the first drugs targeting an integrin or a kinase were introduced in the years 1997 and 2001. (Rask-Andersen, et al. 2011) Transcription factors (TFs) have traditionally been

considered as “non-druggable”. Recently, strategies to target TFs by blocking protein-protein or protein-DNA interactions are emerging (Berg 2008). However, they still do not belong to frequent drug targets of approved drugs. An exception builds the class of nuclear receptors, which comprises the second most frequent gene-family of drug targets (Overington, et al. 2006).
These facts point out that receptors, enzymes and transporters within our top-40 set of genes suggested for mediation of leukemogenic effects of MLL-AF9 might be “druggable”.
Eight of our top-40 genes encode proteins of these classes. Among these is one G-protein-coupled receptor, the taste receptor TAS1R3. Furthermore are two nuclear receptors, the vitamin D receptor (VDR) and the aryl hydrocarbon receptor (AHR).
Among the enzymes is the receptor tyrosine kinase ROR2, the putative endopeptidase RHBDL1, the kinase HIPK2 and the phosphodiesterase PDE4D. The only transporter within our top-40 set is the calcium ion transporting plasma membrane ATPase ATP2B2.

Drugs targeting AHR, VDR and PDE4D already exist (Wishart, et al. 2008).
VDR agonists e.g. reduce parathyroid hormone levels and are employed in secondary hyperparathyroidism associated with chronic kidney disease, in refractory rickets, hypocalcemia and in the management and prevention of osteoporosis.
AHR is targeted by drugs used in rheumatoid arthritis, for the prevention of coronary heart disease, in ventricular tachycardia and in the management of metastatic carcinoma of the prostate.
PDE4 inhibitors, which also target PDE4D, exhibit antidepressant, anti-inflammatory and neuroprotective properties. They are e.g. employed in respiratory disorders.
To our knowledge, TAS1R3, RHBDL1 and PDE4D have not previously been linked to myeloid leukemia and thus represent entirely novel, potentially “druggable” targets for *MLL*-aberrant AML.

9.5 MLL-AF9 associated changes in miRNA expression

In the previous sections we analyzed MLL-AF9 dependent effects on gene expression and the potential involvement in leukemogenesis as well as the prospective druggability of identified targets. Other downstream effects involve miRNAs that might equally lead to the development of novel therapies. To date, miRNA-based cancer therapies have not yet reached clinical application. They are, however, considered as promising strategies since pre-clinical *in vivo* data support the suitability of re-expression of tumor suppressive miRNAs or the targeting of oncogenic miRNAs via antagomiRs in a number of cancer models. The small size of miRNAs

and their low antigenicity may present benefits as compared to protein-coding gene replacement therapies. (Kasinski, et al. 2011)

We hypothesized that the fusion protein MLL-AF9 leads to differential expression of miRNAs thereby supporting the leukemogenic effects of MLL-AF9. The identified leukemogenic miRNAs could then serve as therapeutic targets for the associated leukemia subtype. Therefore, a differential miRNA expression profile was generated after knockdown of endogenous *MLL-AF9* in THP1 cells.

9.5.1 Deregulated miRNAs

We employed a quantitative (TaqMan Low Density Arrays, LDA) as well as a semiquantitative (Agilent microarrays) profiling technique to analyze differential expression of miRNAs after MLL-AF9 depletion in THP1 cells.

With these array systems, 21 out of 664 (3.2%, LDA) and 2 out of 1048 (0.2%, Agilent microarray) analyzed miRNAs were detected as differentially expressed in *MLL-AF9* knockdown versus control treatments ($p<0.05$). In comparison, our gene expression data revealed 6 % of the analyzed (~ 20000) genes of the human genome (International Human Genome Sequencing Consortium 2004) as differentially expressed. Thus, the percentage of detected differentially expressed miRNAs is somewhat lower than that of genes.

No overlapping results between the differentially expressed miRNAs from the two profiling platforms were present in our datasets. Low correlation between LDA and microarray results from the same samples has previously been reported. As the quantitative LDA was evaluated to display a higher sensitivity and specificity, we concentrated on these miRNA results for screening purposes. (Chen, et al. 2009)

A subset of the 21 differentially expressed miRNAs from LDA results was additionally assessed via single-assay qRT-PCR to confirm our results. Here, the majority of these miRNAs (7 out of 11) was confirmed to be differentially expressed.

Little is known, about how and to what extent the administration of an siRNA can disturb endogenous miRNA expression levels. In our study, we observed strikingly high differences in the expression of single miRNAs between the two non-targeting control siRNA treatments or between the two siRNAs designed to knockdown *MLL-AF9*. These observations suggest that siRNAs may have off-target effects not only on mRNA expression but also on miRNAs and corroborates the importance of using adequate controls for off-target effects in siRNA studies.

As example, the miRNA 196b has been previously described to be upregulated by MLL-AF9 (Popovic, et al. 2009; Cierpicki, et al. 2010). In this study however, we observed a clear discrepancy of miR-196b levels when we compared the two non-targeting control siRNA

treatments. Thus miR-196b did not fulfill our criteria for technical validation and was excluded from our results.

The high stringency of our experimental design might thus explain the relatively low number of differentially expressed miRNAs we detected.

Seven out of eleven miRNAs (miR-214, miR-219-5p, miR-432, miR-511, miR-539, miR-589 and miR-758) were confirmed by single assay qRT-PCR to be differentially expressed in MLL-AF9 depleted THP1 cells.

Some of the differentially expressed miRNAs have a genomic location within introns of protein-coding or non-coding genes. These host-genes, however, were not detected as differentially expressed in our data set. This is not surprising, as miRNAs are not necessarily coregulated with their host genes because miRNA processing is a specifically regulated process.

Recently, in a number of *in vivo* studies, miRNAs have been found to be differentially expressed among distinct cytogenetic groups of AML. However, the specific signatures differed among studies, most likely due to the lack of standardized methods used by different groups. (Marcucci, et al. 2011)

Nevertheless, some concordance was detected between our *in vitro* data set and previously published *in vivo* data. This concerned four of our confirmed differentially expressed miRNAs, namely miR-214, miR-219-5p, miR-432 and miR-511 which were reported in various myeloid leukemia subtypes (table 10, page 78). These concordant *in vivo* observations are mostly not specifically derived from AML with *MLL*-aberrations or with *MLL-AF9* translocation, so that they may only weakly support the hypothesis that these miRNAs play a role in *MLL-AF9* positive leukemia.

So far, no link for either miR-432, miR-539, miR-589 or miR-758 to leukemia has been described.

MiR-432 is derived from chromosome 14 and lies within exon 1 of retrotransposon-like 1 (*RTL1*) gene. *RTL1* showed low expression in microarray data and was not coregulated. This gene contains more miRNAs (miR-136, miR-127, miR-433 and miR-431) but these were also not detected as differentially expressed in *MLL-AF9* knockdown. So far, no direct targets of miR-432 have been validated.

Mir-539 is located within intron 1 of the lincRNA *RP11* on human chromosome 14. It has been suggested that its reduced expression might increase proliferation of mast cells in mastocytosis, a disease which is characterized by abnormal accumulation of mast cells (Lee, et al. 2011). Mir-

539 was downregulated in gastric extranodal marginal zone lymphomas compared to gastritis (Thorns, et al. 2012). However, in our data set, miR-539 expression is reduced after *MLL-AF9* knockdown.

MiR-589 lies within an intron of human gene F-box and leucine-rich repeat protein 18 (*FBXL18*) on chromosome 7. No biological role or direct target for human miR-589 has been described up to date.

MiR-758 is located intergenic on human chromosome 14. ATP-binding cassette transporter A1 (*ABCA1*), a major regulator of macrophage cholesterol efflux, is a described target of miR-758 (Ramirez, et al. 2011). However, *ABCA1* was not detected as deregulated after *MLL-AF9* knockdown in THP1 cells.

Two intergenic copies of miR-219-5p exist in the human genome: one on chromosome 6 and one on chromosome 9. MiR-219-5p was upregulated in a childhood myeloid leukemia cell line upon stimulation with either IL3, GM-CSF or G-CSF, supporting a role during leukemic and normal hematopoiesis (Favreau, et al. 2012).

MiR-214 is derived from chromosome 1 and lies in an intron of dynamin 3 gene (DNM3), which showed low expression and was not regulated in microarray data of *MLL-AF9* knockdown. MiR-214 has been described to have pro-metastatic functions in melanoma (Bar-Eli 2011) but on the other hand inhibits the proliferation capacity, migration and invasion ability in cervical tumor (Qiang, et al. 2011). Thus no clear role as onco-miR or tumor-suppressor-miR can be assigned. MiR-214 has been described to target *PTEN* in monocytes and THP1 cells thus leading to delayed apoptosis (Li, et al. 2011). MiR-214 has also been described to be part of a negative feedback loop by targeting the *EZH2* encoding a polycomb-group protein and thus promoting skeletal muscle cell differentiation (Juan, et al. 2009). EZH2 has been shown to be responsible for long-term repopulating potential of hematopoietic stem cells (Kamminga, et al. 2006) suggesting a potential role for miR-214 in leukemogenesis. However *EZH2* was not detected as differentially expressed after *MLL-AF9* knockdown in our study.

MiR-511 is located on chromosome 10 within intron 5 of the gene coding for macrophage mannose receptor 1 (MRC1). In our gene expression microarray analysis, MRC1 gene transcript showed low expression and was not found coregulated with miR-511.

Both, miR-214 and miR-511, were reported to be significantly lower expressed in adrenocortical and hepatocellular carcinomas (Tombol, et al. 2009; Wang, et al. 2012). Estep et al. (2010) found miR-511 significantly lower expressed in the visceral adipose tissue of non-alcoholic steatohepatitis (NASH) patients, a condition in which inflammation plays an important role.

MiR-511 has also been described to be a novel potent modulator of human immune response being upregulated during dendritic cell and macrophage differentiation. Additionally, the first known direct targets of miR-511, *TLR4* and *CD80* were described. (Tserel, et al. 2011)
However, no differential expression of *TRL4* and *CD80* was observed after *MLL-AF9* knockdown, suggesting that other targets might be more prominently regulated in our setting.

9.5.2 MiR-511 in monocytic differentiation and potential target genes

The strongest regulated of our confirmed differentially expressed miRNAs after *MLL-AF9* knockdown, miR-511, was selected for further investigation.
The target prediction algorithms we used identified a wide range of predicted targets for miR-511. Among those, we experimentally assessed nine via expression analysis after miR-511 upregulation in THP1. Though we observed a trend towards the expected downregulation in eight of these transcripts, none of these alterations reached statistical significance.
Because most direct miRNA targets are reduced on mRNA level (Baek, et al. 2008), it might be more straight forward, to analyze a gene expression profile after miR-511 upregulation in THP1 and subsequently search for its direct targets within this set of differentially expressed mRNAs.
Except for miR-511 and miR-137 which seem to be involved in macrophage differentiation (Tserel, et al. 2011), we did not observe overlapping results between our differentially expressed miRNA data set and published information on miRNAs in monocytic differentiation.
We were, however, able to detect a significant upregulation of miR-511 in THP1 cells stimulated to differentiate into monocytes / macrophages by the addition of PMA. This finding further supports the hypothesis that miR-511 is involved in the differentiation processes of monoblasts.

10 Conclusions

This study aimed to identify new potential therapeutic targets for acute myeloid leukemia (AML) with the *MLL-AF9* translocation, a subtype with still poor clinical prognosis. Specifically the identification of leukemogenic downstream effects of the MLL-AF9 aberration both on the cellular phenotype as well as on gene and miRNA expression pattern should generate information on candidate targets.

For this purpose we optimized an experimental approach that utilized a cell line carrying this specific translocation (THP1) in conjunction with RNA interference capable to downregulate MLL-AF9 protein and function. The technical achievements included:

- The successful design of efficient siRNAs that specifically target the breakpoint of *MLL-AF9* while not disturbing wildtype *MLL* or *AF9* expression or producing off-target effects.
- Confirmation of MLL-AF9 knockdown efficiency at transcript level (down to 20%) as well as at functional protein level by analyzing HOXA9 transcript as a surrogate marker, because MLL-AF9 protein showed very low solubility and appeared to be prone to aggregate.
- Elaboration of experimental conditions that ensured a prolonged knockdown of *MLL*-AF9 in cell culture and minimized the masking of MLL-AF9-specific effects by the strong mitogenic influence of fetal bovine serum.

MLL-AF9 knockdown changed the phenotype of THP1 cells characterized by a highly significant reduction of cell diameter of about 0.3 µm. This effect was highly reproducible and persisted over time in culture. Indirect evidence pointed to reduced ribosomal biogenesis and / or to AF9 protein co-aggregation with MLL-AF9 as potential causative mechanisms. No effects of the knockdown on cell proliferation rate, cell cycle or on apoptosis was observed.

After MLL-AF9 knockdown differential gene and miRNA array expression data were evaluated in the biological context; specifically to sort out candidate genes and functions with a high likelihood to be involved in the mediation of MLL-AF9 leukemogenic effects.

1269 genes were detected to be differentially expressed. The data set was technically validated, complied to standard quality criteria and submitted to and accepted by Gene Expression Omnibus (GEO) database under the accession number GSE36592.

Functional gene ontology analysis (GO) revealed several key biological functions and annotation terms as significantly enriched: In particular, functional terms related to differentiation of monoblasts were highly overrepresented. Others include transcripts involved in apoptosis, in calcium and estrogen signaling, in immunosurveillance and in the functional processes of protein folding. Taken together, the analysis provided evidence that depletion of MLL-AF9 leads to a

partial release of the differentiation block in THP1 cells. Other effects might include those on regulation of apoptosis though we observed no induction of apoptosis at phenotypic level, presumably due to missing apoptotic stimuli within our experimental setting. The influence of MLL-AF9 on estrogen signaling is consistent with a known role for estrogen signals in leukemia development and may point to potential efficiency of anti-estrogen treatments in AML. As the evasion of immunosurveillance is a critical feature in sustaining cancer cells, some of the MLL-AF9 regulated genes identified within this functional category might equally be worthwhile targets to be addressed. The influence of MLL-AF9 knockdown on several functional processes of protein folding suggested mechanistic links between the heat-shock / unfolded protein response and myeloid leukemogenesis. This might be caused by low solubility of MLL-AF9 protein which appears to be prone to aggregate.

The functional disease ontology database (FunDO) contains curated preexisting evidence on genes associated with disease entities and was queried with our data set of 1269 differentially expressed genes. The term leukemia turned out both as highly significant and highly enriched being top ranked among all associations covered. Besides the identification of leukemia associated candidate targets, this analysis also validated our experimental approach in that an expected information content related to leukemia was indeed disclosed in our data.

Subsequently, 40 genes were prioritized by a multistep selection approach as likely candidate targets for mediation of MLL-AF9 leukemogenic effects. Eight of these were rated as likely "druggable" and included e.g. the G-protein-coupled receptor TAS1R3, the putative endopeptidase RHBDL1 and the phosphodiesterase PDE4D. These three gene products have not previously been linked to myeloid leukemia.

After *MLL-AF9* knockdown, miRNA profiles revealed 23 miRNAs as significantly differentially expressed. Seven out of eleven prioritized and selected miRNA candidates were confirmed by qRT-PCR, the strongest deregulated miRNA being hsa-miR-511. In THP1 cells differentiated via phorbol 12-myristate 13-acetate (PMA) treatment, miR-511 was significantly upregulated suggesting a potential role of this miRNA in differentiation.

This study yielded the first comprehensive data set for differential miRNA and gene expression after an efficient and prolonged *MLL-AF9* knockdown in THP1 cells. It further identified key biological processes as well as new gene and miRNA candidates highly likely to be involved in mediation of MLL-AF9 leukemogenic effects. Eight of the involved gene products and miR-511 were evaluated as potentially "druggable". Subsequent studies of these candidate targets shall assess their suitability for therapeutic intervention in *MLL-AF9* positive acute myeloid leukemia.

11 References

Immunology Database and Analysis Portal. https://www.immport.org/immportWeb/queryref/geneListDetail.do?fileName=Cykn&fileType=geneSummary&title=Cytokines&displayType=1 . 2011. Electronic Citation

Abedin,M.J., Kashio,Y., Seki,M., Nakamura,K., and Hirashima,M. Potential roles of galectins in myeloid differentiation into three different lineages. *J Leukoc Biol* 2003; 73 (5): 650-6.

Abrink,M., Gobl,A.E., Huang,R., Nilsson,K., and Hellman,L. Human cell lines U-937, THP-1 and Mono Mac 6 represent relatively immature cells of the monocyte-macrophage cell lineage. *Leukemia* 1994; 8 (9): 1579-84.

Afonja,O., Smith,J.E., Jr., Cheng,D.M., Goldenberg,A.S., Amorosi,E., Shimamoto,T., Nakamura,S., et al. *MEIS1* and *HOXA7* genes in human acute myeloid leukemia. *Leuk Res* 2000; 24 (10): 849-55.

Aggarwal,S. and Gupta,S. Increased apoptosis of T cell subsets in aging humans: altered expression of Fas (CD95), Fas ligand, Bcl-2, and Bax. *J Immunol* 1998; 160 (4): 1627-37.

Algarra,I., Garcia-Lora,A., Cabrera,T., Ruiz-Cabello,F., and Garrido,F. The selection of tumor variants with altered expression of classical and nonclassical MHC class I molecules: implications for tumor immune escape. *Cancer Immunol Immunother* 2004; 53 (10): 904-10.

Aljurf,M., Saleh,A.J.M., and Ahmed,S.O. MLL gene in maternal and infantile acute lymphoblastic leukemia and the effect of estrogen. *Leuk Res* 2011; 35 (7): e127.

Allen,J.M., Brachvogel,B., Farlie,P.G., Fitzgerald,J., and Bateman,J.F. The extracellular matrix protein WARP is a novel component of a distinct subset of basement membranes. *Matrix Biol* 2008; 27 (4): 295-305.

An,L.L., Ma,X.T., Yang,Y.H., Lin,Y.M., Song,Y.H., and Wu,K.F. Marked reduction of LL-37/hCAP-18, an antimicrobial peptide, in patients with acute myeloid leukemia. *Int J Hematol* 2005; 81 (1): 45-7.

Andersen,J.S., Lam,Y.W., Leung,A.K.L., Ong,S.E., Lyon,C.E., Lamond,A.I., and Mann,M. Nucleolar proteome dynamics. *Nature* 2005; 433 (7021): 77-83.

Anderson,M.S. and Miller,J. Invariant chain can function as a chaperone protein for class II major histocompatibility complex molecules. *PNAS* 1992; 89 (6): 2282-6.

Ansari,K.I., Hussain,I., Shrestha,B., Kasiri,S., and Mandal,S.S. HOXC6 is transcriptionally regulated via coordination of MLL histone methylase and estrogen receptor in an estrogen environment. *J Mol Biol* 2011; 411 (2): 334-49.

Ansari,K.I., Kasiri,S., Hussain,I., and Mandal,S.S. Mixed lineage leukemia histone methylases play critical roles in estrogen-mediated regulation of HOXC13. *FEBS J* 2009; 276 (24): 7400-11.

Ansari,K.I. and Mandal,S.S. Mixed lineage leukemia: roles in gene expression, hormone signaling and mRNA processing. *FEBS J* 2010; 277 (8): 1790-804.

Anwar,A., Keating,A.K., Joung,D., Sather,S., Kim,G.K., Sawczyn,K.K., Brandao,L., et al. Mer tyrosine kinase (MerTK) promotes macrophage survival following exposure to oxidative stress. *J Leukoc Biol* 2009; 86 (1): 73-9.

Armstrong,S.A., Staunton,J.E., Silverman,L.B., Pieters,R., den Boer,M.L., Minden,M.D., Sallan,S.E., et al. MLL translocations specify a distinct gene expression profile that distinguishes a unique leukemia. *Nat Genet* 2002; 30 (1): 41-7.

Arunachalam,B., Phan,U.T., Geuze,H.J., and Cresswell,P. Enzymatic reduction of disulfide bonds in lysosomes: characterization of a gamma-interferon-inducible lysosomal thiol reductase (GILT). *PNAS* 2000; 97 (2): 745-50.

Aurich-Costa,J., Cadel,S., Gouzy,C., Foulon,T., Cherif,D., and Cohen,P. Assignment of the aminopeptidase B gene (RNPEP) to human chromosome 1 band q32 by in situ hybridization. *Cytogenet Cell Genet* 1997; 79 (1-2): 143-4.

Auwerx,J.H., Deeb,S., Brunzell,J.D., Wolfbauer,G., and Chait,A. Lipoprotein lipase gene expression in THP-1 cells. *Biochemistry* 1989; 28 (11): 4563-7.

Ayton,P.M. and Cleary,M.L. Molecular mechanisms of leukemogenesis mediated by MLL fusion proteins. *Oncogene* 2001; 20 (40): 5695-707.

Babiarz,J.E. and Blelloch,R. 2009. Small RNAs - their biogenesis, regulation and function in embryonic stem cells. *In* StemBook. Harvard Stem Cell Institute, Cambridge (MA).

Bachmann,M., Dragoi,C., Poleganov,M.A., Pfeilschifter,J., and Muhl,H. Interleukin-18 directly activates T-bet expression and function via p38 mitogen-activated protein kinase and nuclear factor-kappaB in acute myeloid leukemia-derived predendritic KG-1 cells. *Mol Cancer Ther* 2007; 6 (2): 723-31.

Baek,D., Villen,J., Shin,C., Camargo,F.D., Gygi,S.P., and Bartel,D.P. The impact of microRNAs on protein output. *Nature* 2008; 455 (7209): 64-71.

Balgobind,B.V., Hollink,I.H., Arentsen-Peters,S.T., Zimmermann,M., Harbott,J., Beverloo,B., von Bergh,A.R., et al. Integrative analysis of type-I and type-II aberrations underscores the genetic heterogeneity of pediatric acute myeloid leukemia. *Haematologica* 2011; 96 (10): 1478-87.

Banisadr,G., Gosselin,R.D., Mechighel,P., Rostene,W., Kitabgi,P., and Melik,P.S. Constitutive neuronal expression of CCR2 chemokine receptor and its colocalization with neurotransmitters in normal rat brain: functional effect of MCP-1/CCL2 on calcium mobilization in primary cultured neurons. *J Comp Neurol* 2005; 492 (2): 178-92.

Bar-Eli,M. Searching for the 'melano-miRs': miR-214 drives melanoma metastasis. *EMBO J* 2011; 30 (10): 1880-1.

Barrett,T., Troup,D.B., Wilhite,S.E., Ledoux,P., Evangelista,C., Kim,I.F., Tomashevsky,M., et al. NCBI GEO: archive for functional genomics data sets – 10 years on. *Nucleic Acids Res* 2011; 39 (suppl 1): D1005-D1010.

Bartel,D.P. MicroRNAs: genomics, biogenesis, mechanism, and function. *Cell* 2004; 116 (2): 281-97.

Baum,P., Fundel-Clemens,K., Kreuz,S., Kontermann,R.E., Weith,A., Mennerich,D., and Rippmann,J.F. Off-target analysis of control siRNA molecules reveals important differences in the cytokine profile and inflammation response of human fibroblasts. *Oligonucleotides* 2010; 20 (1): 17-26.

Bei,L., Lu,Y., and Eklund,E.A. HOXA9 activates transcription of the gene encoding gp91Phox during myeloid differentiation. *J Biol Chem* 2005; 280 (13): 12359-70.

Bender-Götze,C., Walther,J., Rampf,U., Haas,R., Graubner,U., Müller-Weihrich,S., and Baier,U. 2003. Besonderheiten der akuten Leikämien im Kindesalter. Tumorzentrum München, ed. *In* Leukämien, myelodysplastische und myeloproliferative Syndrome. Tumorzentrum München und W. Zuckschwerdt Verlag München, München, pp 77-96.

Benjamini,Y. and Hochberg,Y. Controlling the false discovery rate: a practical and powerful approach to multiple testing. *J R Statist Soc B* 1995; 57 (1): 289-300.

Berg,T. Inhibition of transcription factors with small organic molecules. *Curr Opin Chem Biol* 2008; 12 (4): 464-71.

Bies,J., Sramko,M., Fares,J., Rosu-Myles,M., Zhang,S., Koller,R., and Wolff,L. Myeloid-specific inactivation of p15Ink4b results in monocytosis and predisposition to myeloid leukemia. *Blood* 2010; 116 (6): 979-87.

Bond,H.M., Mesuraca,M., Amodio,N., Mega,T., Agosti,V., Fanello,D., Pelaggi,D., et al. Early hematopoietic zinc finger protein - zinc finger protein 521: A candidate regulator of diverse immature cells. *Int J Biochem Cell Biol* 2008; 40 (5): 848-54.

Bortner,C.D. and Cidlowski,J.A. A necessary role for cell shrinkage in apoptosis. *Biochem Pharmacol* 1998; 56 (12): 1549-59.

Boyd,K.E., Xiao,Y.Y., Fan,K., Poholek,A., Copeland,N.G., Jenkins,N.A., and Perkins,A.S. Sox4 cooperates with Evi1 in AKXD-23 myeloid tumors via transactivation of proviral LTR. *Blood* 2006; 107 (2): 733-41.

Breccia,M. and Alimena,G. NF-kappaB as a potential therapeutic target in myelodysplastic syndromes and acute myeloid leukemia. *Expert Opin Ther Targets* 2010; 14 (11): 1157-76.

Bullinger,L., Dohner,K., Bair,E., Frohling,S., Schlenk,R.F., Tibshirani,R., Dohner,H., et al. Use of gene-expression profiling to identify prognostic subclasses in adult acute myeloid leukemia. *N Engl J Med* 2004; 350 (16): 1605-16.

Bunaciu,R.P. and Yen,A. Activation of the aryl hydrocarbon receptor AhR promotes retinoic acid induced differentiation of myeloblastic leukemia cells by restricting expression of the stem cell transcription factor Oct4. *Cancer Res* 2011; 71 (6): 2371-80.

Burns,K., Duggan,B., Atkinson,E.A., Famulski,K.S., Nemer,M., Bleackley,R.C., and Michalak,M. Modulation of gene expression by calreticulin binding to the glucocorticoid receptor. *Nature* 1994; 367 (6462): 476-80.

Calin,G.A., Dumitru,C.D., Shimizu,M., Bichi,R., Zupo,S., Noch,E., Aldler,H., et al. Frequent deletions and down-regulation of micro- RNA genes miR15 and miR16 at 13q14 in chronic lymphocytic leukemia. *PNAS* 2002; 99 (24): 15524-9.

Calin,G.A., Liu,C.G., Sevignani,C., Ferracin,M., Felli,N., Dumitru,C.D., Shimizu,M., et al. MicroRNA profiling reveals distinct signatures in B cell chronic lymphocytic leukemias. *PNAS* 2004; 101 (32): 11755-60.

Callahan,M.K., Garg,M., and Srivastava,P.K. Heat-shock protein 90 associates with N-terminal extended peptides and is required for direct and indirect antigen presentation. *PNAS* 2008; 105 (5): 1662-7.

Carlberg,C. and Seuter,S. A genomic perspective on vitamin D signaling. *Anticancer Res* 2009; 29 (9): 3485-93.

Castiello,L., Stroncek,D.F., Finn,M.W., Wang,E., Marincola,F.M., Clayberger,C., Krensky,A.M., et al. 15 kDa Granulysin versus GM-CSF for monocytes differentiation: analogies and differences at the transcriptome level. *J Transl Med* 2011; 9 41.

Ceolotto,G., Gallo,A., Miola,M., Sartori,M., Trevisan,R., Del Prato,S., Semplicini,A., et al. Protein kinase C activity is acutely regulated by plasma glucose concentration in human monocytes in vivo. *Diabetes* 1999; 48 (6): 1316-22.

Chacko,E. and Ranganathan,S. Comprehensive splicing graph analysis of alternative splicing patterns in chicken, compared to human and mouse. *BMC Genomics* 2009; 10 Suppl 1 S5.

Chen,W., Kumar,A.R., Hudson,W.A., Li,Q., Wu,B., Staggs,R.A., Lund,E.A., et al. Malignant transformation initiated by Mll-AF9: gene dosage and critical target cells. *Cancer Cell* 2008; 13 (5): 432-40.

Chen,Y., Gelfond,J., McManus,L., and Shireman,P. Reproducibility of quantitative RT-PCR array in miRNA expression profiling and comparison with microarray analysis. *BMC Genomics* 2009; 10 (1): 407.

Cheng,C.S., Johnson,T.L., and Hoffmann,A. Epigenetic control: slow and global, nimble and local. *Genes Dev* 2008; 22 (9): 1110-4.

Chowdhury,T. and Brady,H.J.M. Insights from clinical studies into the role of the MLL gene in infant and childhood leukemia. *Blood Cells Mol Dis* 2003; 40 (2): 192-9.

Cierpicki,T., Risner,L.E., Grembecka,J., Lukasik,S.M., Popovic,R., Omonkowska,M., Shultis,D.D., et al. Structure of the MLL CXXC domain-DNA complex and its functional role in MLL-AF9 leukemia. *Nat Struct Mol Biol* 2010; 17 (1): 62-8.

Cimmino,A., Calin,G.A., Fabbri,M., Iorio,M.V., Ferracin,M., Shimizu,M., Wojcik,S.E., et al. miR-15 and miR-16 induce apoptosis by targeting BCL2. *PNAS* 2005; 102 (39): 13944-9.

Clapham,D.E. Calcium signaling. *Cell* 2007; 131 (6): 1047-58.

Collins,E.C., Appert,A., Ariza-McNaughton,L., Pannell,R., Yamada,Y., and Rabbitts,T.H. Mouse Af9 is a controller of embryo patterning, like Mll, whose human homologue fuses with Af9 after chromosomal translocation in leukemia. *Mol Cell Biol* 2002; 22 (20): 7313-24.

Cordes,K.R., Srivastava,D., and Ivey,K.N. MicroRNAs in cardiac development. *Pediatr Cardiol* 2010; 31 (3): 349-56.

Corral,J., Lavenir,I., Impey,H., Warren,A.J., Forster,A., Larson,T.A., Bell,S., et al. An Mll-AF9 fusion gene made by homologous recombination causes acute leukemia in chimeric mice: a method to create fusion oncogenes. *Cell* 1996; 85 (6): 853-61.

Creutzig,U., Zimmermann,M., Ritter,J., Reinhardt,D., Hermann,J., Henze,G., Jurgens,H., et al. Treatment strategies and long-term results in paediatric patients treated in four consecutive AML-BFM trials. *Leukemia* 2005; 19 (12): 2030-42.

Daga,A., Podesta,M., Capra,M.C., Piaggio,G., Frassoni,F., and Corte,G. The retroviral transduction of HOXC4 into human CD34(+) cells induces an in vitro expansion of clonogenic and early progenitors. *Exp Hematol* 2000; 28 (5): 569-74.

Dedhar,S., Rennie,P.S., Shago,M., Hagesteijn,C.Y., Yang,H., Filmus,J., Hawley,R.G., et al. Inhibition of nuclear hormone receptor activity by calreticulin. *Nature* 1994; 367 (6462): 480-3.

Demiroglu,A., Steer,E.J., Heath,C., Taylor,K., Bentley,M., Allen,S.L., Koduru,P., et al. The t(8;22) in chronic myeloid leukemia fuses BCR to FGFR1: transforming activity and specific inhibition of FGFR1 fusion proteins. *Blood* 2001; 98 (13): 3778-83.

Deschler,B. and Lubbert,M. Acute myeloid leukemia: epidemiology and etiology. *Cancer* 2006; 107 (9): 2099-107.

Dey,B.R., Spence,S.L., Nissley,P., and Furlanetto,R.W. Interaction of human suppressor of cytokine signaling (SOCS)-2 with the insulin-like growth factor-I receptor. *J Biol Chem* 1998; 273 (37): 24095-101.

Ding,Y. and Lawrence,C.E. Statistical prediction of single-stranded regions in RNA secondary structure and application to predicting effective antisense target sites and beyond. *Nucleic Acids Res* 2001; 29 (5): 1034-46.

Dinger,M.E., Amaral,P.P., Mercer,T.R., Pang,K.C., Bruce,S.J., Gardiner,B.B., Askarian-Amiri,M.E., et al. Long noncoding RNAs in mouse embryonic stem cell pluripotency and differentiation. *Genome Res* 2008; 18 (9): 1433-45.

Dobson,C.L., Warren,A.J., Pannell,R., Forster,A., Lavenir,I., Corral,J., Smith,A.J., et al. The mll-AF9 gene fusion in mice controls myeloproliferation and specifies acute myeloid leukaemogenesis. *EMBO J* 1999; 18 (13): 3564-74.

Dominguez-Soto,A., Sierra-Filardi,E., Puig-Kroger,A., Perez-Maceda,B., Gomez-Aguado,F., Corcuera,M.T., Sanchez-Mateos,P., et al. Dendritic cell-specific ICAM-3-grabbing nonintegrin expression on M2-polarized and tumor-associated macrophages is macrophage-CSF dependent and enhanced by tumor-derived IL-6 and IL-10. *J Immunol* 2011; 186 (4): 2192-200.

Dong,H., Zitt,C., Auriga,C., Hatzelmann,A., and Epstein,P.M. Inhibition of PDE3, PDE4 and PDE7 potentiates glucocorticoid-induced apoptosis and overcomes glucocorticoid resistance in CEM T leukemic cells. *Biochem Pharmacol* 2010; 79 (3): 321-9.

Dorsam,S.T., Ferrell,C.M., Dorsam,G.P., Derynck,M.K., Vijapurkar,U., Khodabakhsh,D., Pau,B., et al. The transcriptome of the leukemogenic homeoprotein HOXA9 in human hematopoietic cells. *Blood* 2004; 103 (5): 1676-84.

Drexler,H.G., Quentmeier,H., and MacLeod,R.A. Malignant hematopoietic cell lines: in vitro models for the study of MLL gene alterations. *Leukemia* 2004; 18 (2): 227-32.

Du,P., Feng,G., Flatow,J., Song,J., Holko,M., Kibbe,W.A., and Lin,S.M. From disease ontology to disease-ontology lite: statistical methods to adapt a general-purpose ontology for the test of gene-ontology associations. *Bioinformatics* 2009; 25 (12): i63-i68.

Dusso,A.S., Brown,A.J., and Slatopolsky,E. Vitamin D. *Am J Physiol Renal Physiol* 2005; 289 (1): F8-28.

Dweep,H., Sticht,C., Pandey,P., and Gretz,N. miRWalk - Database: Prediction of possible miRNA binding sites by "walking" the genes of three genomes. *J Biomed Inform* 2011; 44 (5): 839-47.

Edgar,A.J., Birks,E.J., Yacoub,M.H., and Polak,J.M. Cloning of dexamethasone-induced transcript: a novel glucocorticoid-induced gene that is upregulated in emphysema. *Am J Respir Cell Mol Biol* 2001; 25 (1): 119-24.

Ehrenhofer-Murray,A.E. Chromatin dynamics at DNA replication, transcription and repair. *Eur J Biochem* 2004; 271 (12): 2335-49.

Eklund,E.A. The role of HOX genes in malignant myeloid disease. *Curr Opin Hematol* 2007; 14 (2): 85-9.

El Beialy,W., Galal,N., Deyama,Y., Yoshimura,Y., Suzuki,K., Tei,K., and Totsuka,Y. Effects of estrogen on PMCA 2 and 4 in human fibroblast-like synovial cells and mouse macrophage-like cells. *Endocr J* 2010; 57 (1): 93-7.

Elwess,N.L., Filoteo,A.G., Enyedi,A., and Penniston,J.T. Plasma membrane Ca2+ pump isoforms 2a and 2b are unusually responsive to calmodulin and Ca2+. *J Biol Chem* 1997; 272 (29): 17981-6.

Erfurth,F.E., Popovic,R., Grembecka,J., Cierpicki,T., Theisler,C., Xia,Z.B., Stuart,T., et al. MLL protects CpG clusters from methylation within the Hoxa9 gene, maintaining transcript expression. *PNAS* 2008; 105 (21): 7517-22.

Estep,M., Armistead,D., Hossain,N., Elarainy,H., Goodman,Z., Baranova,A., Chandhoke,V., et al. Differential expression of miRNAs in the visceral adipose tissue of patients with non-alcoholic fatty liver disease. *Aliment Pharmacol Ther* 2010; 32 (3): 487-97.

Faber,J., Krivtsov,A.V., Stubbs,M.C., Wright,R., Davis,T.N., van den Heuvel-Eibrink,M., Zwaan,C.M., et al. HOXA9 is required for survival in human MLL-rearranged acute leukemias. *Blood* 2009; 113 (11): 2375-85.

Falcon,S. and Gentleman,R. Using GOstats to test gene lists for GO term association. *Bioinformatics* 2007; 23 (2): 257-8.

Favaro,P.M., de Souza,M.S., Traina,F., Basseres,D.S., Costa,F.F., and Saad,S.T. Human leukocyte formin: a novel protein expressed in lymphoid malignancies and associated with Akt. *Biochem Biophys Res Commun* 2003; 311 (2): 365-71.

Favreau,A.J. and Sathyanarayana,P. miR-590-5p, miR-219-5p, miR-15b and miR-628-5p are commonly regulated by IL-3, GM-CSF and G-CSF in acute myeloid leukemia. *Leuk Res* 2012; 36 (3): 334-41.

Flatow,J., et al. FunDO: Exploring Genes Using Functional Disease Ontology Annotations (http://projects.bioinformatics.northwestern.edu/fundo). 2009. Computer Program

Fleige,S. and Pfaffl,M.W. RNA integrity and the effect on the real-time qRT-PCR performance. *Mol Aspects Med* 2006; 27 (2-3): 126-39.

Foran,J.M. New prognostic markers in acute myeloid leukemia: perspective from the clinic. *Hematology Am Soc Hematol Educ Program* 2010; 2010 47-55.

Gabet,Y., Baniwal,S.K., Leclerc,N., Shi,Y., Kohn-Gabet,A.E., Cogan,J., Dixon,A., et al. Krox20/EGR2 deficiency accelerates cell growth and differentiation in the monocytic lineage and decreases bone mass. *Blood* 2010; 116 (19): 3964-71.

Gamper,N., Fillon,S., Feng,Y., Friedrich,B., Lang,P.A., Henke,G., Huber,S.M., et al. K+ channel activation by all three isoforms of serum- and glucocorticoid-dependent protein kinase SGK. *Pflugers Arch* 2002; 445 (1): 60-6.

Gan,T., Jude,C.D., Zaffuto,K., and Ernst,P. Developmentally induced Mll1 loss reveals defects in postnatal haematopoiesis. *Leukemia* 2010; 24 (10): 1732-41.

Garzon,R., Volinia,S., Liu,C.G., Fernandez-Cymering,C., Palumbo,T., Pichiorri,F., Fabbri,M., et al. MicroRNA signatures associated with cytogenetics and prognosis in acute myeloid leukemia. *Blood* 2008; 111 (6): 3183-9.

Geijtenbeek,T.B., Torensma,R., van Vliet,S.J., van Duijnhoven,G.C., Adema,G.J., van Kooyk,Y., and Figdor,C.G. Identification of DC-SIGN, a novel dendritic cell-specific ICAM-3 receptor that supports primary immune responses. *Cell* 2000; 100 (5): 575-85.

Gemelli,C., Orlandi,C., Zanocco,M.T., Martello,A., Vignudelli,T., Ferrari,F., Montanari,M., et al. The vitamin D3/Hox-A10 pathway supports MafB function during the monocyte differentiation of human CD34+ hemopoietic progenitors. *J Immunol* 2008; 181 (8): 5660-72.

Gentleman,R.C., Carey,V.J., Bates,D.M., Bolstad,B., Dettling,M., Dudoit,S., Ellis,B., et al. Bioconductor: open software development for computational biology and bioinformatics. *Genome Biol* 2004; 5 (10): R80.

Ghannam,G., Takeda,A., Camarata,T., Moore,M.A., Viale,A., and Yaseen,N.R. The oncogene Nup98-HOXA9 induces gene transcription in myeloid cells. *J Biol Chem* 2004; 279 (2): 866-75.

Glasser,L. Functional differentiation in acute monoblastic leukemia. *Am J Clin Pathol* 1981; 75 (1): 122-5.

Gocek,E., Kielbinski,M., Baurska,H., Haus,O., Kutner,A., and Marcinkowska,E. Different susceptibilities to 1,25-dihydroxyvitamin D3-induced differentiation of AML cells carrying various mutations. *Leuk Res* 2010; 34 (5): 649-57.

Gombart,A.F., Borregaard,N., and Koeffler,H.P. Human cathelicidin antimicrobial peptide (CAMP) gene is a direct target of the vitamin D receptor and is strongly up-regulated in myeloid cells by 1,25-dihydroxyvitamin D3. *FASEB J* 2005; 19 (9): 1067-77.

Goyert,S.M., Ferrero,E., Rettig,W.J., Yenamandra,A.K., Obata,F., and Le Beau,M.M. The CD14 monocyte differentiation antigen maps to a region encoding growth factors and receptors. *Science* 1988; 239 (4839): 497-500.

Grandy,D.K., Zhang,Y.A., Bouvier,C., Zhou,Q.Y., Johnson,R.A., Allen,L., Buck,K., et al. Multiple human D5 dopamine receptor genes: a functional receptor and two pseudogenes. *PNAS* 1991; 88 (20): 9175-9.

Gresko,E., Ritterhoff,S., Sevilla-Perez,J., Roscic,A., Frobius,K., Kotevic,I., Vichalkovski,A., et al. PML tumor suppressor is regulated by HIPK2-mediated phosphorylation in response to DNA damage. *Oncogene* 2009; 28 (5): 698-708.

Grinnell,F. Fibronectin and wound healing. *J Cell Biochem* 1984; 26 (2): 107-16.

Guenther,M.G., Jenner,R.G., Chevalier,B., Nakamura,T., Croce,C.M., Canaani,E., and Young,R.A. Global and Hox-specific roles for the MLL1 methyltransferase. *PNAS* 2005; 102 (24): 8603-8.

Guerzoni,C., Bardini,M., Mariani,S.A., Ferrari-Amorotti,G., Neviani,P., Panno,M.L., Zhang,Y., et al. Inducible activation of CEBPB, a gene negatively regulated by BCR/ABL, inhibits proliferation and promotes differentiation of BCR/ABL-expressing cells. *Blood* 2006; 107 (10): 4080-9.

Gupta,R.A., Shah,N., Wang,K.C., Kim,J., Horlings,H.M., Wong,D.J., Tsai,M.C., et al. Long non-coding RNA HOTAIR reprograms chromatin state to promote cancer metastasis. *Nature* 2010; 464 (7291): 1071-6.

Hammond,S.M. MicroRNAs as oncogenes. *Curr Opin Genet Dev* 2006; 16 (1): 4-9.

Hasegawa,Y., Takahashi,N., Forrest,A.R., Shin,J.W., Kinoshita,Y., Suzuki,H., and Hayashizaki,Y. CC chemokine ligand 2 and leukemia inhibitory factor cooperatively promote pluripotency in mouse induced pluripotent cells. *Stem Cells* 2011; 29 (8): 1196-205.

Haynes,C.M. and Ron,D. The mitochondrial UPR - protecting organelle protein homeostasis. *J Cell Sci* 2010; 123 (Pt 22): 3849-55.

He,H., Hua,X., and Yan,J. Epigenetic regulations in hematopoietic Hox code. *Oncogene* 2011a; 30 (4): 379-88.

He,N., Chan,C.K., Sobhian,B., Chou,S., Xue,Y., Liu,M., Alber,T., et al. Human Polymerase-Associated Factor complex (PAFc) connects the Super Elongation Complex (SEC) to RNA polymerase II on chromatin. *PNAS* 2011b; 108 (36): E636-E645.

Heldens,L., Hensen,S.M., Onnekink,C., van Genesen,S.T., Dirks,R.P., and Lubsen,N.H. An atypical unfolded protein response in heat shocked cells. *PLoS One* 2011; 6 (8): e23512.

Hess,J., Angel,P., and Schorpp-Kistner,M. AP-1 subunits: quarrel and harmony among siblings. *J Cell Sci* 2004; 117 (Pt 25): 5965-73.

Hollink,I.H., Van den Heuvel-Eibrink MM, and Zwaan,C.M. CEBPA resembles Roman god Janus. *Blood* 2009; 113 (26): 6501-2.

Hsieh,J.J., Ernst,P., Erdjument-Bromage,H., Tempst,P., and Korsmeyer,S.J. Proteolytic cleavage of MLL generates a complex of N- and C-terminal fragments that confers protein stability and subnuclear localization. *Mol Cell Biol* 2003; 23 (1): 186-94.

Hua,S., Kittler,R., and White,K.P. Genomic antagonism between retinoic acid and estrogen signaling in breast cancer. *Cell* 2009; 137 (7): 1259-71.

Huang,D.W., Sherman,B.T., and Lempicki,R.A. Bioinformatics enrichment tools: paths toward the comprehensive functional analysis of large gene lists. *Nucleic Acids Res* 2009a; 37 (1): 1-13.

Huang,D.W., Sherman,B.T., and Lempicki,R.A. Systematic and integrative analysis of large gene lists using DAVID bioinformatics resources. *Nat Protocols* 2009b; 4 (1): 44-57.

Hutvagner,G. Small RNA asymmetry in RNAi: Function in RISC assembly and gene regulation. *FEBS Lett* 2005; 579 (26): 5850-7.

Hwang,H.W. and Mendell,J.T. MicroRNAs in cell proliferation, cell death, and tumorigenesis. *Br J Cancer* 2006; 94 (6): 776-80.

Ichijo,H., Nishida,E., Irie,K., ten Dijke,P., Saitoh,M., Moriguchi,T., Takagi,M., et al. Induction of apoptosis by ASK1, a mammalian MAPKKK that activates SAPK/JNK and p38 signaling pathways. *Science* 1997; 275 (5296): 90-4.

International Human Genome Sequencing Consortium Finishing the euchromatic sequence of the human genome. *Nature* 2004; 431 (7011): 931-45.

Itoh,M., Fu,L., and Tohda,S. NF-kappaB activation induced by Notch ligand stimulation in acute myeloid leukemia cells. *Oncol Rep* 2009; 22 (3): 631-4.

Iwasaki,T., Katsumi,A., Kiyoi,H., Tanizaki,R., Ishikawa,Y., Ozeki,K., Kobayashi,M., et al. Prognostic implication and biological roles of RhoH in acute myeloid leukaemia. *Eur J Haematol* 2008; 81 (6): 454-60.

Jackson,A.L. and Linsley,P.S. Recognizing and avoiding siRNA off-target effects for target identification and therapeutic application. *Nat Rev Drug Discov* 2010; 9 (1): 57-67.

Jacobson,E.M., Hugo,E.R., Tuttle,T.R., Papoian,R., and Ben Jonathan,N. Unexploited therapies in breast and prostate cancer: blockade of the prolactin receptor. *Trends Endocrinol Metab* 2010; 21 (11): 691-8.

Jaleco,A.C., Neves,H., Hooijberg,E., Gameiro,P., Clode,N., Haury,M., Henrique,D., et al. Differential effects of Notch ligands Delta-1 and Jagged-1 in human lymphoid differentiation. *J Exp Med* 2001; 194 (7): 991-1002.

Jansen,M.W., van,d.V., V, and van Dongen,J.J. Efficient and easy detection of MLL-AF4, MLL-AF9 and MLL-ENL fusion gene transcripts by multiplex real-time quantitative RT-PCR in TaqMan and LightCycler. *Leukemia* 2005; 19 (11): 2016-8.

Johnnidis,J.B., Harris,M.H., Wheeler,R.T., Stehling-Sun,S., Lam,M.H., Kirak,O., Brummelkamp,T.R., et al. Regulation of progenitor cell proliferation and granulocyte function by microRNA-223. *Nature* 2008; 451 (7182): 1125-9.

Jongen-Lavrencic,M., Sun,S.M., Dijkstra,M.K., Valk,P.J., and Lowenberg,B. MicroRNA expression profiling in relation to the genetic heterogeneity of acute myeloid leukemia. *Blood* 2008; 111 (10): 5078-85.

Juan,A.H., Kumar,R.M., Marx,J.G., Young,R.A., and Sartorelli,V. Mir-214-dependent regulation of the polycomb protein Ezh2 in skeletal muscle and embryonic stem cells. *Mol Cell* 2009; 36 (1): 61-74.

Juszczynski,P., Rodig,S.J., Ouyang,J., O'Donnell,E., Takeyama,K., Mlynarski,W., Mycko,K., et al. MLL-rearranged B lymphoblastic leukemias selectively express the immunoregulatory carbohydrate-binding protein galectin-1. *Clin Cancer Res* 2010; 16 (7): 2122-30.

Kaderi,M.A., Kanduri,M., Buhl,A.M., Sevov,M., Cahill,N., Gunnarsson,R., Jansson,M., et al. LPL is the strongest prognostic factor in a comparative analysis of RNA-based markers in early chronic lymphocytic leukemia. *Haematologica* 2011; 96 (8): 1153-60.

Kamminga,L.M., Bystrykh,L.V., de Boer,A., Houwer,S., Douma,J., Weersing,E., Dontje,B., et al. The Polycomb group gene Ezh2 prevents hematopoietic stem cell exhaustion. *Blood* 2006; 107 (5): 2170-9.

Kang,S., Elf,S., Dong,S., Hitosugi,T., Lythgoe,K., Guo,A., Ruan,H., et al. Fibroblast growth factor receptor 3 associates with and tyrosine phosphorylates p90 RSK2, leading to RSK2 activation that mediates hematopoietic transformation. *Mol Cell Biol* 2009; 29 (8): 2105-17.

Kasinski,A.L. and Slack,F.J. Epigenetics and genetics. MicroRNAs en route to the clinic: progress in validating and targeting microRNAs for cancer therapy. *Nat Rev Cancer* 2011; 11 (12): 849-64.

Katunuma,N., Matsunaga,Y., and Saibara,T. Mechanism and regulation of antigen processing by cathepsin B. *Adv Enzyme Regul* 1994; 34 145-58.

Kaufmann,S.H., Desnoyers,S., Ottaviano,Y., Davidson,N.E., and Poirier,G.G. Specific proteolytic cleavage of poly(ADP-ribose) polymerase: an early marker of chemotherapy-induced apoptosis. *Cancer Res* 1993; 53 (17): 3976-85.

Kauss,M.A., Reiterer,G., Bunaciu,R.P., and Yen,A. Human myeloblastic leukemia cells (HL-60) express a membrane receptor for estrogen that signals and modulates retinoic acid-induced cell differentiation. *Exp Cell Res* 2008; 314 (16): 2999-3006.

Kawagoe,H., Kawagoe,R., and Sano,K. Targeted down-regulation of MLL-AF9 with antisense oligodeoxyribonucleotide reduces the expression of the HOXA7 and -A10 genes and induces apoptosis in a human leukemia cell line, THP-1. *Leukemia* 2001; 15 (11): 1743-9.

Kawakami,Y., Esteban,C.R., Matsui,T., Rodriguez-Leon,J., Kato,S., and Izpisua Belmonte,J.C. Sp8 and Sp9, two closely related buttonhead-like transcription factors, regulate Fgf8 expression and limb outgrowth in vertebrate embryos. *Development* 2004; 131 (19): 4763-74.

Kelly,L.M., Englmeier,U., Lafon,I., Sieweke,M.H., and Graf,T. MafB is an inducer of monocytic differentiation. *EMBO J* 2000; 19 (9): 1987-97.

Kestler,H.A. and Kuhl,M. From individual Wnt pathways towards a Wnt signalling network. *Philos Trans R Soc Lond B Biol Sci* 2008; 363 (1495): 1333-47.

Kida,Y., Shimizu,T., and Kuwano,K. Opposing roles of activator protein-1 and CCAAT/enhancer binding protein beta in the regulation of inducible granulysin gene expression in a human monocytic cell line, THP-1. *Immunology* 2002; 107 (4): 507-16.

Kishimoto,K., Kaneko,S., Ohmori,K., Tamura,T., and Hasegawa,K. Olopatadine suppresses the migration of THP-1 monocytes induced by S100A12 protein. *Mediators Inflamm* 2006; 2006 (1): 42726.

Kiss,F., Simon,A., Csathy,L., Hevessy,Z., Katona,E., Kiss,C., and Kappelmayer,J. A coagulation factor becomes useful in the study of acute leukemias: studies with blood coagulation factor XIII. *Cytometry A* 2008; 73 (3): 194-201.

Kitchens,R.L. Role of CD14 in cellular recognition of bacterial lipopolysaccharides. *Chem Immunol* 2000; 74 61-82.

Klco,J.M., Kulkarni,S., Kreisel,F.H., Nguyen,T.D., Hassan,A., and Frater,J.L. Immunohistochemical analysis of monocytic leukemias: usefulness of CD14 and Kruppel-like factor 4, a novel monocyte marker. *Am J Clin Pathol* 2011; 135 (5): 720-30.

Kobayashi,T., Deak,M., Morrice,N., and Cohen,P. Characterization of the structure and regulation of two novel isoforms of serum- and glucocorticoid-induced protein kinase. *Biochem J* 1999; 344 Pt 1 189-97.

Kohlmann,A., Schoch,C., Dugas,M., Schnittger,S., Hiddemann,W., Kern,W., and Haferlach,T. New insights into MLL gene rearranged acute leukemias using gene expression profiling: shared pathways, lineage commitment, and partner genes. *Leukemia* 2005; 19 (6): 953-64.

Koivusalo,M., Kapus,A., and Grinstein,S. Sensors, transducers, and effectors that regulate cell size and shape. *J Biol Chem* 2009; 284 (11): 6595-9.

Kondos,H., Anastasiadou,E., Photopoulou,A., Cary,P., Aleporou-Marinou,V., and Pataryas,T. Elevated levels of the chromosomal protein HMG 17 in chronic myelogenic leukemia. *Biochem Mol Biol Int* 1995; 36 (4): 803-9.

Krivtsov,A.V., Twomey,D., Feng,Z., Stubbs,M.C., Wang,Y., Faber,J., Levine,J.E., et al. Transformation from committed progenitor to leukaemia stem cell initiated by MLL-AF9. *Nature* 2006; 442 (7104): 818-22.

Kroon,E., Krosl,J., Thorsteinsdottir,U., Baban,S., Buchberg,A.M., and Sauvageau,G. Hoxa9 transforms primary bone marrow cells through specific collaboration with Meis1a but not Pbx1b. *EMBO J* 1998; 17 (13): 3714-25.

Kufe,D., Pollock,R., Weichselbaum,R., Bast,R.J., Gansler,T., Holland,J., and Frei,E. 2003. *In* Cancer Medicine 6. BC Decker Inc., Hamilton (Canada).

La Rocca,R., Fulciniti,M., Lakshmikanth,T., Mesuraca,M., Ali,T.H., Mazzei,V., Amodio,N., et al. Early Hematopoietic Zinc Finger Protein Prevents Tumor Cell Recognition by Natural Killer Cells. *J Immunol* 2009; 182 (8): 4529-37.

Landthaler,M., Yalcin,A., and Tuschl,T. The human DiGeorge syndrome critical region gene 8 and Its D. melanogaster homolog are required for miRNA biogenesis. *Curr Biol* 2004; 14 (23): 2162-7.

Langer,T., Metzler,M., Reinhardt,D., Viehmann,S., Borkhardt,A., Reichel,M., Stanulla,M., et al. Analysis of t(9;11) chromosomal breakpoint sequences in childhood acute leukemia: almost identical MLL breakpoints in therapy-related AML after treatment without etoposides. *Genes Chromosomes Cancer* 2003; 36 (4): 393-401.

Lawrence,H.J., Helgason,C.D., Sauvageau,G., Fong,S., Izon,D.J., Humphries,R.K., and Largman,C. Mice bearing a targeted interruption of the homeobox gene *HOXA9* have defects in myeloid, erythroid, and lymphoid hematopoiesis. *Blood* 1997; 89 (6): 1922-30.

Lee,Y.N., Brandal,S., Noel,P., Wentzel,E., Mendell,J.T., McDevitt,M.A., Kapur,R., et al. KIT signaling regulates MITF expression through miRNAs in normal and malignant mast cell proliferation. *Blood* 2011; 117 (13): 3629-40.

Legdeur,M.C., Broekhoven,M.G., Schuurhuis,G.J., Beelen,R.H., and Ossenkoppele,G.J. Monocyte-chemoattractant-protein-1-mediated migration of human monocytes towards blasts from patients with acute myeloid leukemia. *Cancer Immunol Immunother* 2001; 50 (1): 16-22.

Lennartsson,A., Garwicz,D., Lindmark,A., and Gullberg,U. The proximal promoter of the human cathepsin G gene conferring myeloid-specific expression includes C/EBP, c-myb and PU.1 binding sites. *Gene* 2005; 356 193-202.

Lessard,F., Morin,F., Ivanchuk,S., Langlois,F., Stefanovsky,V., Rutka,J., and Moss,T. The ARF tumor suppressor controls ribosome biogenesis by regulating the RNA polymerase I transcription factor TTF-I. *Mol Cell* 2010; 38 (4): 539-50.

Leung,M.F., Lin,T.S., and Sartorelli,A.C. Changes in actin and actin-binding proteins during the differentiation of HL-60 leukemia cells. *Cancer Res* 1992; 52 (11): 3063-6.

Li,L.M., Hou,D.X., Guo,Y.L., Yang,J.W., Liu,Y., Zhang,C.Y., and Zen,K. Role of microRNA-214-targeting phosphatase and tensin homolog in advanced glycation end product-induced apoptosis delay in monocytes. *J Immunol* 2011; 186 (4): 2552-60.

Li,Q., Kopecky,K.J., Mohan,A., Willman,C.L., Appelbaum,F.R., Weick,J.K., and Issa,J.P. Estrogen receptor methylation is associated with improved survival in adult acute myeloid leukemia. *Clin Cancer Res* 1999; 5 (5): 1077-84.

Li,X.L., Arai,Y., Harada,H., Shima,Y., Yoshida,H., Rokudai,S., Aikawa,Y., et al. Mutations of the HIPK2 gene in acute myeloid leukemia and myelodysplastic syndrome impair. *Oncogene* 2007; 26 (51): 7231-9.

Li,Z., Huang,H., Li,Y., Jiang,X., Chen,P., Arnovitz,S., Radmacher,M.D., et al. Up-regulation of a HOXA-PBX3 homeobox-gene signature following down-regulation of miR-181 is associated with adverse prognosis in patients with cytogenetically-abnormal AML. *Blood* 2012.

Li,Z., Luo,R.T., Mi,S., Sun,M., Chen,P., Bao,J., Neilly,M.B., et al. Consistent deregulation of gene expression between human and murine MLL rearrangement leukemias. *Cancer Res* 2009; 69 (3): 1109-16.

Lim,L.P., Lau,N.C., Garrett-Engele,P., Grimson,A., Schelter,J.M., Castle,J., Bartel,D.P., et al. Microarray analysis shows that some microRNAs downregulate large numbers of target mRNAs. *Nature* 2005; 433 (7027): 769-73.

Lin,C., Smith,E.R., Takahashi,H., Lai,K.C., Martin-Brown,S., Florens,L., Washburn,M.P., et al. AFF4, a component of the ELL/P-TEFb elongation complex and a shared subunit of MLL chimeras, can link transcription elongation to leukemia. *Mol Cell* 2010; 37 (3): 429-37.

Liu,A., Takahashi,M., Toba,K., Zheng,Z., Hashimoto,S., Nikkuni,K., Furukawa,T., et al. Regulation of the expression of MHC class I and II by class II transactivator (CIITA) in hematopoietic cells. *Hematol Oncol* 1999; 17 (4): 149-60.

Lu,J., Getz,G., Miska,E.A., Alvarez-Saavedra,E., Lamb,J., Peck,D., Sweet-Cordero,A., et al. MicroRNA expression profiles classify human cancers. *Nature* 2005; 435 (7043): 834-8.

Lutherborrow,M., Bryant,A., Jayaswal,V., Agapiou,D., Palma,C., Yang,Y.H., and Ma,D.D. Expression profiling of cytogenetically normal acute myeloid leukemia identifies microRNAs that target genes involved in monocytic differentiation. *Am J Hematol* 2011; 86 (1): 2-11.

Lyo,D., Xu,L., and Foster,D.A. Phospholipase D stabilizes HDM2 through an mTORC2/SGK1 pathway. *Biochem Biophys Res Commun* 2010; 396 (2): 562-5.

Mace,O.J., Lister,N., Morgan,E., Shepherd,E., Affleck,J., Helliwell,P., Bronk,J.R., et al. An energy supply network of nutrient absorption coordinated by calcium and T1R taste receptors in rat small intestine. *J Physiol* 2009; 587 (1): 195-210.

Magg,T., Hartrampf,S., and Albert,M.H. Stable nonviral gene transfer into primary human T cells. *Hum Gene Ther* 2009; 20 (9): 989-98.

Mai,T., Zan,H., Zhang,J., Hawkins,J.S., Xu,Z., and Casali,P. Estrogen receptors bind to and activate the HOXC4/HoxC4 promoter to potentiate HoxC4-mediated activation-induced cytosine deaminase induction, immunoglobulin class switch DNA recombination, and somatic hypermutation. *J Biol Chem* 2010; 285 (48): 37797-810.

Manning,G., Whyte,D.B., Martinez,R., Hunter,T., and Sudarsanam,S. The protein kinase complement of the human genome. *Science* 2002; 298 (5600): 1912-34.

Mao,J.H., Wu,D., Kim,I.J., Kang,H.C., Wei,G., Climent,J., Kumar,A., et al. Hipk2 cooperates with p53 to suppress gamma-ray radiation-induced mouse thymic lymphoma. *Oncogene* 2012; 31 (9): 1176-80.

MAQC Consortium The MicroArray Quality Control (MAQC) project shows inter- and intraplatform reproducibility of gene expression measurements. *Nat Biotechnol* 2006; 24 (9): 1151-61.

Marcucci,G., Mrozek,K., Radmacher,M.D., Garzon,R., and Bloomfield,C.D. The prognostic and functional role of microRNAs in acute myeloid leukemia. *Blood* 2011; 117 (4): 1121-9.

Margaritis,T. and Holstege,F.C.P. Poised RNA Polymerase II Gives Pause for Thought. *Cell* 2008; 133 (4): 581-4.

Martin,J., Anamika,K., and Srinivasan,N. Classification of protein kinases on the basis of both kinase and non-kinase regions. *PLoS One* 2010; 5 (9): e12460.

Martino,V., Bianchera,A., Reia,L., Bussolati,O., Fazzina,R., Marino,F., Montemurro,L., et al. Down-regulation of *HOXA4*, *HOXA7*, *HOXA10*, *HOXA11* and *MEIS1* during monocyte-macrophage differentiation in THP-1 cells. *Molecular Medicine Reports* 2009; 2 241-4.

Martino,V., Tonelli,R., Montemurro,L., Franzoni,M., Marino,F., Fazzina,R., and Pession,A. Down-regulation of *MLL-AF9*, *MLL* and *MYC* expression is not obligatory for monocyte-macrophage maturation in AML-M5 cell lines carrying t(9;11)(p22;q23). *Oncol Rep* 2006; 15 (1): 207-11.

Matikainen,S. and Hurme,M. Comparison of retinoic acid and phorbol myristate acetate as inducers of monocytic differentiation. *Int J Cancer* 1994; 57 (1): 98-103.

Matsubara,E., Sakai,I., Yamanouchi,J., Fujiwara,H., Yakushijin,Y., Hato,T., Shigemoto,K., et al. The role of zinc finger protein 521/early hematopoietic zinc finger protein in erythroid cell differentiation. *J Biol Chem* 2009; 284 (6): 3480-7.

Mazur,G., Wrobel,T., Butrym,A., Kapelko-Slowik,K., Poreba,R., and Kuliczkowski,K. Increased monocyte chemoattractant protein 1 (MCP-1/CCL-2) serum level in acute myeloid leukemia. *Neoplasma* 2007; 54 (4): 285-9.

McCarthy,D.M., San Miguel,J.F., Freake,H.C., Green,P.M., Zola,H., Catovsky,D., and Goldman,J.M. 1,25-dihydroxyvitamin D3 inhibits proliferation of human promyelocytic leukaemia (HL60) cells and induces monocyte-macrophage differentiation in HL60 and normal human bone marrow cells. *Leuk Res* 1983; 7 (1): 51-5.

Melillo,L., Musto,P., Tomasi,P., Cascavilla,N., Bodenizza,C., Ladogana,S., and Carotenuto,M. Serum beta 2-microglobulin in malignant lymphoproliferative disorders. *Tumori* 1988; 74 (2): 129-35.

Mellor,H. and Parker,P.J. The extended protein kinase C superfamily. *Biochem J* 1998; 332 (Pt 2) 281-92.

Mestdagh,P., Van Vlierberghe,P., De Weer,A., Muth,D., Westermann,F., Speleman,F., and Vandesompele,J. A novel and universal method for microRNA RT-qPCR data normalization. *Genome Biol* 2009; 10 (6): R64.

Meyer,C., Schneider,B., Jakob,S., Strehl,S., Attarbaschi,A., Schnittger,S., Schoch,C., et al. The MLL recombinome of acute leukemias. *Leukemia* 2006; 20 (5): 777-84.

Mi,S., Li,Z., Chen,P., He,C., Cao,D., Elkahloun,A., Lu,J., et al. Aberrant overexpression and function of the miR-17-92 cluster in MLL-rearranged acute leukemia. *PNAS* 2010; 107 (8): 3710-5.

Middeldorf,I., Galm,O., Osieka,R., Jost,E., Herman,J.G., and Wilop,S. Sequence of administration and methylation of SOCS3 may govern response to gemtuzumab ozogamicin in combination with conventional chemotherapy in patients with refractory or relapsed acute myelogenous leukemia (AML). *Am J Hematol* 2010; 85 (7): 477-81.

Milech,N., Kees,U.R., and Watt,P.M. Novel alternative PBX3 isoforms in leukemia cells with distinct interaction specificities. *Genes Chromosomes Cancer* 2001; 32 (3): 275-80.

Minami,Y., Oishi,I., Endo,M., and Nishita,M. Ror-family receptor tyrosine kinases in noncanonical Wnt signaling: their implications in developmental morphogenesis and human diseases. *Dev Dyn* 2010; 239 (1): 1-15.

Minamoto,S., Ikegame,K., Ueno,K., Narazaki,M., Naka,T., Yamamoto,H., Matsumoto,T., et al. Cloning and functional analysis of new members of STAT induced STAT inhibitor (SSI) family: SSI-2 and SSI-3. *Biochem Biophys Res Commun* 1997; 237 (1): 79-83.

Mirro,J., Kitchingman,G.R., Williams,D.L., Murphy,S.B., Zipf,T.F., and Stass,S.A. Mixed lineage leukemia: the implications for hematopoietic differentiation. *Blood* 1986; 68 (2): 597-9.

Mishra,B.P., Ansari,K.I., and Mandal,S.S. Dynamic association of MLL1, H3K4 trimethylation with chromatin and Hox gene expression during the cell cycle. *FEBS J* 2009; 276 (6): 1629-40.

Mizoguchi,Y., Fujita,N., Taki,T., Hayashi,Y., and Hamamoto,K. Juvenile myelomonocytic leukemia with t(7;11)(p15;p15) and NUP98-HOXA11 fusion. *Am J Hematol* 2009; 84 (5): 295-7.

Mobasheri,M.B., Modarressi,M.H., Shabani,M., Asgarian,H., Sharifian,R.A., Vossough,P., and Shokri,F. Expression of the testis-specific gene, TSGA10, in Iranian patients with acute lymphoblastic leukemia (ALL). *Leuk Res* 2006; 30 (7): 883-9.

Moellering,R.E., Cornejo,M., Davis,T.N., Del Bianco,C., Aster,J.C., Blacklow,S.C., Kung,A.L., et al. Direct inhibition of the NOTCH transcription factor complex. *Nature* 2009; 462 (7270): 182-8.

Mohan,M., Lin,C., Guest,E., and Shilatifard,A. Licensed to elongate: a molecular mechanism for MLL-based leukaemogenesis. *Nat Rev Cancer* 2010; 10 (10): 721-8.

Moretti,P., Simmons,P., Thomas,P., Haylock,D., Rathjen,P., Vadas,M., and D'Andrea,R. Identification of homeobox genes expressed in human haemopoietic progenitor cells. *Gene* 1994; 144 (2): 213-9.

Mueller,B.U., Pabst,T., Fos,J., Petkovic,V., Fey,M.F., Asou,N., Buergi,U., et al. ATRA resolves the differentiation block in t(15;17) acute myeloid leukemia by restoring PU.1 expression. *Blood* 2006; 107 (8): 3330-8.

Murata-Ohsawa,M., Tohda,S., Kogoshi,H., and Nara,N. The Notch ligand, Delta-1, reduces TNF-alpha-induced growth suppression and apoptosis by decreasing activation of caspases in U937 cells. *Int J Mol Med* 2004; 14 (5): 861-6.

Nagata,C., Iwasa,S., Shiraki,M., and Shimizu,H. Estrogen and alpha-fetoprotein levels in maternal and umbilical cord blood samples in relation to birth weight. *Cancer Epidemiol Biomarkers Prev* 2006; 15 (8): 1469-72.

Naka,K., Hoshii,T., and Hirao,A. Novel therapeutic approach to eradicate tyrosine kinase inhibitor resistant chronic myeloid leukemia stem cells. *Cancer Sci* 2010; 101 (7): 1577-81.

Nakagawa,Y., Hasegawa,M., Kurata,M., Yamamoto,K., Abe,S., Inoue,M., Takemura,T., et al. Expression of IAP-family proteins in adult acute mixed lineage leukemia (AMLL). *Am J Hematol* 2005; 78 (3): 173-80.

Nakajima,K., Asakura,T., Oike,H., Morita,Y., Shimizu-Ibuka,A., Misaka,T., Sorimachi,H., et al. Neoculin, a taste-modifying protein, is recognized by human sweet taste receptor. *Neuroreport* 2006; 17 (12): 1241-4.

Nakamura,T., Canaani,E., and Croce,C.M. Oncogenic All1 fusion proteins target Drosha-mediated microRNA processing. *PNAS* 2007; 104 (26): 10980-5.

National Center for Biotechnology Information . Gene Database. http://www.ncbi.nlm.nih.gov/sites/entrez?db=gene . 2012. Electronic Citation

Nature Publishing Group Whither RNAi? *Nat Cell Biol* 2003; 5 (6): 489-90.

Neumann,F., Gattermann,N., Barthelmes,H.U., Haas,R., and Germing,U. Levels of beta 2 microglobulin have a prognostic relevance for patients with myelodysplastic syndrome with regard to survival and the risk of transformation into acute myelogenous leukemia. *Leuk Res* 2009; 33 (2): 232-6.

Nielsen,J., Christiansen,J., Lykke-Andersen,J., Johnsen,A.H., Wewer,U.M., and Nielsen,F.C. A family of insulin-like growth factor II mRNA-binding proteins represses translation in late development. *Mol Cell Biol* 1999; 19 (2): 1262-70.

Norwood,K., Wang,R.Y., Hirschmann-Jax,C., Andreeff,M., Brenner,M.K., Goodell,M.A., and Wulf,G.G. An in vivo propagated human acute myeloid leukemia expressing ABCA3. *Leuk Res* 2004; 28 (3): 295-9.

Okoshi,R., Kubo,N., Nakashima,K., Shimozato,O., Nakagawara,A., and Ozaki,T. CREB represses p53-dependent transactivation of MDM2 through the complex formation with p53 and contributes to p53-mediated apoptosis in response to glucose deprivation. *Biochem Biophys Res Commun* 2011; 406 (1): 79-84.

Oltval,Z.N., Milliman,C.L., and Korsmeyer,S.J. Bcl-2 heterodimerizes in vivo with a conserved homolog, Bax, that accelerates programed cell death. *Cell* 1993; 74 (4): 609-19.

Onishi,H., Kino,Y., Morita,T., Futai,E., Sasagawa,N., and Ishiura,S. MBNL1 associates with YB-1 in cytoplasmic stress granules. *J Neurosci Res* 2008; 86 (9): 1994-2002.

Osborne,J.D., Flatow,J., Holko,M., Lin,S.M., Kibbe,W.A., Zhu,L.J., Danila,M.I., et al. Annotating the human genome with Disease Ontology. *BMC Genomics* 2009; 10 Suppl 1 S6.

Overington,J.P., Al Lazikani,B., and Hopkins,A.L. How many drug targets are there? *Nat Rev Drug Discov* 2006; 5 (12): 993-6.

Panagopoulos,I., Isaksson,M., Billstrom,R., Strombeck,B., Mitelman,F., and Johansson,B. Fusion of the NUP98 gene and the homeobox gene HOXC13 in acute myeloid leukemia with t(11;12)(p15;q13). *Genes Chromosomes Cancer* 2003; 36 (1): 107-12.

Park,J., Leong,M.L., Buse,P., Maiyar,A.C., Firestone,G.L., and Hemmings,B.A. Serum and glucocorticoid-inducible kinase (SGK) is a target of the PI 3-kinase-stimulated signaling pathway. *EMBO J* 1999; 18 (11): 3024-33.

Paroo,Z., Ye,X., Chen,S., and Liu,Q. Phosphorylation of the human microRNA-generating complex mediates MAPK/Erk signaling. *Cell* 2009; 139 (1): 112-22.

Pascall,J.C. and Brown,K.D. Characterization of a mammalian cDNA encoding a protein with high sequence similarity to the Drosophila regulatory protein Rhomboid. *FEBS Lett* 1998; 429 (3): 337-40.

Pession,A., Martino,V., Tonelli,R., Beltramini,C., Locatelli,F., Biserni,G., Franzoni,M., et al. MLL-AF9 oncogene expression affects cell growth but not terminal differentiation and is downregulated during monocyte-macrophage maturation in AML-M5 THP-1 cells. *Oncogene* 2003; 22 (54): 8671-6.

Phillips,C.L., Gerbing,R., Alonzo,T., Perentesis,J.P., Harley,I.T., Meshinchi,S., Bhatla,D., et al. MDM2 polymorphism increases susceptibility to childhood acute myeloid leukemia: a report from the Children's Oncology Group. *Pediatr Blood Cancer* 2010; 55 (2): 248-53.

Phinney,D.G., Gray,A.J., Hill,K., and Pandey,A. Murine mesenchymal and embryonic stem cells express a similar Hox gene profile. *Biochem Biophys Res Commun* 2005; 338 (4): 1759-65.

Pieters,J., Bakke,O., and Dobberstein,B. The MHC class II-associated invariant chain contains two endosomal targeting signals within its cytoplasmic tail. *J Cell Sci* 1993; 106 (Pt 3) 831-46.

Pina,C., May,G., Soneji,S., Hong,D., and Enver,T. MLLT3 regulates early human erythroid and megakaryocytic cell fate. *Cell Stem Cell* 2008; 2 (3): 264-73.

Pogna,E.A., Clayton,A.L., and Mahadevan,L.C. Signalling to chromatin through post-translational modifications of HMGN. *Biochim Biophys Acta* 2010; 1799 (1-2): 93-100.

Popovic,R., Riesbeck,L.E., Velu,C.S., Chaubey,A., Zhang,J., Achille,N.J., Erfurth,F.E., et al. Regulation of mir-196b by MLL and its overexpression by MLL fusions contributes to immortalization. *Blood* 2009; 113 (14): 3314-22.

Porkka,K., Laakkonen,P., Hoffman,J.A., Bernasconi,M., and Ruoslahti,E. A fragment of the HMGN2 protein homes to the nuclei of tumor cells and tumor endothelial cells in vivo. *PNAS* 2002; 99 (11): 7444-9.

Qiang,R., Wang,F., Shi,L.Y., Liu,M., Chen,S., Wan,H.Y., Li,Y.X., et al. Plexin-B1 is a target of miR-214 in cervical cancer and promotes the growth and invasion of HeLa cells. *Int J Biochem Cell Biol* 2011; 43 (4): 632-41.

R Development Core Team 2008. *In* R: A language and environment for statistical computing. R Foundation for Statistical Computing, Vienna, Austria.

Raimondi,S.C., Chang,M.N., Ravindranath,Y., Behm,F.G., Gresik,M.V., Steuber,C.P., Weinstein,H.J., et al. Chromosomal Abnormalities in 478 Children With Acute Myeloid Leukemia: Clinical Characteristics and Treatment Outcome in a Cooperative Pediatric Oncology Group Study - POG 8821. *Blood* 1999; 94 (11): 3707-16.

Ramirez,C.M., Davalos,A., Goedeke,L., Salerno,A.G., Warrier,N., Cirera-Salinas,D., Suarez,Y., et al. MicroRNA-758 regulates cholesterol efflux through posttranscriptional repression of ATP-binding cassette transporter A1. *Arterioscler Thromb Vasc Biol* 2011; 31 (11): 2707-14.

Rask-Andersen,M., Almen,M.S., and Schioth,H.B. Trends in the exploitation of novel drug targets. *Nat Rev Drug Discov* 2011; 10 (8): 579-90.

Rico-Bautista,E., Flores-Morales,A., and Fernβ ndez-Pθrez,L. Suppressor of cytokine signaling (SOCS) 2, a protein with multiple functions. *Cytokine Growth Factor Rev* 2006; 17 (6): 431-9.

Rimsza,L.M., Roberts,R.A., Miller,T.P., Unger,J.M., LeBlanc,M., Braziel,R.M., Weisenberger,D.D., et al. Loss of MHC class II gene and protein expression in diffuse large B-cell lymphoma is related to decreased tumor immunosurveillance and poor patient survival regardless of other prognostic factors: a follow-up study from the Leukemia and Lymphoma Molecular Profiling Project. *Blood* 2004; 103 (11): 4251-8.

Ripoll,V.M., Irvine,K.M., Ravasi,T., Sweet,M.J., and Hume,D.A. Gpnmb Is Induced in Macrophages by IFN-+¦ and Lipopolysaccharide and Acts as a Feedback Regulator of Proinflammatory Responses. *J Immunol* 2007; 178 (10): 6557-66.

Roghanian,A., Jones,D.C., Pattisapu,J.V., Wolfe,J., Young,N.T., and Behnam,B. Filament-associated TSGA10 protein is expressed in professional antigen presenting cells and interacts with vimentin. *Cell Immunol* 2010; 265 (2): 120-6.

Ross,M.E., Mahfouz,R., Onciu,M., Liu,H.C., Zhou,X., Song,G., Shurtleff,S.A., et al. Gene expression profiling of pediatric acute myelogenous leukemia. *Blood* 2004; 104 (12): 3679-87.

Rozovskaia,T., Ravid-Amir,O., Tillib,S., Getz,G., Feinstein,E., Agrawal,H., Nagler,A., et al. Expression profiles of acute lymphoblastic and myeloblastic leukemias with ALL-1 rearrangements. *PNAS* 2003; 100 (13): 7853-8.

Ruan,G.R., Qin,Y.Z., Chen,S.S., Li,J.L., Ma,X., Chang,Y., Wang,Y.Z., et al. Abnormal expression of the programmed cell death 5 gene in acute and chronic myeloid leukemia. *Leuk Res* 2006; 30 (9): 1159-65.

Ruan,G.R., Zhao,H.S., Chang,Y., Li,J.L., Qin,Y.Z., Liu,Y.R., Chen,S.S., et al. Adenovirus-mediated PDCD5 gene transfer sensitizes K562 cells to apoptosis induced by idarubicin in vitro and in vivo. *Apoptosis* 2008; 13 (5): 641-8.

Rucker,F.G., Sander,S., Dohner,K., Dohner,H., Pollack,J.R., and Bullinger,L. Molecular profiling reveals myeloid leukemia cell lines to be faithful model systems characterized by distinct genomic aberrations. *Leukemia* 2006; 20 (6): 994-1001.

Ruggero,D. and Pandolfi,P.P. Does the ribosome translate cancer? *Nat Rev Cancer* 2003; 3 (3): 179-92.

Salesse,S. and Verfaillie,C.M. BCR/ABL-mediated increased expression of multiple known and novel genes that may contribute to the pathogenesis of chronic myelogenous leukemia. *Mol Cancer Ther* 2003; 2 (2): 173-82.

Satoh,A., Graham,G.M., Bryant,S.V., and Gardiner,D.M. Neurotrophic regulation of epidermal dedifferentiation during wound healing and limb regeneration in the axolotl (Ambystoma mexicanum). *Dev Biol* 2008; 319 (2): 321-35.

Savli,H., Aalto,Y., Nagy,B., Knuutila,S., and Pakkala,S. Gene expression analysis of 1,25(OH)2D3-dependent differentiation of HL-60 cells: a cDNA array study. *Br J Haematol* 2002; 118 (4): 1065-70.

Schardt,J.A., Mueller,B.U., and Pabst,T. Activation of the unfolded protein response in human acute myeloid leukemia. *Methods Enzymol* 2011; 489 227-43.

Scholl,T., Mahanta,S.K., and Strominger,J.L. Specific complex formation between the type II bare lymphocyte syndrome-associated transactivators CIITA and RFX5. *PNAS* 1997; 94 (12): 6330-4.

Schroeder,A., Mueller,O., Stocker,S., Salowsky,R., Leiber,M., Gassmann,M., Lightfoot,S., et al. The RIN: an RNA integrity number for assigning integrity values to RNA measurements. *BMC Mol Biol* 2006; 7 (1): 3.

Schubert,I., Kellner,C., Stein,C., Kugler,M., Schwenkert,M., Saul,D., Mentz,K., et al. A single-chain triplebody with specificity for CD19 and CD33 mediates effective lysis of mixed lineage leukemia cells by dual targeting. *MAbs* 2011; 3 (1): 21-30.

Schuetz,A., Nana,D., Rose,C., Zocher,G., Milanovic,M., Koenigsmann,J., Blasig,R., et al. The structure of the Klf4 DNA-binding domain links to self-renewal and macrophage differentiation. *Cell Mol Life Sci* 2011; 68 (18): 3121-31.

Schuler,A., Schwieger,M., Engelmann,A., Weber,K., Horn,S., Muller,U., Arnold,M.A., et al. The MADS transcription factor Mef2c is a pivotal modulator of myeloid cell fate. *Blood* 2008; 111 (9): 4532-41.

Schwende,H., Fitzke,E., Ambs,P., and Dieter,P. Differences in the state of differentiation of THP-1 cells induced by phorbol ester and 1,25-dihydroxyvitamin D3. *J Leukoc Biol* 1996; 59 (4): 555-61.

Scott,E., Hexner,E., Perl,A., and Carroll,M. Targeted signal transduction therapies in myeloid malignancies. *Curr Oncol Rep* 2010; 12 (6): 358-65.

Sergeev,I.N. Calcium signaling in cancer and vitamin D. *J Steroid Biochem Mol Biol* 2005; 97 (1-2): 145-51.

Shiina,T., Hosomichi,K., Inoko,H., and Kulski,J.K. The HLA genomic loci map: expression, interaction, diversity and disease. *J Hum Genet* 2009; 54 (1): 15-39.

Shimane,M., Tani,K., Hibino,H., Setoyama,M., Takahashi,S., Tojo,A., Yodoi,J., et al. Significant expression of G-CSF-induced gene-1 (GIG-1) protein in myeloid cells and NK cells. *J Leukoc Biol* 1999; 65 (1): 109-16.

Shin,D.M., Zuba-Surma,E.K., Wu,W., Ratajczak,J., Wysoczynski,M., Ratajczak,M.Z., and Kucia,M. Novel epigenetic mechanisms that control pluripotency and quiescence of adult bone marrow-derived Oct4(+) very small embryonic-like stem cells. *Leukemia* 2009; 23 (11): 2042-51.

Slany,R.K. The molecular biology of mixed lineage leukemia. *Haematologica* 2009; 94 (7): 984-93.

Smith,L.L., Yeung,J., Zeisig,B.B., Popov,N., Huijbers,I., Barnes,J., Wilson,A.J., et al. Functional crosstalk between Bmi1 and MLL/Hoxa9 axis in establishment of normal hematopoietic and leukemic stem cells. *Cell Stem Cell* 2011; 8 (6): 649-62.

Smyth,G.K. Linear models and empirical bayes methods for assessing differential expression in microarray experiments. *Stat Appl Genet Mol Biol* 2004; 3 Article3.

Smyth,G.K. 2005. *In* Limma: linear models for microarray data. Springer, New York.

Sohal,J., Chase,A., Mould,S., Corcoran,M., Oscier,D., Iqbal,S., Parker,S., et al. Identification of four new translocations involving FGFR1 in myeloid disorders. *Genes Chromosomes Cancer* 2001; 32 (2): 155-63.

Somervaille,T.C.P. and Cleary,M.L. Identification and characterization of leukemia stem cells in murine MLL-AF9 acute myeloid leukemia. *Cancer Cell* 2006; 10 (4): 257-68.

Spicer,A.P., Joo,A., and Bowling,R.A., Jr. A hyaluronan binding link protein gene family whose members are physically linked adjacent to chondroitin sulfate proteoglycan core protein genes: the missing links. *J Biol Chem* 2003; 278 (23): 21083-91.

Standart,N. and Jackson,R.J. MicroRNAs repress translation of m7Gppp-capped target mRNAs in vitro by inhibiting initiation and promoting deadenylation. *Genes Dev* 2007; 21 (16): 1975-82.

Stavropoulou,V., Brault,L., and Schwaller,J. Insights into molecular pathways for targeted therapeutics in acute leukemia. *Swiss Med Wkly* 2010; 140 w13068.

Steinbach,D., Gillet,J.P., Sauerbrey,A., Gruhn,B., Dawczynski,K., Bertholet,V., de Longueville,F., et al. ABCA3 as a possible cause of drug resistance in childhood acute myeloid leukemia. *Clin Cancer Res* 2006; 12 (14 Pt 1): 4357-63.

Stoskus,M., Gineikiene,E., Valceckiene,V., Valatkaite,B., Pileckyte,R., and Griskevicius,L. Identification of characteristic IGF2BP expression patterns in distinct B-ALL entities. *Blood Cells Mol Dis* 2011; 46 (4): 321-6.

Stumpel,D.J., Schotte,D., Lange-Turenhout,E.A., Schneider,P., Seslija,L., de Menezes,R.X., Marquez,V.E., et al. Hypermethylation of specific microRNA genes in MLL-rearranged infant acute lymphoblastic leukemia: major matters at a micro scale. *Leukemia* 2011; 25 (3): 429-39.

Su,L., Zhao,H., Sun,C., Zhao,B., Zhao,J., Zhang,S., Su,H., et al. Role of Hmbox1 in endothelial differentiation of bone-marrow stromal cells by a small molecule. *ACS Chem Biol* 2010; 5 (11): 1035-43.

Sun,H., Tu,X., and Baserga,R. A mechanism for cell size regulation by the insulin and insulin-like growth factor-I receptors. *Cancer Res* 2006a; 66 (23): 11106-9.

Sun,R., Iribarren,P., Zhang,N., Zhou,Y., Gong,W., Cho,E.H., Lockett,S., et al. Identification of neutrophil granule protein cathepsin G as a novel chemotactic agonist for the G protein-coupled formyl peptide receptor. *J Immunol* 2004; 173 (1): 428-36.

Sun,X., Wang,E., Jones,D.M., Shen,H., Johnson,M.M., Issa,J.P., Amin,H., et al. SOX4 gene expression in human leukemic and benign hematopoietic cells. *AACR Meeting Abstracts* 2006b; 2006 (1): 714-a.

Suzuki,H., Forrest,A.R., van Nimwegen,E., Daub,C.O., Balwierz,P.J., Irvine,K.M., Lassmann,T., et al. The transcriptional network that controls growth arrest and differentiation in a human myeloid leukemia cell line. *Nat Genet* 2009; 41 (5): 553-62.

Swingler,S., Brichacek,B., Jacque,J.M., Ulich,C., Zhou,J., and Stevenson,M. HIV-1 Nef intersects the macrophage CD40L signalling pathway to promote resting-cell infection. *Nature* 2003; 424 (6945): 213-9.

Tabayashi,T., Ishimaru,F., Takata,M., Kataoka,I., Nakase,K., Kozuka,T., and Tanimoto,M. Characterization of the short isoform of Helios overexpressed in patients with T-cell malignancies. *Cancer Sci* 2007; 98 (2): 182-8.

Taft,R.J., Pang,K.C., Mercer,T.R., Dinger,M., and Mattick,J.S. Non-coding RNAs: regulators of disease. *J Pathol* 2010; 220 (2): 126-39.

Tanaka,N., Kawasaki,K., Nejime,N., Kubota,Y., Nakamura,K., Kunitomo,M., Takahashi,K., et al. P2Y receptor-mediated Ca(2+) signaling increases human vascular endothelial cell permeability. *J Pharmacol Sci* 2004a; 95 (2): 174-80.

Tanaka,R., Ono,T., Sato,S., Nakada,T., Koizumi,F., Hasegawa,K., Nakagawa,K., et al. Over-expression of the testis-specific gene TSGA10 in cancers and its immunogenicity. *Microbiol Immunol* 2004b; 48 (4): 339-45.

Tassaneetrithep,B., Burgess,T.H., Granelli-Piperno,A., Trumpfheller,C., Finke,J., Sun,W., Eller,M.A., et al. DC-SIGN (CD209) mediates dengue virus infection of human dendritic cells. *J Exp Med* 2003; 197 (7): 823-9.

Taubes,G. Misfolding the way to disease. *Science* 1996; 271 (5255): 1493-5.

Teplova,M. and Patel,D.J. Structural insights into RNA recognition by the alternative-splicing regulator muscleblind-like MBNL1. *Nat Struct Mol Biol* 2008; 15 (12): 1343-51.

Territo,M.C. and Cline,M.J. Monocyte function in man. *J Immunol* 1977; 118 (1): 187-92.

Thorns,C., Kuba,J., Bernard,V., Senft,A., Szymczak,S., Feller,A.C., and Bernd,H.W. Deregulation of a distinct set of microRNAs is associated with transformation of gastritis into MALT lymphoma. *Virchows Arch* 2012.

Ting,J.P. and Trowsdale,J. Genetic control of MHC class II expression. *Cell* 2002; 109 Suppl S21-S33.

Tombol,Z., Szabo,P.M., Molnar,V., Wiener,Z., Tolgyesi,G., Horanyi,J., Riesz,P., et al. Integrative molecular bioinformatics study of human adrenocortical tumors: microRNA, tissue-specific target prediction, and pathway analysis. *Endocr Relat Cancer* 2009; 16 (3): 895-906.

Tosi,G., Jabrane-Ferrat,N., and Peterlin,B.M. Phosphorylation of CIITA directs its oligomerization, accumulation and increased activity on MHCII promoters. *EMBO J* 2002; 21 (20): 5467-76.

Travers,J., Blagg,J., and Workman,P. Epigenetics: Targeting leukemia on the DOT. *Nat Chem Biol* 2011; 7 (10): 663-5.

Tserel,L., Runnel,T., Kisand,K., Pihlap,M., Bakhoff,L., Kolde,R., Peterson,H., et al. MicroRNA expression profiles of human blood monocyte-derived dendritic cells and macrophages reveal miR-511 as putative positive regulator of toll-like receptor 4. *J Biol Chem* 2011; 286 (30): 26487-95.

Tsuchiya,S., Yamabe,M., Yamaguchi,Y., Kobayashi,Y., Konno,T., and Tada,K. Establishment and characterization of a human acute monocytic leukemia cell line (THP-1). *Int J Cancer* 1980; 26 (2): 171-6.

UniProt Consortium Reorganizing the protein space at the Universal Protein Resource (UniProt). *Nucleic Acids Res* 2012; 40 (Database issue): D71-D75.

Valk,P.J., Verhaak,R.G., Beijen,M.A., Erpelinck,C.A., Barjesteh van Waalwijk van Doorn-Khosrovani, Boer,J.M., Beverloo,H.B., et al. Prognostically useful gene-expression profiles in acute myeloid leukemia. *N Engl J Med* 2004; 350 (16): 1617-28.

Vandesompele,J., De Preter,K., Pattyn,F., Poppe,B., Van Roy,N., De Paepe,A., and Speleman,F. Accurate normalization of real-time quantitative RT-PCR data by geometric averaging of multiple internal control genes. *Genome Biol* 2002; 3 (7): research0034.

VanHouten,J., Sullivan,C., Bazinet,C., Ryoo,T., Camp,R., Rimm,D.L., Chung,G., et al. PMCA2 regulates apoptosis during mammary gland involution and predicts outcome in breast cancer. *PNAS* 2010; 107 (25): 11405-10.

Vert,J.P., Foveau,N., Lajaunie,C., and Vandenbrouck,Y. An accurate and interpretable model for siRNA efficacy prediction. *BMC Bioinformatics* 2006; 7 (1): 520.

Vinante,F., Rigo,A., Tecchio,C., Patuzzo,C., Ricetti,M.M., Morosato,L., Cassatella,M.A., et al. Preferential release of high amounts of interleukin-8 by myeloid blasts showing monocytic differentiation. *Haematologica* 1996; 81 (3): 195-200.

Wada,J., Ota,K., Kumar,A., Wallner,E.I., and Kanwar,Y.S. Developmental regulation, expression, and apoptotic potential of galectin-9, a beta-galactoside binding lectin. *J Clin Invest* 1997; 99 (10): 2452-61.

Waldegger,S., Barth,P., Raber,G., and Lang,F. Cloning and characterization of a putative human serine/threonine protein kinase transcriptionally modified during anisotonic and isotonic alterations of cell volume. *PNAS* 1997; 94 (9): 4440-5.

Wang,H. and Eckel,R.H. Lipoprotein lipase: from gene to obesity. *Am J Physiol Endocrinol Metab* 2009; 297 (2): E271-E288.

Wang,H., Zhao,L.N., Li,K.Z., Ling,R., Li,X.J., and Wang,L. Overexpression of ribosomal protein L15 is associated with cell proliferation in gastric cancer. *BMC Cancer* 2006; 6: 91.

Wang,J., Xiang,G., Mitchelson,K., and Zhou,Y. Microarray profiling of monocytic differentiation reveals miRNA-mRNA intrinsic correlation. *J Cell Biochem* 2011; 112 (9): 2443-53.

Wang,W., Zhao,L.J., Tan,Y.X., Ren,H., and Qi,Z.T. MiR-138 induces cell cycle arrest by targeting cyclin D3 in hepatocellular carcinoma. *Carcinogenesis* 2012.

Weiss,E.H., Lilienfeld,B.G., Muller,S., Muller,E., Herbach,N., Kessler,B., Wanke,R., et al. HLA-E/human beta2-microglobulin transgenic pigs: protection against xenogeneic human anti-pig natural killer cell cytotoxicity. *Transplantation* 2009; 87 (1): 35-43.

Weterman,M.A., Ajubi,N., van Dinter,I.M., Degen,W.G., van Muijen,G.N., Ruitter,D.J., and Bloemers,H.P. nmb, a novel gene, is expressed in low-metastatic human melanoma cell lines and xenografts. *Int J Cancer* 1995; 60 (1): 73-81.

Wiederschain,D., Kawai,H., Shilatifard,A., and Yuan,Z.M. Multiple mixed lineage leukemia (MLL) fusion proteins suppress p53-mediated response to DNA damage. *J Biol Chem* 2005; 280 (26): 24315-21.

Wishart,D.S., Knox,C., Guo,A.C., Cheng,D., Shrivastava,S., Tzur,D., Gautam,B., et al. DrugBank: a knowledgebase for drugs, drug actions and drug targets. *Nucleic Acids Res* 2008; 36 (Database issue): D901-D906.

Wu,J.J., Cantor,A., and Moscinski,L.C. beta2 Integrins are characteristically absent in acute promyelocytic leukemia and rapidly upregulated in vivo upon differentiation with all-trans retinoic acid. *Leuk Res* 2007; 31 (1): 49-57.

Wu,K., Katiyar,S., Li,A., Liu,M., Ju,X., Popov,V.M., Jiao,X., et al. Dachshund inhibits oncogene-induced breast cancer cellular migration and invasion through suppression of interleukin-8. *PNAS* 2008; 105 (19): 6924-9.

Yan,W., Arai,A., Aoki,M., Ichijo,H., and Miura,O. ASK1 is activated by arsenic trioxide in leukemic cells through accumulation of reactive oxygen species and may play a negative role in induction of apoptosis. *Biochem Biophys Res Commun* 2007; 355 (4): 1038-44.

Yasuhara,F., Gomes,G.R., Siu,E.R., Suenaga,C.I., Marostica,E., Porto,C.S., and Lazari,M.F. Effects of the antiestrogen fulvestrant (ICI 182,780) on gene expression of the rat efferent ductules. *Biol Reprod* 2008; 79 (3): 432-41.

Yokoyama,A., Kitabayashi,I., Ayton,P.M., Cleary,M.L., and Ohki,M. Leukemia proto-oncoprotein MLL is proteolytically processed into 2 fragments with opposite transcriptional properties. *Blood* 2002; 100 (10): 3710-8.

Yu,B.D., Hanson,R.D., Hess,J.L., Horning,S.E., and Korsmeyer,S.J. MLL, a mammalian trithorax-group gene, functions as a transcriptional maintenance factor in morphogenesis. *PNAS* 1998; 95 (18): 10632-6.

Yu,B.D., Hess,J.L., Horning,S.E., Brown,G.A.J., and Korsmeyer,S.J. Altered Hox expression and segmental identity in Mll-mutant mice. *Nature* 1995; 378 (6556): 505-8.

Yuan,J., Takeuchi,M., Negishi,M., Oguro,H., Ichikawa,H., and Iwama,A. Bmi1 is essential for leukemic reprogramming of myeloid progenitor cells. *Leukemia* 2011a; 25 (8): 1335-43.

Yuan,Y., Niu,C.C., Deng,G., Li,Z.Q., Pan,J., Zhao,C., Yang,Z.L., et al. The Wnt5a/Ror2 noncanonical signaling pathway inhibits canonical Wnt signaling in K562 cells. *Int J Mol Med* 2011b; 27 (1): 63-9.

Zelphati,O. and Szoka,F.C., Jr. Mechanism of oligonucleotide release from cationic liposomes. *PNAS* 1996; 93 (21): 11493-8.

Zhang,B., Wu,K.F., Cao,Z.Y., Rao,Q., Ma,X.T., Zheng,G.G., and Li,G. IL-18 increases invasiveness of HL-60 myeloid leukemia cells: up-regulation of matrix metalloproteinases-9 (MMP-9) expression. *Leuk Res* 2004; 28 (1): 91-5.

Zhang,F., Sjoholm,A., and Zhang,Q. Growth hormone signaling in pancreatic beta-cells - calcium handling regulated by growth hormone. *Mol Cell Endocrinol* 2009; 297 (1-2): 50-7.

Zhang,J., Schneider,C., Ottmers,L., Rodriguez,R., Day,A., Markwardt,J., and Schneider,B.L. Genomic scale mutant hunt identifies cell size homeostasis genes in S. cerevisiae. *Curr Biol* 2002; 12 (23): 1992-2001.

Zhang,J.Y., Chan,E.K., Peng,X.X., and Tan,E.M. A novel cytoplasmic protein with RNA-binding motifs is an autoantigen in human hepatocellular carcinoma. *J Exp Med* 1999; 189 (7): 1101-10.

Zhang,M., Chen,S., Li,Q., Ling,Y., Zhang,J., and Yu,L. Characterization of a novel human HMBOX1 splicing variant lacking the homeodomain and with attenuated transcription repressor activity. *Mol Biol Rep* 2010; 37 (6): 2767-72.

Zheng,C., Li,L., Haak,M., Brors,B., Frank,O., Giehl,M., Fabarius,A., et al. Gene expression profiling of CD34+ cells identifies a molecular signature of chronic myeloid leukemia blast crisis. *Leukemia* 2006; 20 (6): 1028-34.

Zhu,N. and Wang,Z. Calreticulin expression is associated with androgen regulation of the sensitivity to calcium ionophore-induced apoptosis in LNCaP prostate cancer cells. *Cancer Res* 1999; 59 (8): 1896-902.

12 Abbreviations

Abbreviation	Full name
adj. *p*-value	adjusted *p*-value (adjusted for multiple testing)
AF9	ALL1-fused gene from chromosome 9. Alias: myeloid/lymphoid or mixed-lineage leukemia (trithorax homolog, Drosophila); translocated to, 3 (*MLLT3*)
ALL	acute lymphoblastic leukemia
AML	acute myeloid leukemia
B-ALL	acute B lymphoblastic leukemia
BP	blastic (acute) phase (of CML)
CLL	chronic lymphoblastic leukemia
CML	chronic myeloid leukemia
CP	chronic phase (of CML)
C_T	threshold cycle (represents expression strength of qRT-PCR data)
DAPI	4,6-diamidino-2-phenylindole
DotCom	Dot1 complex
FAB type	leukemia subtypes according to French-American-British classification system
FCM	flow cytometry
FI	fluorescent signal intensity
G-CSF	granulocyte colony-stimulating factor
GM-CSF	granulocyte-macrophage colony-stimulating factor
GMP	granulocyte macrophage progenitors
GOA	gene ontology annotation
HLA	human leukocyte antigen
HSC	hematopoietic stem cell
in vitro	here: studies in cells (cell culture)
in vivo	here: studies in whole organisms
in silico	computational
kb	kilo base
LDA	TaqMan low density array (a high throughput qRT-PCR technique, which was employed here to screen miRNA expression)
lincRNA	large intervening non-coding RNA
LNGFR	low-affinity nerve growth factor receptor (NGFR), a truncated version is employed as a surface selection marker
$\log_2$FC	logarithmic (to the base 2) fold change
LSC	leukemia stem cells
MHC	major histocompatibility complex
miR	microRNA (employed when a certain miRNA is described (e.g. miR-511)
miRNA	microRNA
MLL	mixed-lineage leukemia gene
n.a.	not available
ncRNA	non-coding RNA
nt	nucleotide

n-tg	non-targeting (control siRNAs, which are designed not to target any mRNA)
nts	nucleotides
OMIM	Online Mendelian Inheritance in Man® (An Online Catalog of Human Genes and Genetic Disorders)
PMA	phorbol 12-myristate 13-acetate
ROI	region of interest (regions selected for image analysis by Cellscreen microscopy)
"pool 1"	Pooled RNA samples of five independent *MLL-AF9* knockdown experiments performed in THP1 cells which were employed for array profiling methods (gene and miRNA expression).
"pool 2"	Pooled RNA samples of further two independent *MLL-AF9* knockdown experiments performed in THP1 cells which were employed for data validation.
rRNA	ribosomal RNA
RT	room temperature
SAM	significance analysis of microarray
SEC	super elongation complex

13 Supplementary data

Supplementary table 1: **Primer sequences used for qRT-PCR**

Gene name	Primer	Sequence 5'-3'	Design
AF9	forward	CAACGTTACCGCCATTTG	own
AF9	reverse	GTCTGGGATGGTGTGAAG	own
AFF1	forward	CGTAGGGTCCCAGTCAAGTG	own
AFF1	reverse	ACTGCTGTTGAGGGCCAAGG	own
AFF4	forward	GACCAAGCTGAACAGCTTTCC	own
AFF4	reverse	AAGGGCCAACTGACATGATCG	own
ARHGAP26	forward	CGAACTGGCCAAGGATTTCG	own
ARHGAP26	reverse	GACGTTTCTCCTGCACGTAG	own
BAX	forward	ATGGACGGGTCCGGGGAGCAGCCC	(Aggarwal, et al. 1998)
BAX	reverse	GGTGAGCACTCCCGCCACAAAGAT	(Aggarwal, et al. 1998)
BCL-2	forward	CGACGACTTCTCCCGCCGCTACCGC	(Aggarwal, et al. 1998)
BCL-2	reverse	CCGCATGCTGGGGCCGTACAGTTCC	(Aggarwal, et al. 1998)
CALR	forward	GCCGAGCCTGCCGTCTACTTCA	own
CALR	reverse	AGGCTCGAAACTGGCCGACAG	own
CEBPB	forward	CAAACCAACCGCACATGCAG	own
CEBPB	reverse	AACAGCAACAAGCCCGTAGG	own
CIITA	forward	GTGGGAGCCGAGAGCTTGGC	own
CIITA	reverse	ATGGTGGGCGTCCACATCGC	own
DACH1	forward	GACGAAACGGCGTGAACAAG	own
DACH1	reverse	CACTGCGGTCAGCCTCTATC	own
EGR2	forward	ACATCTACCCGGTGGAGGAC	own
EGR2	reverse	CAGAGGTGACGCTGGATGAG	own
EMP1	forward	CCAACATTAGCTGCAGTGAC	own
EMP1	reverse	AAGAGCTGGAACACGAAGAC	own
FGFR1	forward	TGGCCTTGACCTCCAACCAG	own
FGFR1	reverse	TGAGTCCGCCATTGGCAAGC	own
FGFR3	forward	ACCTGGACCGTGTCCTTACC	own
FGFR3	reverse	CTGCACCTGGAGGCAAGATG	own
FOS	forward	CGTACTCCAACCGCATCTGCA	own
FOS	reverse	CTCCGGTTGCGGCATTTGGC	own
FUCA1	forward	GCTACGCCGACTTCGGACCG	own
FUCA1	reverse	CCCGATGAGGCCCCACGTCT	own
HOXA10	forward	GCAAAGCCTCGCCGGAGAAGG	own
HOXA10	reverse	CTGTCCGTGAGGTGGACGCTG	own
HOXA9	forward	CACCAGACGAACAGTGAGGA	(Faber, et al. 2009)
HOXA9	reverse	TGGTCAGTAGGCCTTGAGGT	(Faber, et al. 2009)
IGF2BP2	forward	CTCGTGACCAAACGCCAGATG	own
IGF2BP2	reverse	GCGACTCCCTGAGGGTATTTC	own
IL8	forward	ACCACACTGCGCCAACACAG	own
IL8	reverse	TCTCTTGGCCCTTGGCCTCAA	own
KCTD12	forward	CCGACATCGTGGAGCTGAAC	own
KCTD12	reverse	CGTCCCGGTCCAGAAAGAAG	own
KIF26A	forward	GCAGACACGGTCCGAGAATG	own
KIF26A	reverse	TGCTGCCAGGGTTGTCCTTG	own
MAFB	forward	GAAGCACCACCTGGAGAATG	own

Gene name	Primer	Sequence 5'-3'	Design
MAFB	reverse	GCGAGTTTCTCGCACTTGAC	own
MAPRE2	forward	ACCTCGTGCAGAGACTAATGG	own
MAPRE2	reverse	TGATGGTAACGGCAGATTGGG	own
MDM2	forward	GAATCTACAGGGACGCCATCG	own
MDM2	reverse	CCCTGCCTGATACACAGTAAC	own
MDM2-001	forward	GCTGGGAACCTCTTGATTGTG	own
MDM2-001	reverse	GTGGTGACAGGGTGCTCTAAC	own
MEF2C	forward	ATAACTCCCAGTCGGCTCAG	own
MEF2C	reverse	GCGGTGTTAAACCCAGACAG	own
MLL1	forward	GTCCAGAGCAGAGCAAAC	own
MLL1	reverse	CAAAGTGCCTGCATTCTCC	own
MLL-AF9	forward	GCTCCCCGCCCAAGTATC	own
MLL-AF9	reverse	GGGATGGTGTGAAGCTGGAG	own
NOTCH2	forward	ATATGCTCAGCCGGGATACC	own
NOTCH2	reverse	TGGCAGTGTCCTGGAATGTC	own
RPL13A	forward	CCTGGAGGAGAAGAGGAAAGAGA	(Vandesompele, et al. 2002)
RPL13A	reverse	TTGAGGACCTCTGTGTATTTGTCAA	(Vandesompele, et al. 2002)
SOCS2	forward	GCTCGGTCAGACAGGATGG	(Zheng, et al. 2006)
SOCS2	reverse	TCGATTCGAAGATTAGTTGGTCC	(Zheng, et al. 2006)
SULF2	forward	GTACAAGGCCAGCTATGTCC	own
SULF2	reverse	GGACTGTGTCGTTCTCTAGG	own
TGFBR1	forward	AAGCCAGCCATTGCTCATAG	own
TGFBR1	reverse	GATGTCAGCACGTTTGAAGG	own
TSAPAN14	forward	GGCTGGAGTTGTCTTCCTTG	own
TSAPAN14	reverse	CAGCACCACAGGGTCGATTC	own
UBC	forward	ATTTGGGTCGCGGTTCTTG	(Vandesompele, et al. 2002)
UBC	reverse	TGCCTTGACATTCTCGATGGT	(Vandesompele, et al. 2002)
VASH1	forward	ATGACTTCCGCAAGGAGCTG	own
VASH1	reverse	TTTCACTGCGGCTGTTCCTG	own
VDR	forward	GCCGCATCACCAAGGACAAC	own
VDR	reverse	ATCTCCCGCTTCCTCTGCAC	own
ZNF521	forward	GGTGAAACTTGATATCAATGGCC	(La Rocca, et al. 2009)
ZNF521	reverse	GGAGTTTGGCAGGAGAGTCA	(La Rocca, et al. 2009)

Supplementary table 2: **All 1345 probes, which were differentially expressed after *MLL-AF9* knockdown in THP1 cells.** Besides expression changes between *MLL-AF9* knockdown and control samples in THP1 cells from microarray data, supplementary table 2 includes the information if gene expression was validated by qRT-PCR (validated if qRT-PCR data showed $log_2FC>\pm0.3$ in corresponding direction) and if all or only some of the probes against the transcripts of a gene were differentially expressed (all or only single transcription variants may be affected). adj. *p*-value, *p*-value corrected for multiple testing as described in material and methods section 7.3.1. Ave Expr, average expression strength (due to signal intensity). Column "1)": * all probes against the transcripts of this gene were differentially expressed, # not all probes against the transcripts of this gene were differentially expressed.

Probe name	Systematic name	Gene name	*p*-value	adj. *p*-value	Ave Expr	log_2FC	1)	confirmed via qRT-PCR
A_23_P140876	NM_001089	ABCA3	0.02	0.45	8.15	3.12E-01		
A_23_P100539	NM_001171	ABCC6	0.00	0.26	8.87	-4.02E-01		
A_33_P3399598	AK125109	ABCD4	0.01	0.38	5.57	4.59E-01	#	
A_33_P3283713	NM_015407	ABHD14A	0.01	0.32	13.05	-3.77E-01	*	
A_23_P202520	NM_001003408	ABLIM1	0.00	0.18	6.2	4.61E-01	#	
A_23_P356616	NM_145804	ABTB2	0.01	0.38	9.64	-3.68E-01		
A_23_P89799	NM_006111	ACAA2	0.00	0.17	10.86	6.10E-01		
A_32_P215318	NM_198839	ACACA	0.00	0.22	8.21	-4.36E-01	#	
A_23_P10182	NM_003500	ACOX2	0.00	0.23	6.66	4.27E-01		
A_33_P3395008	NM_001142807	ACOXL	0.00	0.17	7.81	-4.97E-01		
A_23_P54488	NM_015162	ACSBG1	0.01	0.30	7.73	4.28E-01	#	
A_33_P3217983	NM_203380	ACSL5	0.02	0.47	11.65	-3.01E-01		
A_23_P66328	NM_182617	ACSM2B	0.02	0.45	5.73	-3.13E-01		
A_23_P148829	NM_080431	ACTRT2	0.00	0.24	5.94	4.85E-01		
A_23_P360754	NM_005099	ADAMTS4	0.02	0.41	6.34	-4.08E-01	#	
A_23_P49816	NM_018404	ADAP2	0.01	0.31	9.23	4.44E-01		
A_33_P3337161	NM_139247	ADCY4	0.01	0.41	6.83	3.60E-01	#	
A_24_P100742	NM_014189	ADD1	0.02	0.48	7.47	-3.45E-01		
A_23_P55477	NM_000676	ADORA2B	0.01	0.40	10.14	3.74E-01		
A_23_P137931	NM_000677	ADORA3	0.01	0.39	6.89	4.70E-01	#	
A_24_P221092	AF289615	AF289615	0.00	0.10	8.26	5.31E-01		
A_24_P286079	NM_014423	AFF4	0.02	0.46	9.51	-3.58E-01	#	
A_23_P7099	NM_000027	AGA	0.01	0.32	10.53	-3.80E-01		
A_23_P103720	NM_024758	AGMAT	0.02	0.46	9.25	-3.80E-01		
A_23_P69810	NM_032717	AGPAT9	0.00	0.06	8.21	6.34E-01		
A_33_P3279470	NM_001138	AGRP	0.01	0.36	6.2	3.77E-01		
A_33_P3316800	NM_001621	AHR	0.00	0.23	8.21	4.44E-01	*	
A_23_P215566	NM_001621	AHR	0.01	0.32	9.1	3.81E-01	*	
A_33_P3367077	AI669688	AI669688	0.00	0.17	6.75	4.67E-01		
A_33_P3258712	AK056005	AK056005	0.00	0.18	8.64	-4.58E-01		
A_33_P3326812	AK056267	AK056267	0.02	0.46	8.84	-3.19E-01		
A_33_P3244991	AK091251	AK091251	0.01	0.30	7.66	3.97E-01		
A_32_P30831	AK125393	AK125393	0.01	0.41	7.19	-3.56E-01		
A_33_P3422471	AK126796	AK126796	0.01	0.34	5.42	-3.88E-01		
A_33_P3307980	AK131345	AK131345	0.02	0.41	9.06	-3.34E-01		
A_23_P303978	AK311383	AK311383	0.01	0.32	5.6	-4.22E-01		
A_32_P49668	AK311627	AK311627	0.00	0.22	6.41	5.80E-01	*	
A_24_P349207	AK311627	AK311627	0.01	0.40	7.78	3.91E-01	*	
A_33_P3238433	NM_001135168	ALDH3A1	0.02	0.48	6.75	-3.13E-01	#	
A_23_P104464	NM_000698	ALOX5	0.00	0.07	8.03	7.55E-01		
A_23_P85941	NM_006492	ALX3	0.00	0.25	5.8	4.94E-01		

Probe name	Systematic name	Gene name	*p*-value	adj. *p*-value	Ave Expr	log_2FC	1)	confirmed via qRT-PCR
A_33_P3262138	NM_022662	ANAPC1	0.02	0.44	9.05	-3.21E-01	#	
A_23_P27147	NM_001002244	ANAPC11	0.00	0.12	16.22	-6.98E-01		
A_33_P3291279	NM_001029870	ANKRD56	0.00	0.24	5.54	4.32E-01		
A_23_P94501	NM_000700	ANXA1	0.01	0.39	11.49	4.30E-01		
A_32_P148345	NM_001002857	ANXA2	0.00	0.13	8.18	-5.38E-01	#	
A_23_P16976	NM_001153	ANXA4	0.01	0.40	13.03	-3.31E-01		
A_23_P145718	NM_001637	AOAH	0.02	0.43	9.1	3.96E-01		
A_33_P3258782	NM_003916	AP1S2	0.01	0.35	10.56	3.80E-01	#	
A_23_P217384	NM_003916	AP1S2	0.01	0.38	11.3	4.39E-01	#	
A_24_P287691	NM_005829	AP3S2	0.02	0.43	10.23	-3.21E-01		
A_33_P3295655	NM_001163	APBA1	0.00	0.17	5.9	4.68E-01	*	
A_23_P101905	NM_005883	APC2	0.00	0.24	7.45	-5.64E-01		
A_23_P54770	NM_018690	APOB48R	0.01	0.39	11.22	3.44E-01		
A_33_P3360097	NM_000485	APRT	0.02	0.43	14.21	-6.90E-01		
A_23_P372834	NM_198098	AQP1	0.00	0.19	6.16	-5.21E-01	#	
A_23_P112482	NM_004925	AQP3	0.00	0.27	8.29	-5.25E-01		
A_33_P3217786	NR_002817	AQP7P1	0.01	0.40	5.73	-3.45E-01	*	
A_23_P113111	NM_000044	AR	0.00	0.09	10.42	-5.41E-01		
A_33_P3228305	NM_015071	ARHGAP26	0.00	0.18	10.43	5.02E-01		yes
A_33_P3323722	NM_005737	ARL4C	0.00	0.13	8.23	4.94E-01		
A_24_P943997	NM_178815	ARL5B	0.02	0.46	7.5	-3.02E-01		
A_24_P167473	NM_005719	ARPC3	0.01	0.30	16.01	-3.94E-01		
A_33_P3775007	NM_018482	ASAP1	0.01	0.41	8.59	3.33E-01		
A_33_P3414883	AK302556	ATMIN	0.01	0.36	6.2	-5.15E-01	#	
A_23_P148879	NM_000702	ATP1A2	0.00	0.15	7.65	-6.14E-01	*	
A_33_P3359771	NM_000702	ATP1A2	0.00	0.24	5.52	-4.23E-01	*	
A_33_P3393851	U15688	ATP2B2	0.00	0.08	5.72	-6.92E-01	#	
A_23_P87616	NM_001002031	ATP5G2	0.00	0.04	16.04	-6.69E-01		
A_23_P11353	NM_005765	ATP6AP2	0.02	0.45	12.61	-3.42E-01		
A_24_P276932	NM_001039362	ATP6V1C2	0.02	0.42	7.86	-3.29E-01		
A_24_P391368	NM_013236	ATXN10	0.00	0.12	11.78	-5.48E-01	*	
A_33_P3231367	NM_013236	ATXN10	0.01	0.35	10.36	-3.72E-01	*	
A_33_P3679768	AW303581	AW303581	0.02	0.48	10.09	-3.05E-01		
A_33_P3422701	AX746590	AX746590	0.02	0.44	6.16	3.49E-01		
A_33_P3346806	AX747590	AX747590	0.01	0.38	5.51	-3.68E-01	#	
A_33_P3244784	AX747898	AX747898	0.02	0.45	9.53	-3.10E-01		
A_33_P3708763	AX748036	AX748036	0.02	0.44	5.37	-3.15E-01		
A_23_P37441	NM_004048	B2M	0.00	0.15	17.63	-4.72E-01		
A_24_P913716	NM_145236	B3GNT7	0.01	0.39	10.34	3.53E-01	#	
A_23_P101380	NM_198540	B3GNT8	0.02	0.45	9.38	3.17E-01		
A_23_P152678	NM_015681	B9D1	0.01	0.35	7.65	-3.73E-01	#	
A_23_P49539	NM_001080519	BAHCC1	0.02	0.46	11.02	-3.20E-01		
A_33_P3262575	NM_018842	BAIAP2L1	0.01	0.35	5.6	-4.13E-01	#	
A_24_P182122	BC061915	BC061915	0.01	0.39	14.02	-3.36E-01		
A_33_P3328990	BC067767	BC067767	0.00	0.18	5.77	-5.67E-01		
A_23_P34930	NM_005872	BCAS2	0.02	0.43	12.39	-3.32E-01		
A_24_P935986	NM_005504	BCAT1	0.01	0.32	10.94	-3.97E-01	#	
A_24_P411186	NM_022893	BCL11A	0.01	0.37	8.29	3.64E-01	*	
A_33_P3249595	NM_138559	BCL11A	0.01	0.40	6.55	3.49E-01	*	
A_23_P57856	NM_001130845	BCL6	0.01	0.35	9.26	4.60E-01		
A_23_P109171	NM_001195	BFSP1	0.00	0.22	8.31	-5.01E-01		
A_33_P3269976	BG675116	BG675116	0.02	0.44	5.8	-5.28E-01		

Probe name	Systematic name	Gene name	*p*-value	adj. *p*-value	Ave Expr	log_2FC	1)	confirmed via qRT-PCR
A_32_P75581	NM_152414	BHLHE22	0.00	0.10	13.31	-6.19E-01		
A_24_P303989	NM_005180	BMI1	0.02	0.45	9.88	-3.28E-01	#	
A_33_P3219651	NM_133468	BMPER	0.01	0.30	6.11	-4.02E-01	#	
A_33_P3368301	NM_212552	BOLA3	0.01	0.31	10.6	-5.77E-01	#	
A_23_P42935	NM_004333	BRAF	0.02	0.47	8.49	-3.02E-01		
A_23_P99452	NM_000059	BRCA2	0.02	0.44	8.6	-5.64E-01		
A_24_P183264	NM_001037637	BTF3	0.02	0.45	14.04	-3.19E-01		
A_23_P105900	NR_026983	BTF3L1	0.00	0.26	14.25	-4.26E-01		
A_33_P3228427	BX103560	BX103560	0.00	0.04	5.56	6.66E-01		
A_32_P221748	BX350880	BX350880	0.02	0.45	8.4	-3.58E-01		
A_32_P86739	NM_001010911	C10orf114	0.00	0.08	9.15	-7.76E-01		
A_24_P372553	NM_015608	C10orf137	0.00	0.22	8.39	-4.54E-01	*	
A_32_P152767	NM_207371	C10orf140	0.00	0.02	8.17	-9.26E-01	#	
A_33_P3280784	NM_025125	C10orf57	0.01	0.33	7.31	-3.81E-01		
A_33_P3291454	NM_198515	C10orf96	0.02	0.46	7.88	-5.34E-01		
A_23_P202773	NM_001039496	C11orf20	0.02	0.48	6.7	-3.68E-01		
A_33_P3306898	NM_012194	C11orf41	0.02	0.42	5.79	3.41E-01	#	
A_24_P252846	NM_138787	C11orf74	0.02	0.42	9	-3.67E-01		
A_23_P345928	NM_032230	C12orf26	0.01	0.31	9.4	-4.63E-01		
A_23_P128375	NM_032829	C12orf34	0.02	0.45	9.02	-3.37E-01		
A_23_P151179	NM_022895	C12orf43	0.02	0.45	8.35	-3.43E-01		
A_23_P53763	NM_025113	C13orf18	0.00	0.13	11.48	-5.03E-01		
A_23_P15285	NM_024109	C16orf68	0.01	0.28	10.61	-4.10E-01		
A_24_P364954	NM_024648	C17orf101	0.02	0.46	10.17	-3.13E-01		
A_23_P392126	NM_001076680	C17orf108	0.02	0.41	7.29	-3.45E-01		
A_23_P164100	NM_181707	C17orf64	0.01	0.38	6.54	-3.45E-01		
A_33_P3379268	NM_207103	C17orf87	0.02	0.46	5.63	3.44E-01		
A_33_P3411945	NM_001136482	C19orf38	0.00	0.25	7.03	4.65E-01		
A_23_P153360	NM_024104	C19orf42	0.01	0.33	11.91	-3.74E-01	#	
A_23_P330561	NM_174918	C19orf59	0.01	0.40	12.65	3.57E-01		
A_23_P74668	NM_152290	C1orf158	0.00	0.21	8.31	-7.77E-01		
A_24_P190877	NM_030934	C1orf25	0.00	0.12	7.32	-5.70E-01		
A_23_P1014	NR_026761	C1orf97	0.00	0.17	9.54	-5.32E-01		
A_33_P3400843	NM_001008223	C1QL4	0.01	0.30	6.28	3.95E-01		
A_33_P3404601	NM_000063	C2	0.00	0.25	6.83	6.17E-01	#	
A_23_P68486	NM_080821	C20orf108	0.02	0.47	10.1	3.35E-01		
A_23_P372096	AK097804	C20orf112	0.00	0.23	8.69	4.92E-01	*	
A_33_P3271284	NM_080616	C20orf112	0.00	0.26	5.87	3.99E-01	*	
A_33_P3364989	NM_001024675	C20orf134	0.01	0.38	6.93	3.91E-01		
A_23_P17490	NM_001009924	C20orf30	0.01	0.40	12.04	-3.59E-01	#	
A_23_P166431	NM_015372	C22orf24	0.01	0.33	5.93	-6.13E-01		
A_33_P3250887	NM_001123225	C22orf41	0.02	0.44	6.3	-6.52E-01	#	
A_24_P28811	NR_023391	C2orf14	0.01	0.35	9.02	-6.12E-01	#	
A_23_P28652	NM_016085	C2orf28	0.00	0.19	10.89	-4.61E-01		
A_23_P108761	NM_017546	C2orf29	0.01	0.39	10.61	-3.40E-01		
A_23_P39542	NM_001017927	C2orf76	0.00	0.20	9.88	-4.55E-01		
A_33_P3242174	NM_206895	C2orf82	0.01	0.39	7.68	-3.55E-01		
A_33_P3237507	NM_207405	C4orf50	0.02	0.46	5.68	3.29E-01		
A_24_P110558	NM_001007189	C5orf53	0.01	0.34	8.79	3.80E-01		
A_24_P388940	NM_001042493	C6orf162	0.01	0.40	8.53	-3.38E-01		
A_33_P3372674	NR_026784	C6orf164	0.01	0.31	5.69	-4.05E-01	*	
A_23_P122532	NM_021184	C6orf47	0.01	0.35	9.82	4.03E-01		

Probe name	Systematic name	Gene name	*p*-value	adj. *p*-value	Ave Expr	log_2FC	1)	confirmed via qRT-PCR
A_33_P3247644	NM_152793	C7orf41	0.01	0.31	7.6	3.94E-01	#	
A_33_P3431595	NM_173687	C8orf31	0.02	0.46	8.18	-3.59E-01		
A_23_P422115	NM_001048265	C9orf116	0.01	0.36	7.79	-3.70E-01	*	
A_33_P3217649	NM_001048265	C9orf116	0.02	0.48	6.38	-2.95E-01	*	
A_33_P3375145	NM_203403	C9orf150	0.00	0.06	6.46	6.13E-01		
A_23_P312837	NR_026663	C9orf70	0.01	0.35	5.37	3.77E-01		
A_24_P915196	NM_153045	C9orf91	0.02	0.45	8.89	3.21E-01		
A_24_P943922	NM_020925	CACHD1	0.02	0.44	5.73	3.36E-01		
A_33_P3218960	NM_021098	CACNA1H	0.02	0.43	5.86	-3.39E-01		
A_33_P3292854	NM_004343	CALR	0.00	0.11	17.05	-5.13E-01		yes
A_23_P253791	NM_004345	CAMP	0.01	0.30	8.04	4.61E-01		
A_23_P341349	NM_023083	CAPN10	0.01	0.39	9.9	-7.73E-01	#	
A_24_P902728	NM_203364	CAPRIN1	0.02	0.47	9.1	-3.13E-01	#	
A_23_P380379	AF251056	CAPS2	0.02	0.45	5.46	3.39E-01	#	
A_33_P3322353	NM_006136	CAPZA2	0.01	0.38	10.27	-3.49E-01	*	
A_32_P224666	NM_006136	CAPZA2	0.02	0.41	8.82	-3.34E-01	*	
A_23_P434890	NM_014550	CARD10	0.02	0.43	8.96	-3.32E-01		
A_23_P166306	NM_000071	CBS	0.00	0.10	11.1	-5.73E-01		
A_33_P3333975	NM_001024916	CBWD5	0.02	0.42	13.8	-3.94E-01	*	
A_33_P3222018	NM_016587	CBX3	0.01	0.34	7.35	-3.63E-01	#	
A_23_P65983	NM_033212	CCDC102A	0.01	0.38	6.91	-4.29E-01		
A_23_P73540	NM_033626	CCDC120	0.01	0.35	8.25	-3.66E-01		
A_33_P3356230	NM_001004306	CCDC144NL	0.01	0.39	7.02	-3.85E-01		
A_33_P3324854	NM_024768	CCDC48	0.00	0.07	5.68	7.04E-01	#	
A_33_P3246613	NM_001031737	CCDC78	0.02	0.41	11.05	-8.04E-01		
A_24_P289170	NM_001080414	CCDC88C	0.01	0.30	7.5	4.15E-01	#	
A_23_P89431	NM_002982	CCL2	0.00	0.00	6.89	1.61E+00		
A_23_P215491	NM_002991	CCL24	0.01	0.37	11.44	-4.59E-01		
A_33_P3305780	NM_001039780	CCNI2	0.01	0.40	5.48	-4.24E-01		
A_23_P212354	NM_001123041	CCR2	0.00	0.26	14.15	4.01E-01	#	
A_24_P131066	NM_004258	CD101	0.00	0.23	5.85	4.38E-01		
A_33_P3284508	NM_000591	CD14	0.00	0.01	8.02	1.05E+00		
A_23_P61466	NM_174941	CD163L1	0.01	0.41	11.02	-3.56E-01		
A_24_P380536	NM_006016	CD164	0.02	0.48	11.06	-3.48E-01	#	
A_23_P257815	NM_005582	CD180	0.01	0.37	6.03	4.16E-01		
A_23_P113572	NM_001770	CD19	0.01	0.37	8.5	3.52E-01		
A_24_P305345	NM_021155	CD209	0.00	0.09	8.15	7.31E-01	*	
A_33_P3272493	NM_001144897	CD209	0.01	0.27	6.15	4.40E-01	*	
A_24_P186539	NM_021155	CD209	0.01	0.38	6.43	3.98E-01	*	
A_23_P85453	NM_016382	CD244	0.01	0.41	10.08	3.88E-01	#	
A_24_P159434	NM_007261	CD300A	0.01	0.30	7.22	3.88E-01	*	
A_23_P55020	NM_139018	CD300LF	0.01	0.31	9.31	4.19E-01		
A_23_P111583	NM_001001547	CD36	0.00	0.15	10.88	5.96E-01		
A_23_P57036	NM_001250	CD40	0.00	0.24	7.45	-4.16E-01		
A_23_P70095	NM_001025158	CD74	0.00	0.03	9.93	7.65E-01		
A_24_P274795	NM_018719	CDCA7L	0.02	0.44	12.4	-3.51E-01	#	
A_23_P38732	NM_001792	CDH2	0.02	0.47	5.47	-3.28E-01	#	
A_23_P110643	NM_016508	CDKL3	0.02	0.48	8.2	-3.27E-01		
A_33_P3411628	NM_058197	CDKN2A	0.01	0.34	6.16	6.48E-01	#	
A_23_P78526	NM_020219	CEACAM19	0.02	0.45	9.57	-3.33E-01		
A_23_P411296	NM_005194	CEBPB	0.00	0.14	12.34	5.27E-01		yes
A_33_P3262635	NM_177405	CECR1	0.02	0.41	11.21	3.62E-01		

Probe name	Systematic name	Gene name	*p*-value	adj. *p*-value	Ave Expr	log_2FC	1)	confirmed via qRT-PCR
A_32_P148710	NM_005507	CFL1	0.01	0.41	13.22	-3.54E-01	#	
A_23_P22444	NM_002621	CFP	0.01	0.31	7.69	-4.23E-01		
A_23_P163306	NM_032866	CGNL1	0.00	0.08	7.79	-7.38E-01		
A_33_P3376971	NM_024111	CHAC1	0.01	0.30	8.39	-4.19E-01	#	
A_24_P379727	NM_032309	CHCHD5	0.01	0.32	9.94	-4.14E-01		
A_24_P85317	NM_001042572	CHD2	0.02	0.47	7.19	-3.08E-01	#	
A_23_P34888	NM_021797	CHIA	0.01	0.41	5.92	-4.60E-01		
A_23_P105571	NM_020244	CHPT1	0.02	0.46	9.76	-3.37E-01		
A_23_P40847	NM_004267	CHST2	0.01	0.34	6.92	3.75E-01		
A_24_P44514	NM_006384	CIB1	0.01	0.32	12.12	-3.89E-01		
A_33_P3308914	NM_006383	CIB2	0.01	0.35	8.48	-3.66E-01		
A_32_P209960	NM_000246	CIITA	0.00	0.02	7.96	8.28E-01	#	yes
A_23_P88134	NM_032630	CINP	0.02	0.43	8.79	-5.31E-01		
A_23_P48056	NM_006825	CKAP4	0.00	0.14	9.2	-6.03E-01		
A_24_P215804	NM_016951	CKLF	0.01	0.40	7.85	-3.47E-01	#	
A_32_P206698	NM_001826	CKS1B	0.02	0.47	12.03	-3.08E-01	#	
A_23_P311232	NM_015282	CLASP1	0.01	0.39	9.28	-3.34E-01	#	
A_33_P3415097	NM_001830	CLCN4	0.00	0.13	8.15	5.00E-01	*	
A_33_P3367596	NM_001830	CLCN4	0.01	0.32	5.92	3.85E-01	*	
A_33_P3229032	NM_002975	CLEC11A	0.01	0.39	17.03	-3.33E-01		
A_33_P3410659	NM_001129998	CLEC12B	0.00	0.27	6.21	4.74E-01	#	
A_33_P3410654	NM_205852	CLEC12B	0.01	0.38	7.25	5.52E-01	#	
A_33_P3260572	NM_024692	CLIP4	0.02	0.42	7.03	-3.25E-01	#	
A_23_P376591	NM_206808	CLYBL	0.02	0.48	8.61	-3.77E-01		
A_23_P371239	NM_198390	CMIP	0.01	0.36	9.17	4.00E-01		
A_23_P106661	NM_052999	CMTM1	0.02	0.48	6.3	-2.97E-01		
A_33_P3372682	NR_024009	CN5H6.4	0.02	0.45	7.19	-4.24E-01		
A_23_P153183	NM_001168648	CNKSR2	0.01	0.39	5.65	3.43E-01	#	
A_23_P53288	NM_014255	CNPY2	0.01	0.27	15.12	-5.72E-01		
A_33_P3296240	NM_017738	CNTLN	0.01	0.38	8.5	-3.43E-01	*	
A_23_P9135	NM_033655	CNTNAP3	0.02	0.47	7.29	-3.33E-01	*	
A_32_P80850	NM_021110	COL14A1	0.00	0.13	6.75	-5.33E-01	#	
A_23_P31124	NM_030820	COL21A1	0.02	0.43	5.44	-3.37E-01		
A_24_P365975	NM_005202	COL8A2	0.01	0.27	7.38	4.84E-01	#	
A_23_P389525	NM_152516	COMMD1	0.00	0.18	11.13	-4.54E-01		
A_23_P105625	NM_032314	COQ5	0.01	0.38	11.34	-3.57E-01		
A_23_P106761	NM_007074	CORO1A	0.00	0.22	12.74	4.40E-01		
A_32_P98502	NM_004255	COX5A	0.02	0.48	14.56	-4.02E-01		
A_33_P3397066	CR736467	CR736467	0.01	0.39	5.72	-3.40E-01		
A_32_P29806	NM_003805	CRADD	0.00	0.25	10.62	-4.30E-01		
A_23_P33465	NM_024324	CRELD2	0.00	0.10	13.42	-5.51E-01		
A_33_P3232688	ENST00000381524	CSF2RA	0.01	0.32	9.97	3.77E-01	#	
A_23_P149892	NM_018590	CSGALNACT2	0.01	0.39	9.84	4.17E-01	#	
A_33_P3246017	AK091252	CTAGE5	0.01	0.38	5.39	-3.61E-01	#	
A_23_P81880	NM_005730	CTDSP2	0.02	0.45	14.07	3.36E-01	#	
A_33_P3287631	NM_147780	CTSB	0.01	0.35	8.31	4.24E-01		
A_23_P140384	NM_001911	CTSG	0.00	0.27	18.38	-4.28E-01		
A_33_P3354291	CU013345	CU013345	0.02	0.46	5.61	-3.10E-01		
A_33_P3210303	CU688821	CU688821	0.01	0.30	5.52	3.91E-01		
A_33_P3313528	CU693037	CU693037	0.02	0.46	6.03	3.54E-01		
A_33_P3375859	NR_002712	CXCR2P	0.02	0.45	7.29	3.28E-01		
A_23_P114299	NM_001504	CXCR3	0.00	0.27	7.91	-5.28E-01		

Probe name	Systematic name	Gene name	*p*-value	adj. *p*-value	Ave Expr	log_2FC	1)	confirmed via qRT-PCR
A_23_P102000	NM_001008540	CXCR4	0.00	0.15	14.4	5.10E-01		
A_24_P365767	NM_000397	CYBB	0.02	0.43	11.14	3.98E-01		
A_33_P3285868	NM_134268	CYGB	0.02	0.47	13.02	-3.73E-01		
A_23_P90626	NM_004288	CYTIP	0.02	0.47	7.17	3.73E-01		
A_33_P3209200	DA858408	DA858408	0.00	0.12	6.85	-5.17E-01		
A_33_P3316786	NM_080759	DACH1	0.00	0.15	13.03	-5.42E-01	*	
A_23_P32577	NM_080759	DACH1	0.00	0.18	11.41	-5.95E-01	*	
A_23_P106056	NM_001344	DAD1	0.02	0.45	14.05	-4.01E-01		
A_33_P3262742	NM_001017920	DAPL1	0.01	0.33	5.59	-4.09E-01	*	
A_23_P165598	NM_001017920	DAPL1	0.02	0.42	6.69	-3.87E-01	*	
A_23_P26439	NM_001042610	DBNDD1	0.01	0.41	6.65	-3.84E-01		
A_23_P75038	NM_014881	DCLRE1A	0.02	0.45	10.65	-3.51E-01		
A_23_P76622	NM_001922	DCT	0.01	0.30	6.25	-3.98E-01		
A_23_P44166	NM_016286	DCXR	0.02	0.48	12.71	-3.03E-01		
A_33_P3372910	NM_014314	DDX58	0.01	0.39	7.8	-4.72E-01	#	
A_23_P31816	NM_005217	DEFA3	0.00	0.01	8.5	1.36E+00		
A_23_P326080	NM_001925	DEFA4	0.00	0.25	10.17	-4.14E-01		
A_33_P3290174	NM_206918	DEGS2	0.02	0.45	8.73	-3.78E-01		
A_23_P78608	NM_024898	DENND1C	0.02	0.45	10.48	3.38E-01		
A_24_P541919	NM_144973	DENND5B	0.00	0.14	7.38	-4.90E-01	#	
A_24_P144377	NM_014015	DEXI	0.00	0.08	14.11	-5.60E-01		
A_32_P211045	NM_000791	DHFR	0.00	0.09	11.02	-6.08E-01	#	
A_33_P3359368	NM_001082488	DHRS4L1	0.01	0.33	8.66	-3.91E-01	#	
A_23_P80778	NM_032839	DIRC2	0.00	0.26	9.55	4.51E-01	#	
A_33_P3349252	AL512723	DKFZP547L112	0.02	0.48	9.83	-4.85E-01		
A_33_P3254460	NM_206539	DLK2	0.01	0.32	7.16	-4.33E-01		
A_23_P167920	NM_005618	DLL1	0.02	0.45	9.45	-5.44E-01		
A_32_P142818	NM_178120	DLX1	0.00	0.11	9.92	6.23E-01	#	
A_23_P28598	NM_004405	DLX2	0.01	0.38	7.33	5.11E-01		
A_23_P157895	NM_021240	DMRT3	0.02	0.43	5.9	-3.39E-01		
A_23_P33583	NM_018897	DNAH7	0.01	0.41	5.46	3.64E-01		
A_33_P3290687	NM_022365	DNAJC1	0.00	0.06	10.18	-6.32E-01	*	
A_24_P225604	NM_018981	DNAJC10	0.01	0.36	11.44	-3.61E-01	*	
A_23_P25913	NM_031427	DNAL1	0.01	0.38	8.46	-3.98E-01		
A_23_P119266	NM_001375	DNASE2	0.02	0.46	8.93	4.06E-01		
A_23_P16722	NM_014689	DOCK10	0.00	0.10	11.57	5.81E-01		
A_33_P3228564	NM_001144875	DOK3	0.02	0.46	8.54	-3.42E-01	#	
A_33_P3286046	NM_015448	DPCD	0.01	0.41	9.19	-3.99E-01	#	
A_33_P3423185	AK024141	DPF3	0.02	0.46	5.57	-4.16E-01	#	
A_33_P3402963	NM_001012728	DPRX	0.01	0.37	5.58	-3.89E-01		
A_24_P149036	NM_001387	DPYSL3	0.00	0.23	8.77	5.09E-01		
A_23_P427299	DQ786249	DQ786249	0.01	0.34	7.44	3.85E-01	*	
A_32_P145051	DQ786249	DQ786249	0.02	0.43	6.58	3.42E-01	*	
A_32_P54274	NM_000798	DRD5	0.00	0.02	7.62	-9.56E-01	*	
A_24_P862886	NM_000798	DRD5	0.00	0.05	6.49	-7.95E-01	*	
A_23_P4494	NM_024422	DSC2	0.00	0.17	8.13	-4.67E-01		
A_23_P19226	NM_013352	DSE	0.01	0.37	7.34	-3.92E-01		
A_23_P110712	NM_004417	DUSP1	0.00	0.13	6.36	6.07E-01		
A_33_P3359012	NM_004420	DUSP8	0.02	0.48	10.79	-3.87E-01	#	
A_23_P158257	NM_012148	DUX3	0.00	0.15	5.59	4.74E-01		
A_23_P211126	NM_130436	DYRK1A	0.00	0.19	10.45	-5.06E-01	#	
A_33_P3366082	NM_032565	EBPL	0.02	0.43	11.86	-3.26E-01	#	

Probe name	Systematic name	Gene name	*p*-value	adj. *p*-value	Ave Expr	log_2FC	1)	confirmed via qRT-PCR
A_32_P47701	NM_001402	EEF1A1	0.00	0.25	16.05	-4.07E-01	#	
A_33_P3387272	NM_001402	EEF1A1	0.02	0.42	15.59	-3.24E-01	#	
A_33_P3411744	NR_004428	EGOT	0.01	0.41	6.14	-3.36E-01		
A_23_P46936	NM_000399	EGR2	0.00	0.08	8.45	8.13E-01		yes
A_23_P130961	NM_001972	ELANE	0.00	0.16	16.61	-4.70E-01		
A_23_P58506	NM_012081	ELL2	0.01	0.41	10.86	3.45E-01		
A_33_P3359900	NM_198449	EMB	0.00	0.08	12.88	-6.24E-01	*	
A_24_P684186	NM_198449	EMB	0.00	0.11	14.34	-6.18E-01	*	
A_23_P76488	NM_001423	EMP1	0.00	0.08	6.55	7.35E-01		yes
A_23_P106682	NM_001424	EMP2	0.01	0.38	8.4	3.78E-01		
A_23_P502336	NM_013447	EMR2	0.02	0.47	8.44	-3.38E-01		
A_24_P69095	NM_003633	ENC1	0.00	0.24	6.26	4.92E-01		
A_32_P120604	ENST00000219090	ENST00000219090	0.02	0.45	8.6	3.22E-01		
A_24_P288993	ENST00000244249	ENST00000244249	0.00	0.07	11.61	-6.56E-01		
A_33_P3257050	ENST00000314232	ENST00000314232	0.01	0.35	6.83	-5.11E-01		
A_23_P140614	ENST00000314246	ENST00000314246	0.00	0.10	10.17	-5.37E-01		
A_33_P3377090	ENST00000314747	ENST00000314747	0.02	0.48	5.36	-2.99E-01		
A_33_P3312217	ENST00000330110	ENST00000330110	0.00	0.23	5.36	-4.74E-01	#	
A_33_P3216568	ENST00000356191	ENST00000356191	0.02	0.46	5.9	3.42E-01		
A_33_P3418611	ENST00000357491	ENST00000357491	0.02	0.43	11.25	-4.06E-01		
A_33_P3391521	ENST00000366589	ENST00000366589	0.02	0.47	6.02	-3.80E-01		
A_33_P3418576	ENST00000367101	ENST00000367101	0.02	0.48	6.16	2.96E-01		
A_33_P3220813	ENST00000367652	ENST00000367652	0.01	0.38	5.96	3.76E-01		
A_33_P3332487	ENST00000368689	ENST00000368689	0.02	0.46	5.53	-3.12E-01		
A_33_P3228402	ENST00000373495	ENST00000373495	0.01	0.41	6.15	-3.43E-01		
A_33_P3230788	ENST00000374440	ENST00000374440	0.01	0.40	8.88	-5.88E-01		
A_33_P3378680	ENST00000378013	ENST00000378013	0.01	0.30	5.54	4.10E-01		
A_33_P3216192	ENST00000381654	ENST00000381654	0.00	0.17	10.81	-4.64E-01		
A_33_P3312194	ENST00000392178	ENST00000392178	0.02	0.44	6.13	3.56E-01		
A_33_P3224265	ENST00000394333	ENST00000394333	0.02	0.43	8.65	-4.02E-01		
A_33_P3272352	ENST00000397064	ENST00000397064	0.02	0.46	12.04	-3.04E-01		
A_33_P3374684	ENST00000398617	ENST00000398617	0.02	0.43	7.86	-8.76E-01		
A_33_P3291329	ENST00000398917	ENST00000398917	0.00	0.01	7.82	-9.77E-01		
A_33_P3392213	ENST00000399125	ENST00000399125	0.01	0.34	11.7	-3.67E-01		
A_23_P331908	ENST00000399269	ENST00000399269	0.00	0.19	7.58	-4.73E-01		
A_33_P3278159	ENST00000399539	ENST00000399539	0.01	0.31	9.5	-6.37E-01		
A_33_P3424217	ENST00000399670	ENST00000399670	0.00	0.00	7.93	1.19E+00		
A_33_P3243230	ENST00000401931	ENST00000401931	0.00	0.09	6.89	5.51E-01		
A_23_P255827	ENST00000402782	ENST00000402782	0.00	0.05	9.43	-7.02E-01		
A_33_P3220302	ENST00000416014	ENST00000416014	0.01	0.38	5.23	-3.67E-01		
A_24_P280897	ENST00000418275	ENST00000418275	0.00	0.23	13.79	-4.64E-01		
A_24_P306469	ENST00000420126	ENST00000420126	0.00	0.14	11.29	-4.86E-01		
A_24_P15388	ENST00000424969	ENST00000424969	0.00	0.18	5.35	-5.64E-01		
A_24_P238570	ENST00000430873	ENST00000430873	0.02	0.45	5.93	3.27E-01		
A_33_P3244640	ENST00000432765	ENST00000432765	0.01	0.38	6.56	-3.47E-01		
A_24_P58242	ENST00000435613	ENST00000435613	0.00	0.09	10.93	-7.06E-01		
A_33_P3271711	ENST00000449914	ENST00000449914	0.01	0.38	7.26	-3.92E-01		
A_32_P76853	ENST00000450802	ENST00000450802	0.00	0.24	12.12	-4.25E-01		
A_33_P3302662	ENST00000461758	ENST00000461758	0.01	0.30	7.45	4.15E-01		
A_33_P3218975	NM_001776	ENTPD1	0.00	0.08	7.02	6.43E-01	*	
A_33_P3218980	NM_001776	ENTPD1	0.00	0.09	7.56	7.43E-01	*	
A_23_P4536	NM_012307	EPB41L3	0.02	0.45	8.45	4.53E-01		

Probe name	Systematic name	Gene name	*p*-value	adj. *p*-value	Ave Expr	log_2FC	1)	confirmed via qRT-PCR
A_24_P257579	NM_022140	EPB41L4A	0.00	0.17	5.39	4.90E-01	#	
A_33_P3248325	AK290895	EPB41L5	0.02	0.44	7.09	-3.22E-01	#	
A_23_P34537	NM_000120	EPHX1	0.01	0.33	9.69	-3.70E-01		
A_33_P3325018	NM_015701	ERLEC1	0.02	0.46	12.13	-3.13E-01	#	
A_23_P164042	NM_001433	ERN1	0.02	0.43	6.24	3.28E-01		
A_33_P3226425	NM_001034025	ERP29	0.02	0.44	10.12	-3.21E-01	#	
A_33_P3226678	NM_001145127	EVPLL	0.01	0.27	6.34	-4.09E-01	#	
A_24_P368943	NM_001989	EVX1	0.00	0.26	10.14	-6.25E-01		
A_23_P205177	NM_000504	F10	0.02	0.44	5.79	-4.20E-01	#	
A_32_P140139	NM_000129	F13A1	0.02	0.46	5.67	3.25E-01	#	
A_23_P94879	NM_000506	F2	0.01	0.34	5.74	-3.96E-01		
A_23_P117298	NM_000131	F7	0.01	0.34	5.86	4.03E-01		
A_23_P133438	NM_019018	FAM105A	0.00	0.15	10.98	4.74E-01	*	
A_32_P51848	NM_019018	FAM105A	0.01	0.35	7.11	3.94E-01	*	
A_23_P120973	NM_017911	FAM118A	0.02	0.43	7.63	-3.22E-01		
A_23_P142688	NM_024293	FAM134A	0.02	0.46	9.78	3.03E-01	*	
A_23_P398172	NM_020819	FAM135A	0.02	0.45	7.98	3.46E-01	#	
A_23_P100001	NM_207446	FAM174B	0.02	0.48	8.74	-2.96E-01		
A_33_P3290573	NM_017633	FAM46A	0.00	0.05	12.96	-7.42E-01	*	
A_33_P3410599	NM_017633	FAM46A	0.00	0.08	13.72	-6.96E-01	*	
A_23_P379327	NM_001040450	FAM63B	0.02	0.46	8.95	-4.18E-01		
A_33_P3316410	NR_026789	FAM66A	0.02	0.46	6.74	-3.04E-01	#	
A_33_P3217364	NM_001083124	FAM75A3	0.02	0.48	7.3	3.01E-01	#	
A_33_P3222045	NM_201400	FAM86A	0.01	0.30	8.6	-4.07E-01	#	
A_33_P3374878	NM_024582	FAT4	0.02	0.46	5.45	3.21E-01	#	
A_32_P220463	NR_024356	FBLL1	0.01	0.38	7.43	-3.82E-01	*	
A_23_P211631	NM_006486	FBLN1	0.00	0.08	7.83	-5.85E-01	#	
A_23_P406385	NM_153350	FBXL16	0.02	0.46	5.68	3.11E-01		
A_33_P3259507	NM_012166	FBXO10	0.02	0.44	9.28	-3.32E-01		
A_23_P168847	NM_172366	FBXO16	0.01	0.38	8.1	-3.91E-01		
A_23_P395566	NM_024735	FBXO31	0.02	0.46	7.93	-3.34E-01	#	
A_23_P164773	NM_002002	FCER2	0.00	0.04	6.36	8.75E-01		
A_23_P85716	NM_021642	FCGR2A	0.00	0.23	9.97	-4.87E-01	#	
A_33_P3327617	NM_201563	FCGR2C	0.02	0.44	9.02	-3.80E-01		
A_33_P3255509	NM_001161357	FCHO1	0.01	0.30	10.96	3.78E-01		
A_23_P500501	NM_000142	FGFR3	0.01	0.36	8.55	-4.97E-01	#	
A_33_P3332018	NM_006682	FGL2	0.00	0.04	7.01	9.40E-01		
A_23_P103932	NM_001042747	FGR	0.00	0.06	10.69	6.31E-01		
A_33_P3278330	AK131224	FLJ16124	0.01	0.33	5.95	-6.64E-01		
A_33_P3711933	NM_152432	FLJ32810	0.01	0.41	6.54	3.47E-01	#	
A_32_P473302	NR_015375	FLJ35024	0.01	0.33	7.18	-4.21E-01		
A_33_P3259890	BC042169	FLJ35946	0.01	0.30	5.46	-6.21E-01		
A_33_P3331426	AK095105	FLJ37786	0.01	0.37	7.42	-3.66E-01	#	
A_24_P194661	AK095698	FLJ38379	0.00	0.16	6.51	-5.79E-01		
A_33_P3543288	AK124832	FLJ42842	0.02	0.44	5.58	-5.44E-01		
A_23_P256059	NR_029406	FLJ43681	0.02	0.42	14.55	-3.37E-01		
A_33_P3227482	AK125932	FLJ43944	0.01	0.41	5.67	-3.33E-01		
A_33_P3248900	NR_028324	FLJ45445	0.01	0.34	12.83	-4.21E-01	#	
A_23_P47168	NM_013280	FLRT1	0.02	0.46	6.98	3.79E-01		
A_24_P390668	NM_005892	FMNL1	0.01	0.38	9.58	3.55E-01	*	
A_23_P417942	NM_001024948	FNBP1L	0.02	0.43	7.72	-3.82E-01		
A_23_P53176	NM_016725	FOLR1	0.01	0.32	7.16	-3.71E-01		

Probe name	Systematic name	Gene name	*p*-value	adj. *p*-value	Ave Expr	log_2FC	1)	confirmed via qRT-PCR
A_23_P47709	NM_000803	FOLR2	0.01	0.30	6.2	-4.80E-01	#	
A_23_P106194	NM_005252	FOS	0.00	0.06	11.15	8.78E-01		yes
A_23_P429998	NM_006732	FOSB	0.00	0.01	7.24	1.05E+00		
A_32_P34920	NM_004472	FOXD1	0.00	0.10	9.33	-6.32E-01		
A_32_P119248	NM_207305	FOXD4	0.02	0.42	9.17	-3.38E-01		
A_24_P15391	NM_001135649	FOXI3	0.02	0.45	6.19	-3.93E-01		
A_33_P3261173	NM_005479	FRAT1	0.02	0.44	6.12	3.21E-01	#	
A_33_P3364112	NM_006654	FRS2	0.00	0.27	9.08	-4.32E-01		
A_33_P3411075	NM_003088	FSCN1	0.00	0.12	12.22	-6.32E-01		
A_33_P3225022	NM_206965	FTCD	0.02	0.41	5.79	-3.25E-01	*	
A_23_P11543	NM_000147	FUCA1	0.00	0.04	10.19	6.82E-01		yes
A_33_P3406493	NM_005458	GABBR2	0.02	0.43	5.87	3.19E-01		
A_32_P25514	NM_198904	GABRG2	0.00	0.19	7.24	-6.04E-01		
A_24_P910667	AF220235	GAFA3	0.02	0.47	6.54	7.18E-01		
A_23_P374844	NM_015973	GAL	0.00	0.07	12.66	-6.11E-01		
A_33_P3402350	CR598865	GAPDHP32	0.02	0.48	5.79	-3.00E-01		
A_24_P85942	NM_181453	GCC2	0.00	0.18	9.96	-4.99E-01	*	
A_23_P122662	NM_018988	GFOD1	0.02	0.46	10.59	3.08E-01		
A_33_P3408953	NM_199127	GGTLC2	0.01	0.40	9.66	-3.34E-01	#	
A_23_P214411	NM_006708	GLO1	0.01	0.38	12.39	-3.65E-01		
A_32_P19294	NM_144669	GLT1D1	0.00	0.13	7.6	5.70E-01		
A_24_P392925	NM_001014985	GLTPD2	0.01	0.30	6.51	3.86E-01		
A_33_P3285580	NM_145262	GLYCTK	0.01	0.34	7.19	3.97E-01	#	
A_23_P209954	NM_006433	GNLY	0.01	0.30	5.4	3.83E-01	*	
A_24_P323072	NM_178332	GNRH2	0.00	0.24	7.88	-4.14E-01	#	
A_33_P3332474	NM_001001413	GOLGA6L1	0.00	0.23	7.58	-5.90E-01		
A_33_P3239101	NM_001164465	GOLGA6L10	0.02	0.45	6.9	-3.26E-01	#	
A_33_P3220025	NM_001145004	GOLGA6L6	0.00	0.16	9.73	-5.72E-01	#	
A_24_P50972	NM_001145004	GOLGA6L6	0.00	0.26	11.22	-5.41E-01	#	
A_32_P231086	NM_198181	GOLGA6L9	0.02	0.48	11.15	-3.01E-01	#	
A_24_P98277	NM_001002296	GOLGA7	0.02	0.45	9.81	-3.30E-01	#	
A_32_P2392	NM_181077	GOLGA8A	0.01	0.28	10.53	-3.92E-01	#	
A_32_P119569	NR_033350	GOLGA8E	0.00	0.07	9.94	-6.01E-01	*	
A_33_P3262833	NR_033350	GOLGA8E	0.00	0.13	11.19	-4.91E-01	*	
A_24_P229669	NR_024074	GOLGA9P	0.00	0.08	10.16	-6.91E-01		
A_33_P3210671	NM_207328	GPAT2	0.00	0.25	5.69	4.24E-01	#	
A_23_P209904	NM_002081	GPC1	0.02	0.46	9.24	-3.85E-01		
A_23_P112874	NM_004466	GPC5	0.00	0.11	5.92	-5.21E-01		
A_33_P3375467	NM_177483	GPLD1	0.02	0.46	5.42	-3.48E-01	#	
A_23_P378416	NM_001001996	GPM6B	0.01	0.35	7.62	-3.71E-01	*	
A_23_P134426	NM_001005340	GPNMB	0.00	0.00	8.48	1.24E+00		
A_24_P334718	NM_181791	GPR141	0.01	0.36	6.9	3.49E-01		
A_23_P14165	NM_005292	GPR18	0.02	0.46	9.96	3.40E-01		
A_33_P3375368	NM_005301	GPR35	0.01	0.38	7.44	4.07E-01		
A_23_P37892	NM_133443	GPT2	0.01	0.30	9.28	-3.99E-01		
A_24_P418816	NM_015696	GPX7	0.02	0.45	9.78	-3.23E-01		
A_23_P257962	NM_007327	GRIN1	0.01	0.33	5.43	-4.07E-01	#	
A_33_P3423365	NM_001127663	GSN	0.00	0.19	12.31	-4.84E-01	#	
A_23_P115407	NM_146421	GSTM1	0.01	0.40	10.27	-3.55E-01		
A_23_P12343	NM_000849	GSTM3	0.00	0.23	14.35	-4.82E-01		
A_23_P153945	NM_001006636	GTDC1	0.01	0.29	9.53	-3.99E-01		
A_24_P274640	NM_001042490	GTF2H2D	0.01	0.37	12.42	-3.55E-01		

Probe name	Systematic name	Gene name	*p*-value	adj. *p*-value	Ave Expr	log_2FC	1)	confirmed via qRT-PCR
A_33_P3375646	AK296003	GTPBP6	0.02	0.45	6.53	-3.58E-01	#	
A_33_P3388192	NM_144594	GTSF1	0.02	0.47	14.04	-3.21E-01		
A_33_P3362933	NM_002099	GYPA	0.01	0.40	7.9	3.31E-01	#	
A_23_P117602	NM_004131	GZMB	0.00	0.24	6.3	4.25E-01		
A_23_P128993	NM_033423	GZMH	0.01	0.35	6.22	-3.98E-01		
A_23_P121182	NM_012260	HACL1	0.02	0.47	12.1	-3.07E-01		
A_33_P3318946	NM_021817	HAPLN2	0.00	0.02	11.35	-1.20E+00		
A_33_P3382887	ENST00000426779	hCG_1659830	0.00	0.01	7.16	-2.19E+00		
A_24_P290013	NR_024363	hCG_1990547	0.02	0.47	7.95	-3.04E-01	#	
A_33_P3281036	NR_026790	HCG11	0.01	0.40	12.12	-3.64E-01		
A_24_P17870	NM_006674	HCP5	0.00	0.10	8.19	8.01E-01		
A_24_P55250	NM_016063	HDDC2	0.00	0.26	11.8	-9.88E-01	*	
A_33_P3212650	BC001671	HDDC2	0.02	0.45	12.63	-3.09E-01	*	
A_23_P122796	NM_016063	HDDC2	0.01	0.37	8.45	-3.54E-01		
A_23_P258689	NM_017802	HEATR2	0.01	0.27	11.35	-4.08E-01	#	
A_23_P59349	NM_016217	HECA	0.02	0.46	12.92	3.17E-01		
A_32_P166693	NM_020733	HEG1	0.00	0.06	10.29	6.24E-01		
A_23_P368805	NM_007072	HHLA2	0.00	0.08	5.67	5.83E-01	#	
A_24_P363548	NM_005338	HIP1	0.01	0.40	7.64	4.18E-01		
A_24_P681011	NM_022740	HIPK2	0.00	0.15	7.21	5.02E-01	*	
A_23_P7976	NM_005321	HIST1H1E	0.00	0.01	11.74	-9.68E-01		
A_23_P30813	NM_003541	HIST1H4K	0.02	0.48	11.01	-3.33E-01	#	
A_23_P137909	NM_003493	HIST3H3	0.01	0.27	16.01	-3.96E-01		
A_23_P217958	NM_033500	HK1	0.00	0.13	9.35	5.44E-01		
A_32_P175739	NM_000189	HK2	0.01	0.30	10.76	4.22E-01	#	
A_33_P3424800	NM_005514	HLA-B	0.00	0.06	14.75	-6.40E-01	#	
A_24_P50245	NM_006120	HLA-DMA	0.00	0.08	9.43	6.40E-01	*	
A_23_P42306	NM_006120	HLA-DMA	0.00	0.08	9.82	7.00E-01	*	
A_32_P351968	NM_002118	HLA-DMB	0.00	0.00	8.74	1.49E+00		
A_23_P30913	NM_033554	HLA-DPA1	0.00	0.00	10.41	1.60E+00	*	
A_33_P3234277	NM_033554	HLA-DPA1	0.00	0.01	9.81	1.33E+00	*	
A_24_P166443	NM_002121	HLA-DPB1	0.00	0.00	10.22	1.54E+00	*	
A_23_P258769	NM_002121	HLA-DPB1	0.00	0.00	11.09	1.63E+00	*	
A_33_P3271651	NM_002121	HLA-DPB1	0.00	0.00	9.37	1.65E+00	*	
A_33_P3271635	NM_002121	HLA-DPB1	0.00	0.00	8.48	1.45E+00	*	
A_24_P288836	NR_001435	HLA-DPB2	0.00	0.01	7.7	9.36E-01	#	
A_33_P3293049	NM_002122	HLA-DQA1	0.00	0.01	6.29	9.62E-01	*	
A_33_P3273884	NM_002122	HLA-DQA1	0.00	0.09	5.8	5.93E-01	*	
A_24_P852756	NM_020056	HLA-DQA2	0.00	0.07	5.57	5.94E-01		
A_23_P136683	NM_002123	HLA-DQB1	0.00	0.02	9.08	9.42E-01	*	
A_33_P3424222	NM_002123	HLA-DQB1	0.00	0.06	10.51	8.09E-01	*	
A_23_P8108	AK304543	HLA-DQB1	0.00	0.11	10.95	5.98E-01	*	
A_23_P19510	NR_003937	HLA-DQB2	0.00	0.06	7.67	6.68E-01		
A_32_P87697	NM_019111	HLA-DRA	0.00	0.04	11.64	8.73E-01		
A_24_P343233	NM_002124	HLA-DRB1	0.00	0.06	13.17	7.35E-01		
A_33_P3383912	NM_022555	HLA-DRB3	0.00	0.13	11.32	5.59E-01		
A_24_P370472	NM_021983	HLA-DRB4	0.00	0.22	10.37	4.53E-01		
A_23_P45099	NM_002125	HLA-DRB5	0.00	0.12	13.09	5.98E-01		
A_33_P3379967	NM_001098478	HLA-F	0.00	0.24	8.76	5.27E-01	#	
A_33_P3323448	NM_178582	HM13	0.02	0.46	6.76	6.11E-01	#	
A_24_P932736	ENST00000397358	HMBOX1	0.00	0.01	6.48	-9.46E-01	#	
A_23_P148990	NM_031935	HMCN1	0.01	0.40	5.53	3.74E-01		

Probe name	Systematic name	Gene name	*p*-value	adj. *p*-value	Ave Expr	log_2FC	1)	confirmed via qRT-PCR
A_32_P41487	NM_005517	HMGN2	0.02	0.44	18.01	-3.15E-01	#	
A_24_P132099	NM_138730	HMGN3	0.01	0.30	13.61	-4.02E-01		
A_24_P397515	NM_006353	HMGN4	0.02	0.43	9.89	3.65E-01		
A_24_P136161	NM_001013631	HNRNPCL1	0.01	0.38	9.25	-3.69E-01		
A_33_P3264528	NM_005523	HOXA11	0.00	0.13	9.78	-4.95E-01		
A_24_P280983	NR_002795	HOXA11AS	0.01	0.38	11.5	-3.53E-01		
A_23_P70968	NM_006896	HOXA7	0.00	0.26	6.69	-4.07E-01		
A_23_P500998	NM_152739	HOXA9	0.00	0.14	11.59	-5.65E-01	#	
A_33_P3300975	NM_014620	HOXC4	0.00	0.04	7.38	-7.64E-01		
A_23_P139527	NM_002150	HPD	0.00	0.11	6.18	-5.93E-01		
A_33_P3320241	XM_001722088	HPX-2	0.00	0.05	5.35	7.51E-01	#	
A_23_P142125	NM_002152	HRC	0.00	0.26	8.26	-5.38E-01		
A_33_P3309231	NM_172002	HSCB	0.00	0.10	15.71	-5.76E-01	#	
A_23_P63209	NM_181755	HSD11B1	0.00	0.22	12.59	-4.73E-01		
A_33_P3335042	NM_016142	HSD17B12	0.02	0.42	10.34	-3.20E-01	#	
A_23_P11859	NM_016371	HSD17B7	0.01	0.40	10.22	-3.81E-01		
A_33_P3510335	NM_213655	HSN2	0.01	0.28	8.11	-4.06E-01		
A_23_P162874	NM_005348	HSP90AA1	0.01	0.38	14.17	-3.74E-01		
A_33_P3408212	NM_003299	HSP90B1	0.01	0.31	12.62	-4.01E-01	#	
A_33_P3401252	NR_003130	HSP90B3P	0.01	0.39	13.84	-3.39E-01		
A_23_P88303	NM_021979	HSPA2	0.02	0.42	7.54	-3.54E-01		
A_33_P3418511	NR_027756	HTA	0.02	0.42	5.84	3.27E-01		
A_24_P153820	BC028351	HYDIN	0.02	0.48	5.67	2.97E-01	#	
A_33_P3209351	NM_013417	IARS	0.01	0.41	10.14	-3.31E-01	#	
A_33_P3209346	NM_013417	IARS	0.02	0.47	7.85	-3.30E-01	#	
A_23_P152655	NM_000873	ICAM2	0.02	0.48	9.1	-3.05E-01		
A_23_P119143	NM_003259	ICAM5	0.00	0.15	6.28	6.29E-01		
A_23_P153745	NM_006332	IFI30	0.00	0.06	10	9.14E-01		
A_33_P3337540	NM_000874	IFNAR2	0.00	0.17	12.33	-4.91E-01	#	
A_23_P406135	NM_015662	IFT172	0.02	0.44	11.79	-3.26E-01		
A_33_P3242973	NM_006548	IGF2BP2	0.01	0.27	7.47	-4.15E-01	*	
A_23_P250156	NM_006548	IGF2BP2	0.02	0.48	10.33	-3.36E-01	*	
A_23_P119943	NM_000597	IGFBP2	0.01	0.32	7.73	-3.68E-01		
A_33_P3372004	NM_005849	IGSF6	0.00	0.06	6.43	6.44E-01		
A_32_P114284	NM_001079526	IKZF2	0.00	0.10	8.09	-5.96E-01	#	
A_23_P203173	NM_001558	IL10RA	0.00	0.13	9.55	5.27E-01		
A_23_P72077	NM_001559	IL12RB2	0.00	0.26	8.21	-4.39E-01		
A_24_P73599	NM_172217	IL16	0.00	0.20	6.44	4.94E-01	*	
A_23_P61057	NM_004513	IL16	0.01	0.30	7.88	4.39E-01	*	
A_23_P104798	NM_001562	IL18	0.01	0.38	8.35	-3.79E-01		
A_33_P3228322	NM_173042	IL18BP	0.01	0.41	6.62	-3.30E-01		
A_23_P91850	NM_144717	IL20RB	0.02	0.43	9.48	-3.73E-01		
A_33_P3290394	NM_000206	IL2RG	0.02	0.47	7.37	-3.09E-01	#	
A_32_P87013	NM_000584	IL8	0.00	0.06	7.75	6.47E-01		yes
A_23_P109907	NM_175924	ILDR1	0.00	0.11	15.02	-5.11E-01		
A_33_P3290403	NM_014214	IMPA2	0.02	0.42	9.8	3.34E-01	*	
A_23_P50081	NM_014214	IMPA2	0.02	0.47	13.56	3.04E-01	*	
A_23_P122924	NM_002192	INHBA	0.01	0.38	6.43	4.10E-01		
A_33_P3397995	NM_001130699	IPCEF1	0.02	0.45	9.28	3.70E-01	#	
A_32_P21474	NM_001010844	IRAK1BP1	0.02	0.45	7.57	-3.82E-01		
A_33_P3352970	NM_001570	IRAK2	0.01	0.38	8.2	3.73E-01		
A_23_P206022	NM_001004439	ITGA11	0.02	0.48	6.8	-3.04E-01		

Probe name	Systematic name	Gene name	*p*-value	adj. *p*-value	Ave Expr	log_2FC	1)	confirmed via qRT-PCR
A_23_P128084	NM_002206	ITGA7	0.02	0.47	12.78	3.50E-01		
A_23_P206806	NM_002209	ITGAL	0.00	0.22	10.63	5.68E-01		
A_23_P50907	NM_002210	ITGAV	0.02	0.42	11.25	-3.35E-01		
A_23_P312132	NM_000887	ITGAX	0.00	0.24	10.43	6.17E-01	#	
A_23_P104199	NM_133376	ITGB1	0.02	0.45	9.99	-3.21E-01		
A_23_P76529	NM_000889	ITGB7	0.01	0.34	9.44	3.69E-01		
A_23_P171074	NM_004867	ITM2A	0.00	0.06	7.46	-7.55E-01		
A_24_P379820	NM_030926	ITM2C	0.01	0.41	10.37	-3.33E-01	#	
A_24_P835500	NM_001034841	ITPRIPL2	0.00	0.13	8.95	4.91E-01		
A_23_P106024	NM_002226	JAG2	0.02	0.42	6.73	-4.83E-01		
A_23_P427217	NM_032776	JMJD1C	0.01	0.36	9.26	-3.95E-01		
A_23_P429950	NM_000216	KAL1	0.02	0.42	7.13	3.69E-01		
A_33_P3209866	NM_153186	KANK1	0.01	0.30	8.83	-4.00E-01	#	
A_33_P3260530	NM_181712	KANK4	0.02	0.47	5.68	-3.10E-01	*	
A_23_P101516	NM_004977	KCNC3	0.01	0.38	7.73	3.42E-01	#	
A_23_P3177	NM_022054	KCNK13	0.00	0.18	6.45	4.76E-01		
A_23_P119573	NM_002248	KCNN1	0.00	0.26	5.59	4.27E-01		
A_23_P150648	NR_024627	KCNQ1DN	0.01	0.41	5.61	3.54E-01		
A_33_P3395823	NM_172109	KCNQ2	0.00	0.17	8.04	-8.12E-01	#	
A_33_P3240512	NM_138444	KCTD12	0.00	0.16	11.66	5.39E-01	#	yes
A_23_P211504	NM_016657	KDELR3	0.01	0.36	5.67	-3.69E-01		
A_33_P3297621	NM_015047	KIAA0090	0.02	0.43	9.95	-3.43E-01	#	
A_23_P324490	NM_014686	KIAA0355	0.01	0.38	9.08	-3.69E-01		
A_23_P206310	NM_014732	KIAA0513	0.02	0.42	7.33	3.75E-01		
A_24_P295601	NM_014741	KIAA0652	0.02	0.47	10.41	-3.10E-01	#	
A_23_P116168	NM_032424	KIAA1826	0.02	0.47	9.01	3.14E-01		
A_23_P126888	NM_017596	KIF21B	0.01	0.32	9.62	3.76E-01	#	
A_32_P27917	NM_015656	KIF26A	0.00	0.03	5.98	8.37E-01		no
A_33_P3414683	NM_145754	KIFC2	0.01	0.38	6.3	3.41E-01	#	
A_23_P315451	NM_199180	KIRREL2	0.02	0.47	8.33	-3.15E-01	#	
A_23_P32233	NM_004235	KLF4	0.01	0.30	7.8	4.82E-01		
A_23_P64898	NM_005810	KLRG1	0.02	0.46	7.07	-3.35E-01	#	
A_33_P3306207	NM_198508	KLRG2	0.00	0.13	11.51	-4.91E-01	#	
A_24_P11791	NM_002268	KPNA4	0.01	0.40	13.01	-3.62E-01		
A_33_P3364520	NM_181602	KRTAP6-1	0.02	0.45	6.34	3.12E-01		
A_23_P89780	NM_198129	LAMA3	0.01	0.31	7.12	-3.81E-01	#	
A_33_P3223780	NM_002292	LAMB2	0.00	0.24	5.51	4.51E-01	#	
A_33_P3413815	NR_004405	LAMB2L	0.01	0.28	8.87	4.59E-01		
A_33_P3338121	NM_001017402	LAMB3	0.01	0.29	10.05	-4.72E-01		
A_33_P3238007	NM_178043	LARP1B	0.01	0.38	9.25	-3.52E-01	#	
A_23_P89187	NM_006148	LASP1	0.00	0.23	12.13	-5.94E-01		
A_32_P48466	NM_152505	LCA5L	0.02	0.47	5.56	3.16E-01		
A_33_P3382746	NM_005356	LCK	0.00	0.13	6.35	5.20E-01	#	
A_23_P215931	NM_015344	LEPROTL1	0.02	0.42	11.44	-3.60E-01	#	
A_23_P166459	NM_002305	LGALS1	0.01	0.33	15.05	-4.05E-01		
A_23_P120902	NM_006498	LGALS2	0.00	0.02	7.38	1.02E+00		
A_33_P3365437	NM_020204	LHX9	0.00	0.00	7.64	-1.34E+00	*	
A_23_P327562	NM_020204	LHX9	0.00	0.04	6.04	-7.22E-01	*	
A_32_P70158	NM_006864	LILRB3	0.00	0.08	5.79	6.64E-01	#	
A_33_P3408762	NM_005572	LMNA	0.01	0.34	13.19	3.95E-01	#	
A_32_P33561	NR_024407	LOC100009676	0.02	0.47	7.33	-3.04E-01	#	
A_33_P3301297	XR_039256	LOC100128086	0.00	0.20	6.28	-6.35E-01		

Probe name	Systematic name	Gene name	*p*-value	adj. *p*-value	Ave Expr	log_2FC	1)	confirmed via qRT-PCR
A_32_P100641	XM_001719779	LOC100128139	0.01	0.40	6.63	3.66E-01		
A_33_P3326447	AK125272	LOC100128276	0.00	0.17	7.42	6.01E-01		
A_33_P3339990	AK123323	LOC100128429	0.02	0.46	5.9	3.66E-01		
A_33_P3383071	AK126077	LOC100128437	0.02	0.46	5.99	-3.37E-01	#	
A_32_P834166	AF128541	LOC100128843	0.02	0.46	6.69	4.78E-01		
A_33_P3318763	BM457408	LOC100128994	0.00	0.02	7.75	-9.53E-01	*	
A_33_P3265872	XM_001717144	LOC100128994	0.00	0.03	8.74	-1.01E+00	*	
A_32_P91042	NR_027406	LOC100129034	0.01	0.37	8.59	3.67E-01		
A_33_P3333560	XM_001715999	LOC100129101	0.02	0.42	6.44	-3.52E-01		
A_33_P3261953	XR_037125	LOC100129536	0.00	0.26	6.27	4.01E-01		
A_33_P3409580	AK097764	LOC100129722	0.00	0.00	10.26	-1.32E+00		
A_33_P3263284	NR_024563	LOC100130238	0.02	0.46	10.06	-7.55E-01	#	
A_33_P3400334	AK127532	LOC100130372	0.01	0.28	5.53	4.11E-01		
A_33_P3404671	NR_024567	LOC100130557	0.02	0.44	10.65	-3.17E-01	#	
A_24_P76078	ENST00000437256	LOC100130794	0.01	0.37	12.91	-3.78E-01		
A_33_P3239579	AK296298	LOC100131060	0.00	0.10	5.87	5.33E-01		
A_33_P3373573	XM_001717835	LOC100131316	0.02	0.42	5.58	3.23E-01		
A_33_P3315704	XM_001721221	LOC100131778	0.02	0.48	6.42	3.26E-01		
A_33_P3258127	AY203946	LOC100132188	0.02	0.47	5.61	3.33E-01		
A_33_P3308101	AK128836	LOC100132217	0.01	0.40	8.81	-5.54E-01	#	
A_33_P3223631	AK128836	LOC100132217	0.02	0.44	7.9	-3.48E-01	#	
A_24_P167877	NM_001135865	LOC100132247	0.01	0.32	15.98	3.69E-01	#	
A_33_P3244369	XR_037592	LOC100132541	0.02	0.46	7.53	-4.26E-01	#	
A_24_P367421	XM_001718703	LOC100132816	0.00	0.07	9.3	-6.24E-01	*	
A_33_P3334738	XM_001718703	LOC100132816	0.01	0.41	6.54	-3.59E-01	*	
A_33_P3413795	AV727532	LOC100133008	0.00	0.10	9.07	-7.89E-01	#	
A_33_P3388909	AK128414	LOC100133077	0.02	0.45	5.99	3.11E-01		
A_33_P3405864	XM_001716939	LOC100133165	0.00	0.17	5.98	-4.56E-01		
A_33_P3256480	XR_038016	LOC100133478	0.00	0.26	8.1	-5.91E-01		
A_33_P3292602	XM_001722336	LOC100133737	0.02	0.45	12.1	-3.27E-01	#	
A_33_P3366493	XR_037443	LOC100133990	0.00	0.14	7.97	-6.66E-01		
A_33_P3337742	XM_001714782	LOC100134002	0.02	0.47	8.88	-4.58E-01		
A_33_P3281905	NR_021493	LOC100144604	0.01	0.36	9.52	-3.64E-01		
A_33_P3419003	XM_002342467	LOC100289258	0.00	0.17	17.53	-4.66E-01		
A_33_P3395237	XM_001724470	LOC134505	0.02	0.43	10.8	-4.03E-01		
A_33_P3387656	XM_002343801	LOC139431	0.00	0.17	5.81	1.66E+00		
A_33_P3406572	AK091704	LOC149773	0.02	0.46	6.01	-7.48E-01		
A_33_P3404641	NR_027034	LOC150381	0.00	0.23	7.3	-5.11E-01		
A_32_P81676	NR_024281	LOC157627	0.00	0.19	5.79	4.84E-01		
A_33_P3348011	NR_002936	LOC222699	0.01	0.37	7.26	-4.59E-01		
A_33_P3711318	AK001439	LOC257152	0.02	0.48	9.39	-6.73E-01		
A_33_P3394140	NR_024431	LOC283050	0.01	0.29	6	3.97E-01		
A_33_P3235761	NR_024349	LOC284023	0.02	0.43	5.89	-3.33E-01		
A_32_P13151	NR_027995	LOC284232	0.02	0.47	7	-7.03E-01	#	
A_33_P3387766	NR_015417	LOC284276	0.01	0.30	6.36	-3.80E-01	#	
A_32_P232808	NR_029390	LOC284412	0.01	0.39	5.45	3.64E-01		
A_33_P3362148	NR_026963	LOC284900	0.02	0.41	6.19	4.81E-01	#	
A_33_P3802966	BM559483	LOC285740	0.02	0.45	6.06	4.18E-01	#	
A_33_P3548190	BC043259	LOC338864	0.00	0.19	6.01	8.79E-01		
A_33_P3414880	XM_001726300	LOC339192	0.01	0.39	6.97	4.54E-01		
A_33_P3398618	NR_001443	LOC339240	0.02	0.45	5.57	3.10E-01	*	
A_33_P3472460	BC041488	LOC339260	0.00	0.13	7.35	-5.40E-01		

Probe name	Systematic name	Gene name	*p*-value	adj. *p*-value	Ave Expr	log_2FC	1)	confirmed via qRT-PCR
A_33_P3793307	AK023856	LOC339803	0.00	0.10	8.74	-5.89E-01		
A_33_P3429242	BC041468	LOC339988	0.01	0.38	8.11	3.45E-01		
A_24_P135579	XM_293026	LOC344382	0.01	0.30	9.75	-3.83E-01		
A_33_P3282641	AK309325	LOC344887	0.01	0.34	7.17	-3.86E-01	#	
A_33_P3422740	NR_027002	LOC388692	0.01	0.32	8.94	-6.35E-01	#	
A_33_P3364293	NR_027420	LOC389834	0.00	0.24	8.68	-7.11E-01	#	
A_33_P3357626	XM_001716257	LOC390998	0.00	0.24	10.71	-6.15E-01		
A_33_P3366396	XM_001720500	LOC392435	0.00	0.08	5.5	5.52E-01		
A_33_P3546363	BQ950045	LOC400128	0.00	0.18	13.49	-4.86E-01		
A_33_P3388588	ENST00000378340	LOC400558	0.01	0.40	13.22	-7.90E-01		
A_33_P3328360	NR_027033	LOC400931	0.00	0.18	11.57	-4.63E-01	#	
A_33_P3257910	NM_001168214	LOC401097	0.00	0.10	6.85	-5.74E-01	*	
A_23_P305245	NM_001168214	LOC401097	0.00	0.18	7.88	-5.18E-01	*	
A_33_P3358601	ENST00000382123	LOC402778	0.01	0.38	5.65	3.59E-01		
A_33_P3227899	NR_015361	LOC440896	0.00	0.22	9.93	-4.24E-01		
A_33_P3212375	BC063653	LOC441239	0.02	0.47	6.71	-3.22E-01		
A_33_P3403053	BC066990	LOC441242	0.00	0.00	7.21	-1.11E+00		
A_24_P161813	NR_024380	LOC441666	0.00	0.25	8.17	-4.74E-01	#	
A_33_P3273266	NR_024380	LOC441666	0.01	0.27	10.14	-4.46E-01	#	
A_24_P84008	ENST00000454093	LOC441722	0.00	0.21	10.06	-5.12E-01		
A_33_P3620246	AK302879	LOC441728	0.00	0.24	8.4	-4.11E-01	#	
A_33_P3391316	AK125677	LOC441956	0.01	0.37	6.58	-3.49E-01		
A_33_P3250273	XR_040018	LOC442132	0.02	0.45	6.81	-3.45E-01	#	
A_24_P647682	NR_003598	LOC442308	0.00	0.23	9.59	-5.17E-01		
A_33_P3860067	BC009388	LOC554174	0.01	0.28	6.37	-4.31E-01		
A_32_P57702	NR_033245	LOC641746	0.01	0.41	12.44	-3.47E-01		
A_33_P3328973	AK129565	LOC642384	0.02	0.43	6.26	3.48E-01		
A_33_P3401307	AK123703	LOC643441	0.00	0.05	5.25	7.26E-01		
A_24_P366415	XM_001721772	LOC643997	0.01	0.37	15.38	-3.95E-01		
A_33_P3596355	BG033631	LOC644242	0.00	0.23	5.64	4.69E-01		
A_33_P3332175	XM_001714131	LOC644310	0.02	0.41	11.81	-3.25E-01		
A_33_P3576034	BX248273	LOC644919	0.02	0.48	5.77	-2.97E-01		
A_33_P3329352	XM_001717733	LOC644992	0.01	0.29	8.33	-4.43E-01		
A_33_P3384900	BC014600	LOC645339	0.00	0.01	7.09	-1.13E+00		
A_33_P3259447	NR_027024	LOC645752	0.00	0.07	5.65	-6.54E-01	*	
A_33_P3276153	NR_027024	LOC645752	0.00	0.21	9.59	-4.66E-01	*	
A_33_P3260511	XR_036884	LOC646070	0.01	0.35	5.77	4.87E-01	#	
A_33_P3259861	XM_001726976	LOC646396	0.01	0.38	8.57	3.83E-01	#	
A_24_P332651	XM_001726994	LOC650157	0.00	0.07	7.4	-6.16E-01		
A_33_P3240340	XR_015456	LOC727796	0.01	0.35	10	-8.62E-01		
A_33_P3384312	XM_001720692	LOC727872	0.02	0.47	5.88	-5.73E-01		
A_33_P3292814	CR747917	LOC727878	0.00	0.07	7.48	-6.19E-01		
A_33_P3327687	AK090681	LOC727993	0.02	0.45	6.1	3.36E-01		
A_33_P3248580	XR_039169	LOC728217	0.01	0.28	9.76	-4.29E-01		
A_24_P213354	XR_015710	LOC729046	0.01	0.38	14.74	-3.43E-01		
A_24_P66932	NR_033244	LOC729080	0.02	0.47	8.88	-3.15E-01		
A_32_P36143	CR602569	LOC729088	0.02	0.46	7.67	-3.37E-01		
A_24_P267686	XR_037423	LOC729314	0.01	0.31	7.53	3.99E-01		
A_33_P3222341	BC037261	LOC729822	0.01	0.34	7.63	3.65E-01		
A_33_P3240972	XR_037628	LOC729900	0.01	0.35	8.33	-3.83E-01		
A_33_P3407618	NR_026811	LOC80154	0.01	0.37	5.57	-4.31E-01	*	
A_33_P3789382	NR_027182	LOC84989	0.00	0.02	9.34	-1.06E+00		

Probe name	Systematic name	Gene name	*p*-value	adj. *p*-value	Ave Expr	log_2FC	1)	confirmed via qRT-PCR
A_24_P781615	NR_002773	LOC90586	0.02	0.46	5.77	3.04E-01		
A_23_P39799	NM_032603	LOXL3	0.02	0.46	6.82	3.06E-01	#	
A_23_P146233	NM_000237	LPL	0.00	0.06	9.33	7.06E-01		
A_23_P87150	NM_004811	LPXN	0.00	0.22	8.79	4.32E-01		
A_23_P124837	NM_002332	LRP1	0.00	0.18	5.76	4.50E-01		
A_23_P155463	NM_024512	LRRC2	0.00	0.01	6.48	-1.43E+00	#	
A_23_P61487	NM_018205	LRRC20	0.01	0.40	9.61	-3.43E-01		
A_23_P143857	NM_052953	LRRC3B	0.01	0.28	6.18	-4.32E-01		
A_33_P3263217	NM_022143	LRRC4	0.00	0.26	6.47	-4.01E-01		
A_32_P190049	NM_001099678	LRRC58	0.01	0.40	9.22	3.69E-01		
A_23_P157527	NM_033402	LRRCC1	0.00	0.08	9.17	-6.44E-01		
A_23_P13382	NM_001013254	LSP1	0.00	0.25	5.46	4.25E-01	#	
A_23_P211252	NM_001001438	LSS	0.02	0.44	8.37	-3.31E-01	#	
A_33_P3221064	NM_001042544	LTBP4	0.02	0.45	12.33	-3.31E-01	#	
A_24_P7584	NM_025262	LY6G5C	0.01	0.40	7.13	3.33E-01		
A_33_P3281028	NM_080676	MACROD2	0.02	0.46	6.17	7.46E-01	#	
A_23_P17345	NM_005461	MAFB	0.00	0.23	9.1	6.65E-01	*	yes
A_33_P3220837	NM_005461	MAFB	0.01	0.29	11.28	5.65E-01	*	yes
A_23_P103110	NM_012323	MAFF	0.02	0.45	6.57	3.92E-01		
A_33_P3564409	AK094541	MAGED4B	0.02	0.47	5.8	3.14E-01	#	
A_33_P3329444	NM_182574	MAMSTR	0.00	0.05	6.54	7.06E-01	#	
A_23_P103601	NM_020379	MAN1C1	0.02	0.43	10.42	3.50E-01	#	
A_23_P105409	NM_006301	MAP3K12	0.00	0.24	6.81	4.47E-01		
A_23_P207319	NM_003954	MAP3K14	0.01	0.41	8.19	3.66E-01		
A_23_P134125	NM_005923	MAP3K5	0.02	0.46	10.71	3.12E-01	#	
A_23_P5002	NM_001042600	MAP4K1	0.00	0.21	9.27	4.46E-01		
A_33_P3409513	NM_002751	MAPK11	0.02	0.48	8.15	-4.42E-01	#	
A_24_P89835	NM_139021	MAPK15	0.00	0.08	5.44	5.79E-01	#	
A_23_P418015	NM_014268	MAPRE2	0.02	0.46	10.54	-3.68E-01		
A_23_P102242	NM_022826	MARCH7	0.01	0.39	10.09	-3.38E-01		
A_23_P214222	NM_002356	MARCKS	0.01	0.29	9.69	4.27E-01		
A_23_P310	NM_023009	MARCKSL1	0.01	0.30	8.48	-5.11E-01		
A_23_P101992	NM_006770	MARCO	0.00	0.04	10.32	7.40E-01		
A_23_P97677	NM_002379	MATN1	0.02	0.45	5.74	3.21E-01	#	
A_33_P3854030	NM_018328	MBD5	0.02	0.47	6.53	3.63E-01		
A_23_P357811	NM_021038	MBNL1	0.02	0.47	14.74	-3.42E-01		
A_24_P808100	NM_014060	MCTS1	0.01	0.36	8.36	3.54E-01	*	
A_23_P105730	NM_020128	MDM1	0.00	0.26	7.16	-4.17E-01		
A_24_P233915	NM_201542	MED8	0.02	0.45	10.69	-3.29E-01	#	
A_23_P320739	NM_002397	MEF2C	0.00	0.23	10.5	-6.01E-01		
A_32_P129894	NM_001080497	MEGF9	0.01	0.30	8.99	3.86E-01		
A_33_P3402091	NM_006343	MERTK	0.00	0.01	6.21	1.04E+00		
A_23_P164057	NM_002404	MFAP4	0.00	0.13	11.18	-6.41E-01		
A_33_P3270315	NR_026666	MGC16384	0.01	0.33	8.61	3.80E-01	*	
A_23_P110167	NM_002413	MGST2	0.02	0.42	13.19	-3.66E-01		
A_23_P2041	NM_032867	MICALCL	0.01	0.40	6.22	3.46E-01		
A_24_P230916	NM_001077702	MIER1	0.02	0.42	11.19	-3.52E-01	#	
A_32_P108156	NR_001458	MIR155HG	0.01	0.29	6.96	4.17E-01		
A_23_P211680	NM_015166	MLC1	0.01	0.36	15.99	-3.54E-01		
A_33_P3301306	NM_170606	MLL3	0.02	0.43	11.25	-3.65E-01	#	
A_24_P116535	NM_002428	MMP15	0.01	0.30	9.49	-3.82E-01		
A_23_P137935	NM_002432	MNDA	0.00	0.25	13.44	4.42E-01		

Probe name	Systematic name	Gene name	*p*-value	adj. *p*-value	Ave Expr	log_2FC	1)	confirmed via qRT-PCR
A_23_P31064	NM_015529	MOXD1	0.00	0.20	11.28	-4.52E-01		
A_24_P153568	NM_001039396	MPEG1	0.02	0.43	6.16	4.58E-01	#	
A_23_P60579	NM_002435	MPI	0.01	0.37	9.66	-3.65E-01		
A_33_P3215953	NM_024569	MPZL1	0.02	0.42	8.26	-5.46E-01	#	
A_23_P357207	NM_138409	MRAP2	0.02	0.42	6.88	-4.66E-01		
A_24_P279797	NM_001031727	MRI1	0.02	0.47	9.2	-3.11E-01		
A_23_P3979	NM_015971	MRPS7	0.01	0.40	11.7	-3.52E-01		
A_23_P36120	NM_022349	MS4A6A	0.01	0.38	11.09	3.40E-01	#	
A_33_P3379326	NM_138715	MSR1	0.00	0.09	5.7	6.61E-01	#	
A_24_P148796	NM_020998	MST1	0.02	0.48	10.46	3.07E-01		
A_33_P3368313	NM_005951	MT1H	0.01	0.29	7.96	-4.97E-01	#	
A_23_P423695	NM_006454	MXD4	0.01	0.34	10.11	-3.95E-01	#	
A_23_P128362	NM_206819	MYBPC1	0.00	0.27	5.63	-4.08E-01	#	
A_23_P127385	NM_000256	MYBPC3	0.02	0.44	7.5	-3.14E-01		
A_23_P201655	NM_012333	MYCBP	0.02	0.46	12.37	-3.01E-01		
A_23_P377212	NM_138336	MYEOV2	0.00	0.12	5.62	7.31E-01	#	
A_33_P3235004	NM_005964	MYH10	0.00	0.17	5.64	-5.91E-01		
A_23_P59738	NM_021223	MYL7	0.01	0.35	5.96	3.68E-01		
A_33_P3539345	NM_004999	MYO6	0.00	0.22	9.85	-5.07E-01		
A_23_P422350	NM_000260	MYO7A	0.01	0.32	6.9	-4.90E-01	#	
A_23_P1320	NM_021245	MYOZ1	0.00	0.10	6.83	-5.61E-01		
A_23_P251785	NM_024561	NAA16	0.01	0.30	10.14	-5.10E-01	#	
A_24_P66679	NM_001011713	NAA30	0.02	0.46	6.41	-3.22E-01	#	
A_23_P59888	NR_002182	NACAP1	0.01	0.36	12.5	-4.42E-01		
A_33_P3346461	AK311046	NAIP	0.00	0.25	7	4.37E-01	*	
A_23_P110473	NM_004536	NAIP	0.00	0.07	9.84	6.03E-01		
A_24_P703830	NM_001098622	NANOS3	0.02	0.42	6.76	-3.81E-01		
A_33_P3405068	NM_020443	NAV1	0.00	0.08	6.46	6.85E-01	*	
A_24_P102880	NM_020443	NAV1	0.02	0.46	5.54	3.41E-01	*	
A_32_P199429	ENST00000400546	NCAM2	0.02	0.41	8.62	-4.53E-01	#	
A_33_P3299854	NM_002486	NCBP1	0.01	0.35	10.2	-3.60E-01	#	
A_33_P3369393	NM_000265	NCF1	0.01	0.38	11.3	5.03E-01	#	
A_23_P138194	NM_000433	NCF2	0.00	0.13	9.67	6.19E-01		
A_23_P120442	NM_181659	NCOA3	0.01	0.28	9.29	4.23E-01		
A_33_P3344423	NM_001145467	NCR3	0.01	0.40	5.84	-3.33E-01	*	
A_33_P3413188	NR_024493	NCRNA00087	0.02	0.46	9.21	-3.09E-01	#	
A_33_P3279362	NR_027021	NCRNA00110	0.00	0.24	5.66	4.30E-01	#	
A_24_P273143	NR_024204	NCRNA00152	0.01	0.38	10.36	-3.38E-01		
A_33_P3275350	NM_014286	NCS1	0.00	0.23	6.32	-4.24E-01		
A_33_P3404508	NM_001144027	NDOR1	0.00	0.18	8.99	-4.83E-01	#	
A_33_P3403666	NM_001144026	NDOR1	0.02	0.45	6.51	3.11E-01	#	
A_23_P145777	NM_002489	NDUFA4	0.00	0.03	16.02	-7.16E-01		
A_23_P77440	NM_173164	NFATC3	0.01	0.38	10.08	3.47E-01		
A_24_P412512	NM_016350	NIN	0.00	0.23	9.32	-4.86E-01	#	
A_23_P48109	NM_016533	NINJ2	0.00	0.08	10.29	-6.36E-01		
A_33_P3250840	NM_144599	NIPA1	0.00	0.13	11.26	-5.04E-01		
A_23_P120860	NM_003634	NIPSNAP1	0.02	0.45	9.52	-3.16E-01		
A_23_P51376	NM_024522	NKAIN1	0.02	0.48	6.51	-3.23E-01		
A_23_P119042	NM_005601	NKG7	0.01	0.39	11.94	-3.44E-01		
A_23_P207125	NM_020795	NLGN2	0.01	0.30	7.31	3.88E-01		
A_23_P101434	NM_033297	NLRP12	0.00	0.23	5.93	4.26E-01		
A_23_P60387	NM_017617	NOTCH1	0.02	0.44	8.44	3.50E-01		

Probe name	Systematic name	Gene name	*p*-value	adj. *p*-value	Ave Expr	log_2FC	1)	confirmed via qRT-PCR
A_23_P200792	NM_024408	NOTCH2	0.00	0.08	11.78	5.62E-01	#	yes
A_24_P83544	NP239768	NP239768	0.00	0.22	10.51	-4.79E-01		
A_33_P3209497	NP511207	NP511207	0.02	0.46	8.31	4.46E-01		
A_33_P3261869	NM_182795	NPM2	0.00	0.25	8.74	-4.10E-01	#	
A_23_P124905	NM_002522	NPTX1	0.00	0.01	8.39	-1.00E+00		
A_33_P3237775	NM_005693	NR1H3	0.00	0.25	9.63	-4.43E-01		
A_33_P3403117	NM_005654	NR2F1	0.01	0.30	8.01	-3.92E-01		
A_24_P238333	NM_014886	NSA2	0.02	0.47	12.78	-3.18E-01	#	
A_23_P1199	NM_014142	NUDT5	0.01	0.36	11.77	-3.60E-01		
A_33_P3402489	NM_006187	OAS3	0.02	0.46	7.26	-4.40E-01	#	
A_23_P121702	NM_001014446	OCIAD2	0.01	0.34	12.36	-4.05E-01		
A_33_P3376090	NM_001004452	OR1J4	0.00	0.25	6.8	-4.15E-01		
A_33_P3243118	NM_001004704	OR4C6	0.02	0.47	5.74	4.01E-01		
A_24_P302574	NM_022353	OSGEPL1	0.00	0.13	9.46	-5.51E-01		
A_23_P254852	NM_194248	OTOF	0.00	0.11	10.98	5.14E-01		
A_33_P3326647	AK128214	OTOG	0.00	0.18	5.28	-4.77E-01	#	
A_23_P403284	NM_014562	OTX1	0.00	0.19	12.44	-4.51E-01	#	
A_33_P3214481	NM_001142595	P4HA1	0.02	0.44	9.79	-4.13E-01		
A_23_P30363	NM_004199	P4HA2	0.01	0.38	8.62	-4.06E-01	#	
A_33_P3252043	NM_000918	P4HB	0.01	0.35	17.62	-3.58E-01	#	
A_23_P82693	NM_002568	PABPC1	0.01	0.41	16.46	-3.28E-01		
A_33_P3271105	NM_001135654	PABPC4	0.01	0.37	8.45	-3.52E-01	#	
A_32_P123514	NM_001114734	PABPC4L	0.02	0.46	8.77	-3.11E-01		
A_23_P258088	NM_020804	PACSIN1	0.00	0.20	6.54	-4.59E-01		
A_24_P77681	NM_006451	PAIP1	0.01	0.38	10.87	-4.17E-01	#	
A_33_P3384287	NM_002579	PALM	0.00	0.17	10.54	-4.69E-01		
A_32_P133244	NM_002582	PARN	0.02	0.44	10.71	-3.50E-01		
A_32_P144342	NM_006437	PARP4	0.02	0.42	8.68	-3.25E-01	#	
A_23_P121898	NM_024615	PARP8	0.00	0.07	11.73	-6.27E-01		
A_23_P71821	NM_006195	PBX3	0.00	0.14	11.51	-5.13E-01	*	
A_33_P3348887	NM_006195	PBX3	0.00	0.18	10.87	-4.83E-01	*	
A_32_P137980	NM_032973	PCDH11Y	0.01	0.33	5.41	-3.72E-01	*	
A_23_P57709	NM_013363	PCOLCE2	0.02	0.44	11.3	3.26E-01		
A_24_P14731	NM_013271	PCSK1N	0.01	0.34	10.87	-4.80E-01		
A_33_P3394809	NM_002861	PCYT2	0.01	0.39	10.99	-3.46E-01	#	
A_24_P339611	NM_004708	PDCD5	0.00	0.07	12.56	-8.18E-01	*	
A_32_P22338	NM_013374	PDCD6IP	0.00	0.16	11.33	-4.63E-01	#	
A_33_P3389653	NM_001165899	PDE4D	0.01	0.38	9.25	-3.44E-01	#	
A_33_P3326992	NM_014644	PDE4DIP	0.00	0.10	6.96	7.20E-01	*	
A_23_P200801	NM_001002811	PDE4DIP	0.00	0.15	7.53	6.25E-01	*	
A_33_P3323803	NM_014644	PDE4DIP	0.00	0.24	7.49	6.68E-01	*	
A_33_P3272090	NM_014644	PDE4DIP	0.01	0.29	6.43	5.71E-01	*	
A_33_P3286774	AK024906	PDE4DIP	0.02	0.43	6.03	4.23E-01	*	
A_33_P3308223	NM_014644	PDE4DIP	0.02	0.45	5.74	3.35E-01	*	
A_23_P64913	NM_006205	PDE6H	0.01	0.32	6.19	4.24E-01		
A_24_P243749	NM_002612	PDK4	0.00	0.25	6.8	4.82E-01		
A_24_P279870	NM_024411	PDYN	0.02	0.44	6.18	-3.75E-01		
A_33_P3424057	NM_006210	PEG3	0.01	0.29	5.98	-3.92E-01	#	
A_23_P65532	NM_021255	PELI2	0.01	0.40	10.06	3.62E-01		
A_23_P213908	NM_032177	PHAX	0.00	0.22	11.22	-4.91E-01		
A_24_P915692	NM_007350	PHLDA1	0.01	0.35	6.22	3.95E-01		
A_33_P3311083	BC070094	PHLDB3	0.02	0.47	6.27	7.55E-01	#	

Probe name	Systematic name	Gene name	*p*-value	adj. *p*-value	Ave Expr	log_2FC	1)	confirmed via qRT-PCR
A_23_P34307	NM_005482	PIGK	0.01	0.41	10.49	-3.74E-01	#	
A_23_P143484	NM_153681	PIGP	0.01	0.41	10.83	-3.88E-01		
A_23_P66543	NM_014308	PIK3R5	0.02	0.48	6.85	3.02E-01		
A_33_P3235987	NM_006223	PIN4	0.01	0.38	10.39	-3.95E-01	#	
A_33_P3235262	NM_001135219	PIP5KL1	0.01	0.36	9.31	-3.56E-01		
A_23_P84189	NM_181671	PITPNC1	0.01	0.39	7.63	3.57E-01		
A_33_P3240328	NM_002653	PITX1	0.01	0.32	8.69	-3.79E-01	#	
A_33_P3317628	NM_007183	PKP3	0.02	0.46	5.71	3.09E-01		
A_33_P3241316	NM_213600	PLA2G4F	0.02	0.46	5.49	3.44E-01	#	
A_33_P3306146	NM_001145031	PLAU	0.02	0.45	9.29	3.17E-01	*	
A_23_P24104	NM_002658	PLAU	0.01	0.34	12.63	4.05E-01		
A_23_P254801	NM_002660	PLCG1	0.01	0.41	7.95	-3.38E-01		
A_33_P3254946	NM_024927	PLEKHH3	0.01	0.40	11.27	-3.77E-01		
A_23_P30254	NM_006622	PLK2	0.02	0.45	9.29	3.59E-01		
A_33_P3413048	NM_017514	PLXNA3	0.00	0.27	9.68	-4.12E-01		
A_33_P3339103	NM_203290	POLR1C	0.00	0.23	11.71	-4.82E-01	#	
A_33_P3237784	NM_203473	PORCN	0.02	0.44	9.03	3.19E-01		
A_33_P3882624	NM_015450	POT1	0.00	0.01	8.6	-9.39E-01		
A_23_P373724	NM_003622	PPFIBP1	0.01	0.34	8.81	-4.30E-01	#	
A_24_P203226	NM_178230	PPIAL4A	0.02	0.46	15.82	-3.76E-01	*	
A_24_P304723	NM_000942	PPIB	0.00	0.26	13.55	-4.00E-01		
A_23_P422724	NM_000943	PPIC	0.01	0.37	10.36	-4.02E-01		
A_23_P213661	NM_015216	PPIP5K2	0.02	0.43	11.02	-3.24E-01		
A_32_P150030	NM_003620	PPM1D	0.02	0.43	10.16	-3.22E-01	#	
A_23_P35414	NM_005398	PPP1R3C	0.01	0.32	7.47	-4.59E-01		
A_33_P3397399	AK301582	PPP3CB	0.01	0.34	8.38	-3.84E-01	#	
A_33_P3214293	NM_000945	PPP3R1	0.02	0.45	8.31	-6.27E-01	#	
A_23_P356330	NM_015704	PPPDE2	0.02	0.42	8.44	-4.64E-01		
A_33_P3388491	NM_001040125	PQLC2	0.01	0.32	18.36	-6.14E-01		
A_23_P114232	NM_006406	PRDX4	0.00	0.20	14.77	-4.82E-01		
A_23_P413641	NM_020820	PREX1	0.02	0.46	12.9	3.15E-01		
A_23_P44139	NM_000947	PRIM2	0.02	0.46	11.38	-5.05E-01	#	
A_24_P916496	NM_002737	PRKCA	0.01	0.39	12.34	4.48E-01		
A_23_P250564	NM_005400	PRKCE	0.00	0.08	8	5.87E-01		
A_23_P205567	NM_006255	PRKCH	0.00	0.27	6.66	-4.35E-01		
A_23_P1374	NM_006257	PRKCQ	0.00	0.21	7.07	-4.42E-01		
A_24_P165656	NM_005813	PRKD3	0.00	0.19	9.26	-4.64E-01		
A_24_P671164	NM_000949	PRLR	0.00	0.07	7.39	6.41E-01	*	
A_23_P167468	NM_000949	PRLR	0.00	0.10	6.96	6.16E-01	*	
A_33_P3416757	NM_000949	PRLR	0.01	0.32	6.23	5.01E-01	*	
A_33_P3379922	NM_000312	PROC	0.01	0.28	6.3	3.91E-01	#	
A_33_P3403102	NM_175922	PRR18	0.01	0.29	6.38	-3.89E-01	#	
A_23_P121637	NM_003619	PRSS12	0.00	0.05	11.42	-7.21E-01		
A_23_P102864	NM_002772	PRSS7	0.00	0.08	5.67	6.12E-01		
A_33_P3298775	NM_214710	PRSSL1	0.00	0.25	14.38	-8.20E-01		
A_23_P142345	NM_002777	PRTN3	0.02	0.43	15.61	-3.37E-01		
A_23_P259692	NM_058179	PSAT1	0.01	0.41	11.13	-7.66E-01		
A_24_P48587	NM_172341	PSENEN	0.01	0.34	11.82	-3.60E-01		
A_32_P435367	NM_002810	PSMD4	0.02	0.47	15.05	-3.11E-01		
A_23_P48997	NM_003978	PSTPIP1	0.01	0.39	10.63	3.74E-01		
A_24_P102821	NM_000952	PTAFR	0.00	0.04	8.1	6.98E-01	#	
A_33_P3229918	NM_138296	PTCRA	0.00	0.21	8.51	4.31E-01		

Probe name	Systematic name	Gene name	*p*-value	adj. *p*-value	Ave Expr	log_2FC	1)	confirmed via qRT-PCR
A_33_P3298159	NM_000954	PTGDS	0.02	0.46	12.58	-3.51E-01	#	
A_23_P148047	NM_000958	PTGER4	0.02	0.43	13.3	4.59E-01		
A_33_P3346403	NM_001099285	PTMA	0.01	0.31	16.62	-3.76E-01	#	
A_23_P161352	NM_014241	PTPLA	0.00	0.16	10.31	-4.86E-01	*	
A_33_P3235410	BC027709	PTPLA	0.01	0.30	7.37	-3.80E-01	*	
A_23_P210015	NM_014369	PTPN18	0.01	0.33	10.83	4.11E-01	*	
A_33_P3309468	NM_002850	PTPRS	0.01	0.30	10.51	-4.02E-01	#	
A_23_P121064	NM_002852	PTX3	0.01	0.34	6.6	-3.67E-01		
A_23_P130194	NM_006907	PYCR1	0.01	0.37	13.63	-3.47E-01	*	
A_33_P3271930	NM_153824	PYCR1	0.02	0.45	7.55	-3.27E-01	*	
A_23_P34233	NM_014298	QPRT	0.02	0.43	13.41	-3.91E-01		
A_23_P75800	NM_013401	RAB3IL1	0.01	0.41	5.85	-3.25E-01		
A_23_P121222	NM_020165	RAD18	0.02	0.48	8.68	-4.80E-01		
A_33_P3272390	NM_006267	RANBP2	0.00	0.25	9.84	-4.47E-01	#	
A_23_P3371	NM_002891	RASGRF1	0.02	0.45	6.3	-3.27E-01	#	
A_23_P166400	NM_001007279	RASL10A	0.00	0.14	8.61	-5.72E-01		
A_33_P3232562	NM_005610	RBBP4	0.02	0.45	10.44	-3.64E-01	#	
A_33_P3240702	NM_002894	RBBP8	0.02	0.43	10.65	-4.53E-01		
A_23_P132910	NM_019027	RBM47	0.01	0.40	9.15	4.26E-01	#	
A_33_P3382648	NM_001006121	RBMY1B	0.00	0.15	5.59	5.49E-01	#	
A_23_P75283	NM_006744	RBP4	0.02	0.46	5.96	-3.16E-01		
A_23_P67339	NM_020650	RCN3	0.02	0.46	8.55	3.43E-01		
A_23_P203023	NM_002906	RDX	0.02	0.44	9.84	-3.30E-01	#	
A_23_P83028	NM_021111	RECK	0.01	0.38	10.32	3.76E-01	#	
A_23_P19182	NM_016606	REEP2	0.02	0.47	7.57	-3.54E-01		
A_33_P3262789	NM_138393	REEP6	0.01	0.40	9.23	-3.68E-01	#	
A_33_P3312682	NM_020695	REXO1	0.02	0.47	13.78	3.19E-01		
A_24_P20032	NM_000449	RFX5	0.00	0.26	12.48	-4.04E-01	#	
A_23_P320578	NM_002928	RGS16	0.00	0.21	10.08	-5.35E-01	*	
A_23_P217845	NM_002928	RGS16	0.01	0.35	7.77	-3.93E-01	*	
A_23_P302550	NM_130782	RGS18	0.02	0.48	10.99	3.54E-01		
A_23_P46045	NM_003617	RGS5	0.00	0.14	6.25	-5.20E-01	#	
A_23_P26468	NM_003961	RHBDL1	0.01	0.30	11.19	-1.13E+00		
A_23_P58132	NM_004310	RHOH	0.02	0.45	5.43	3.29E-01		
A_23_P73667	NM_001031745	RIBC1	0.02	0.45	6.75	-3.09E-01	#	
A_24_P305570	NM_018993	RIN2	0.02	0.46	6.79	3.97E-01		
A_23_P151820	NM_024832	RIN3	0.01	0.36	7.98	4.12E-01		
A_24_P8088	NM_153005	RIOK1	0.02	0.48	10.45	-3.29E-01		
A_23_P385500	NM_178841	RNF166	0.02	0.48	7.48	-3.79E-01		
A_24_P333019	NM_007219	RNF24	0.00	0.19	9.86	4.51E-01		
A_24_P415601	NM_002939	RNH1	0.01	0.40	13	3.44E-01		
A_24_P48408	NM_003799	RNMT	0.02	0.46	8.69	-3.48E-01	*	
A_33_P3258091	NM_020216	RNPEP	0.02	0.46	13.53	-3.15E-01		
A_23_P100499	NM_024589	ROGDI	0.01	0.28	8.94	4.11E-01		
A_33_P3298535	NM_080748	ROMO1	0.01	0.30	15.14	-3.83E-01	*	
A_23_P143414	NM_080748	ROMO1	0.02	0.46	14.41	-3.41E-01	*	
A_23_P121885	NM_031916	ROPN1L	0.00	0.23	7.18	-4.50E-01		
A_23_P158318	NM_004560	ROR2	0.00	0.06	5.98	8.05E-01	#	
A_32_P42725	XR_040330	RP11-403I13.9	0.00	0.25	7.3	-4.99E-01	#	
A_23_P90143	NM_012423	RPL13A	0.01	0.39	17.99	-3.43E-01	*	
A_32_P118258	NM_000982	RPL21	0.01	0.30	17.96	-3.83E-01	*	
A_23_P26713	NM_000978	RPL23	0.01	0.39	18	-3.33E-01	#	

Probe name	Systematic name	Gene name	*p*-value	adj. *p*-value	Ave Expr	log_2FC	1)	confirmed via qRT-PCR
A_33_P3382560	NM_000984	RPL23A	0.01	0.35	15.62	-1.09E+00	#	
A_33_P3295066	NR_026673	RPL23P8	0.01	0.38	16.9	-3.54E-01		
A_33_P3299319	NM_001136137	RPL28	0.02	0.45	7.31	3.11E-01	#	
A_24_P7085	NR_002778	RPL29P2	0.01	0.41	14.07	-4.45E-01		
A_23_P7221	NM_033625	RPL34	0.00	0.17	17.01	-4.61E-01	#	
A_23_P44956	NM_000996	RPL35A	0.02	0.46	18	-3.10E-01		
A_23_P142724	NM_000998	RPL37A	0.02	0.46	17.99	-3.29E-01	#	
A_32_P225604	NM_000969	RPL5	0.00	0.22	17.58	-4.36E-01	*	
A_33_P3246163	NM_000969	RPL5	0.01	0.41	17.92	-3.35E-01	*	
A_24_P63262	NM_002950	RPN1	0.01	0.39	11.9	-3.68E-01		
A_32_P3476	NM_203400	RPRML	0.01	0.32	5.69	-3.75E-01	#	
A_32_P14894	NM_001014	RPS10	0.02	0.45	17.19	-3.41E-01	#	
A_32_P14744	NM_001019	RPS15A	0.01	0.29	16.99	-3.84E-01	#	
A_23_P47357	NM_001028	RPS25	0.02	0.45	17.56	-3.32E-01		
A_23_P116694	NM_001029	RPS26	0.00	0.05	16.8	-8.48E-01	#	
A_23_P157196	NR_026676	RPS2P32	0.00	0.27	16.13	-7.42E-01	#	
A_23_P35791	NM_003942	RPS6KA4	0.02	0.46	10.48	3.10E-01		
A_24_P465772	NR_026825	RPSAP52	0.02	0.43	14.77	-3.26E-01		
A_23_P133691	NM_021244	RRAGD	0.01	0.28	10.51	4.15E-01		
A_23_P54605	NM_015659	RSL1D1	0.02	0.46	12.13	-3.16E-01	#	
A_24_P203502	XM_001714653	RSL24D1P11	0.01	0.29	9.34	-3.90E-01		
A_23_P102950	NM_080860	RSPH1	0.01	0.41	6.06	-4.01E-01		
A_33_P3390335	NM_012425	RSU1	0.01	0.39	10.83	-3.78E-01	#	
A_33_P3362371	NM_201430	RTN3	0.02	0.47	8.36	-3.67E-01	#	
A_33_P3341841	NM_001004312	RTP2	0.01	0.30	5.78	4.67E-01		
A_32_P161762	NM_004348	RUNX2	0.02	0.43	6.27	4.63E-01	#	
A_23_P74001	NM_005621	S100A12	0.00	0.25	7.05	8.38E-01	*	
A_33_P3385785	NM_005621	S100A12	0.01	0.36	6.44	5.36E-01	*	
A_23_P115467	NM_002962	S100A5	0.00	0.27	7.43	5.84E-01		
A_23_P119448	NM_014931	SAPS1	0.02	0.43	8.96	-3.41E-01		
A_24_P158421	NM_020150	SAR1A	0.02	0.47	11.49	-3.79E-01	#	
A_23_P90484	NM_017827	SARS2	0.00	0.06	9.91	-7.39E-01		
A_24_P237443	NM_018990	SASH3	0.00	0.12	9.85	5.88E-01		
A_23_P259741	NM_002971	SATB1	0.02	0.45	12.63	-3.56E-01		
A_33_P3352019	NM_182826	SCARA3	0.01	0.31	5.53	4.00E-01	#	
A_33_P3417459	NR_023358	SCARNA9L	0.00	0.19	8.35	-4.71E-01		
A_33_P3228023	NM_021626	SCPEP1	0.01	0.41	8.6	3.40E-01	*	
A_23_P366366	NM_014766	SCRN1	0.02	0.47	9.38	-3.46E-01	#	
A_23_P17012	NM_024583	SCRN3	0.02	0.45	6.75	-3.32E-01	#	
A_23_P109034	NM_002999	SDC4	0.01	0.35	7.85	3.70E-01		
A_23_P208009	NM_033280	SEC11C	0.01	0.34	13.78	-4.07E-01		
A_23_P23438	NM_022367	SEMA4A	0.01	0.30	9.35	3.80E-01		
A_24_P261169	NM_006378	SEMA4D	0.01	0.37	8.03	3.86E-01	#	
A_33_P3372727	NM_003966	SEMA5A	0.00	0.10	5.99	5.69E-01		
A_33_P3284919	NM_030913	SEMA6C	0.01	0.34	8.17	-3.81E-01	#	
A_33_P3376644	NM_015571	SENP6	0.00	0.25	8.84	4.93E-01	*	
A_33_P3386429	NM_015571	SENP6	0.01	0.33	7.24	4.84E-01	*	
A_23_P121926	NM_005410	SEPP1	0.02	0.43	5.59	-3.30E-01		
A_33_P3329686	NM_002688	SEPT5	0.02	0.41	8.2	-3.50E-01	#	
A_23_P218111	NM_001002236	SERPINA1	0.02	0.42	7.29	3.41E-01	#	
A_23_P313981	NM_005024	SERPINB10	0.00	0.12	7.36	5.05E-01		
A_24_P245379	NM_002575	SERPINB2	0.00	0.01	9.14	8.16E-01		

Probe name	Systematic name	Gene name	*p*-value	adj. *p*-value	Ave Expr	log_2FC	1)	confirmed via qRT-PCR
A_24_P147461	NM_001031848	SERPINB8	0.00	0.07	10.15	6.67E-01		
A_23_P35082	NM_031459	SESN2	0.02	0.47	7.96	3.11E-01		
A_32_P456318	NM_080743	SFRS13B	0.01	0.39	7.96	-3.95E-01		
A_33_P3305840	NM_001031684	SFRS7	0.02	0.45	13.99	-3.28E-01	#	
A_24_P333857	NM_032291	SGIP1	0.01	0.39	6.25	-3.62E-01	*	
A_23_P19673	NM_005627	SGK1	0.00	0.01	8.39	1.10E+00		
A_32_P163125	NM_147156	SGMS1	0.00	0.08	8.11	7.54E-01		
A_33_P3333033	AK125203	SGSM2	0.02	0.44	11.41	-3.20E-01	#	
A_24_P686965	NM_001103161	SH2D5	0.00	0.10	7.27	6.23E-01		
A_32_P205624	NM_012435	SHC2	0.00	0.24	6.29	-4.13E-01	#	
A_33_P3417339	NM_020859	SHROOM3	0.02	0.48	5.54	-3.47E-01	#	
A_33_P3382498	NM_001098612	SIGLEC14	0.02	0.48	9.15	3.54E-01	#	
A_33_P3211734	NM_001102396	SIKE1	0.00	0.24	12.45	-4.34E-01	*	
A_33_P3383261	NM_001102396	SIKE1	0.01	0.35	12.68	-3.62E-01	*	
A_24_P937855	NM_001102396	SIKE1	0.01	0.39	9.01	-3.53E-01	*	
A_23_P216340	NM_001045556	SLA	0.00	0.16	11.34	4.67E-01		
A_24_P13311	NM_145648	SLC15A4	0.01	0.39	9.89	3.51E-01	*	
A_33_P3481987	NM_213606	SLC16A12	0.00	0.14	17.67	-4.82E-01		
A_23_P118741	NM_201566	SLC16A13	0.02	0.47	5.64	3.20E-01		
A_23_P137097	NM_006517	SLC16A2	0.00	0.13	7.63	-6.48E-01		
A_23_P93213	NM_153320	SLC22A7	0.02	0.42	5.63	3.45E-01	#	
A_23_P25204	NM_213611	SLC25A3	0.01	0.32	17.02	-4.17E-01		
A_23_P408455	NM_001104647	SLC25A36	0.02	0.45	11.12	-3.21E-01	#	
A_24_P64100	AF495725	SLC25A37	0.02	0.43	11.1	3.17E-01	#	
A_33_P3281537	ENST00000271857	SLC27A3	0.01	0.32	5.59	5.17E-01	#	
A_33_P3251108	NM_004733	SLC33A1	0.02	0.46	8.47	-5.17E-01		
A_33_P3261737	NM_005660	SLC35A2	0.00	0.17	7.98	-5.13E-01	*	
A_23_P69840	NM_080670	SLC35A4	0.02	0.45	10.17	3.23E-01	#	
A_33_P3369799	NM_001008783	SLC35D3	0.02	0.47	7.28	-3.42E-01		
A_23_P413888	NM_001029858	SLC35F1	0.01	0.32	7.99	-4.08E-01	#	
A_33_P3474319	NM_198277	SLC37A2	0.00	0.22	6.56	5.82E-01	#	
A_24_P382467	NM_144564	SLC39A3	0.01	0.38	10.51	-3.56E-01		
A_24_P46093	NM_003043	SLC6A6	0.01	0.41	11.31	3.50E-01	#	
A_32_P147078	NM_021097	SLC8A1	0.00	0.01	6.79	1.15E+00	#	
A_24_P136866	NM_021097	SLC8A1	0.01	0.30	5.7	4.27E-01	#	
A_33_P3319542	NM_015063	SLC8A2	0.02	0.46	5.27	-3.07E-01		
A_23_P389141	NM_144990	SLFNL1	0.02	0.45	6.72	-3.30E-01		
A_23_P48936	NM_005902	SMAD3	0.02	0.46	10.8	3.16E-01		
A_23_P70818	NM_005631	SMO	0.02	0.48	8.36	-3.41E-01		
A_23_P163567	NM_018667	SMPD3	0.02	0.43	8.61	-3.79E-01		
A_23_P72117	NM_006714	SMPDL3A	0.00	0.12	6	5.05E-01		
A_24_P83922	NM_003093	SNRPC	0.00	0.25	8.78	-4.76E-01	#	
A_33_P3320152	NM_003094	SNRPE	0.00	0.24	12.04	-4.53E-01	*	
A_33_P3265355	NM_003094	SNRPE	0.01	0.38	13.74	-3.56E-01	*	
A_24_P347624	NM_022804	SNURF	0.01	0.33	12.82	-3.77E-01		
A_23_P154585	NM_001042633	SNX21	0.01	0.41	7.3	3.48E-01	#	
A_23_P128215	NM_003877	SOCS2	0.00	0.03	12.73	-1.07E+00		yes
A_23_P207058	NM_003955	SOCS3	0.00	0.14	7.32	5.27E-01		
A_23_P77103	NM_003104	SORD	0.02	0.46	10.74	-3.30E-01	#	
A_23_P87049	NM_003105	SORL1	0.00	0.07	12.21	5.93E-01		
A_23_P85703	NM_005686	SOX13	0.02	0.45	6.37	3.43E-01	#	
A_24_P911676	NM_003107	SOX4	0.00	0.04	8.25	-8.40E-01		

Probe name	Systematic name	Gene name	*p*-value	adj. *p*-value	Ave Expr	log_2FC	1)	confirmed via qRT-PCR
A_33_P3383184	ENST00000394967	SP9	0.00	0.00	6.67	-1.19E+00	#	
A_33_P3382924	NM_003118	SPARC	0.01	0.39	9.23	-3.68E-01		
A_33_P3299000	NM_031952	SPATA9	0.01	0.29	6.28	-4.65E-01	#	
A_33_P3332666	NM_020126	SPHK2	0.01	0.36	7	3.67E-01	#	
A_23_P49060	NM_181642	SPINT1	0.02	0.43	8.35	3.32E-01		
A_23_P27795	NM_021102	SPINT2	0.00	0.13	11.11	-5.09E-01		
A_24_P551028	NM_001001664	SPOPL	0.02	0.46	9.73	3.20E-01		
A_23_P7313	NM_001040058	SPP1	0.01	0.32	5.37	3.81E-01		
A_24_P388810	NM_003135	SRP19	0.01	0.35	10.83	-3.59E-01		
A_23_P136978	NM_014467	SRPX2	0.02	0.47	5.67	-3.91E-01		
A_23_P102060	NM_006751	SSFA2	0.01	0.41	11.95	4.32E-01		
A_23_P250800	NM_006100	ST3GAL6	0.01	0.35	10.89	3.69E-01		
A_33_P3380751	NM_003034	ST8SIA1	0.00	0.15	6.96	-6.10E-01	#	
A_33_P3291484	NM_005668	ST8SIA4	0.01	0.32	9.26	4.04E-01	#	
A_33_P3364696	NM_213622	STAMBP	0.01	0.29	9.87	-4.92E-01		
A_33_P3382147	AY082592	STARD13	0.02	0.42	10.26	3.52E-01	#	
A_23_P344481	NM_152709	STOX1	0.02	0.47	7.05	-3.12E-01	#	
A_24_P163237	NM_020225	STOX2	0.01	0.38	9.43	3.52E-01		
A_24_P203308	NM_182489	STRA8	0.00	0.19	6.55	-5.45E-01		
A_23_P104734	NM_152713	STT3A	0.02	0.45	10.99	-4.14E-01		
A_23_P156788	NM_003764	STX11	0.01	0.34	8.16	3.66E-01		
A_23_P154605	NM_018837	SULF2	0.00	0.11	8.32	6.60E-01		yes
A_23_P106773	NM_177528	SULT1A2	0.00	0.10	9.84	-6.73E-01		
A_32_P223189	NR_002190	SUMO1P3	0.01	0.37	9.49	-3.67E-01		
A_24_P89971	NM_033161	SURF4	0.01	0.38	12.1	-3.44E-01	#	
A_33_P3370461	NR_024187	SUZ12P	0.00	0.08	16.4	-7.61E-01	#	
A_23_P722	NM_003176	SYCP1	0.00	0.01	10.41	-9.74E-01		
A_23_P210675	NM_014258	SYCP2	0.00	0.25	6.92	5.48E-01		
A_23_P9255	NM_003177	SYK	0.01	0.39	12.53	3.34E-01		
A_33_P3324839	NM_006772	SYNGAP1	0.01	0.33	5.89	4.52E-01	#	
A_33_P3284404	NM_145731	SYNGR1	0.01	0.40	11.55	-3.41E-01	*	
A_33_P3397658	ENST00000394243	SYNPO	0.00	0.07	6.7	-6.15E-01	*	
A_23_P344531	NM_007286	SYNPO	0.00	0.14	7.23	-4.89E-01	*	
A_33_P3390868	NM_133477	SYNPO2	0.00	0.08	10.15	-8.07E-01	#	
A_33_P3237201	NM_001135805	SYT1	0.01	0.41	5.42	4.16E-01	#	
A_33_P3214899	NM_001136504	SYT2	0.01	0.41	5.59	3.39E-01	*	
A_33_P3286973	ENST00000339381	TAS1R3	0.00	0.00	9.8	-2.01E+00	#	
A_24_P330633	NM_000353	TAT	0.01	0.38	6.42	4.57E-01		
A_33_P3216292	NM_018421	TBC1D2	0.01	0.41	11.2	3.91E-01		
A_24_P168994	NM_178571	TBC1D26	0.01	0.39	6.63	-3.50E-01		
A_33_P3327539	NM_015130	TBC1D9	0.01	0.34	7.03	3.81E-01	#	
A_23_P90357	NM_001060	TBXA2R	0.01	0.38	9.24	-3.74E-01	#	
A_33_P3325808	XM_001723171	tcag7.1058	0.02	0.44	7.46	-3.47E-01		
A_23_P147641	NM_003195	TCEA2	0.02	0.43	8.57	3.20E-01	#	
A_23_P34375	NM_003196	TCEA3	0.00	0.23	5.53	4.55E-01		
A_32_P18470	NM_001012979	TCEAL5	0.01	0.40	9.59	-3.57E-01		
A_32_P192545	NM_001006938	TCEAL6	0.01	0.39	10.4	-3.47E-01	#	
A_23_P254816	NM_004609	TCF15	0.01	0.38	10.99	3.81E-01		
A_33_P3381684	NM_007113	TCHH	0.01	0.27	5.73	-4.08E-01	*	
A_32_P98072	NM_007113	TCHH	0.02	0.43	8.17	-4.92E-01	*	
A_23_P40611	NM_000355	TCN2	0.02	0.44	5.6	-3.63E-01		
A_32_P38283	NM_174910	TCTE3	0.01	0.39	6.78	-4.44E-01		

Probe name	Systematic name	Gene name	*p*-value	adj. *p*-value	Ave Expr	log_2FC	1)	confirmed via qRT-PCR
A_33_P3404779	NM_001013632	TCTEX1D4	0.00	0.19	6.15	4.49E-01	*	
A_23_P82000	NM_003214	TEAD3	0.01	0.34	8.38	-5.00E-01		
A_23_P112412	NM_017746	TEX10	0.01	0.38	11.33	-3.43E-01		
A_23_P10518	NM_016521	TFDP3	0.00	0.08	7.74	-7.50E-01		
A_33_P3398634	NM_007162	TFEB	0.01	0.32	11.48	-4.09E-01	#	
A_24_P345822	NM_006070	TFG	0.02	0.44	11.96	-3.46E-01		
A_33_P3331451	NM_004612	TGFBR1	0.00	0.23	9.38	4.52E-01		yes
A_33_P3320112	THC2471881	THC2471881	0.00	0.05	5.47	6.50E-01		
A_33_P3337931	THC2502236	THC2502236	0.00	0.17	8.9	4.66E-01		
A_33_P3371305	THC2507457	THC2507457	0.02	0.42	5.52	3.31E-01		
A_33_P3372161	THC2507627	THC2507627	0.01	0.29	15.99	-3.94E-01		
A_33_P3273424	THC2516883	THC2516883	0.01	0.41	5.48	3.56E-01		
A_33_P3375002	THC2518870	THC2518870	0.00	0.02	8.6	-9.00E-01		
A_33_P3235454	THC2542270	THC2542270	0.00	0.00	8.04	-1.68E+00		
A_24_P127312	THC2554858	THC2554858	0.01	0.37	12.87	-4.00E-01		
A_33_P3292130	THC2566648	THC2566648	0.02	0.43	12.08	6.11E-01		
A_33_P3322046	THC2596076	THC2596076	0.00	0.22	6.91	-7.67E-01		
A_33_P3255782	THC2600290	THC2600290	0.02	0.43	16.96	-3.32E-01		
A_33_P3230493	THC2727687	THC2727687	0.00	0.23	5.43	5.17E-01		
A_33_P3325384	THC2752493	THC2752493	0.00	0.14	7.33	-5.18E-01		
A_23_P149375	NM_053055	THEM4	0.00	0.18	9.41	-5.05E-01	#	
A_24_P400324	NM_015204	THSD7A	0.01	0.33	10.28	-4.62E-01		
A_23_P208937	NM_024760	TLE6	0.02	0.46	6.1	3.27E-01	*	
A_24_P193498	NM_078474	TM2D3	0.01	0.41	8.91	-3.38E-01		
A_23_P116037	NM_003273	TM7SF2	0.01	0.38	9.36	-3.45E-01		
A_23_P204702	NM_003217	TMBIM6	0.02	0.48	13.97	-2.96E-01	#	
A_23_P346093	NM_152468	TMC8	0.02	0.45	9.09	3.19E-01	#	
A_23_P355067	NM_019026	TMCO1	0.02	0.48	12.2	-3.85E-01		
A_32_P87649	NM_001008740	TMCO2	0.00	0.18	6.74	-4.84E-01		
A_23_P26173	NM_007364	TMED3	0.01	0.33	13	-3.74E-01		
A_32_P123088	NM_001164468	TMED7-TICAM2	0.02	0.45	8.4	-3.10E-01	#	
A_33_P3282566	NM_017728	TMEM104	0.00	0.23	10.75	-4.32E-01	#	
A_24_P119131	NM_001080825	TMEM120B	0.01	0.34	7.42	-4.03E-01	#	
A_23_P13524	NM_032273	TMEM126A	0.02	0.45	12.71	-3.14E-01		
A_24_P161959	NM_199337	TMEM179B	0.00	0.20	10.17	-4.83E-01		
A_23_P255601	NM_032508	TMEM185A	0.02	0.46	9.14	-3.09E-01		
A_32_P40288	NM_052913	TMEM200A	0.01	0.37	5.37	-4.08E-01		
A_24_P371281	NM_025246	TMEM22	0.01	0.38	6.25	-4.95E-01		
A_33_P3230219	NM_033504	TMEM54	0.00	0.12	9.93	-5.23E-01		
A_24_P100673	NM_016454	TMEM85	0.01	0.30	13.31	-4.10E-01	*	
A_23_P114952	NM_016456	TMEM9	0.02	0.48	9.67	-3.19E-01		
A_24_P307289	NM_198154	TMEM95	0.01	0.31	9.14	-4.19E-01		
A_23_P68106	NM_021103	TMSB10	0.02	0.47	13.81	-3.26E-01		
A_24_P374516	NM_021109	TMSB4X	0.02	0.46	15.25	3.26E-01		
A_32_P2452	NM_175861	TMTC1	0.01	0.36	8.67	3.62E-01	#	
A_23_P104942	NM_015959	TMX2	0.01	0.39	11.69	-4.41E-01		
A_23_P139722	NM_001065	TNFRSF1A	0.00	0.27	11.12	-4.64E-01		
A_23_P30666	NM_014452	TNFRSF21	0.01	0.35	10.7	3.93E-01		
A_33_P3397865	NM_003283	TNNT1	0.01	0.28	11.2	3.97E-01		
A_33_P3321711	NM_006809	TOMM34	0.00	0.09	9.98	-5.78E-01	#	
A_24_P15754	NM_006114	TOMM40	0.02	0.45	10.42	-3.23E-01	#	
A_23_P336644	NM_145034	TOR1AIP2	0.01	0.36	8.84	-3.48E-01	#	

Probe name	Systematic name	Gene name	*p*-value	adj. *p*-value	Ave Expr	log_2FC	1)	confirmed via qRT-PCR
A_24_P327050	NM_016209	TRAPPC2L	0.02	0.44	12.55	-3.19E-01		
A_33_P3319905	AK292162	TREM1	0.02	0.46	6.08	3.04E-01	#	
A_33_P3424367	NM_033219	TRIM14	0.02	0.46	8.41	3.07E-01	#	
A_23_P402778	NM_138700	TRIM40	0.00	0.24	5.56	4.37E-01		
A_23_P425880	NM_007118	TRIO	0.00	0.13	6.61	5.30E-01	*	
A_33_P3415500	ENST00000344204	TRIO	0.00	0.25	7.17	5.06E-01	*	
A_23_P71170	NM_018646	TRPV6	0.01	0.31	5.67	3.92E-01	#	
A_23_P17103	NM_025244	TSGA10	0.01	0.39	7.02	1.03E+00	#	
A_23_P215070	NM_018718	TSGA14	0.01	0.38	8.75	-3.94E-01		
A_23_P361014	NM_020856	TSHZ3	0.00	0.05	7.7	7.27E-01		
A_23_P160167	NM_005727	TSPAN1	0.02	0.46	6.85	-3.18E-01		
A_24_P135483	NM_030927	TSPAN14	0.00	0.24	8.57	4.16E-01	*	yes
A_23_P171143	NM_003270	TSPAN6	0.01	0.34	8.06	-3.76E-01		
A_23_P254031	NM_007344	TTF1	0.01	0.33	9.61	-3.98E-01	#	
A_33_P3385993	NM_001008409	TTLL9	0.01	0.41	6.18	3.99E-01	#	
A_23_P11397	NR_001537	TTTY13	0.00	0.24	6.41	-4.24E-01		
A_23_P113656	NM_006087	TUBB4	0.00	0.18	6.06	4.87E-01		
A_23_P127150	NM_006659	TUBGCP2	0.02	0.47	11.43	-3.17E-01		
A_23_P3450	NM_014444	TUBGCP4	0.02	0.42	9.59	-3.36E-01		
A_23_P434398	NM_153235	TXLNB	0.00	0.23	6.36	-5.42E-01		
A_23_P200199	NM_015913	TXNDC12	0.01	0.29	12.22	-4.78E-01		
A_33_P3209386	NM_032731	TXNDC17	0.02	0.46	8.41	-3.61E-01		
A_23_P259611	NM_016616	TXNDC3	0.02	0.47	10.13	5.38E-01		
A_23_P97700	NM_006472	TXNIP	0.02	0.45	13.39	3.53E-01		
A_23_P141917	NM_003331	TYK2	0.02	0.45	8.66	3.11E-01		
A_23_P123866	NM_016525	UBAP1	0.02	0.47	9.87	-3.21E-01		
A_33_P3310989	NM_014847	UBAP2L	0.01	0.39	9.22	-3.35E-01	*	
A_24_P13032	NM_003338	UBE2D1	0.01	0.39	10.02	-3.97E-01		
A_23_P78563	NM_024292	UBL5	0.00	0.08	14.98	-6.13E-01		
A_23_P166333	NM_005659	UFD1L	0.01	0.30	12.2	-4.55E-01	#	
A_24_P313109	NM_016617	UFM1	0.02	0.48	8.13	-4.32E-01	#	
A_23_P204980	NM_020121	UGGT2	0.00	0.14	11.8	-5.01E-01	#	
A_23_P69617	NM_003728	UNC5C	0.01	0.35	6.99	-3.78E-01	#	
A_23_P171366	NM_004651	USP11	0.02	0.46	11.36	-3.10E-01	#	
A_24_P322908	NM_001145073	USP27X	0.01	0.41	6.38	3.77E-01	*	
A_23_P67829	NM_025076	UXS1	0.02	0.48	11.43	-3.05E-01		
A_23_P77000	NM_014909	VASH1	0.00	0.14	10.95	4.88E-01		yes
A_23_P115492	NM_024749	VASH2	0.01	0.32	7.24	-3.75E-01		
A_23_P400449	NM_020927	VAT1L	0.01	0.39	6.01	-3.46E-01		
A_23_P144959	NM_004385	VCAN	0.00	0.24	6.06	4.72E-01		
A_32_P33083	NM_016378	VCX2	0.02	0.44	12.13	3.28E-01	#	
A_23_P162589	NM_001017535	VDR	0.00	0.06	10.66	6.70E-01		yes
A_24_P294982	NM_016485	VTA1	0.01	0.41	10.45	-3.66E-01	*	
A_23_P42368	NM_016485	VTA1	0.02	0.48	10.08	-3.04E-01	*	
A_23_P10785	NM_145206	VTI1A	0.01	0.34	8.41	-3.70E-01		
A_33_P3395743	NM_022834	VWA1	0.00	0.01	7.92	-1.01E+00	#	
A_33_P3416668	NM_022834	VWA1	0.01	0.30	5.96	3.81E-01	#	
A_23_P52986	NM_152718	VWCE	0.01	0.36	7.67	-6.18E-01	*	
A_33_P3414487	NM_017528	WBSCR22	0.02	0.47	12.75	-3.07E-01		
A_24_P83379	NM_178583	WDFY3	0.01	0.30	10.56	-3.92E-01	#	
A_24_P389038	NM_005452	WDR46	0.02	0.46	9.58	3.14E-01		
A_23_P49021	NM_025234	WDR61	0.01	0.37	12.41	-3.61E-01		

Probe name	Systematic name	Gene name	*p*-value	adj. *p*-value	Ave Expr	log_2FC	1)	confirmed via qRT-PCR
A_23_P106617	NM_021197	WFDC1	0.00	0.05	7.11	-6.40E-01		
A_24_P769359	NM_018979	WNK1	0.00	0.08	11.74	-5.48E-01		
A_23_P102117	NM_025216	WNT10A	0.01	0.31	5.72	4.88E-01		
A_23_P34176	NM_015691	WWC3	0.01	0.38	7.72	3.85E-01		
A_23_P120845	NM_005080	XBP1	0.00	0.25	12.54	-4.05E-01		
A_23_P218793	NM_022098	XPNPEP3	0.02	0.45	7.6	-3.16E-01		
A_33_P3363515	CR610241	XRCC3	0.01	0.32	16.96	-4.72E-01	#	
A_23_P166135	NM_012255	XRN2	0.02	0.43	11.12	-3.45E-01		
A_23_P47226	NM_020470	YIF1A	0.02	0.45	13.18	-3.12E-01	#	
A_33_P3613000	NM_001105539	ZBTB10	0.02	0.47	6.93	8.13E-01		
A_23_P218807	NM_017590	ZC3H7B	0.01	0.37	9.22	-3.72E-01		
A_23_P51853	NM_032283	ZDHHC18	0.01	0.39	8.25	3.40E-01		
A_24_P374427	NM_178566	ZDHHC21	0.02	0.46	7.33	-3.04E-01	#	
A_23_P355447	NM_174976	ZDHHC22	0.00	0.26	6.21	4.71E-01	#	
A_23_P161183	NM_022494	ZDHHC6	0.01	0.34	9.44	-4.08E-01		
A_23_P99540	NM_004926	ZFP36L1	0.01	0.38	7.08	4.51E-01	*	
A_33_P3417865	NM_004926	ZFP36L1	0.02	0.43	7.14	3.45E-01	*	
A_23_P101960	NM_006887	ZFP36L2	0.00	0.12	12.73	5.53E-01		
A_33_P3222744	NM_015852	ZNF117	0.01	0.30	10.55	-4.15E-01		
A_23_P84910	NM_003446	ZNF157	0.02	0.45	8.25	-3.65E-01		
A_24_P22981	NM_021047	ZNF253	0.02	0.48	7.27	-3.49E-01		
A_32_P144908	NM_203282	ZNF254	0.02	0.46	14.25	-3.21E-01	#	
A_23_P209032	NM_018443	ZNF302	0.00	0.26	8.68	-4.22E-01		
A_33_P3343442	XR_079205	ZNF316	0.01	0.36	11.6	-3.64E-01		
A_33_P3302736	NM_001166012	ZNF397OS	0.01	0.33	6.8	-4.19E-01	#	
A_33_P3736691	NM_025189	ZNF430	0.01	0.34	8.85	-4.11E-01	#	
A_23_P101476	NM_030824	ZNF442	0.01	0.38	6.92	-3.56E-01		
A_23_P67278	NM_005815	ZNF443	0.02	0.46	7.27	-3.38E-01		
A_23_P115861	NM_145312	ZNF485	0.01	0.36	7.04	-3.60E-01		
A_24_P332862	NM_001076678	ZNF493	0.01	0.37	10.44	-5.70E-01	#	
A_23_P159027	NM_015461	ZNF521	0.00	0.03	11.22	-7.29E-01	*	yes
A_33_P3219398	NM_015461	ZNF521	0.00	0.08	9.34	-7.08E-01	*	yes
A_32_P139229	NM_213598	ZNF543	0.02	0.46	8.11	3.22E-01		
A_23_P416751	NM_173530	ZNF610	0.01	0.39	6.22	-3.73E-01		
A_24_P205036	NM_001001411	ZNF676	0.01	0.34	7.1	-3.67E-01	#	
A_32_P68148	NR_027130	ZNF738	0.01	0.40	11.24	-8.41E-01	#	
A_33_P3344816	NM_001004301	ZNF813	0.02	0.43	7.66	-3.53E-01	#	
A_24_P323967	NM_001145434	ZNF880	0.02	0.46	7.25	-3.39E-01	#	
A_24_P358619	NM_001080409	ZNF99	0.00	0.22	8.6	-4.56E-01	#	
A_24_P162373	NM_032173	ZNRF3	0.02	0.48	10.46	3.20E-01	#	
A_33_P3229276	NM_001007072	ZSCAN2	0.02	0.47	6.97	-2.99E-01	#	
A_24_P153324	A_24_P153324	A_24_P153324	0.00	0.08	13.6	-5.75E-01		
A_24_P161914	A_24_P161914	A_24_P161914	0.01	0.28	11.62	-3.94E-01		
A_24_P170395	A_24_P170395	A_24_P170395	0.01	0.39	6.19	-3.52E-01		
A_24_P187023	A_24_P187023	A_24_P187023	0.01	0.33	15.07	-4.02E-01		
A_24_P221485	A_24_P221485	A_24_P221485	0.01	0.33	6.14	-4.85E-01		
A_24_P24724	A_24_P24724	A_24_P24724	0.02	0.47	12.21	-1.10E+00		
A_24_P306964	A_24_P306964	A_24_P306964	0.02	0.42	13.23	-3.29E-01		
A_24_P307306	A_24_P307306	A_24_P307306	0.01	0.36	8.33	-3.70E-01		
A_24_P307384	A_24_P307384	A_24_P307384	0.00	0.22	8.44	-5.98E-01		
A_24_P349387	A_24_P349387	A_24_P349387	0.00	0.17	15.68	-7.06E-01		
A_24_P358305	A_24_P358305	A_24_P358305	0.01	0.30	7.54	-3.92E-01		

Probe name	Systematic name	Gene name	*p*-value	adj. *p*-value	Ave Expr	log_2FC	1)	confirmed via qRT-PCR
A_24_P374973	A_24_P374973	A_24_P374973	0.01	0.37	8.17	-5.37E-01		
A_24_P384200	A_24_P384200	A_24_P384200	0.00	0.23	8.67	-4.78E-01		
A_24_P401100	A_24_P401100	A_24_P401100	0.02	0.43	17	-3.18E-01		
A_24_P409824	A_24_P409824	A_24_P409824	0.01	0.38	7.28	-7.36E-01		
A_24_P418536	A_24_P418536	A_24_P418536	0.00	0.19	10.44	-5.49E-01		
A_24_P42014	A_24_P42014	A_24_P42014	0.00	0.13	17.02	-4.84E-01		
A_24_P662366	A_24_P662366	A_24_P662366	0.00	0.18	8.61	-4.68E-01		
A_24_P739582	A_24_P739582	A_24_P739582	0.01	0.35	6.45	-4.95E-01		
A_24_P878388	A_24_P878388	A_24_P878388	0.01	0.34	15.53	-3.62E-01		
A_24_P92267	A_24_P92267	A_24_P92267	0.02	0.42	7.15	-3.54E-01		
A_32_P212373	A_32_P212373	A_32_P212373	0.01	0.41	10.77	-3.92E-01		
A_33_P3213561	A_33_P3213561	A_33_P3213561	0.00	0.08	9.42	-7.15E-01		
A_33_P3227556	A_33_P3227556	A_33_P3227556	0.02	0.42	8.74	-3.36E-01		
A_33_P3230676	A_33_P3230676	A_33_P3230676	0.00	0.11	5.47	5.54E-01		
A_33_P3235184	A_33_P3235184	A_33_P3235184	0.00	0.15	10.81	-5.20E-01		
A_33_P3235831	A_33_P3235831	A_33_P3235831	0.01	0.32	7.7	-3.91E-01		
A_33_P3238461	A_33_P3238461	A_33_P3238461	0.02	0.45	16.01	-1.07E+00		
A_33_P3249002	A_33_P3249002	A_33_P3249002	0.00	0.27	14.05	-4.41E-01		
A_33_P3249066	A_33_P3249066	A_33_P3249066	0.01	0.38	7.69	-4.42E-01		
A_33_P3259239	A_33_P3259239	A_33_P3259239	0.01	0.30	5.46	3.99E-01		
A_33_P3263157	A_33_P3263157	A_33_P3263157	0.01	0.38	11.09	8.13E-01		
A_33_P3263629	A_33_P3263629	A_33_P3263629	0.02	0.45	5.59	3.52E-01		
A_33_P3265260	A_33_P3265260	A_33_P3265260	0.00	0.27	5.41	-4.65E-01		
A_33_P3279456	A_33_P3279456	A_33_P3279456	0.01	0.34	15.62	-1.03E+00		
A_33_P3279526	A_33_P3279526	A_33_P3279526	0.01	0.37	7.94	-3.91E-01		
A_33_P3284584	A_33_P3284584	A_33_P3284584	0.00	0.13	9.58	-6.49E-01		
A_33_P3285097	A_33_P3285097	A_33_P3285097	0.01	0.38	6.05	3.48E-01		
A_33_P3288079	A_33_P3288079	A_33_P3288079	0.02	0.41	5.69	4.36E-01		
A_33_P3298612	A_33_P3298612	A_33_P3298612	0.01	0.34	5.59	3.79E-01		
A_33_P3299436	A_33_P3299436	A_33_P3299436	0.01	0.34	17.6	-3.68E-01		
A_33_P3302657	A_33_P3302657	A_33_P3302657	0.01	0.31	6.35	3.95E-01		
A_33_P3304081	A_33_P3304081	A_33_P3304081	0.00	0.26	9.32	-4.14E-01		
A_33_P3304097	A_33_P3304097	A_33_P3304097	0.01	0.38	6.34	3.38E-01		
A_33_P3305325	A_33_P3305325	A_33_P3305325	0.01	0.38	5.83	3.86E-01		
A_33_P3309684	A_33_P3309684	A_33_P3309684	0.02	0.48	15.42	-3.10E-01		
A_33_P3312564	A_33_P3312564	A_33_P3312564	0.02	0.44	13.28	-3.41E-01		
A_33_P3315027	A_33_P3315027	A_33_P3315027	0.02	0.45	18.01	-3.14E-01		
A_33_P3331791	A_33_P3331791	A_33_P3331791	0.00	0.12	9.26	-5.00E-01		
A_33_P3334428	A_33_P3334428	A_33_P3334428	0.01	0.38	5.49	3.43E-01		
A_33_P3344765	A_33_P3344765	A_33_P3344765	0.02	0.45	9.21	-3.48E-01		
A_33_P3346526	A_33_P3346526	A_33_P3346526	0.00	0.08	6.03	-7.63E-01		
A_33_P3351529	A_33_P3351529	A_33_P3351529	0.01	0.41	17.62	-3.30E-01		
A_33_P3354479	A_33_P3354479	A_33_P3354479	0.01	0.32	17.62	-3.70E-01		
A_33_P3359846	A_33_P3359846	A_33_P3359846	0.00	0.15	7.1	-6.92E-01		
A_33_P3360204	A_33_P3360204	A_33_P3360204	0.02	0.47	9.47	-3.17E-01		
A_33_P3365963	A_33_P3365963	A_33_P3365963	0.01	0.30	11.29	-4.05E-01		
A_33_P3389558	A_33_P3389558	A_33_P3389558	0.01	0.33	5.46	3.99E-01		
A_33_P3393986	A_33_P3393986	A_33_P3393986	0.02	0.48	5.63	-4.46E-01		
A_33_P3395403	A_33_P3395403	A_33_P3395403	0.00	0.24	6.96	5.39E-01		
A_33_P3396434	A_33_P3396434	A_33_P3396434	0.01	0.39	18.04	-3.60E-01		
A_33_P3407230	A_33_P3407230	A_33_P3407230	0.02	0.42	7.34	-3.25E-01		
A_33_P3408665	A_33_P3408665	A_33_P3408665	0.00	0.25	12.4	-4.69E-01		

Probe name	Systematic name	Gene name	*p*-value	adj. *p*-value	Ave Expr	log_2FC	1)	confirmed via qRT-PCR
A_33_P3410019	A_33_P3410019	A_33_P3410019	0.00	0.27	9.57	-4.13E-01		
A_33_P3416414	A_33_P3416414	A_33_P3416414	0.01	0.38	6.94	-6.94E-01		
A_33_P3416787	A_33_P3416787	A_33_P3416787	0.01	0.29	5.56	-4.75E-01		
A_33_P3423845	A_33_P3423845	A_33_P3423845	0.00	0.23	8.75	-4.35E-01		

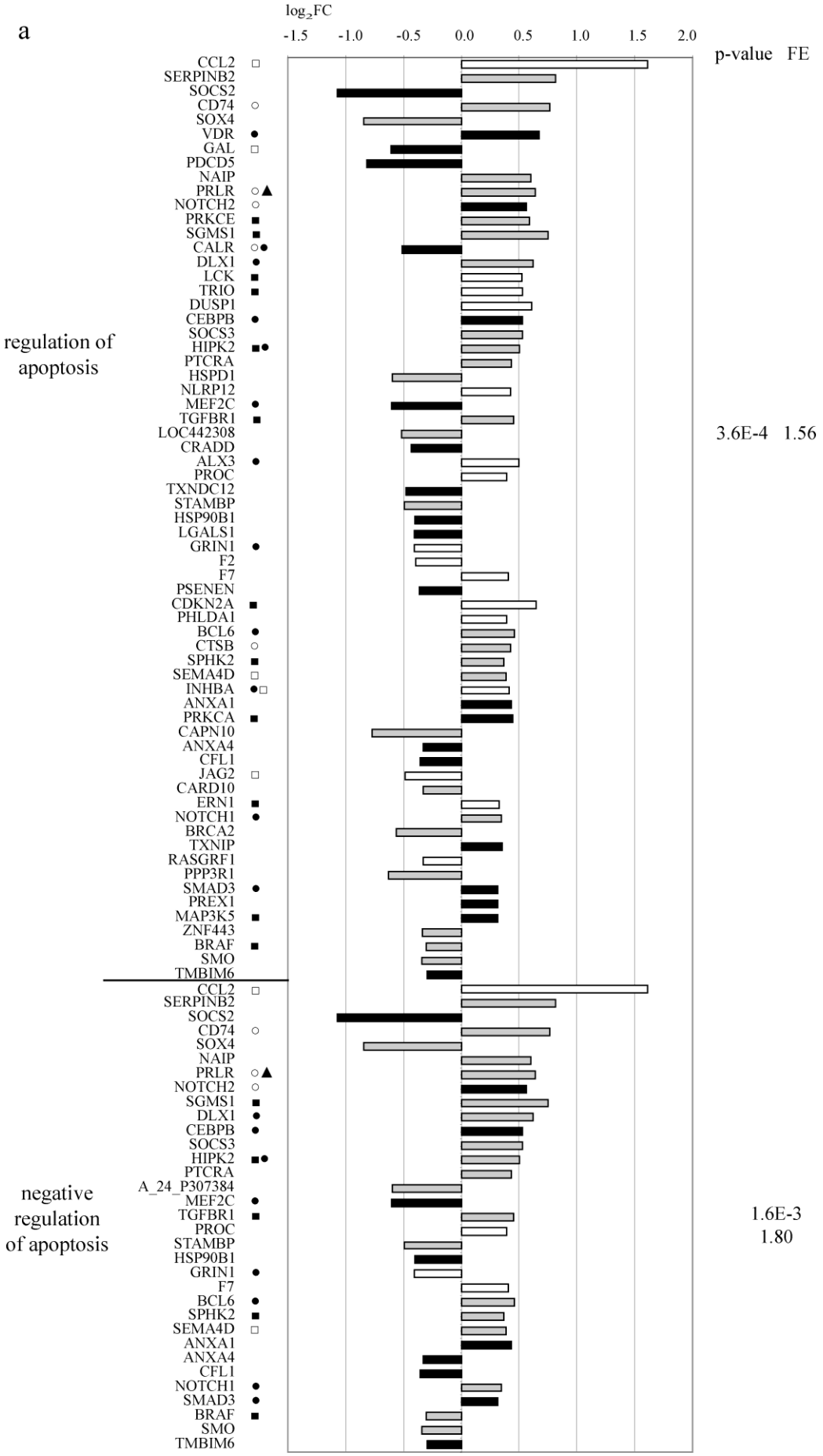

Figure legend on page 175

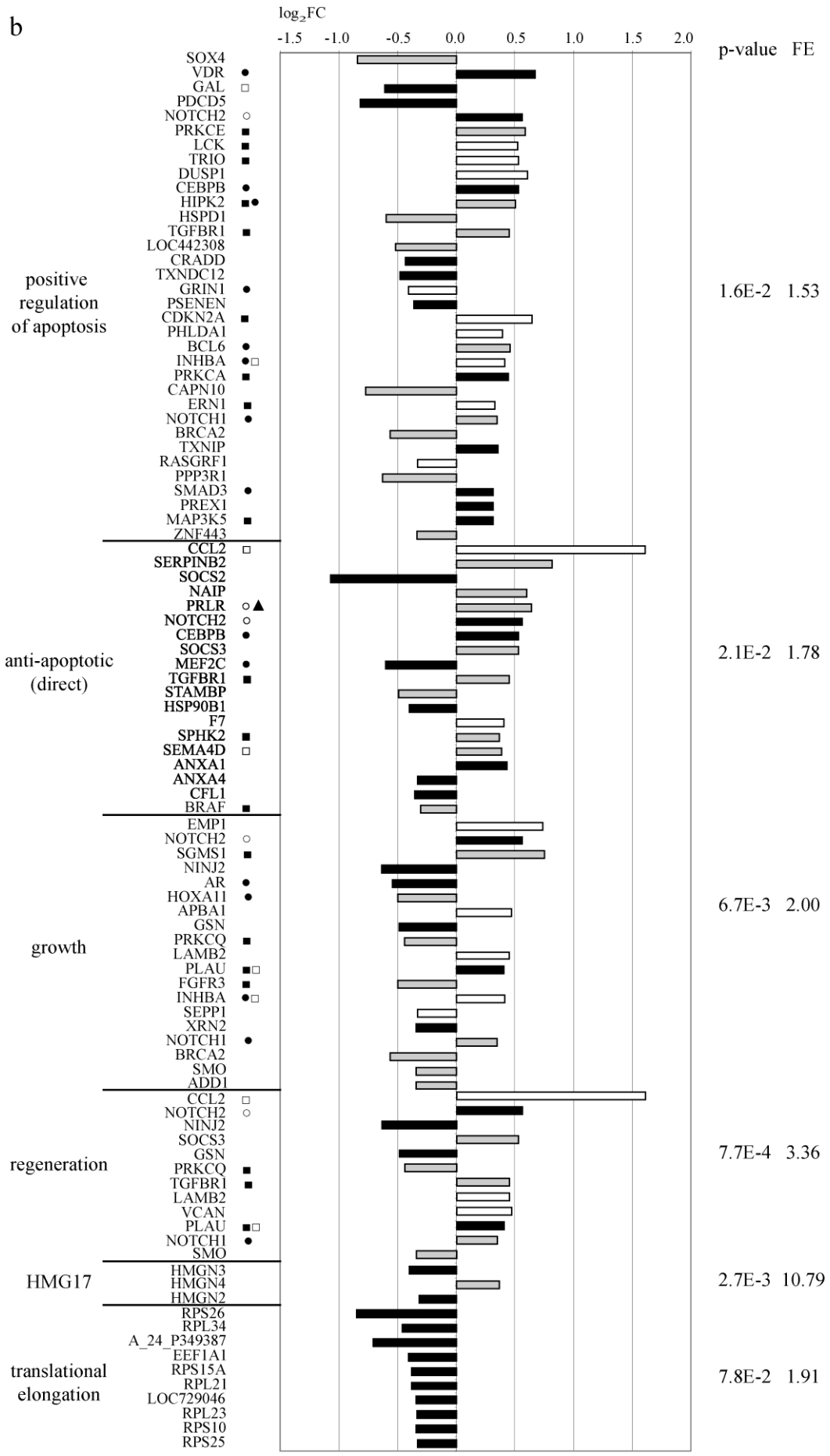

Figure legend on page 175

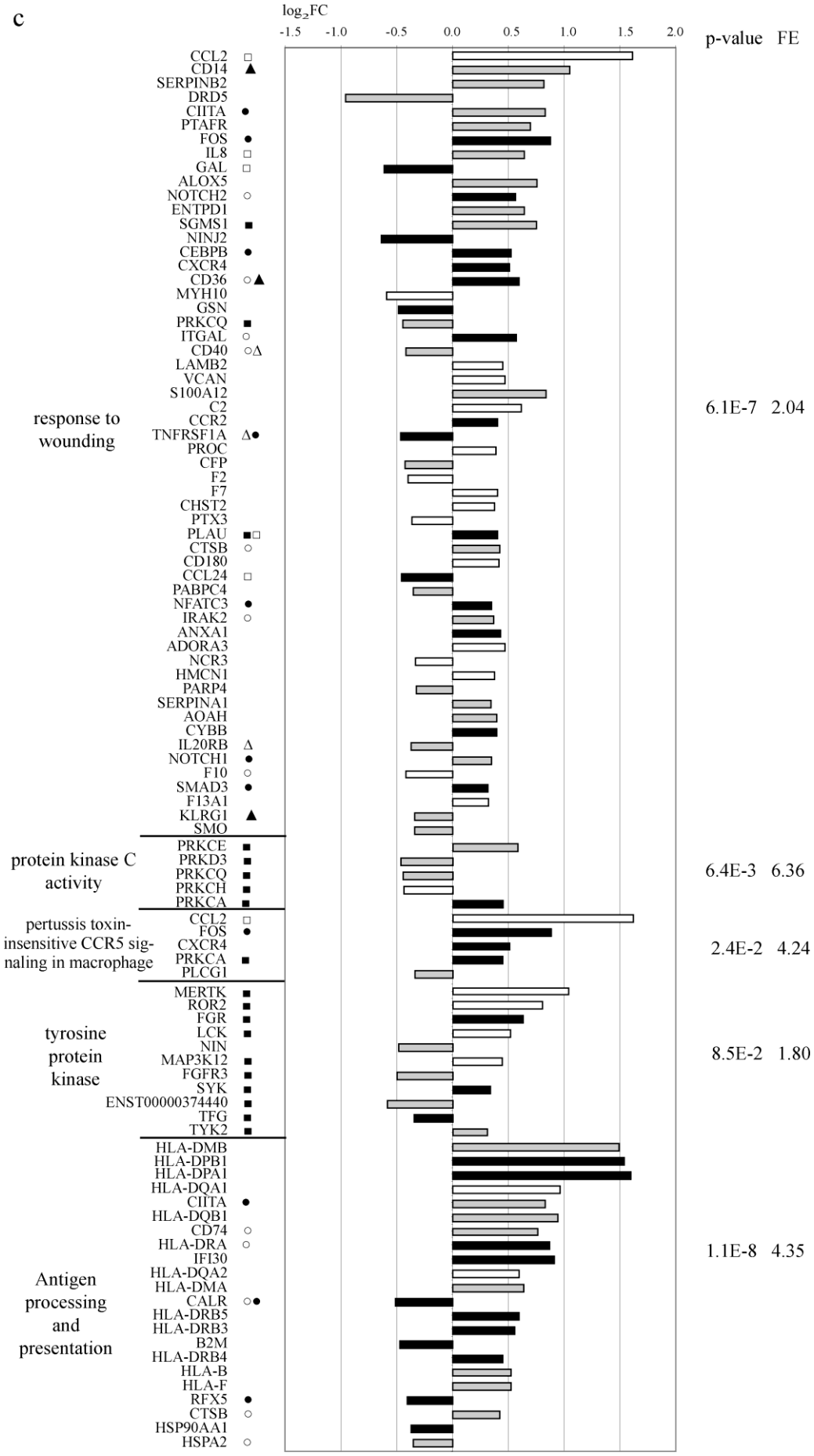

Figure legend on page 175

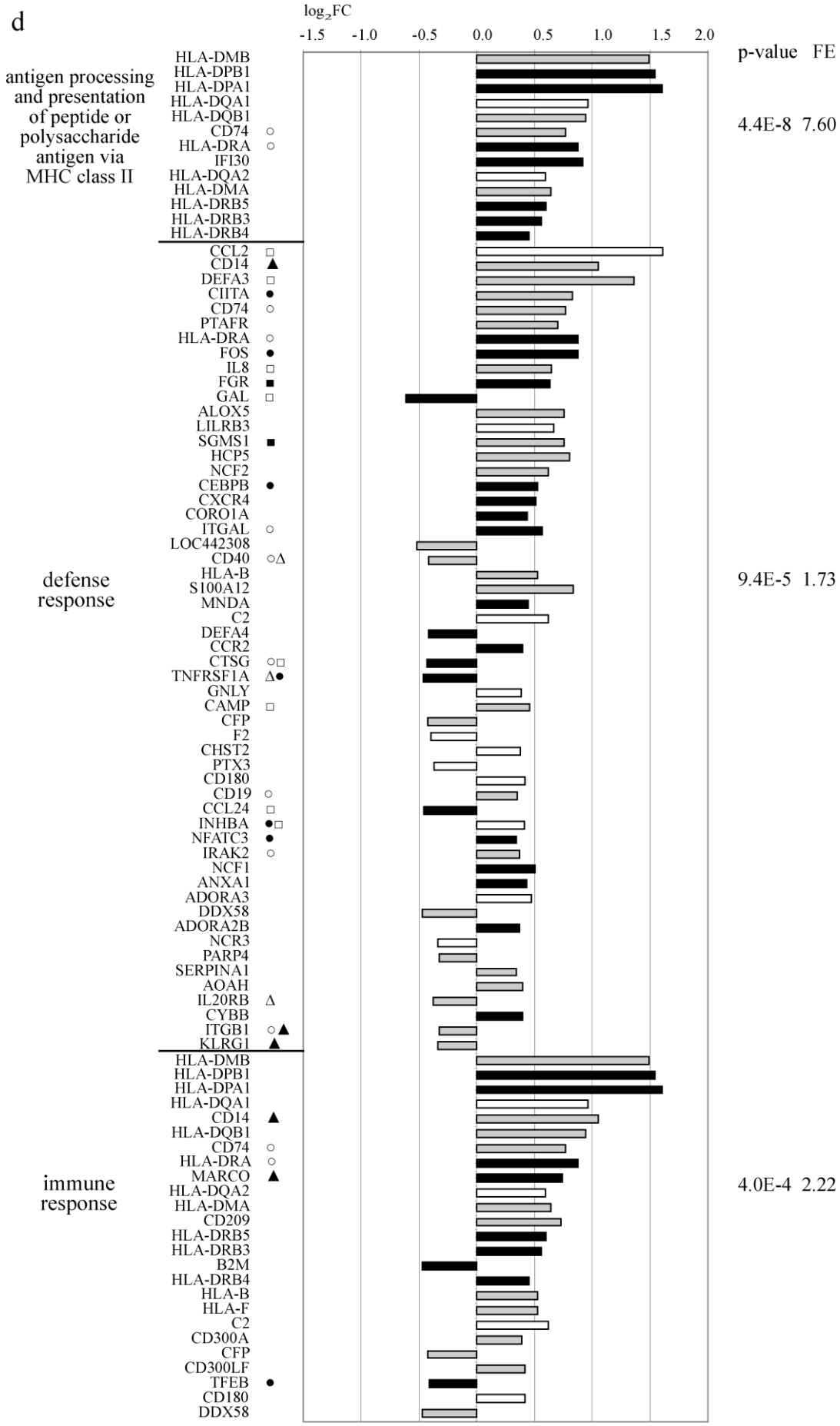

Figure legend on page 175

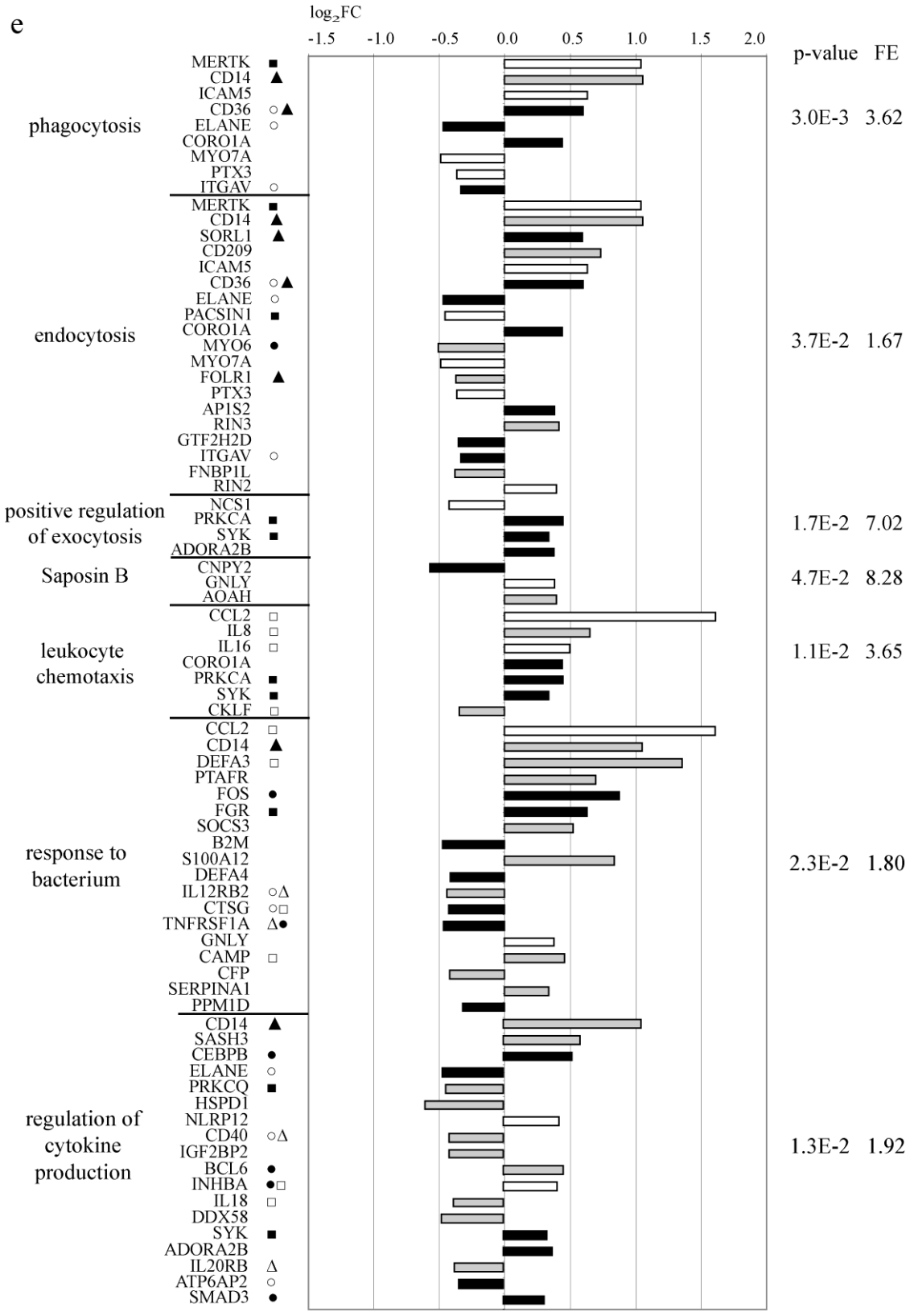

Figure legend on page 175

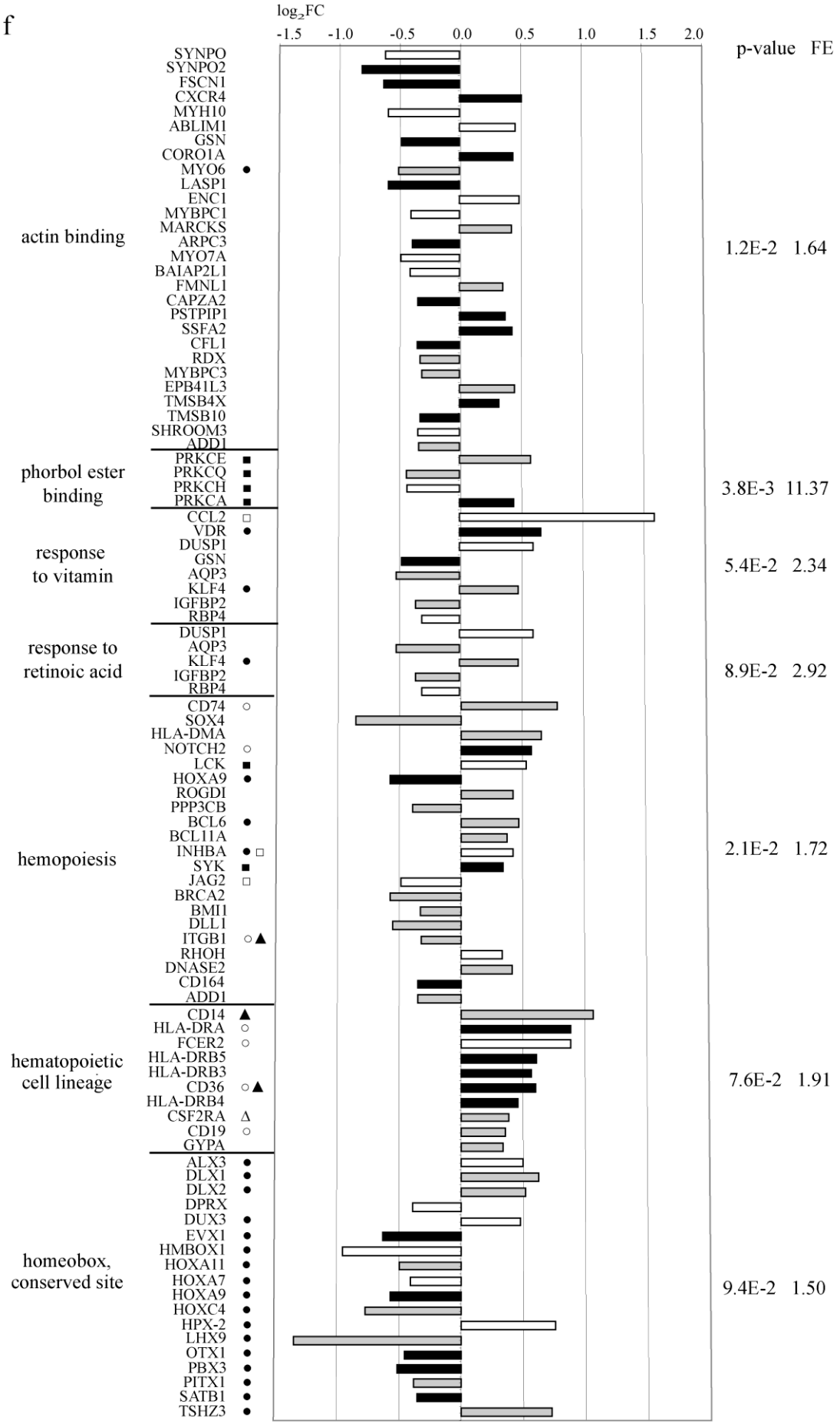

Figure legend on page 175

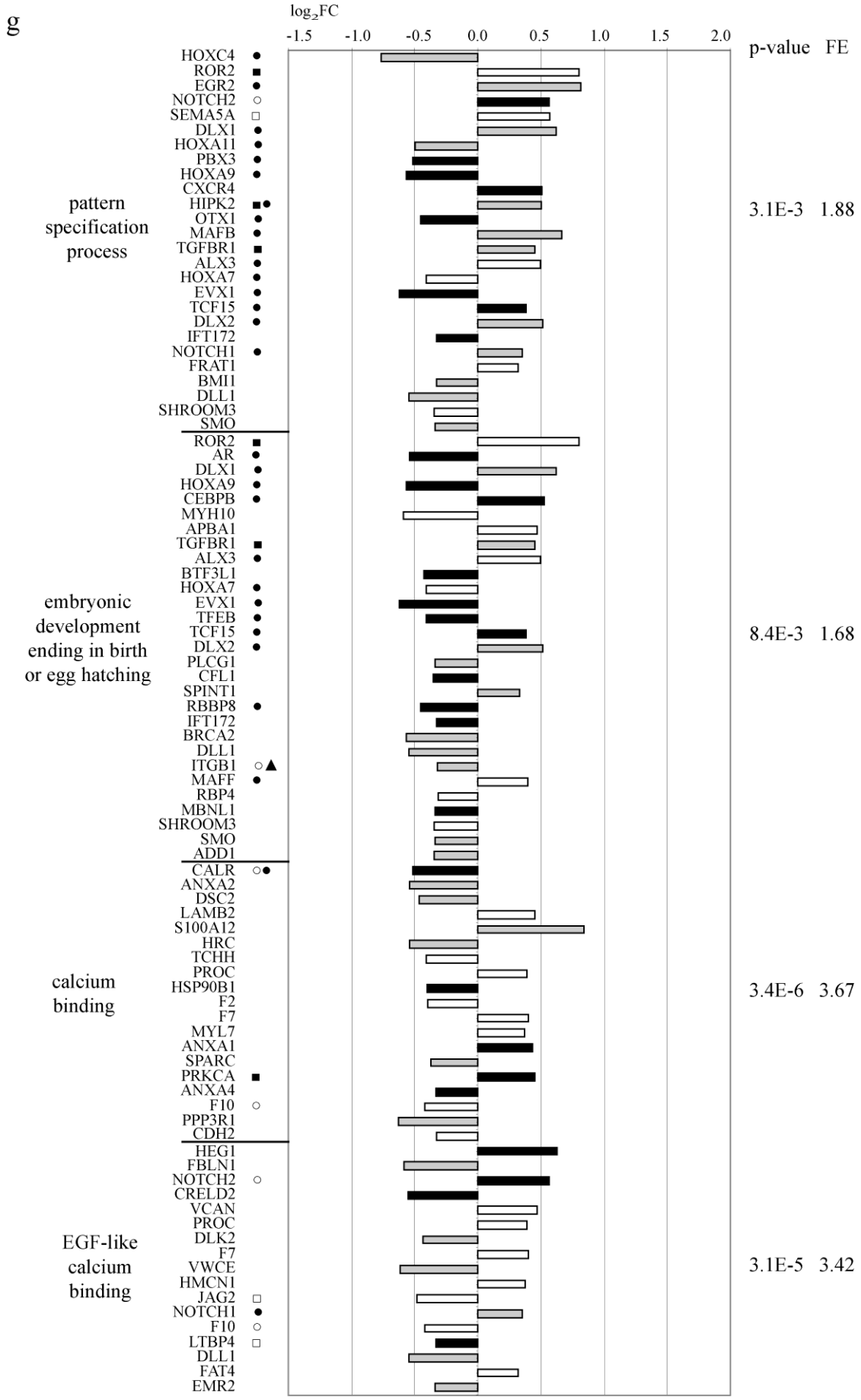

Figure legend on page 175

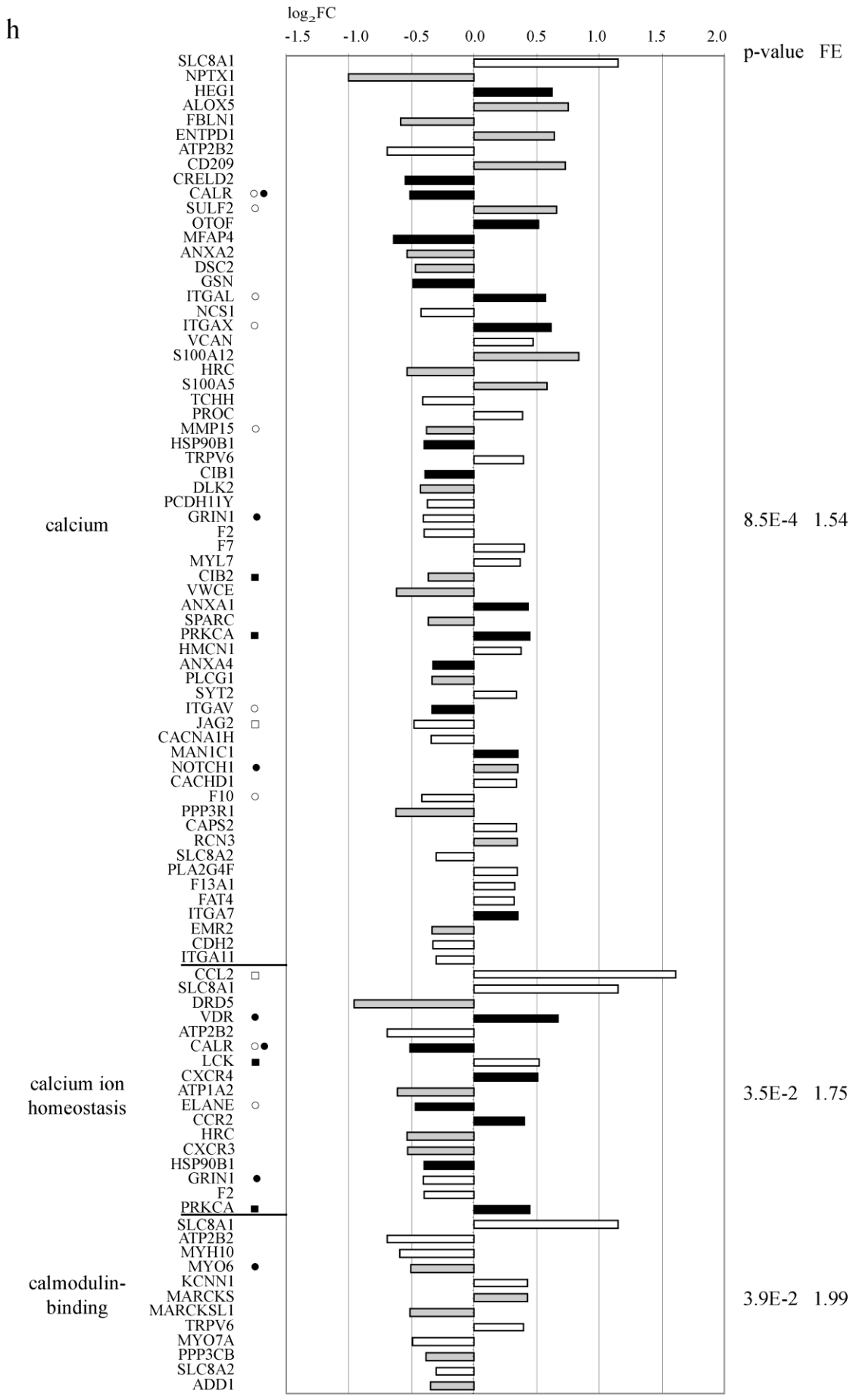

Figure legend on page 175

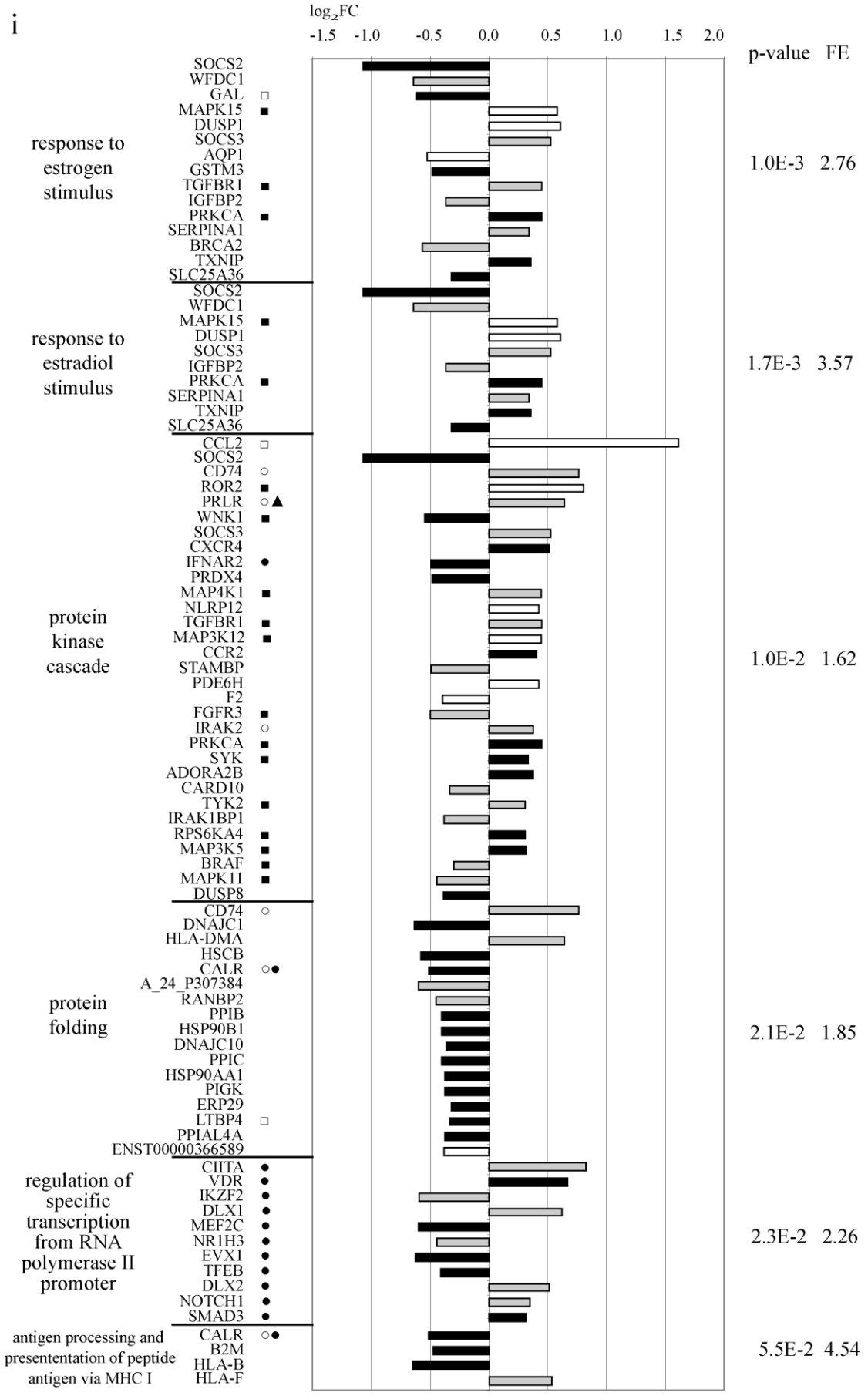

Figure legend on page 175

Supplementary figure 1 a-i: **Expression of all *MLL-AF9* knockdown-associated genes which mapped to functional annotation terms considered to be of biological relevance.** On the left the functional annotation term is given, followed by the encompassed genes and a sign for additional important categories to which they belong (□ cytokine, ■ kinase, ○ cell surface protein, ● transcription factor, Δ cytokine receptor, ▲ other receptor). Their logarithmic fold-change in *MLL-AF9* knockdown versus control treatments in THP1 cells are given on the x-axis. The color of bars indicates expression strength according to microarrays fluorescent signal intensities: ■ high, ▣ medium and □ low expression (classified as described in material and methods). On the right side of the graph the *p*-value and the fold enrichment (FE) of the annotation term are given. Within each term the genes are sorted according to their *p*-value of differential expression.

Supplementary table 3: **Biological roles and rating concerning mediation of MLL-AF9 leukemogenic effects of selected differentially expressed genes after *MLL-AF9* knockdown.** Rating categories (based on biological role and differential expression, see material and methods 7.4, page 32): +++ highly likely candidates and ++ likely candidates for mediation of *MLL-AF9* leukemogenic effects, + genes whose regulation is coherent with its functional role in malignancies, ○ genes with a currently undefined role in malignancies due to a lack of relevant literature, - genes whose regulation is incoherent with its functional role in malignancies. The column on the right gives the basis of selection of this gene for further literature research. GOA, higher-order term of gene ontology annotation.

Gene Rating category	**log_2 FC**	**Official full name** Biological role	**Selection criteria**
ABCA3 -	0.31	**ATP-binding cassette, subfamily A (ABC1), member 3** A ATP-binding cassette (ABC) transporter which is overexpressed in AML and might be involved in drug resistance of leukemic primitive progenitor cells (Norwood, et al. 2004; Steinbach, et al. 2006).	FunDO
AFF4 +	-0.36	**AF4/FMR2 family, member 4** A rare translocation partner of *MLL* in leukemia and a component of the super elongation complex (SEC). SEC is believed to be recruited by many MLL-fusion proteins to activate translational elongation of target genes (Mohan, et al. 2010). AFF4 is required for SEC stability and proper transcriptional elongation (Lin, et al. 2010).	FunDO
AHR ++	0.44	**aryl hydrocarbon receptor** AHR is a nuclear receptor. Upregulation of AHR has been shown to promote retinoic acid–induced differentiation of myeloblastic leukemia cells. Additionally, AHR acts as a E3 ubiquitin ligase and is important for estrogen receptor alpha and androgen receptor degradation. (Bunaciu, et al. 2011)	FunDO
ALOX5 -	0.76	**Arachidonate 5-lipoxygenase** Enzyme in the synthesis of leukotrienes (mediators of inflammatory and allergic conditions) from arachidonic acid. ALOX5 has functions in oxidative stress, inflammation and cancer and supports CML stem cell maintenance. (Naka, et al. 2010)	GOA: calcium associated
ATP2B2 ++	-0.69	**ATPase, Ca++ transporting, plasma membrane 2** A plasma membrane pump which is activated by calmodulin and whose rat homolog (97.9% identical to human) maintains low free cytosolic Ca^{2+} concentration (Elwess, et al. 1997). ATP2B2 is downregulated in PMA differentiated U937 monocytes (Wang, et al. 2011). Overexpression of ATP2B2 in breast cancer cells lowers intracellular calcium and protects from apoptosis (VanHouten, et al. 2010). Estradiol and estrogen decreases ATP2B2 expression and activity (El Beialy, et al. 2010).	GOA: calcium associated
B2M +	-0.47	**Beta-2-microglobulin** A serum protein found in association with the major histocompatibility complex (MHC) class I heavy chain. Elevated B2M serum levels are of prognostic value in CLL and multiple myeloma (Melillo, et al. 1988) and predictive of the risk of a myelodysplastic syndrome evolving into an AML (Neumann, et al. 2009).	FunDO

Gene Rating category	**log_2 FC**	**Official full name** Biological role	**Selection criteria**
BMI1 ++	-0.33	**BMI1 polycomb ring finger oncogene** BMI1 is a polycomb group protein described to be essential for reprogramming of myeloid progenitors into leukemia stem cells (Yuan, et al. 2011a) and, together with HOXA9, for the self-renewal capacity of LSC transformed by MLL-AF9 (Smith, et al. 2011). BMI1 is downregulated in PMA differentiated U937 monocytes (Wang, et al. 2011).	in concordance with patient study (Valk, et al. 2004)
CALR +++	-0.51	**Calreticulin** CALR acts as a major Ca(2+)-binding (storage) protein in the lumen of the endoplasmic reticulum (Burns, et al. 1994). It can also act as an important modulator of the regulation of gene transcription by nuclear hormone receptors (Dedhar, et al. 1994). In this context, CALR can inhibit the transcriptional activities of retinoic acid receptor and was shown to inhibit retinoic acid-induced differentiation in neuronal cells (Dedhar, et al. 1994). It is a chaperone and well-established effector of the unfolded protein response (Schardt, et al. 2011). The chaperone CALR inhibits the translation of CEBPA, which is a key myeloid transcription factor and a frequent target for disruption in AML (Schardt, et al. 2011).	FunDO
CAMP +	0.46	**Cathelicidin antimicrobial peptide** An antimicrobial protein found in monocytes and other leukocytes. A direct target of the vitamin D receptor, which is strongly upregulated in myeloid cells by 1,25-dihydroxyvitamin D3. (Gombart, et al. 2005) Lower CAMP protein expression was detected in neutrophils of AML patients (An, et al. 2005).	FunDO
CCL2 +++	1.61	**Chemokine (C-C motif) ligand 2** The second strongest regulated gene transcript was chemokine (C-C motif) ligand 2 (CCL2) with a *p*-value of 1.11E-6. CCL2 binds to chemokine (C-C motif) receptor 2 and 4 (CCR2 and CCR4), the former of which is also upregulated in a *MLL-AF9* knockdown specific manner in our data set. CCL2 displays chemotactic activity for monocytes and basophils. It is upregulated in PMA differentiated U937 monocytes (Wang, et al. 2011). AML blasts have been described to produce different amounts of CCL2 which influences the number of monocytes migrating towards AML blasts (Legdeur, et al. 2001). Plasma levels of CCL2 are decreased in patients with AML of the subtype M4 and M5 (Mazur, et al. 2007). Thus, low levels of CCL2 might lead to reduced immunosurveillance of M4 and M5 blasts. In this context, CCL2 has been proposed for adoptive immunotherapy (Legdeur, et al. 2001). In induced pluripotent mouse stem cells, Ccl2 induces the key transcription factor genes for pluripotency, Klf4, Nanog, Sox2 and Tbx3 (Hasegawa, et al. 2011). KLF4, which is also a marker for and inducer of monocytic and terminal macrophage differentiation (Klco, et al. 2011; Schuetz, et al. 2011), is also upregulated in a *MLL-AF9* knockdown specific manner in our data set.	FunDO, $log_2FC>\pm1$, GOA: differentiation, calcium associated, other
CD14 ○	1.05	**CD14 molecule** A pattern recognition receptor (Kitchens 2000) and myelomonocytic differentiation antigen (Goyert, et al. 1988) and differentiation marker for maturating monocytes (Schwende, et al. 1996; Abrink, et al. 1994).	$log_2FC>\pm1$, GOA: proliferation, cell growth and death; differentiation
CD19 ○	0.35	**CD19 molecule** While normally expressed on B cells, CD19 is also expressed in mixed lineage leukemia cells (Schubert, et al. 2011).	FunDO
CD209 ○	0.73	**CD209 molecule** A transmembrane receptor expressed in dendritic cells and macrophages, recognizing numerous pathogens and playing a role in cell adhesion. (Geijtenbeek, et al. 2000; Dominguez-Soto, et al. 2011; Tassaneetrithep, et al. 2003)	GOA: calcium associated
CD74 ○	0.77	**CD74 molecule, major histocompatibility complex, class II invariant chain** CD74 ensures stabilization, proper folding as well as transport of newly synthesized HLA class II heterodimers to the MHC class II containing compartments (Pieters, et al. 1993; Anderson, et al. 1992).	GOA: other
CEBPB +++	0.53	**CCAAT/enhancer binding protein (C/EBP), beta** CEBPB activates the promoter of PU.1, a tumor suppressor for AML (Mueller, et al. 2006). Activation of CEBPB expression leads to differentiation and reduced proliferation of CML cells. CEBPB is reactivated after imatinib treatment of BCR/ABL CML cells. (Guerzoni, et al. 2006)	in concordance with patient study (Zheng, et al. 2006)

Gene Rating category	**log_2 FC**	**Official full name** Biological role	**Selection criteria**
CIITA +++	0.83	**Class II, major histocompatibility complex, transactivator** Transcriptional coactivator and master controller of MHC class II expression (Ting, et al. 2002). MHC-II is not expressed on leukemia cells of most patients with acute promyelocytic leukemia and some with acute myeloblastic leukemia. It is considered that these leukemia cells are unable to present the antigens to helper T cells which enhances the function of cytotoxic T cells (CTL) against leukemia cells and may therefore escape the immunological surveillance of the body. Although the regulatory mechanism of individual MHC-II expression has still to be elucidated, these findings reveal a possible new strategy using the CIITA gene in immuno-gene therapy for patients with MHC-II negative hematological malignancies. (Liu, et al. 1999) Phosphorylation of CIITA directs its oligomerization, accumulation and increased activity on MHCII promoters (Tosi, et al. 2002).	FunDO, GOA: other
CTSG ○	-0.43	**Cathepsin G** A hematopoietic serine protease with microbicidal and proinflammatory activity which is strongly expressed in neutrophils. CTSG proteolytically degrades engulfed cell debris and displays a variety of pathophysiological effects, among these enhancing hematopoietic progenitor cell mobilization by cleaving CD106 (Sun, et al. 2004) and is putatively regulated by PU.1, c-myb and C/EBP (Lennartsson, et al. 2005).	FunDO
CYBB +	0.40	**Cytochrome b-245, beta polypeptide** An essential component of phagocytic NADPH-oxidase which is responsible for generating microbicidal superoxide and other oxidants (OMIM). CYBB is downregulated in MLL-ENL/MLL-ELL positive myeloid leukemia progenitor cells (Li, et al. 2009). CYBB is a common target gene repressed by HoxA10 and activated by HoxA9 (Bei, et al. 2005).	FunDO
DACH1 ++	-0.54	**Dachshund homolog 1 (Drosophila)** Was shown to be overexpressed in *MLL*-aberrant leukemia (Ross, et al. 2004). DACH1 binds to the IL8 promoter and repressed it through AP1(JUN/FOS)- and NFKB-binding sites. (Wu, et al. 2008) In concordance to this, IL8 is upregulated in a MLL-AF9 dependent manner in this study.	in concordance with patient studies (Ross, et al. 2004; Kohlmann, et al. 2005)
DEFA3 ○	1.36	**Defensin, alpha 3, neutrophil-specific** An antimicrobial gene. In this setting possibly an indicator for differentiation.	$log_2FC>\pm1$, GOA: differentiation
DEXI ++	-0.56	**Dexi homolog (mouse)** DEXI is suspected to be a membrane protein that dimerizes either with itself or another protein. DEXI is a dexamethasone-induced transcript and is overexpressed in emphysematous lung tissue. (Edgar, et al. 2001) Its function is unknown.	in concordance with patient study (Ross, et al. 2004)
DLL1 +++	-0.54	**Delta-like 1 (Drosophila)** DLL1, a Notch ligand, completely inhibited the differentiation of human hematopoietic progenitors into the B cells, while keeping the potency to develop into NK cells (Jaleco, et al. 2001). DLL1 activated the NF-kappaB pathway via Notch in THP-1 cells (Itoh, et al. 2009). DLL1 reduces TNF-alpha induced growth suppression and apoptosis in monoblastic leukemia cell line U937 cells (Murata-Ohsawa, et al. 2004).	FunDO
DRD5 ○	-0.96	**Dopamine receptor D5** A G-protein coupled receptor which stimulates cAMP (Grandy, et al. 1991).	GOA: proliferation, cell growth and death; calcium associated
EGR2 ++	0.81	**Early growth response 2** A transcription factor and tumor suppressor, whose deletion leads to cancer cell proliferation. EGR2 inhibits neutrophil- and activates macrophage-specific genes. It interacts with PU.1, a master transcription factor in macrophage differentiation. (Gabet, et al. 2010) EGR2 is upregulated in PMA differentiated U937 monocytes (Wang, et al. 2011) and EGR2 binding motifs were found activated and being within the 30 'core' motifs explaining the expressional changes after PMA differentiation in THP1 cells (Suzuki, et al. 2009). Its mouse homolog is underexpressed in hematopoietic stem and progenitor cells after Mll-AF9 knock-in (Chen, et al. 2008).	GOA: early development

Gene Rating category	**log_2 FC**	**Official full name** Biological role	**Selection criteria**
F13A1 ○	0.33	**Coagulation factor XIII, A1 polypeptide** The intracellular form of this coagulation factor is expressed in monocytes and macrophages and has been shown to be a marker for AML FAB M4 and M5 blasts (Kiss, et al. 2008).	FunDO
FMNL1 ○	0.36	**Formin-like 1** A formin, which is overexpressed in lymphoid malignancies and has been shown to associate with Akt (a survival regulator in different cell types) (Favaro, et al. 2003). It is upregulated in PMA differentiated U937 monocytes (Wang, et al. 2011).	FunDO
FOS +++	0.88	**FBJ murine osteosarcoma viral oncogene homolog** FOS and FOSB binding motifs were found activated and being within the 30 'core' motifs explaining the expressional changes after PMA differentiation in THP1 cells (Suzuki, et al. 2009). They are components of the dimeric transcription factor AP-1, which mediates subunit and context dependent gene regulation in response to cytokines, growth factors, stress signals, oncogenic stimuli, bacterial and viral infections. AP-1 has effects on proliferation, differentiation and apoptosis (Hess, et al. 2004).	GOA: proliferation, cell growth and death; in concordance with patient study (Zheng, et al. 2006)
FOSB +++	1.05	**FBJ murine osteosarcoma viral oncogene homolog B** see FOS.	$log_2FC>\pm1$, in concordance with patient study (Zheng, et al. 2006)
GNLY ○	0.38	**Granulysin** A antimicrobial and proinflammatory protein, whose transcription has been shown to be induced by AP-1 (Kida, et al. 2002). One isoform induces immune response, chemotaxis and cell adhesion genes in monocytes (Castiello, et al. 2011).	FunDO
GPNMB ++	1.24	**Glycoprotein (transmembrane) nmb** Encodes a putative transmembrane glycoprotein and has been described to be involved in growth delay and reduction of metastatic potential in human melanoma (Weterman, et al. 1995).	$log_2FC>\pm1$
HAPLN2 ○	-1.20	**Hyaluronan and proteoglycan link protein 2** Previously has been assessed as brain specific, although leukocytes were not analyzed in the study (Spicer, et al. 2003). Cell adhesion molecule.	$log_2FC>\pm1$
HIPK2 +++	0.50	**Homeodomain interacting protein kinase 2** A tumor suppressor. In response to DNA damage, HIPK2 phosphorylates the tumor suppressor PML, thus leading to PML stabilization. This phosphorylation is required for the ability of PML to cooperate with HIPK2 for the induction of cell death (Gresko, et al. 2009). Mutations have been found in AML cases (Li, et al. 2007).	FunDO
HLA-B ○	-0.64	**Major histocompatibility complex, class I, B** MHC class I deficient tumor clones may escape T-cell immune responses, but might be more susceptible to NK cell-mediated lysis (Algarra, et al. 2004).	FunDO
HLA-DMB ++	1.49	**Major histo-compatibility complex, class II, DM beta** see HLA-DPA1	$log_2FC>\pm1$, GOA: differentiation
HLA-DPA1 ++	1.60	**Major histo-compatibility complex, class II, DP alpha1** The following three top differential expressed transcripts were two classical and one nonclassical HLA class II gene: HLA-DPA1, HLA-DPB1 and HLA-DMB. HLA class II histocompatibility antigen, DQ beta 1 (ENST00000399670) is also strongly upregulated. MHC class II proteins are selectively expressed in professional antigen presenting cells, besides monocytes these are macrophages, B-cells and dendritic cells (Ting, et al. 2002). Upregulation of these transcripts has been associated with differentiation of monoblasts and THP1 cells were observed to have reduced HLA class II expression levels compared to mature monocytes (Abrink, et al. 1994). In addition, loss of MHC class II gene expression has been shown to be strikingly correlated with poor patient outcome and decreased immunosurveillance in large B-cell lymphoma patients (Rimsza, et al. 2004).	$log_2FC>\pm1$, GOA: differentiation

Gene Rating category	**log_2 FC**	**Official full name** Biological role	**Selection criteria**
HLA-DPB1 ++	1.54	**Major histo-compatibility complex, class II, DP beta 1** Classical HLA class II gene. See HLA-DPA1	FunDO, $log_2FC>\pm1$, GOA: differentiation
HLA-DQA1 ++	0.96	**Major histocompatibility complex, class II, DQ alpha 1** Classical HLA class II gene. See HLA-DPA1	GOA: differentiation
HLA-DQB1 ++	1.19	**Major histo-compatibility complex, class II, DQ beta 1** Classical HLA class II gene. See HLA-DPA1	$log_2FC>\pm1$, GOA: differentiation
HLA-DRB4 ++	0.45	**Major histocompatibility complex, class II, DR beta 4** Classical HLA class II gene. See HLA-DPA1	in concordance with patient study (Rozovskaia, et al. 2003)
HMBOX1 ○	-0.95	**Homeobox containing 1** Transcription factor, transcriptional repressor (Zhang, et al. 2010). Key factor in differentiation of bone marrow stromal cells into vascular endothelial cells (Su, et al. 2010).	GOA: differentiation, early development
HOXA11 ++	-0.50	**Homeobox A11** HOXA11 (together with HOXA4, A7, A10 and MEIS1) is downregulated after PMA induced differentiation in THP1 cells (Martino, et al. 2009). It is also downregulated in PMA differentiated U937 monocytes (Wang, et al. 2011). HOXA11 has been found to be translocated in hematologic malignancies (Panagopoulos, et al. 2003).	FunDO
HOXA7 +	-0.41	**Homeobox A7** A leukemogenic factor which is, like other homeobox genes, frequently upregulated in MLL aberrations and leukemia (Kawagoe, et al. 2001; Afonja, et al. 2000). Its mouse homolog is overexpressed in hematopoietic stem and progenitor cells after Mll-AF9 knock-in (Chen, et al. 2008).	FunDO, in concordance with patient study (Kohlmann, et al. 2005)
HOXA9 +++	-0.57	**Homeobox A9** A well studied homeobox transcription factor whose transcription level is raised by MLL-AF9 through direct interaction between MLL-AF9 protein complex and HOXA9 promoter (Erfurth, et al. 2008; Cierpicki, et al. 2010). It's mouse homolog is overexpressed in hematopoietic stem and progenitor cells after Mll-AF9 knock-in (Chen, et al. 2008). Concerning hematopoiesis, HOXA9 knock-out in mice has little or no effect on earlier progenitors but decreases the number of committed progenitor cell (Lawrence, et al. 1997). Overexpression of Hoxa9 alone does not lead to leukemic transformation of primary bone marrow cells in mice but does in conjunction with Meis1 overexpression (Kroon, et al. 1998). In conjunction with BMI1, HOXA9 is essential for the self-renewal capacity of LSC transformed by MLL-AF9 (Smith, et al. 2011). HOXA9 is downregulated in differentiating THP1 cells after PMA addition (Martino, et al. 2006).	in concordance with patient studies (Ross, et al. 2004; Erfurth, et al. 2008; Kohlmann, et al. 2005; Bullinger, et al. 2004)
HOXC4 ++	-0.76	**Homeobox C4** Estrogen-estrogen receptor (ER) complexes upregulate HOXC4 expression in B cells, thereby inducing activation-induced cytosine deaminase (AID) and thus leading to antibody class switch DNA recombination (CSR) and somatic hypermutation (Mai, et al. 2010). Murine HoxC4 may contribute to stem cell character of mesenchymal stem cells (Phinney, et al. 2005). *In vitro* overexpression induces expansion of committed as well as very early hematopoietic progenitors (Daga, et al. 2000).	GOA: early development
HPX-2 ○	0.75	**Homeobox HPX-2** Homeobox containing gene, cloned from human CD34+ hematopoietic cells (Moretti, et al. 1994). Biological role unknown.	GOA: early development

Gene Rating category	**log_2 FC**	**Official full name** Biological role	**Selection criteria**
IFI30 ○	0.91	**Interferon, gamma-inducible protein 30** A lysosomal thiol reductase constitutively expressed in antigen-presenting cells. This enzyme has an important role in MHC class II-restricted antigen processing. (Arunachalam, et al. 2000)	GOA: differentiation
IGF2BP2 +	-0.42	**Insulin-like growth factor 2 mRNA binding protein 2 (alias IMP-2)** A member of embryonically expressed IGF-II mRNA-binding proteins (IMPs: IMP1 – 3). IMP-1 has been shown to repress IGF2 translation by binding to the 5' UTR of the (IGF2) mRNA (Nielsen, et al. 1999). Overexpressed in MLL-AF4 positive acute lymphoblastic leukemia (B-ALL) (Stoskus, et al. 2011). One isoform was expressed at high levels in several cancer cell lines and was suspected to be involved in transformation leading to hepatocellular carcinoma because novel autoantibody responses against this isoform have been detected in patients and may be a immune system reaction involved in transformation-associated cellular events (Zhang, et al. 1999).	FunDO
IKZF2 ++	-0.60	**IKAROS family zinc finger 2 (Helios)** A hematopoietic specific transcription factor involved in the regulation of lymphocyte development. A short isoform is overexpressed in patients with adult T-cell leukemia / lymphoma (Tabayashi, et al. 2007).	FunDO
IL18 +	-0.38	**Interleukin 18** A proinflammatory cytokine; has been shown to induce maturation in the acute myeloid leukemia cell line KG-1 (dendritic cell progenitors) (Bachmann, et al. 2007). On the other hand, IL18 has been shown to be overexpressed in AML and to upregulate transmigration of HL-60 cells (human promyelocytic leukemia) (Zhang, et al. 2004).	FunDO
IL2RG -	-0.31	**Interleukin 2 receptor, gamma** Heterodimerizes to form a number of interleukin receptors (IL2, IL4, IL7, IL9, IL15, IL21) (OMIM). IL2RG is upregulated by 1,25-dihydroxyvitamin D3 in HL-60 (human promyelocytic leukemia) cells (Savli, et al. 2002).	FunDO
IL8 ++	0.65	**Interleukin 8** A multifunctional CXC chemokine, chemoattractant for neutrophils in inflammation, influences basophils and T cell function, may act as an angiogenic, proliferative, autocrine and metastatic factor. Relevant amounts of IL8 are produced by the great majority of AML with monocytic components (M4 and M5). IL8 is preferential released by myeloid blasts showing monocytic differentiation (Vinante, et al. 1996) Thus, upregulation of these transcripts might be associated with differentiation of monoblasts. DACH1 binds to the IL8 promoter and repressed it through AP1(JUN/FOS)- and NFKB-binding sites. (Wu, et al. 2008)	FunDO, in concordance with patient study (Zheng, et al. 2006)
ITGAL ○	0.57	**Integrin, alpha L / CD11A** Adhesion molecule, upregulated upon differentiation with all-trans retinoic acid in AML patients (Wu, et al. 2007).	FunDO
ITGAX ○	0.62	**Integrin, alpha X / CD11C** Adhesion molecule. Expression strongly correlated with increased white blood cell count in AML, independent of FAB subtype and was upregulated in AML patients upon differentiation with all-trans retinoic acid (Wu, et al. 2007).	FunDO
KLF4 ++	0.48	**Kruppel-like factor 4** A transcription factor and a marker for monocytic and terminal macrophage differentiation (Klco, et al. 2011; Schuetz, et al. 2011). While a Klf4 zincfinger domain mutant induces self-renewal and block of maturation, wild-type KLF4 induces terminal macrophage differentiation (Schuetz, et al. 2011). KLF4 is induced by CCL2 in induced-pluripotent mouse stem cells, along with the other key transcription factor genes for pluripotency, Nanog, Sox2 and Tbx3 (Hasegawa, et al. 2011)	in concordance with patient study (Zheng, et al. 2006)

Gene Rating category	**log_2 FC**	**Official full name** Biological role	**Selection criteria**
LGALS1 ++	-0.41	**Lectin, galactoside-binding, soluble, 1** A galectin. These are a group of proteins which have been implicated in diverse biological processes, including modulation of cell–cell and cell–matrix interactions (Wada, et al. 1997). LGALS1 promotes escape from T-cell–dependent immunity and confers immune privilege to tumor cells. It is a highly sensitive and specific biomarker of *MLL*-rearrangement in B-ALL which is likely induced by a MLL-dependent epigenetic modification. (Juszczynski, et al. 2010)	in concordance with patient studies (Armstrong, et al. 2002; Ross, et al. 2004)
LGALS2 ○	1.02	**Lectin, galactoside-binding, soluble, 2** A galectin. These are a group of proteins which have been implicated in diverse biological processes, including modulation of cell–cell and cell–matrix interactions (Wada, et al. 1997). Surprisingly, LGALS2 was previously neither reasonably detected in untreated nor in differentiated HL-60 cells (Abedin, et al. 2003). However, it is upregulated in PMA differentiated U937 monocytes (Wang, et al. 2011).	$log_2FC>\pm1$,
LHX9 ○	-1.34	**LIM homeobox protein 9** Gene of the LIM homeobox gene family, a developmentally expressed transcription factor with a suggested role in gonadal development.	$log_2FC>\pm1$,, GOA: differentiation, early development
LOC 100129 722 ○	-1.32	**Hypothetical LOC100129722** A long non-coding RNA (lncRNA). LncRNAs are a group of RNAs whose primary role includes to act as epigenetic regulators of protein-coding gene expression. Many associate with chromatin-modifying complexes and there is evidence for two lncRNAs to be associated with MLL. LncRNAs may also play a role in organelle biogenesis and subcellular trafficking (e.g. cytoplasmic-to-nuclear shuttling of transcription factors). (Taft, et al. 2010; Dinger, et al. 2008)	$log_2FC>\pm1$
LOC 84989 ○	-1.06	**Hypothetical LOC84989** A long non-coding RNA. See LOC 100129722.	$log_2FC>\pm1$
LPL ○	0.71	**Lipoprotein lipase** LPL plays a major role in the metabolism and transport of lipids, facilitates lipoprotein particle uptake (e.g. in macrophages) and can mediate the selective uptake of lipoprotein-associated lipids and lipophilic vitamins without the concomitant uptake of the lipoprotein particles (Wang, et al. 2009). LPL mRNA level is controlled by activation of protein kinase C (PKC) and by mobilization of intracellular Ca2+ and is induced by PMA in the THP-1 (Auwerx, et al. 1989). LPL is a prognostic marker in CLL with high expression predicting shorter overall survival (Kaderi, et al. 2011).	FunDO
LRRC2 ○	-1.43	**Leucine rich repeat containing 2** Unknown function.	$log_2FC>\pm1$
MAP3K5 ○	0.31	**Mitogen-activated protein kinase kinase kinase 5** A component of a protein kinase signal transduction cascade, whose overexpression induces apoptosis (Ichijo, et al. 1997). On the other hand, in leukemic cells treated with arsenic trioxide, MAP3K5 has been shown to be activated by reactive oxygen species resulting in negative regulation of apoptosis without activating p38 and JNK (Yan, et al. 2007).	FunDO
MAPRE2 +	-0.37	**Microtubule-associated protein, RP/EB family, member 2** A tubulin binding protein which is activated by the AML associated fusion gene Nup98-HOXA9. Nup98-HOXA9 is a transcription factor whose activity depends on the HOXA9 DNA binding domain. (Ghannam, et al. 2004) Thus downregulation of MAPRE2 might be a secondary effect of reduced expression of HOXA9.	FunDO
MBNL1 +	-0.34	**Muscleblind-like (Drosophila)** A regulator of developmentally programmed alternative splicing and possibly cellular RNA metabolism. MBNL1 is involved in the molecular mechanism of myotonic dystrophy (Teplova, et al. 2008; Onishi, et al. 2008). Its mouse homolog is overexpressed in hematopoietic stem and progenitor cells after Mll-AF9 knock-in (Chen, et al. 2008).	in concordance with patient studies (Ross, et al. 2004; Valk, et al. 2004)

Gene Rating category	**log_2 FC**	**Official full name** Biological role	**Selection criteria**
MEF2C +++	-0.60	**Myocyte enhancer factor 2C** A member of the MADS box transcription enhancer factor 2 (MEF2) family involved in myogenesis. MEF2C promotes myeloid progenitor proliferation (Johnnidis, et al. 2008). Mef2c is upregulated in leukemic stem cells of MLL-associated leukemia (Krivtsov, et al. 2006; Schuler, et al. 2008) and its mouse homolog is overexpressed in hematopoietic stem and progenitor cells after Mll-AF9 knock-in (Chen, et al. 2008). Expression of Mef2c in granulocyte macrophage progenitors increases the number of differentiated myelomonocytic cells, but does not induce serial replating activity. Mef2c is a cooperating oncogene in leukaemogenesis that is unable to induce leukemia when expressed alone. (Krivtsov, et al. 2006)	in concordance with patient studies (Ross, et al. 2004; Valk, et al. 2004)
MERTK ○	1.04	**C-mer proto-oncogene tyrosine kinase** Regulates cytokine secretion and clearance of apoptotic cells by macrophages and promotes macrophage survival in response to oxidative stress (Anwar, et al. 2009).	log_2FC>±1, GOA: proliferation, cell growth and death; differentiation
NAIP -	0.60	**NLR family, apoptosis inhibitory protein** Antiapoptotic protein, overexpressed in acute mixed lineage leukemia and might be involved in drug resistance (Nakagawa, et al. 2005).	FunDO
NKG7 +	-0.34	**Natural killer cell group 7 sequence** NGK7 expression is upregulated by G-CSF and NGK7 protein accumulates during the differentiation of myeloid cells towards mature neutrophils (Shimane, et al. 1999).	in concordance with patient study (Ross, et al. 2004)
NPTX1 ○	-1.00	**Neuronal pentraxin I** NPTX1 rat homolog has been described to be downregulated upon antiestrogen treatment (Yasuhara, et al. 2008).	log_2FC>±1, GOA: calcium associated
PBX3 +++	-0.51	**Pre-B-cell leukemia homeobox 3** One isoform of PBX3 is preferentially expressed in leukemic cells (Milech, et al. 2001). PBX proteins function as part of large complexes with other homeodomain-containing proteins to regulate gene expression during developmental and/or differentiation processes. Overexpression of PBX3 might play a role in BCR/ABL-mediated myeloid differentiation and transformation. (Salesse, et al. 2003)	in concordance with patient studies (Ross, et al. 2004; Bullinger, et al. 2004; Kohlmann, et al. 2005)
PDCD5 -	-0.82	**Programmed cell death 5** A proapoptotic protein, whose translocation to the nucleus has been described as an universal early event in apoptosis. Reduced levels of PDCD5 in AML and CML marrow cells compared to normal donor marrow cells was detected. (Ruan, et al. 2006; Ruan, et al. 2008)	FunDO
PDE4D ++	-0.34	**Phosphodiesterase 4D, cAMP-specific** A protein that degrades cAMP. In primary B cell chronic lymphocytic leukemic (B-CLL) apoptosis could be induced by stimulating the cAMP signaling pathway with a phosphodiesterase4 (PDE4) inhibitor (Dong, et al. 2010).	FunDO
PRLR -	0.64	**Prolactin receptor** A survival factor that supports tumor growth and confers chemoresistance in breast and prostate cancers (Jacobson, et al. 2010). A rise in intracellular Ca2+ elicited by activation of PRLR has been described to be JAK2-dependent (Zhang, et al. 2009).	GOA: other
RHBDL1 ++	-1.13	**Rhomboid, veinlet-like 1** As suggested by gene annotation inferred from electronic annotation, RHBDL1 may posses serine-type endopeptidase activity and be involved in regulated intramembrane proteolysis and the subsequent release of functional polypeptides from their membrane anchors (UniProt Consortium 2012; National Center for Biotechnology Information 2012). RHBDL1 drosophila homolog has been implicated in the positive modulation of epidermal growth factor receptor signaling (Pascall, et al. 1998).	log_2FC>±1
RHOH +	0.33	**Ras homolog gene family, member H** A member of the Rho family of small GTPases. Low expression of RHOH transcript implied negative prognosis in AML patients concerning overall and disease-free survival (Iwasaki, et al. 2008)	FunDO

Gene Rating category	**log_2 FC**	**Official full name** Biological role	**Selection criteria**
RNPEP +	-0.32	**Arginyl aminopeptidase (aminopeptidase B)** RNPEP is an exopeptidase which is proposed to play a role in the final stages of protein precursor processing (Aurich-Costa, et al. 1997).	in concordance with patient study (Ross, et al. 2004)
ROR2 ++	0.81	**Receptor tyrosine kinase-like orphan receptor 2** A receptor / coreceptor for Wnt5a which mediates noncanonical Wnt signaling. Mutations within the human Ror2 gene are responsible for genetic skeletal disorders. Oncogenic and anti-oncogenic roles have been described in a wide array of malignancies. (Minami, et al. 2010) It has been previously hypothesized that Wnt5a is a tumor suppressor in myeloid leukemogenesis acting through the Wnt5a/Ror2 noncanonical signaling pathway that inhibits Wnt canonical signaling (Yuan, et al. 2011b). Wnt-5A is able to trigger calcium release in several cell types (Kestler, et al. 2008).	GOA: early development, other
RPL23A ○	-1.09	**Ribosomal protein L23a** A ribosomal protein. Production of ribosomes is a major metabolic activity, tightly linked to cell growth, proliferation, cell-cycle regulation, senescence and stress response (Andersen, et al. 2005).	$log_2FC>\pm1$,
RPS26 ○	-0.85	**Ribosomal protein S26** A ribosomal protein. See RPL23A.	GOA: proliferation, cell growth and death
S100A12 ++	0.84	**S100 calcium binding protein A12** A calcium-binding protein, with multiple proinflammatory activities including chemotaxis for monocytes and neutrophils (Kishimoto, et al. 2006), which implicates a potential role in immunosurveillance. S100A12 is upregulated in PMA-differentiated U937 monocytes (Wang, et al. 2011).	GOA: proliferation, cell growth and death; calcium associated; in concordance with patient study (Zheng, et al. 2006)
SGK1 -	1.10	**Serum/glucocorticoid regulated kinase 1** A downstream target of phosphoinositide 3-kinase (PI 3-kinase)-stimulated growth factor signaling (Park, et al. 1999), activated by IGF1 and oxidative stress (Kobayashi, et al. 1999), whose transcription is induced upon cell shrinkage in hepatocytes (Waldegger, et al. 1997) and which activates ion channels (Gamper, et al. 2002) and can promote survival (Lyo, et al. 2010).	$log_2FC>\pm1$
SLC8A1 ○	1.15	**Solute carrier family 8, member 1** A bidirectional sodium/calcium exchanger that contributes to the electrical activity of the heart (Mai, et al. 2010).	$log_2FC>\pm1$, GOA: calcium associated
SNRP D2P2 ○	-1.13	**Small nuclear ribonucleoprotein D2 pseudogene 2 (LOC645339)** A processed pseudogene with no evidence for protein coding function, although a 55 amino acid sequence is predicted. Unknown function.	$log_2FC>\pm1$
SOCS2 +++	-1.07	**Suppressor of cytokine signaling 2** A negative regulator of cytokine receptor signaling via the Janus kinase pathway, suppresses the apoptotic effect of LIF (Minamoto, et al. 1997), may play a regulatory role in IGF1 receptor signaling (Dey, et al. 1998) and is induced by a wide number of cytokines and hormones (e.g. estrogen and GM-CSF) (Rico-Bautista, et al. 2006)	FunDO, $log_2FC>\pm1$, GOA: proliferation, cell growth and death; other; in concordance with patient studies (Ross, et al. 2004; Kohlmann, et al. 2005; Zheng, et al. 2006; Valk, et al. 2004)
SOCS3 -	0.53	**Suppressor of cytokine signaling 3** SOCS3 inhibits the therapeutic, CD33-induced, block on proliferation in AML. A trend towards a higher reaction response and longer overall survival in patients with SOCS3 CpG hypermethylation (Middeldorf, et al. 2010).	FunDO

Gene Rating category	**log_2 FC**	**Official full name** Biological role	**Selection criteria**
SOX4 ++	-0.84	**SRY (sex determining region Y)-box 4** A leukemogenic transcription factor in mouse leukemias. SOX4 is overexpressed in human AML samples. (Sun, et al. 2006b) Transcriptional upregulation of SOX4 together with proviral insertions and Evi1 activation or p15INK4b inactivation has been associated with leukemia (Boyd, et al. 2006; Bies, et al. 2010).	GOA: proliferation, cell growth and death
SP9 ++	-1.19	**Sp9 transcription factor homolog (mouse)** SP9 vertebrate homologs have a described role in embryo limb outgrowth (Kawakami, et al. 2004), are involved in the formation of the regeneration epithelium (like Hoxa-9 and Hoxa-13) and were describes as marker for the dedifferentiation of keratinocytes of the mature skin epidermis in the axolotl (Satoh, et al. 2008).	$log_2FC>\pm1$
TAS1R3 ++	-2.01	**Taste receptor, type 1, member 3** A sweet taste receptor and glucose sensor which may be involved in energy supply (Mace, et al. 2009), was the most significant (p = 7.47E-08) and strongest regulated protein coding gene transcript and showed medium expression strength according to FI signal.	$log_2FC>\pm1$
TSGA10 -	1.03	**Testis specific, 10** Influences the function of antigen presenting cells via its interaction with cytoskeletal proteins such as vimentin (Roghanian, et al. 2010) and has been found overexpressed in cancers (Tanaka, et al. 2004b). TSGA10 is potentially involved in cell proliferation and has been found expressed in the bone marrow and peripheral blood of ALL patients (Mobasheri, et al. 2006).	FunDO, $log_2FC>\pm1$
VDR ++	0.67	**Vitamin D (1,25- dihydroxyvitamin D3) receptor** A ligand-inducible transcription factor affecting cellular metabolism, bone formation, cellular growth, differentiation, control of inflammation and calcium homeostasis (Carlberg, et al. 2009; Dusso, et al. 2005). 1,25-dihydroxyvitamin D3 is capable of inducing *in vitro* monocyte/macrophage differentiation of both normal and leukemic myeloid cell lines (Gocek, et al. 2010) and to inhibit growth and promote differentiation of a variety of cell types and thus has suggested to function in preventing cancers (Dusso, et al. 2005). VDR null mice show an increased susceptibility to tumor formation (Carlberg, et al. 2009). 1,25-dihydroxyvitamin D3 induces a sustained increase of intracellular Ca2+ concentration and thus induced apoptosis in breast cancer cell lines (Sergeev 2005).	GOA: other
VWA1 ○	-1.01	**Von Willebrand factor A domain containing 1** Encodes an extracellular matrix protein, which is also expressed in the apical ectodermal ridge of developing limb buds (like SP9) (Allen, et al. 2008).	$log_2FC>\pm1$
ZNF521 +++	-0.73	**Zinc finger protein 521** Highly expressed in the most immature hematopoietic cells and declines with differentiation. Enforced expression leads to proliferation and differentiation block. Overexpression decreases granulo-monocytic and erythroid differentiation. High expression has been associated with MLL-rearrangements and silencing in THP1 cells led to impaired growth and clonogenicity (Bond, et al. 2008) ZNF521 modulates erythroid cell differentiation through direct binding with GATA-1 (Matsubara, et al. 2009). Enhances resistance to NK cell-mediated cytotoxicity in tumor cells involving HLA class I upregulation (La Rocca, et al. 2009).	FunDO, in concordance with patient study (Kohlmann, et al. 2005)

Supplementary table 4: **Overview of all differentially expressed miRNAs from both profiling platforms in *MLL-AF9* knockdown as compared to control THP1 cells.**

	LDA						microarray						
miRNA	differentially expressed	log_2FC	SD log_2FC	mean C_T	p-Value	adjusted p-Value	differentially expressed	log_2FC	SD log_2FC	AveExpr	p-Value	adjusted p-Value	validated via qRT-PCR (single-assay)
hsa-let-7i*	yes	1.86	0.78	34.2	0.04	0.65	n.d.						n.det.
hsa-miR-137	yes	3.04	0.82	33.6	0.01	0.33	n.d.						n.det.
hsa-miR-155*	yes	0.97	0.08	29.7	0.01	0.45	n.d.						n.det.
hsa-miR-214	yes	8.00	0.31	32.0	n.a.	n.a.	n.d.						yes
hsa-miR-219-5p	yes	-5.49	2.44	35.2	0.01	0.33	n.d.						yes
hsa-miR-301a	yes	0.50	0.03	22.1	0.04	0.54	no						n.det
hsa-miR-328	no						yes	0.44	0.17	4.97	0.000	0.000	n.det
hsa-miR-330-3p	yes	0.61	0.12	28.7	0.03	0.54	n.d.						n.det.
hsa-miR-369-3p	yes	2.73	0.77	32.9	0.01	0.33	n.d.						no
hsa-miR-383	yes	10.66	5.30	29.3	n.a.	n.a.	n.d.						n.det.
hsa-miR-432	yes	-1.57	0.32	29.7	0.01	0.448	n.d.						yes
hsa-miR-455-3p	yes	-0.50	0.03	25.9	0.04	0.54	n.d.						n.det.
hsa-miR-511	yes	8.40	1.23	31.6	n.a.	n.a.	n.d.						yes
hsa-miR-539	yes	-1.77	0.64	29.0	0.02	0.45	n.d.						yes
hsa-miR-548a-3p	yes	-1.45	0.63	34.0	0.04	0.54	n.d.						n.det.
hsa-miR-576-5p	yes	6.38	0.14	33.6	n.a.	n.a.	n.d.						no
hsa-miR-582-3p	yes	-0.85	0.05	28.7	0.01	0.33	n.d.						no
hsa-miR-586	yes	6.58	0.10	33.4	n.a.	n.a.	n.d.						n.det.
hsa-miR-589	yes	-1.09	0.14	31.2	0.01	0.33	n.d.						yes
hsa-miR-610	yes	-0.76	0.25	28.3	0.04	0.65	n.d.						n.det.
hsa-miR-744*	no						yes	0.20	0.05	4.74	0.000	0.000	n.det.
hsa-miR-758	yes	-8.30	0.21	31.7	n.a.	n.a.	n.d.						yes
hsa-miR-760	yes	-0.93	0.23	27.2	0.02	0.56	n.d.						no

All miRNAs with $p<0.05$ from either platform are included. LDA, quantitative TaqMan low density array; microarray, semiquantitative Agilent miRNA microarray; C_T and AveExpr values are given as an indicator of expression strength. C_T, threshold cycle of LDA; AveExpr, average expression from microarray data (based on fluorescence signal intensities); n.p., not present on array; n.a. not available (p-value can not be calculated for miRNAs which were turned "on" or "off"); n.d., not detectable; n.det., not determined.

14 Erklärung

Eidesstattliche Erklärung

Ich versichere hiermit an Eides statt, dass die vorgelegte Dissertation von mir selbständig und ohne unerlaubte Hilfe angefertigt ist.

München, den ....
(Unterschrift)

Erklärung

Hiermit erkläre ich,

dass die Dissertation nicht ganz oder in wesentlichen Teilen einer anderen Prüfungskommission vorgelegt worden ist.

dass ich mich anderweitig einer Doktorprüfung ohne Erfolg **nicht** unterzogen habe.

München, den ....
(Unterschrift)